



TECHNISCHE  
UNIVERSITÄT  
WIEN

## DISSERTATION

# Investigation of different bioprocess modes with *Escherichia coli*

ausgeführt zum Zwecke der Erlangung des akademischen Grades eines Doktors der  
technischen Wissenschaften unter der Leitung von

Associate Prof. Dipl.-Ing. Dr.nat.techn. Oliver Spadiut

E166 Institut für Verfahrenstechnik, Umwelttechnik und technische Biowissenschaften

eingereicht an der Technischen Universität Wien

Fakultät für Technische Chemie

von

**Dipl.-Ing. Stefan Kittler**  
Matrikelnummer 01426143

---

Wien, am

---

eigenhändige Unterschrift



## Erklärung zur Verfassung dieser Arbeit:

Hiermit erkläre ich, dass ich diese Arbeit selbstständig verfasst, alle verwendeten Quellen und Hilfsmittel vollständig angegeben habe und Stellen der Arbeit - einschließlich Tabellen und Abbildungen -, die anderen Werken oder dem Internet im Wortlaut oder Sinn entnommen sind, auf jeden Fall unter Angabe der Quelle als Entlehnung kenntlich gemacht habe.

---

Stefan Kittler



## Danksagung

Ich möchte mich besonders bei Oliver Spadiut bedanken, dass ich meine Dissertation in seiner Arbeitsgruppe durchführen konnte und er mich stets unterstützte. Durch die Möglichkeit an vielen spannenden Projekten mitwirken zu können, konnte ich mein Wissen weiter vertiefen. Weiters gilt ein großer Dank an Julian Kopp, der mich seit der Masterarbeit unterstützte und immer für Ratschläge und Hilfe bereitstand. Zudem möchte ich mich bei der IBD Group bedanken, die unglaublich hilfsbereit war und jeden Arbeitstag motivierend und unterhaltsam machte.

Danke an meine Familie und Freunde, die mich auf diesem Weg begleitet und unterstützt haben!

## Abstract

*Escherichia coli* is one of the most used microorganisms in biotechnology. Even though the complexity of this microorganism is low and the production of antibodies or proteins with post-translational modifications is hardly possible, traits, like fast growth rates, inexpensive media, and an almost limitless genetic toolbox, emphasize its widespread utilization. To date, the production of heterologous proteins is primarily carried out in fed-batch cultivations due to high achievable product concentrations within a short time. However, state-of-the-art fed-batch processing is accompanied by large equipment sizes causing increased energy costs as well as high CO<sub>2</sub> emissions and water consumption. The reduction of downtimes is economically and environmentally desirable and could be achieved with repetitive fed-batch or continuous cultivations. Furthermore, a switch towards continuous manufacturing would bring benefits in scale-up, reactor size and facility design, leading to a lower carbon footprint. Due to a continuous harvest of product and longer cultivation times, the downtimes are reduced, resulting in higher yields. However, continuous applications for recombinant protein production with *E. coli* tremendously lack behind other industrial sectors, due to decreasing productivities and instabilities in long-term cultivations.

In my Thesis I investigated i) different *E. coli* expression systems, ii) a variety of process parameters, and iii) different substrates in fed-batch, repetitive fed-batch and continuous cultivations with *E. coli* to generate process knowledge, identify bottlenecks and increase the bioprocess performance. I found that the spatial separation of biomass growth and recombinant protein expression in cascaded continuous cultivations is promising to achieve stable product formation with *E. coli* in long-term cultivations. I proposed a workflow to implement cascaded continuous cultivations, leading to improved space-time yields compared to typical fed-batch cultivations.

In summary, my Thesis sheds light onto different bioprocess modes with the highly important expression host *E. coli* aiming at the generation of process knowledge to transform the typical fed-batch mode to a continuous process.

## Zusammenfassung

*Escherichia coli* ist einer der am häufigsten verwendeten Mikroorganismen in der Biotechnologie. Obwohl der Mikroorganismus eine geringe Komplexität hat und die Produktion von Antikörpern oder Proteinen mit post-translationalen Modifikationen kaum möglich ist, sind Eigenschaften wie schnelle Wachstumsraten, kostengünstige Medien und eine Vielzahl an Möglichkeiten den Organismus genetisch zu verändern, Gründe für die zahlreichen Anwendungen. Die Produktion heterologer Proteine wird derzeit vor allem in Fed-Batch Kultivierungen durchgeführt, da hier in kurzer Zeit hohe Produktkonzentrationen erreicht werden können. Allerdings ist das Fed-Batch Verfahren derzeit mit großen Anlagen verbunden, die zu erhöhten Energiekosten sowie hohen CO<sub>2</sub>-Emissionen und einem hohen Wasserverbrauch führen. Es ist daher wirtschaftlich und umwelttechnisch wünschenswert den Produktionsstillstand zu verringern. Dies kann durch repetitive Fed-Batch oder kontinuierliche Kultivierungen erreicht werden. Darüber hinaus würde eine Umstellung auf eine kontinuierliche Produktion Vorteile beim Scale-up, der Reaktorgröße und dem Anlagenbau bringen, was den CO<sub>2</sub>-Ausstoß verringern würde. Außerdem kann durch eine kontinuierliche Ernte des Produkts und längere Kultivierungszeiten der Produktionsstillstand reduziert werden, wodurch die volumetrischen Ausbeuten erhöht werden. Allerdings sind kontinuierliche Anwendungen für die rekombinante Proteinproduktion mit *E. coli* derzeit aufgrund von abnehmenden Produktivitäten und Instabilitäten bei Langzeitkultivierungen weit hinter jenen von anderen Industriezweigen zurück.

In meiner Dissertation untersuchte ich i) verschiedene *E. coli*-Expressionssysteme, ii) eine Vielzahl von Prozessparametern und iii) verschiedene Substrate in Fed-Batch, repetitiven Fed-Batch und kontinuierlichen Kultivierungen mit *E. coli*, um Informationen über die Prozesse zu sammeln, Probleme und Hürden zu identifizieren und die Prozessausbeute zu steigern. Dabei habe ich festgestellt, dass die räumliche Trennung von Biomassewachstum und rekombinanter Proteinexpression in kaskadierten kontinuierlichen Kultivierungen vielversprechend ist, um eine stabile Produktbildung mit *E. coli* in Langzeitkultivierungen zu erreichen. Daher wurde ein Arbeitsablauf zur Umsetzung kaskadierter kontinuierlicher Kultivierungen entwickelt, wodurch die Raum-Zeit-Ausbeuten im Vergleich zu Fed-Batch Kultivierungen verbessert wurden.

Meine Dissertation beleuchtet verschiedene Bioprozessmodi, durchgeführt mit dem wichtigen Expressionswirt *E. coli*, mit dem Ziel Prozesswissen zu generieren, um die etablierte Fed-Batch Kultivierung in einen kontinuierlichen Prozess umzuwandeln.

# Table of Content

Danksagung .....	I
Abstract .....	II
Zusammenfassung .....	III
Table of Content.....	IV
1. Introduction and Problem Formulation .....	1
1.1. Fed-batch Bioprocesses .....	2
1.1.1. Fed-batch.....	2
1.1.2. Repetitive Fed-batch.....	3
1.2. Continuous Bioprocesses .....	4
1.2.1. Chemostat.....	4
1.2.2. Cascaded Continuous Cultivation .....	5
2. Goal of the Thesis.....	7
3. Results and Discussion.....	9
3.1. Fed-batch Bioprocesses .....	10
3.1.1. Background Information .....	10
3.1.2. Scientific Publication 1 .....	14
3.1.3. Scientific Publication 2 .....	17
3.1.4. Scientific Publication 3 .....	20
3.2. Continuous Bioprocesses .....	23
3.2.1. Background Information .....	23
3.2.2. Scientific Publication 4 .....	26
3.2.3. Scientific Publication 5 .....	28
4. Conclusion and Outlook.....	31
5. References .....	33
6. Scientific Publications.....	40
6.1. Scientific Publication 1 .....	40



6.2.	Scientific Publication 2 .....	59
6.3.	Scientific Publication 3 .....	67
6.4.	Scientific Publication 4 .....	80
6.5.	Scientific Publication 5 .....	91
7.	Appendix .....	102
7.1.	Protein L – More Than Just an Affinity Ligand.....	102
7.2.	Inclusion body production in fed-batch and continuous cultivation .....	115
7.3.	Curriculum vitae.....	137

# 1. Introduction and Problem Formulation

*Escherichia coli* is used for the production of recombinant proteins in academia and in industry. It was first cultivated in the late 70s for the industrial production of polypeptides. Recombinant human insulin expressed in an *E. coli* strain was approved for the pharmaceutical market in 1982, and therefore paved the way for subsequent strain, process, and protein engineering [1, 2]. This first successful market approval using recombinant DNA technology for strain engineering resulted in a high number of approved *E. coli* products that account for almost 25% of all available therapeutics nowadays [1, 3, 4]. Since bacteria have the drawback of not being able to perform post-translational modifications (PTMs), such as glycosylation or disulfide bond formation, the production of antibodies and complex proteins is restricted. However, the obstacle of disulfide bridge formation has been overcome by strain engineering approaches, enabling either the formation of disulfide bonds in the reducing environment of the cytoplasm or translocation into the periplasm using its prevailing oxidizing conditions [5, 6]. The large genetic toolbox, fast growth rates, low costs, and easiness of cultivation are indispensable advantages causing the wide application range of *E. coli* in various biotechnological processes.

The preferred cultivation mode as well as identification of critical process parameters (CPPs) (such as temperature, specific substrate uptake rate, and induction time) are highly strain- and product-dependent [7, 8]. The classical fed-batch is the preferred process mode for the recombinant protein production using *E. coli* since high biomass and product concentrations can be reached within a short time frame and operational handling of this process mode is simple [7, 9]. However, to increase the space-time yield (STY) and develop more economically and environmentally desirable bioprocesses, a switch towards other bioprocess modes is necessary.

## 1.1. Fed-batch Bioprocesses

### 1.1.1. Fed-batch

In fed-batches the substrate is fed constantly to avoid nutrient depletion and increase the cell density while the production of metabolites is reduced or even prevented. The cells and product remain in the reactor until the end of fermentation (Figure 1). Since cell growth and product formation are severely affected by the chosen feeding rate, it is a crucial process parameter [10, 11]. Even though cell densities and volumetric productivity can be increased by using optimal feeding rates and process conditions, induction temperature, cultivation time and inducer have an impact on the process costs and need to be considered [8].

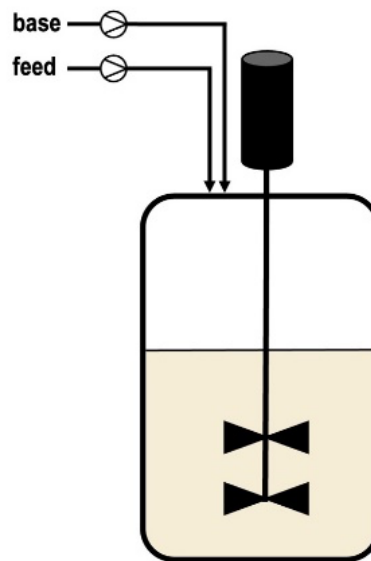


Figure 1: Schematic sketch of a fed-batch cultivation with *E. coli*. After a batch is performed, fresh nutrients are supplied to the reactor using a pre-defined feeding strategy. Commonly, pH control in *E. coli* processes is done solely by the addition of ammoniac, while acid is only added manually if required. Figure adapted from [12].

To control the bioprocess, various feeding strategies can be used. Feed forward strategies are based on determined initial conditions and selected specific growth rates. These strategies benefit from operational simplicity without the need of on-line measurements and control models [11]. However, host physiological changes are not considered and as a result, overfeeding of the cells and subsequent accumulation of the fed primary carbon source is risked. Advanced strategies use a feedback control or soft sensors, such as on-line measurements of oxygen uptake rate (OUR) or carbon evolution rate (CER) [13-15]. Furthermore, static  $pO_2$  or pH values can be targeted to control the applied feeding rate [10, 16]. However, applications of advanced control strategies in industry are scarce as investment costs for software and implementation are often higher than the economic benefit of the improved process performance [11].

In most fed-batch cultivations, first a batch is performed to increase the cell density, subsequently, an exponential feeding profile is applied (non-induced fed-batch) [11, 17]. After a desired cell density is reached, recombinant protein expression is induced, and further substrate is supplied (induced fed-batch). Currently, fed-batch cultivations are favoured for industrial applications due to high achievable volumetric productivities and robustness [7, 9, 11, 18]. However, operation and investment costs are high and production processes suffer from time-dependent product quality [19-21]. Furthermore, sterilization and cleaning steps are required after each production cycle, causing high economic costs and an environmental burden [7, 22]. Most of the time the vessel is not used for the recombinant protein production (~30%) due to biomass growth phases (batch, non-induced fed-batch), sterilization and cleaning, whereby the space-time yield is affected. In the industry, rising energy costs and stricter regulations regarding CO<sub>2</sub> emission likely cause a shift towards different cultivation modes with less downtimes. One way to reduce the number of sterilization and cleaning cycles are repetitive fed-batches.

### 1.1.2. Repetitive Fed-batch

In a repetitive fed-batch the downtime is reduced while the total duration of heterologous protein expression is increased due to repeated production cycles within one cultivation run [23]. In a fed-batch the whole reactor is harvested at the end of a cultivation, whereas in a repetitive fed-batch the reactor is harvested partially after each induced fed-batch phase (=1 cycle). Subsequently, the cell broth is diluted with fresh media and an induced fed-batch is started repeatedly [24-26]. As mentioned before, a repetitive fed-batch allows to increase the STY while the relative amount of time for sterilization and cleaning is lowered with each repeated production cycle [24, 27]. Still, previous results reported that the productivity was declining with each performed production cycle [24, 28, 29]. Furthermore, common problems known from fed-batch cultivations, like scale-up effects affecting biomass yield and product formation are observed. In addition, larger vessel sizes lead to a higher carbon footprint due to increased energy and water consumption [30, 31]. As an alternative, continuous manufacturing would bring benefits in scale-up and facility design, as reduced equipment sizes with significantly less working volume allow small footprint facilities [32, 33].

## 1.2. Continuous Bioprocesses

### 1.2.1. Chemostat

A further step towards intensified equipment utilization is achieved by a switch from batch-wise production to a continuous cultivation [32-34]. So far, continuous cultivation processes are implemented in various industrial sectors, including wastewater treatment, white biotechnology, biogas, and ethanol production [32, 35]. In the red biotechnology, continuous cultivations are implemented mainly with mammalian cells for the production of therapeutics [36-39]. The studies on continuous cultivations go back to the 1950s to Monod and Novick and Szilard [40-42]. Since then, chemostat cultivations have been used to study strain physiology under constant growth conditions [33]. In microbial chemostat cultivations, cells are maintained in a steady-state environment, therefore the culture vessel is supplied continuously with fresh nutrients while simultaneously culture broth is removed, defining the dilution rate ( $D = \frac{\text{feed rate}}{\text{reactor volume}}$ ) (Figure 2) [32].

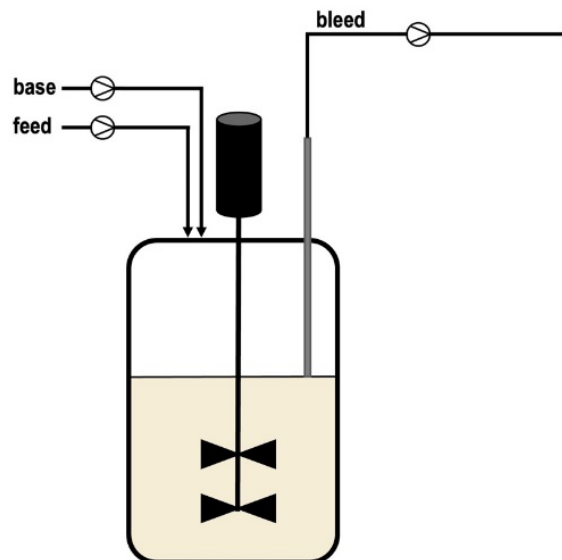


Figure 2: Schematic sketch of a chemostat cultivation with *E. coli*. After a batch is performed, fresh nutrients are supplied to the reactor, using a constant feeding rate, while at the same time fermentation broth is continuously harvested (bleed). The dilution rate is defined by the used feed rate and the reactor volume. Figure adapted from [12].

Continuous manufacturing is associated with benefits regarding reduced equipment size and easier scalability of cultivation processes, lower set-up and operational costs, as well as an increase of product quality and volumetric productivity [21, 32, 34, 35, 43, 44]. Scale-up problems can be circumvented due to more similar equipment in different application scales (research development to production) [18, 32, 43]. The adapted facility design, accompanied by smaller vessel sizes and modular systems, will lead to less water and energy consumption, resulting in small footprint facilities [21, 34]. Furthermore, high feasible dilution rates with *E.*

*E. coli* have the potential to increase the STYs, outperforming fed-batch cultivations [45]. To date, instable and decreasing productivities in chemostat cultivations with *E. coli* are observed, causing that mentioned benefits do not prevail [18, 33, 43]. The occurrence of non-producing subpopulations results in cell heterogeneities and instable recombinant protein expression levels [46-49]. Decoupling of biomass growth and recombinant protein expression in cascaded continuous cultivation led to promising results with stable productivity [18, 35, 48].

### 1.2.2. Cascaded Continuous Cultivation

The declining productivities and instabilities in chemostat continuous cultivations have been circumvented in cascaded continuous cultivations. It is known that recombinant protein expression causes a metabolic burden to the host cells, especially severe when a strong expression systems, like a T7-based pET system, is used [35]. Relying on fed-batches, in which biomass formation and recombinant protein expression are decoupled in a timely manner, these two steps are separated in a cascaded continuous cultivation in two different reactors (Figure 3) [18, 35]. One reactor is solely used for biomass generation, supplying a second culture vessel with fresh biomass. In the second reactor, two volume streams, a biomass stream and a feed stream inducing recombinant protein expression, come together [18, 35, 50].

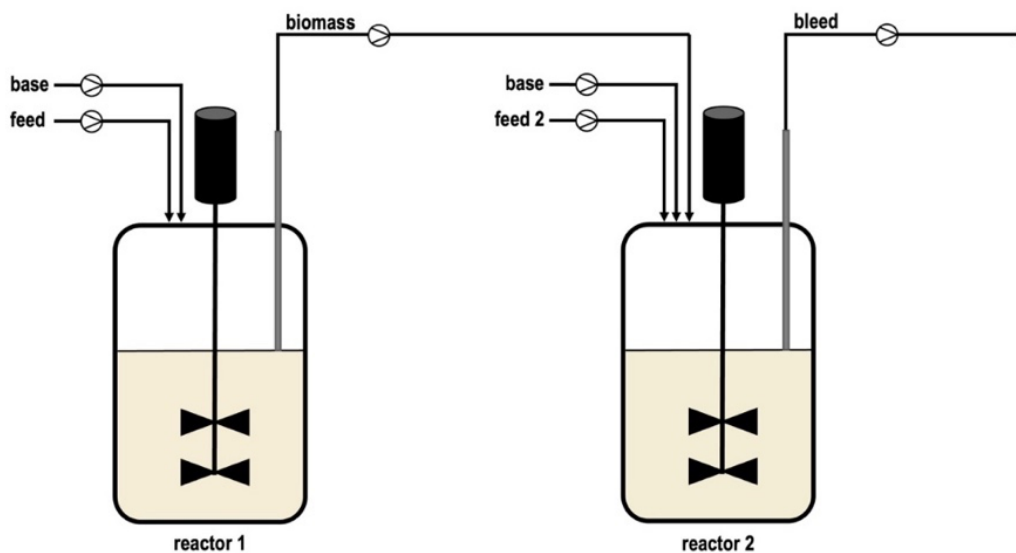


Figure 3: Schematic sketch of cascaded continuous cultivation with *E. coli*. After a batch is performed, fresh nutrients are supplied to the first reactor using a constant feeding rate. The first reactor is solely used to produce biomass, therefore the feed does not contain any inducer (e.g. lactose, arabinose). The biomass is continuously transferred to reactor 2, where additionally a feed with an inducer (feed 2) is applied to initiate recombinant protein expression. From reactor 2 the fermentation broth is continuously harvested (bleed). The dilution rate of reactor 1 is defined by the used feed rate (feed) and the reactor volume. The dilution rate in reactor 2 is defined by the feed rate (feed 2), the biomass flow of reactor 1, and the reactor volume. Figure adapted from [12].

Studies revealed that a separation of these two metabolic pathways (biomass growth and recombinant protein expression) reduce the burden and stress on the microbial host and elongate productivity [18, 35, 50]. Additionally, this operation procedure enables optimal cultivation

conditions for the respective goal (biomass growth, recombinant protein expression) of each vessel [18, 35, 50].

As mentioned before, fed-batch cultivations are used in academia and in industry as gold standard to produce recombinant proteins with *E. coli* (Figure 4). Due to decreasing productivities and low STYs, chemostat cultivations with *E. coli* are not economically feasible to date. Indeed, cascaded continuous cultivations were promising to reach elongated and stable production processes, however, detailed knowledge about critical process parameters is missing and the application of this two-stage cultivation mode is limited to academic studies so far (Figure 4) [18, 35].

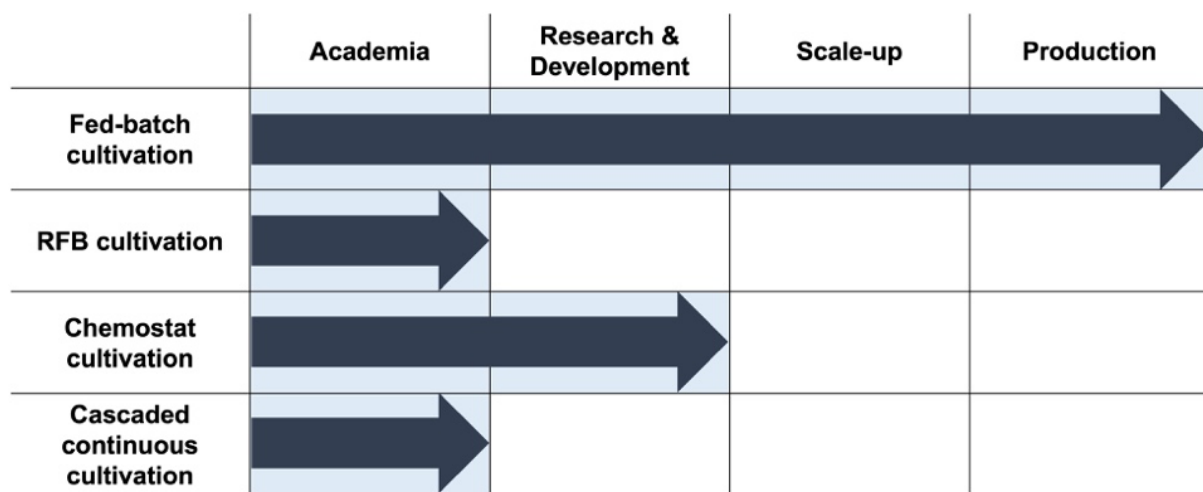


Figure 4: Comparison of the investigated bioprocess modes in this thesis and their predicted application status for *E. coli* in academia and industry. RFB: repetitive fed-batch

## 2. Goal of the Thesis

Although the cultivation of *E. coli* is well established, further process development and optimization should aim to develop more sustainable bioprocesses with larger volumetric throughputs and reduced downtimes. Therefore, I investigated strain, induction mechanism, carbon source and cultivation mode (Figure 5).

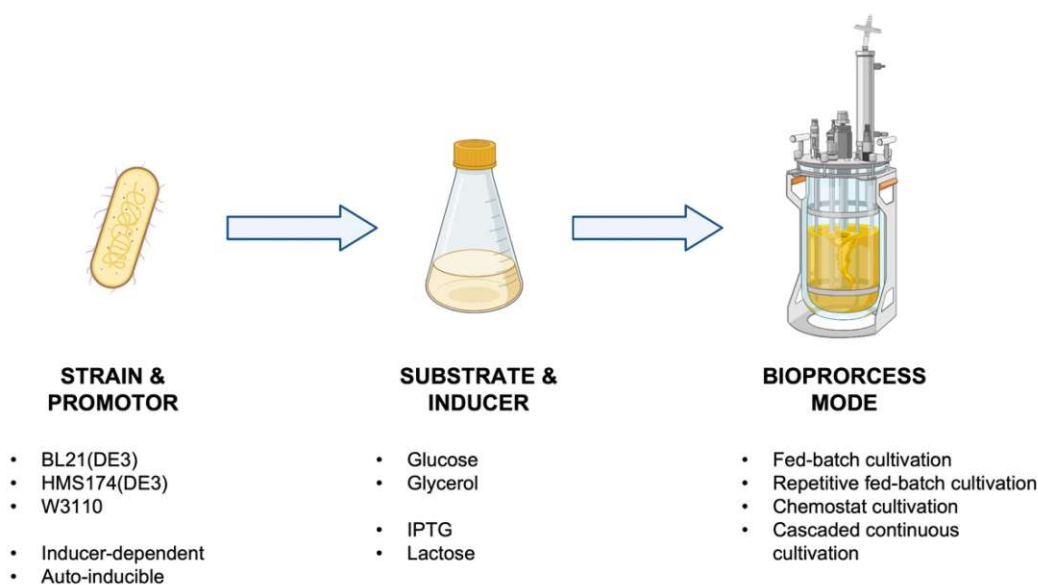


Figure 5: Overview of variables for upstream processing with *E. coli* investigated in this Thesis. IPTG: Isopropyl- $\beta$ -D-thiogalactopyranoside. Created with BioRender.com

To gain process knowledge and develop more efficient and sustainable bioprocesses for the production of recombinant proteins with *E. coli*, the following **five scientific questions** were examined.

1. Can a *phoA*-based expression system increase the soluble expression of a Fab in the *E. coli* periplasm compared to a pET-based expression?

The production of functional Fabs in *E. coli* requires oxidizing conditions for the formation of disulfide bridges, however, strong induction systems, like the T7-based pET expression system, often lead to inclusion body (IB) formation. Thus, we compared the expression to the phosphate ( $\text{PO}_4$ )-sensitive *phoA* expression system in a W3110 strain to increase soluble Fab production in the periplasm. Furthermore, the impact of non-limiting and limiting  $\text{PO}_4$  conditions on strain physiology and productivity were explored to extend the process knowledge of this auto-inducible expression system and evaluate the potential for continuous bioprocessing.



2. To what extent can product formation be increased if a fed-batch cultivation is systematically optimized?

The identification of critical process parameters and their alteration in a multivariate data approach allowed the determination of optimal process conditions to increase the process performance of fed-batch cultivations. In addition, effects of the process conditions on the formation of IBs were studied.

3. Can economic efficiency and equipment utilization be improved in a fed-batch cultivation with *E. coli*?

To increase the economic and environmental benefit, repetitive fed-batches were studied, as less sterilization and cleaning cycles are required in this cultivation mode. The obtained STYs were compared to conventional fed-batches and chemostat cultivations.

4. How do glucose/lactose and glycerol/lactose mixed feeds influence recombinant protein expression in a continuous cultivation?

Induction with lactose increases cell viability and reduces metabolic stress. However, lactose uptake is affected by the uptake rates of the feed's primary carbon source (glucose, glycerol). Glucose is the established substrate for bioprocess with *E. coli*, whereas, in recent studies, glycerol was promising to increase the productivity in recent studies. Therefore, the influence of glucose/lactose and glycerol/lactose mixed feeds on productivity was investigated in chemostat cultivations for the strains BL21(DE3) and HMS174(DE3).

5. How can the set-up and development of a cascaded continuous cultivation be accelerated and simplified?

Spatial separation of biomass growth and protein expression stabilized recombinant protein expression. However, the influence of applied process parameters in cascaded continuous cultivations are still not investigated properly and studies are laborious. Therefore, a workflow was developed to reduce the experimental workload and speed-up the establishment of a cascaded continuous cultivation for stable long-term cultivations.

### 3. Results and Discussion

The scientific publications of this Thesis are assigned to the four investigated process modes, fed-batch (Chapter 3.1.2. and Chapter 3.1.3.), repetitive fed-batch (Chapter 3.1.4.), chemostat (Chapter 3.2.2.), and cascaded continuous cultivations (Chapter 3.2.3.). I will give a detailed background and highlight major findings of each scientific publication in the following chapters. In addition, a Review article that addresses the function of protein L as a universal binding ligand and highlights potential applications (Chapter 7.1) and a book chapter entitled "Inclusion body production in fed-batch and continuous cultivation" (Chapter 7.2.) can be found in the Appendix.

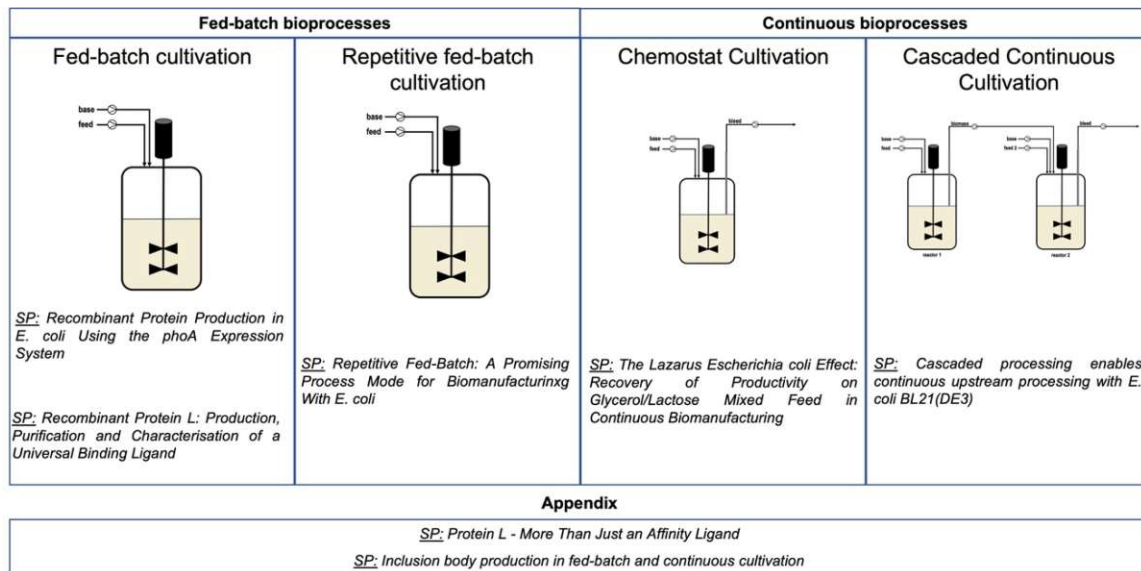


Figure 6: Structure of this PhD Thesis. SP: scientific publication. Figure adapted from [12].

### 3.1. Fed-batch Bioprocesses

#### 3.1.1. Background Information

Theodor Escherich firstly described the Gram-negative bacterium *E. coli* during the mid-1880s, investigating the human gut [51, 52]. Thenceforward, promising studies on the genome and molecular biology caused the rise of recognition, making *E. coli* one of the most important models and production hosts in academia and industry [51-53]. The K-12 and B strains and their derivatives are the most used strains for recombinant protein production [52, 54, 55]. In 1942, Delbrück and Luria first mentioned the ancestor strain B, which was then genetically modified, leading to the common laboratory strain BL21 [52]. Almost 45 years later, Studier and Moffatt introduced the strain BL21(DE3) by integrating the T7 RNA polymerase, originating from a DE3 phage [52, 56]. The integrated T7 polymerase is controlled by the lacUV5 promoter, enabling the use of a T7-based pET expression system [56-58]. The operon naturally expresses lacY ( $\beta$ -Galactosidase-Permease), lacZ ( $\beta$ -Galactosidase), and lacA ( $\beta$ -Galactosid-Transacetylase) and is negatively regulated by the LacI repressor protein. Furthermore, desirable features like low acetate formation rates, fast doubling times, and the lack of two key proteases, Lon and OmpT, cause the popularity of this strain in research and industry [4, 53, 59]. Contrary to the beforehand mentioned BL21(DE3), W3110 is related to the ancestor strain K-12, isolated from a stool sample [52, 60]. This strain is often referred to as wild-type strain and the genome was fully sequenced by Hayashi et al. in 2006 [60, 61]. K-12 strains have higher acetate production levels, leading to lower biomass yields and slower growth rates compared to B-type strains [16, 61]. Still, W3110 is a common strain applied in the biotechnology industry for the large-scale production of therapeutics [16, 62].

Nevertheless, the strain BL21(DE3) with the integrated T7 RNA polymerase caused that the pET-based expression systems are one of the most applied vectors [63, 64]. Up to now, more than 220,000 scientific publications using these expression plasmids are available [63]. The T7 RNA polymerase is under the control of the lacUV5 promoter, while the gene of interest (GoI) is cloned among the T7 promoter and terminator [53, 65-67]. The LacI repressor protein controls the promoter by negative regulation and is inactivated upon induction. Thus, recombinant protein expression starts with the supply of an inducer, which can be Isopropyl- $\beta$ -D-thiogalactopyranoside (IPTG) or the natural analogue lactose [53, 68]. Induction with IPTG is known to put high stress on the expression host and is toxic at high concentrations [18, 69]. Additionally, due to the high metabolic burden, the cell stress increases and consequently, inclusion body (IB) formation is enhanced [46, 69]. However, high expression rates are

achieved and a one-point addition in fed-batch cultivations is sufficient for the induction [70]. To decrease the metabolic burden, the transcription of recombinant proteins can be regulated by limiting the inducer supply [46]. As alternative, lactose, more specifically the formed allolactose, can be used to induce protein expression in pET-based expression systems [46, 66]. Lactose was shown to be a viable alternative to IPTG, increasing cell viability, and has a positive effect on soluble protein formation [68, 71]. In contrast to IPTG, lactose is metabolized, wherefore a continuous supply is required to keep the transcription ongoing [46, 68, 70]. However, the uptake of lactose was shown to be affected by the presence and uptake rates of the carbon source [67-70]. Carbon catabolite repression (CCR) leads to a restricted uptake, and therefore, the substrate (e.g. glucose, glycerol) needs to be fed in limiting amounts. Upon lactose presence, the lactose permease, required for the transport of lactose inside the cell, and the  $\beta$ -galactosidase, which cleaves lactose and forms allolactose, are encoded [66, 68, 71]. Nevertheless, due to the energy dependent transport, a threshold of  $q_{s, \text{glucose/glycerol}}$  is required to provide a sufficient amount of energy for lactose uptake [68, 72]. Overall, the T7 RNA polymerase displays fast transcription rates, being five times faster than native *E. coli* RNA polymerases [4, 58, 65]. However, high expression rates are challenging for the expression of proteins which need to be translocated into the periplasm or require a proper folding inside the cytoplasm. Thus, the recombinant protein expression with a strong promoter system such as the T7-based pET, exhibits a high metabolic burden onto the host cells and could lead to IB formation [71].

To circumvent the formation of IBs and promote the soluble expression of complex proteins like antibodies and fragments, slower expression rates could be beneficial [73, 74]. Especially if the target protein is secreted into the periplasm, increase high expression rates the risk of overloading transport associated proteins [75]. As an alternative, Luo et al. used the *phoA* promoter to express different Fabs. The expression is initiated as soon as the phosphate concentration is decreasing in the fermentation broth [73, 76]. Studies showed that the *phoA*-based expression system is beneficial for the expression of Fabs, especially if secretion into the periplasm is necessary [76]. Despite that, it is crucial to monitor and control the  $\text{PO}_4$  concentration at sufficient levels for high product expression, and at the same time avoid depletion as it affects the cell metabolism and ultimately results in cell lysis [77, 78].

Besides the used promoter system, also protein structure and complexity (disulfide bonds, glycosylation, etc.) cause that heterologous proteins expressed in *E. coli* are either produced in soluble form or as protein aggregates (IBs) [16, 79]. However, the expression in the cytoplasm takes place under reducing conditions, whereby no disulfide bonds are formed and proteins

accumulate as IBs [16]. In addition, high expression rates can overburden chaperones, resulting in the formation of misfolded or even unfolded heterologous proteins [79]. To circumvent the formation of IBs, different strategies are available, (i) strain engineering approaches are applied for the additional expression of foldases and chaperones, deletion of reductases, or expression of periplasmic isomerases to enable a proper folding of complex proteins [16, 80], (ii) translocation of translated proteins into the periplasm, where disulfide bonds are formed [81] and (iii) secretion of heterologous proteins [6].

The cytoplasm is the inner part of a bacterial cell and enables high production yields without the need for complex strain engineering approaches. Furthermore, it can harbour recombinant proteins accounting for up to 30% of the total protein content [6, 16]. On the downside, besides the presence of proteases, also a large amount of host cell proteins (HCPs) and DNA need to be removed during the purification of the target protein. Due to the prevailing reducing conditions and often achieved high expression rates, target proteins could accumulate as IBs. In some cases, the adaption of CPPs, like lowering the temperature during the recombinant protein expression, circumvents this problem. Approaches to improve proper folding of target proteins include media adaptations, different feeding strategies, additional overexpression of chaperones, fusion tags, or strain engineering by deleting reductases located on the *E. coli* genome [6, 82-85]. These mentioned factors are often insufficient and decrease the biomass yield or are not feasible in larger process scale [6]. Alternatively, the expression of recombinant proteins can take place in the periplasm, the space between the inner and outer cell membrane. This is especially desirable when the formation of disulfide bridges is required [6, 16]. The prevailing oxidizing conditions are caused by the Dsb protein family and enable the subsequent formation of disulfide bonds [86]. The addition of an N-terminal signal sequence to the polypeptide chain of the recombinant protein promotes the export into the periplasmic space. However, often low product yields are achieved due to the low number of available transporters which get overloaded rapidly [6, 75]. Furthermore, the periplasm only accounts for approximately 10% of the total cell volume, lowering the achievable product yields [6]. Despite that, a cell disruption process solely targeting the outer membrane could ease the purification due to a decreased amount of HCP, DNA and proteases [16, 87]. To transport the proteins from the cytoplasm into the periplasm, three pathways using the type II secretion system are existing. The secretion is conciliated by (i) the Sec pathway, one of the most applied ways for translocation, (ii) the signal recognition (SRP) pathway, or (iii) the twin-arginine translocation (TAT) pathway [16, 76, 88]. The translocation is guided by linked signal peptides located on the N-terminus of the target protein [89]. In the Sec pathway, the protein is first translated and

subsequently transported into the periplasm, while in the SRP pathway the recombinant protein is translocated during protein translation [90]. In the TAT pathway the protein is first folded in the cytoplasm and then secreted into the periplasm, being not applicable to circumvent the formation of IBs due to the reducing environment in the cytoplasm [90]. So far, the Sec-dependent signal sequences OmpA, LamB, PhoA, and STII have been successfully used for the expression and translocation of recombinant proteins [16, 86]. Furthermore, studies revealed that the used signal sequence effects severely the expression and secretion, depending on the produced protein [88, 89]. A further possibility to localize the produced recombinant proteins is the fermentation broth. Besides the advantages of periplasmic expression, the secretion into the fermentation broth displays advantages in the subsequent downstream processing (DSP) [91, 92]. Cell disruption is not required and the product can be easily separated from the cells by centrifugation and/or filtration. This decreases the number of required purification steps since already a high purity is obtained in the supernatant. Studies showed that different media supplements, such as glycine or Triton, influence the cell membrane integrity [16, 86, 93]. Additionally, CPPs showed to be important not only in the total process performance but also in cell integrity [94-96]. Overall, protein secretion into the fermentation broth is a promising approach which can be applied in continuous bioprocessing and would decrease the costs of the DSP [91, 93, 94].

### 3.1.2. Scientific Publication 1

Can a *phoA*-based expression system increase the soluble expression of a Fab in the *E. coli* periplasm compared to a pET-based expression?

Title: Recombinant Protein Production in *E. coli* Using the *phoA* Expression System

For the soluble production of Fabs in *E. coli* oxidizing conditions are required to facilitate the formation of disulfide bridges. One common approach is the secretion into the periplasmic space via N-terminal signal sequences (e.g. STII, PhoA, OmpA) [16, 86, 97]. However, low expression yields of soluble protein are observed often due to IB formation, protein degradation or insufficient translocation [6, 75]. Strong expression systems with high transcription rates, like the inducible T7-based pET vector (pET system), impose a metabolic burden onto host cells and cause an overload of transport associated proteins, resulting in IB formation [46, 98, 99]. Even though the T7 system is still widely applied in academia and industry, softer induction systems, like the phosphate (PO<sub>4</sub>)-sensitive *phoA* expression system (pAT system), are preferably to increase the soluble protein formation of Fabs [76]. Furthermore, due to the periplasmic expression only the outer cell membrane needs to be disrupted, which would reduce the impurity levels in the supernatant during the purification [100]. Thus, approaches to increase the leakiness of the cell membrane during the cultivation have been investigated since this would enable a “direct” harvest of the target product in continuous bioprocessing [94, 100]. Furthermore, the use of the auto-inducible pAT system enables not only to avoid the addition of inducers, but also the direct control of expression levels in continuous cultivations via adjusted PO<sub>4</sub> concentration in the feed [78, 101]. Therefore, we compared the production of a Fab in *E. coli* using the pET system in a BL21(DE3) strain and the pAT system in a W3110 strain under the same cultivation conditions (T = 30 °C and 35 °C;  $\mu = 0.05 \text{ h}^{-1}$  and  $0.1 \text{ h}^{-1}$ ). Furthermore, we investigated the PO<sub>4</sub> dependent protein expression and its effect on strain physiology.

In all pET cultivations the expressed Fab mainly accumulated as IB, independent from the applied process parameters. Still, IB formation was enhanced at 35 °C compared to 30 °C and an elongated induction time resulted in lower soluble protein levels. The highest soluble Fab concentration was achieved 4 h post induction at 30 °C and a  $\mu = 0.1 \text{ h}^{-1}$ . In the cultivations with the pAT system, protein expression was initiated already before limiting PO<sub>4</sub> conditions were reached (>0.1 mM), indicating a leaky promoter repression. Although IB formation was observed at  $\mu = 0.05 \text{ h}^{-1}$ , indicating a high metabolic stress, the highest soluble Fab titer was reached with this growth rate at 30 °C. Since the cultivation end was determined by PO<sub>4</sub>

starvation, the cultivation time was significantly longer at lower growth rates. In addition, a higher biomass concentration (DCW) was reached using the pAT system, even increasing under  $\text{PO}_4$  limiting conditions. This indicates a metabolic shift from extracellular uptake towards utilization of intracellular stored  $\text{PO}_4$  [102, 103]. This hypothesis was supported by declining intracellular P levels, already starting at non-limiting  $\text{PO}_4$  concentrations in the fermentation broth. Overall, IB formation was depending on the used induction system as well as the applied cultivation conditions. The highest STY in a pAT cultivation ( $T = 30\text{ }^\circ\text{C}$ ;  $\mu = 0.05\text{ h}^{-1}$ ) was 1.3-fold higher compared to the best performing pET cultivation ( $T = 30\text{ }^\circ\text{C}$   $\mu = 0.1\text{ h}^{-1}$ , 4 h induction), even though the cultivation time was almost twice as long (Figure 7).

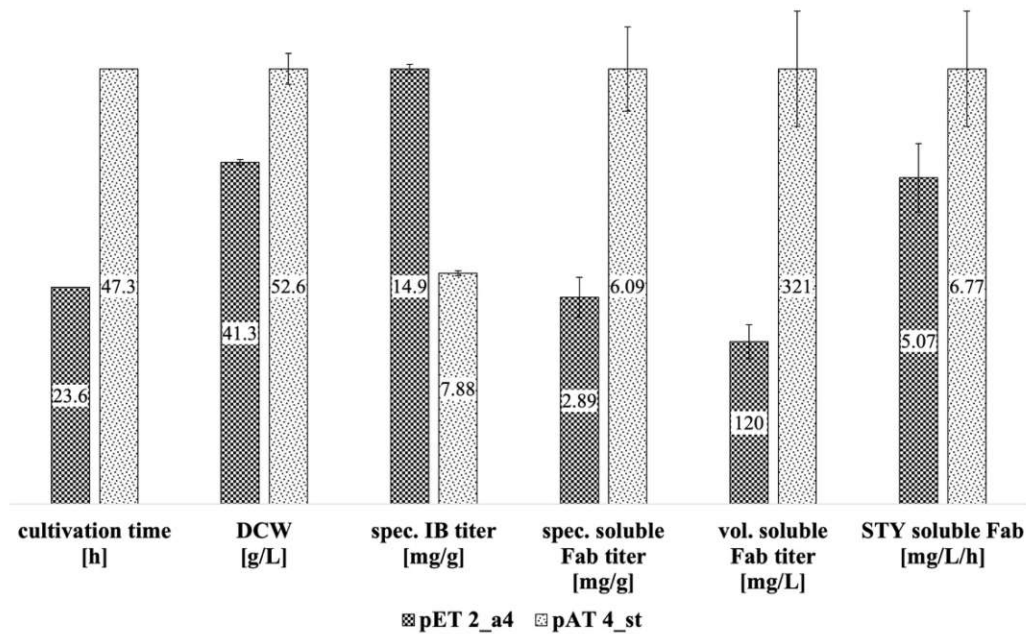


Figure 7: Comparison of the best performing cultivation with the T7-based pET expression system (pET 2\_a4) and the *phoA* expression system (pAT 4\_st). The pET system gave the highest space-time yield (STY) at a  $\mu = 0.1\text{ h}^{-1}$  and  $30\text{ }^\circ\text{C}$  after 4 h of induction. The pAT system performed best at  $\mu = 0.05\text{ h}^{-1}$  and  $30\text{ }^\circ\text{C}$  at  $\text{PO}_4$  starvation.

However, at  $\text{PO}_4$  starvation ( $<0.1\text{ mM}$ ) the cell metabolism started to collapse, and hence potential product is lost due to cell lysis. These results underline the importance of identifying the optimal point of harvest and the necessity of a reliable process control with a time-resolved monitoring of  $\text{PO}_4$ .

In summary, we studied the potential of the pAT system for the soluble periplasmic expression of Fabs and characterized the effects of the  $\text{PO}_4$  depletion, paving the way for further process engineering approaches. Based on the results, we suggest to perform a fed-batch until a concentration close to  $0.1\text{ mM}$  is reached in the reactor. Subsequently, a feed medium with an adjusted  $\text{PO}_4$  concentration should be used to extend the cultivation at this concentration and thus obtain an improved STY.



Authors: Stefan Kittler\*, Thomas Gundinger\*, Sabine Kubicek, Julian Kopp and Oliver Spadiut

\*Authors contributed equally to this work.

Published: *Fermentation*. 2022; 8(4):181. <https://doi.org/10.3390/fermentation8040181>  
IF: 5.123 (2021)

Contribution: This is a shared first authorship with Thomas Gundinger. The study was planned together with Thomas Gundinger and Oliver Spadiut. The experiments and data analysis were performed with Thomas Gundinger and Sabine Kubicek. Julian Kopp and Oliver Spadiut supervised the experiments and reviewed the manuscript. All authors contributed to the article and approved the submitted version.

### 3.1.3. Scientific Publication 2

To what extent can product formation be increased if a fed-batch cultivation is systematically optimized?

Title: Recombinant Protein L: Production, Purification and Characterization of a Universal Binding Ligand

Design of experiments (DoE) enable a structured identification of important process parameters which influence the process performance [101, 104, 105]. Due to the simultaneous alteration of investigated factors, it is also possible to observe interactions, while the experimental workload can be reduced [101, 105]. In previous studies, specific substrate uptake rate ( $q_s$ ) and temperature were identified to affect expression state (soluble and IB) as well as product titer for various proteins [106-109]. Therefore, a DoE approach was used to alter these two process parameters with the aim to increase the soluble protein L production. To adequately describe potential quadratic interactions of the tested parameters, a central composite circumscribed design was applied.

An excess of soluble protein L was obtained for all tested cultivations while the IB titer did not exceed 5% of the final concentration. We hypothesize that the expression state of PpL was not majorly affected by  $q_s$  and induction temperature due to the low complexity of the protein (no disulfide bridges or other posttranslational modifications) [74]. However, the product titer was affected by the tested parameters, as depicted in Figure 8. The specific substrate uptake rate of 0.5 g/g/h led to an increase of the volumetric product titer until 4 to 6 h of induction, depending on the applied temperature (Figure 8). Afterwards the product concentration decreased, accompanied by a stop of biomass growth and subsequent accumulation of glycerol. Specific substrate uptake rates of 0.1 g/g/h and 0.3 g/g/h at lower temperatures ( $\leq 27$  °C) resulted in comparable amounts of PpL after 12 h of induction. The tested temperatures above 31 °C did not lead to an increased product formation. Furthermore, it was observed that the optimal point of harvest (highest product concentration) depended on the used cultivation condition. However, the highest volumetric product titer was reached after 12 h induction time using the center point conditions ( $q_s = 0.3$  g/g/h, temperature 31 °C) (Figure 8).

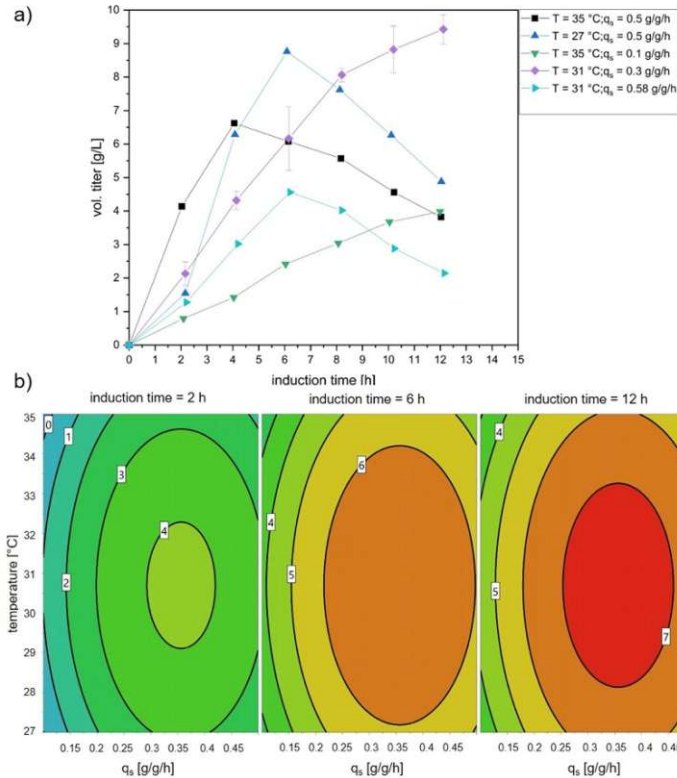


Figure 8: a): Trend of volumetric titer [g/L] of the performed fed-batches during of 12 h induction. b): Contour plot of the volumetric titer [g/L]. The highest titer of about 9 g/L was reached after 12 h using a specific substrate uptake rate ( $q_s$ ) = 0.3 g/g/h and a temperature of 31 °C.

Longer induction times as well as higher specific substrate uptake rates had a positive influence on productivity, whereas the temperature did not affect the volumetric titer significantly. However, too high  $q_s$  and temperature would not increase the product formation (quadratic terms of all tested parameters had a negative impact on the volumetric titer). Furthermore, the interaction terms of the tested parameters had no significant effect on product formation.

In summary, a multivariate data approach was applied and process conditions, leading to the highest product titer were identified (Table 1). The product concentration was increased by more than 400% (at harvest), resulting in a specific product titer of 0.17 g/g with a final biomass concentration of 55 g DCW/L.

Table 1: Summary of the process conditions leading to the highest volumetric product titer.  $q_s$ : specific substrate uptake rate

Factors	Condition	Titer
$q_s$	0.3 g/g/h	
Temperature	31 °C	9.4 ± 0.4 g/L
Induction time	12 h	

Authors: Stefan Kittler\*, Julian Ebner\*, Mihail Besleaga, Johan Larsbrink, Barbara Darnhofer, Ruth Birner-Gruenberger, Silvia Schobesberger, Christopher K. Akhgar, Andreas Schwaighofer, Bernhard Lendl and Oliver Spadiut

\*Authors contributed equally to this work.

Published: *Journal of Biotechnology*. 2022. **359:** p. 108-115.  
<https://doi.org/10.1016/j.jbiotec.2022.10.002>  
IF: 3.595 (2021)

Contribution: This is a shared first authorship with Julian Ebner. I planned with Julian Ebner and Oliver Spadiut the experiments. The USP was performed together with Mihail Besleaga, while Julian Ebner performed the DSP. Mass spectrometry was measured by Barbara Darnhofer and Ruth Birner-Gruenberger. Silvia Schobesberger provided a protocol and helped with the development of the conjugation and ELISA. Christopher K. Akhgar, Andreas Schwaighofer and Bernhard Lendl performed infrared spectroscopy measurements, interpreted the respective data, and wrote their part of the manuscript. Johan Larsbrink performed the structure prediction and performed the respective interpretation. I, Julian Ebner, and Oliver Spadiut wrote the manuscript. All authors approved the submitted version of the manuscript.

### 3.1.4. Scientific Publication 3

#### Can economic efficiency and equipment utilization be improved in a fed-batch cultivation with *E. coli*?

Title: Repetitive Fed-Batch: A Promising Process Mode for Biomanufacturing With *E. coli*

In fed-batches, set-up, sterilization and cleaning of equipment are cost- and time-intensive, thus reducing the productivity of a process (lower STY) [25]. However, more production cycles or longer induction times within one cultivation could improve the process performance, leading to a more economically and environmentally favourable process due to a reduced number of required sterilization and cleaning phases (Figure 9). Therefore, we compared fed-batches, repetitive fed-batches, and chemostat cultivation for two proteins, one expressed in the cytoplasm and one in the periplasm, in terms of product yield and STY.

Cultivation mode	$t_{\text{down}}$	$t_{\text{prod.}}$	Total product
Fed-batch	65.7%	34.3%	$P_{\text{conv.FB}} = V_{\text{Harvest}} * c_{\text{P Harvest}}$
Repetitive fed-batch (2 cycles)	48.9%	51.1%	$P_{\text{RFB 2 phase}} = ((V_{\text{H1}} - \frac{V_{\text{Batch}}}{2}) * c_{\text{PH1}}) + (V_{\text{H2}} * c_{\text{PH2}})$
Repetitive fed-batch (3 cycles)	39.0%	61.0%	$P_{\text{RFB 3 phase}} = ((V_{\text{H1}} - \frac{V_{\text{Batch}}}{2}) * c_{\text{PH1}}) + ((V_{\text{H2}} - \frac{V_{\text{Batch}}}{2}) * c_{\text{PH2}}) + (V_{\text{H3}} * c_{\text{PH3}})$
Chemostat	14.3%	85.7%	$P_{\text{Chemostat}} = \sum (V_{\text{Bleed}} * c_{\text{P Bleed}})$

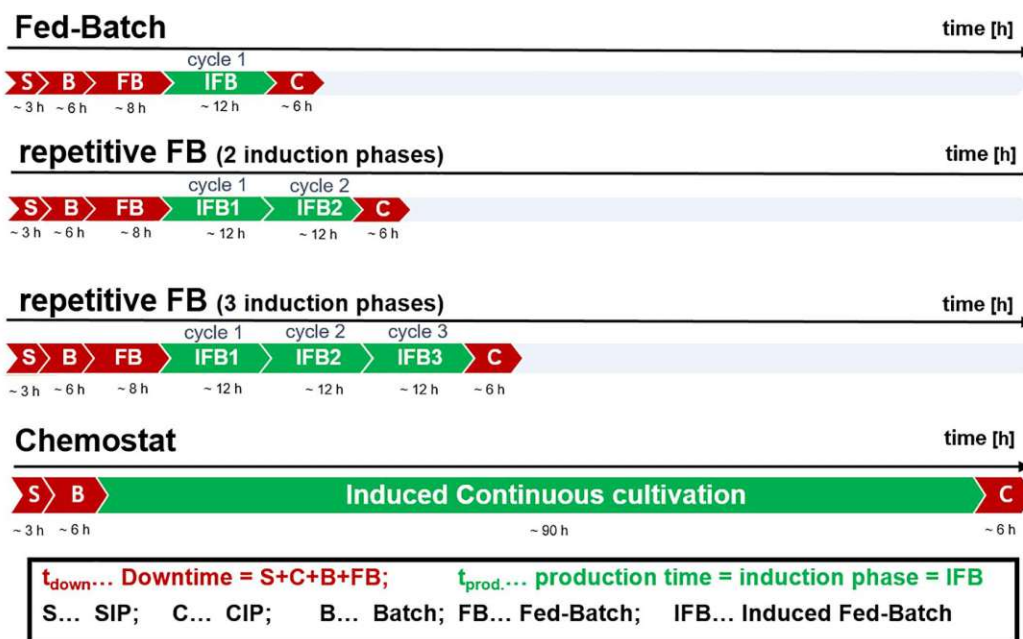


Figure 9: Comparison of the cultivation modes tested within this study. The production time ( $t_{\text{prod.}}$ ) and downtime ( $t_{\text{down}}$ ) is given in percent relative to the total process time. Time for SIP: 3 h; Time for CIP: 6 h (reference values, obtained by the industrial partner); SIP: steam in place; CIP: cleaning in place

First, a fed-batch with an induction time of 12 h was performed (cycle 1), subsequently half of the volume was harvested, and the fermentation broth was diluted with twofold concentrated medium to the starting biomass concentration (end fed-batch). The induced fed-batch was repeated for 12 h (cycle 2). After that, half of the fermentation broth was harvested again. Analogous to the second cycle, a third repeat was performed, resulting in three induction phases of 12 h each. The product amount after each cycle was calculated according to the equations in Figure 9. Since we aimed to increase the process performance (product yield, STY) and develop a more economic and sustainable process, we additionally performed chemostat cultivations for each protein. In theory, chemostat cultivations lead to time-independent productivities in which continuously target protein is harvested resulting in increased STYs [110]. However, the productivity in chemostat cultivation declined for both proteins with the cultivation time, thus being not competitive to the other tested process modes. The repetitive fed-batches led to an increase of the STY for each tested target protein, but the optimal number of cycles differed for the cytoplasmic and the periplasmic protein (Figure 10). For the cytoplasmic protein, the specific productivity ( $q_p$ ) declined with each cycle, but the highest STY was still obtained after two cycles. A different behaviour was observed for the periplasmic protein, the specific productivity was lower throughout the whole process. Additionally, the specific productivity more than doubled from the first to the second cycle, while it slightly decreased in the third cycle, but still, the highest STY was reached after the third production cycle. Moreover, cell leakiness was observed causing an increase of target protein in the fermentation broth with each performed cycle. Since the chemostat cultivation was not competitive under the tested conditions for both proteins, the STY assuming constant productivity at the highest observed  $q_p$  was simulated (ideal chemostat) (Figure 10). Nevertheless, the STY of the chemostat was below the other performed cultivations.

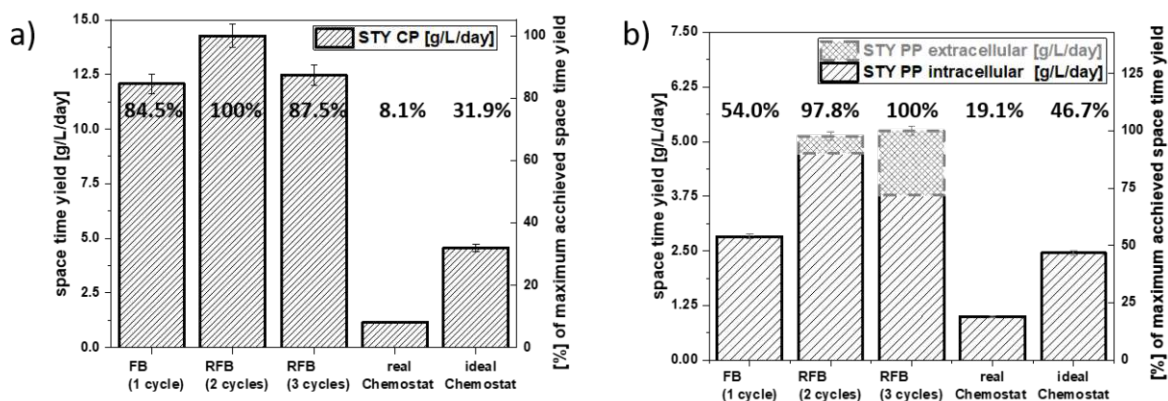


Figure 10: Comparison of the space-time yield (STY) of each process mode for a) cytoplasmic protein and b) periplasmic protein. The values in %, are the relative values referred to the highest obtained STY. The ideal chemostat was simulated, using the highest reached specific productivity, assuming a stable productivity at this level throughout the whole cultivation.

In summary, we showed that repetitive fed-batches are a viable alternative to achieve higher STYs compared to established fed-batches with one induction phase. At the same time, less sterilization and cleaning cycles are required due to repeated production phases. Although the volumetric throughput could be increased, we observed that the specific productivities declined indicating metabolic changes of the cells.

Authors: Stefan Kittler\*, Julian Kopp\*, Christoph Slouka, Christoph Herwig, Oliver Spadiut and David J. Wurm

\*Authors contributed equally to this work.

Published: *Frontiers in Bioengineering and Biotechnology*. 2020 Sec. Bioprocess Engineering; 8: p. 1312. <https://doi.org/10.3389/fbioe.2020.573607>

IF: 6.064 (2022)

Contribution: This is a shared first authorship with Julian Kopp. Julian Kopp planned the experimental design and carried out the data treatment. I performed the cultivations, analytics, and data analysis. Christoph Slouka, Christoph Herwig, and Oliver Spadiut gave major scientific input. David Wurm founded the idea of this study. Julian Kopp and David Wurm wrote the manuscript. Oliver Spadiut reviewed the manuscript. All authors contributed to the article and approved the submitted version.

## 3.2. Continuous Bioprocesses

### 3.2.1. Background Information

Glucose is the preferred carbon source of *E. coli* for metabolization since it leads to the highest growth rates ( $\mu$ ) and has been established as standard substrate, especially in the pharmaceutical biotechnology sector [72, 111]. For various carbon sources, uptake and phosphorylation are catalysed by the phosphoenolpyruvate (PEP) : carbohydrate transferase system (PTS) [112]. Glucose is transported, phosphorylated, and then introduced into glycolysis, leading to the formation of two PEP molecules. In detail, the phosphoryl group is transferred from PEP to EI and then via Histidine protein (HPr) to EIIA<sup>Glc</sup> and EIIB. Finally, glucose is transported by EIIC and phosphorylated during the transport to be further metabolized [113]. After glycolysis, one PEP is processed in the tricarboxylic acid cycle (TCA) while the second molecule takes part in the phosphorylation-transport process of the fed carbohydrate (Figure 11) [72, 114-116].

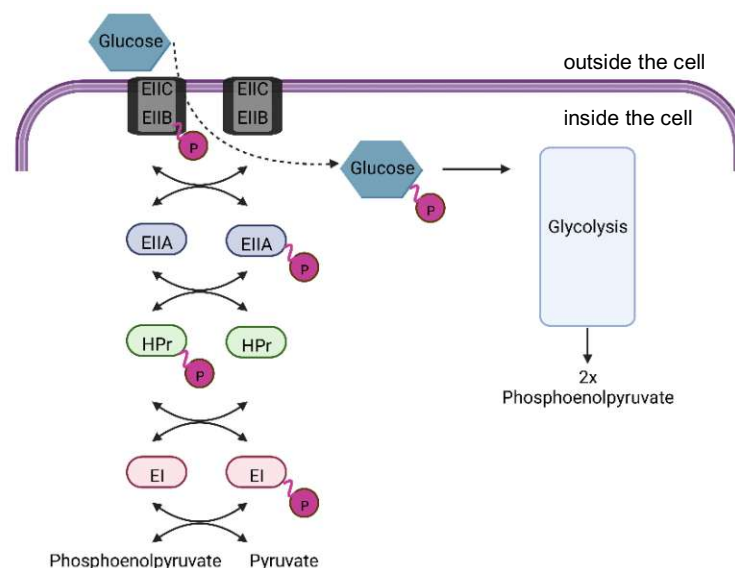


Figure 11: Transport of carbohydrates by the phosphoenolpyruvate (PEP) : carbohydrate transferase system (PTS). The PTS carbohydrate (e.g. glucose) gets transported by EIIC, concomitantly phosphorylated by EIIB, and is then introduced into glycolysis. One of the standardly formed PEP is used for the PTS. Adapted from [114]. Created with BioRender.com

However, with glucose in the cultivation medium, diauxic growth is observed and causes a decrease or even repression of the uptake of other carbohydrates (e.g. lactose) [114]. The uptake is prevented by inducer exclusion and furthermore, the cAMP (cyclic AMP) synthesis is inhibited. Subsequently, CRP (cAMP receptor protein), a transcription factor regulating over 100 operons, which encode among other things proteins that are involved in utilization systems for other sugars, are not activated [114, 116-118]. In addition, the growth on glucose causes the EIIA<sup>Glc</sup> to be predominantly dephosphorylated [112, 116, 119]. Consequently, adenylate



cyclase is not activated (only activated by the phosphorylated EIIA<sup>Glc</sup>), explaining the decreased cAMP levels during the growth on glucose [115, 116, 119]. The first hypothesis was that the cAMP levels play an important role in carbon catabolite repression, leading to decreased lactose uptake rates in cultivations using glucose and lactose. However, cAMP levels in cultivations with solely lactose or glucose are on a comparable level [116, 119]. Subsequent studies showed that the ratio of PEP to pyruvate is mainly responsible for the phosphorylation state of EIIA<sup>Glc</sup> [112, 116]. This means that EIIA<sup>Glc</sup> is predominantly dephosphorylated at low concentrations of PEP compared to pyruvate and vice versa [112, 116]. Therefore, the main factor for the preferred uptake of glucose compared to lactose seems to be caused by inducer exclusion, and not the cAMP levels. While the cAMP-CRP complex is required for the transcription of the *lac* operon, cAMP levels are similar during growth on glucose or lactose [116, 119]. Additionally, the cAMP-CRP complex activates the EIIBC domain of the PTS involved in glucose uptake [116]. However, it was shown that the non-phosphorylated EIIA<sup>Glc</sup> inhibits the *lac* permease, resulting in decreased lactose uptake [112, 113, 119, 120]. These cellular effects have to be considered in pET-based expression systems when induction with lactose is performed while glucose is fed as the primary carbon source.

Alternatively, glycerol has been established as a carbon source for biotechnological processes using *E. coli*. Glycerol is known to be a by-product of the biodiesel production and is from a sustainable point of view a valuable alternative [72, 121, 122]. About 10% w/w of glycerol is produced during biodiesel production, hence, it is highly interesting for upcycling in various biotechnological sectors [123]. Glycerol is transported by diffusion into the cells, where it is subsequently phosphorylated to glycerol 3-phosphate, which can be further metabolized by the cells [113]. Glycerol 3-phosphate is metabolized to dihydroxyacetone phosphate (DHAP), which can then be introduced into glycolysis as well as gluconeogenic pathways (Figure 12) [121].

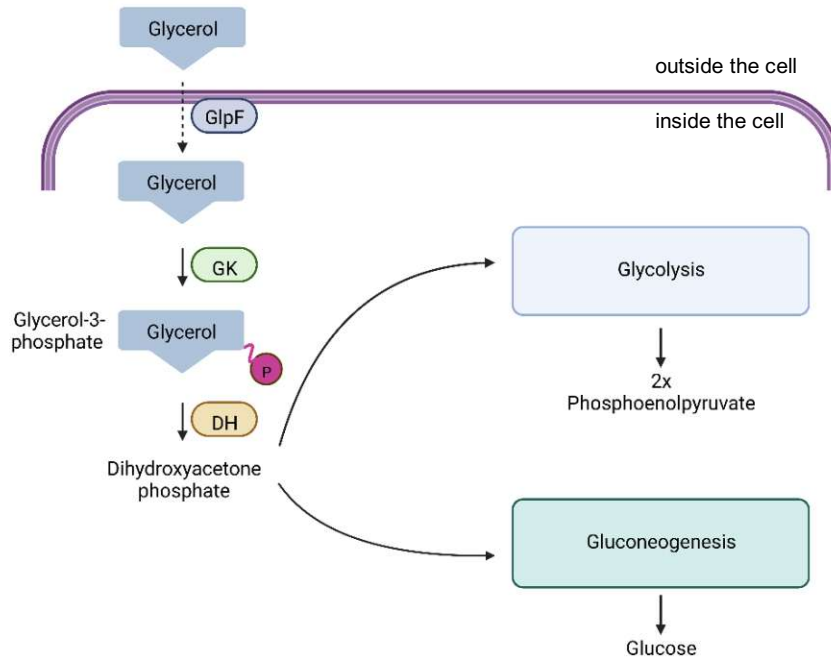


Figure 12: Metabolism of glycerol by *Escherichia coli*. GlpF: glycerol facilitator; GK: glycerol kinase; DH: dehydrogenase. Adapted from [124]. Created with BioRender.com

Biomass yields of glycerol and glucose fed cultivations are comparable since glycerol is utilized efficiently by *E. coli* [72, 121]. Kopp et al. showed that for both carbon sources (glucose and glycerol) lactose uptake rates are depending on the applied feeding rates (specific glucose uptake rates) of the primary carbon source [68, 72]. Glycerol is already established in autoinduction media when cells are grown on a mixture of glucose, glycerol, and lactose [125, 126]. First, due to diauxic growth, glucose is metabolized by the cells and after depletion, induction via the supplied lactose takes place and at the same time glycerol supports growth [125, 126]. Furthermore, glycerol has proven to be a valuable alternative when fed with lactose since it increases cell viability at higher feedings rates compared to glucose fed cultivations [72].

However, galactose accumulates during induction with lactose when the commonly applied strain BL21(DE3) is used, independently of the used carbon source. The strain has deletions of important genes expressing enzymes (galactokinase, galactose-1-phosphate uridylyltransferase and UDP-glucose 4-epimerase) that are involved in the pathway for metabolization of galactose, which is formed during induction with lactose [4]. Alternatively, the strain HMS174(DE3) which originates from the K-12 line, can be cultivated and induced with lactose [4]. The strain has no deletion of important genes involved in the metabolization pathway of galactose [4]. Additionally, this strain harbours genes of the  $\lambda$  prophage, enabling the use of pET-based expression vectors [4].

### 3.2.2. Scientific Publication 4

#### How do glucose/lactose and glycerol/lactose mixed feeds influence recombinant protein expression in a continuous cultivation?

Title: The Lazarus *Escherichia coli* Effect: Recovery of Productivity on Glycerol/Lactose Mixed Feed in Continuous Biomanufacturing

Fed-batch cultivations in industry are linked to large vessel sizes and a high carbon footprint due to high energy and water consumption [30, 31]. The application of continuous cultivations would change facility design since reduced equipment sizes with significantly less working volume can be used [32, 33, 45]. Furthermore, small reactor sizes lead to lower CO<sub>2</sub> emission and less water consumption [32, 127]. However, chemostat cultivations with *E. coli* suffer from declining productivities over time, thus being not competitive for recombinant protein expression compared to other process modes so far [32]. The occurrence of non-producing subpopulations cause that advantages of continuous processing are negligible [47, 48, 128]. Indeed, first improvements to reduce the metabolic stress during recombinant protein expression have been made by switching the inducer from IPTG to lactose. However, lactose uptake depends on the specific uptake rate of the used substrate (glucose or glycerol) [68, 72, 129]. Glucose is established as substrate due to high achievable growth rates, however, glycerol was shown to be a promising alternative in terms of biomass yield and productivity [72, 125]. Therefore, mixed feed approaches of glucose/lactose and glycerol/lactose were studied in chemostat cultivations to boost the STY compared to fed-batches. In addition, the strain HMS174(DE3) was compared with the strain BL21(DE3) to investigate potential influence of galactose during the induction with lactose.

In all chemostat cultivations using BL21(DE3) with glycerol/lactose, the product titer initially decreased, but then a resurgence of the productivity was observed when process duration exceeded 100 hours. The glucose/lactose mixed feed resulted in higher productivities at the beginning of the chemostat cultivation, however, no recovery of the product formation was observed. In contrast, neither with glucose/lactose nor with glycerol/lactose a recovery of the productivity was observed for the strain HMS174(DE3). To sum up, no stable chemostat cultivation for the tested proteins was achieved, independent of the used substrate. Furthermore, the obtained STYs were below the ones of the corresponding fed-batches, thus showing that chemostat cultivations are not competitive so far (Table 2).

Table 2: Average space-time yields (STYs) of the fed-batch cultivations in comparison to the STYs of chemostat cultivation in this study. The cultivation time of chemostat cultivations was calculated to reach the performance of the fed-batch cultivation after 10 h of induction for BL21(DE3). IPTG: Isopropyl- $\beta$ -D-thiogalactopyranoside; FB: fed-batch

	Glucose-IPTG FB STY [g/L/h]	Glycerol/lactose chemostat STY [g/L/h]	Cultivation time to reach FB productivity [h]
GFP	1.28	0.02	581
mCherry	0.87	0.05	167
BBlue	0.56	0.02	215

In summary, we discovered a reproducible reoccurrence of productivity in chemostat cultivations when glycerol/lactose was fed. Hence, the fed primary carbon source (glucose/glycerol) seems to be an important factor to establish continuous cultivations. Furthermore, the declines of productivity were accompanied by changes of the galactose levels. Further investigations might help to understand, the Lazarus effect during the cultivation with glycerol/lactose and the decrease of productivity, along with the occurrence of subpopulations. We believe that transcriptomic and proteomic analyses give a deeper insight and enable a better understanding of observed behaviours during chemostat cultivations.

Authors: Stefan Kittler\*, Julian Kopp\*, Patrick Gwen Veelenturf, Oliver Spadiut, Frank Delvigne, Christoph Herwig and Christoph Slouka

\*Authors contributed equally to this work.

Published: *Frontiers in Bioengineering and Biotechnology*. 2020 Sec. Bioprocess Engineering; 8: p. 993. <https://doi.org/10.3389/fbioe.2020.00993>  
IF: 6.064 (2022)

Contribution: This is a shared first authorship with Julian Kopp. I, Julian Kopp, Patrick Veelenturf, and Christoph Slouka performed the bioreactor cultivations. I, Julian Kopp, and Christoph Slouka evaluated the data. Christoph Herwig, Oliver Spadiut and Christoph Slouka supervised the work. Christoph Herwig and Frank Delvigne gave valuable input for the manuscript. Oliver Spadiut and Christoph Slouka drafted the manuscript. All authors contributed to the article and approved the submitted version.

### 3.2.3. Scientific Publication 5

#### How can the set-up and development of a cascade continuous cultivation be accelerated and simplified?

Title: Cascaded processing enables continuous upstream processing with *E. coli* BL21(DE3)

Continuous cultivations with microbials suffer from a time-dependent decline of productivity, independent of the used inducer or substrate [18]. Indeed, glycerol promotes protein expression and cell viability compared to glucose during induction with lactose [72]. Still, chemostat cultivations have the drawback that recombinant protein expression and biomass growth occur simultaneously, thus, growth inhibition and genetic instabilities are observed [35]. Therefore, biomass and product formation are timely separated in fed-batch cultivations. This knowledge was used for cascaded continuous cultivations in which biomass growth and recombinant protein expression are spatially separated, enabling that each reactor can be operated at optimal conditions (e.g. biomass growth: 37 °C; protein expression: 30 °C). Previous studies have shown that cascaded continuous cultivation resulted in higher STYs compared to fed-batches [18, 35]. However, long term results (>100 h) and effects of process parameters, such as dilution rate and feed ratio (glycerol to lactose concentration), are not well investigated. Therefore, an established model protein (N-Pro) was used to develop a workflow that accelerates the establishment of a cascaded continuous cultivation.

First, the feed ratio (glycerol to lactose) was fixed with a ratio of 2:1 and only biomass and induction feeding (feed 2 in Figure 3) rate was varied in reactor 2. However, to avoid the accumulation of sugar in the reactor, higher induction feed fluxes than 30% of the total volumetric stream were not tested. Highest productivities were obtained for a biomass flux of 70% and an induction feed flux of 30% (of the total volume stream entering reactor 2). Subsequently, these parameters were fixed while the dilution rate and the feed ratio in the induction feed were varied in a DoE approach. Highest specific productivities ( $q_p$ ) and STY were obtained by applying dilution rates higher than  $0.15 \text{ h}^{-1}$  and using a higher concentration of glycerol than lactose in the induction feed (ratio >2). Based on these results, we reduced the design space and suggest an additional initial screening to investigate physiological parameters of unknown strains and products (Figure 13). Therefore, the proposed workflow contains two phases: In phase I, strain physiological parameters, like maximum growth rate and inducer uptake rates at different substrate uptake rates, are screened. In phase II, the results of phase I are combined with the constricted design space to find optimal cultivation conditions for cascaded continuous processing.

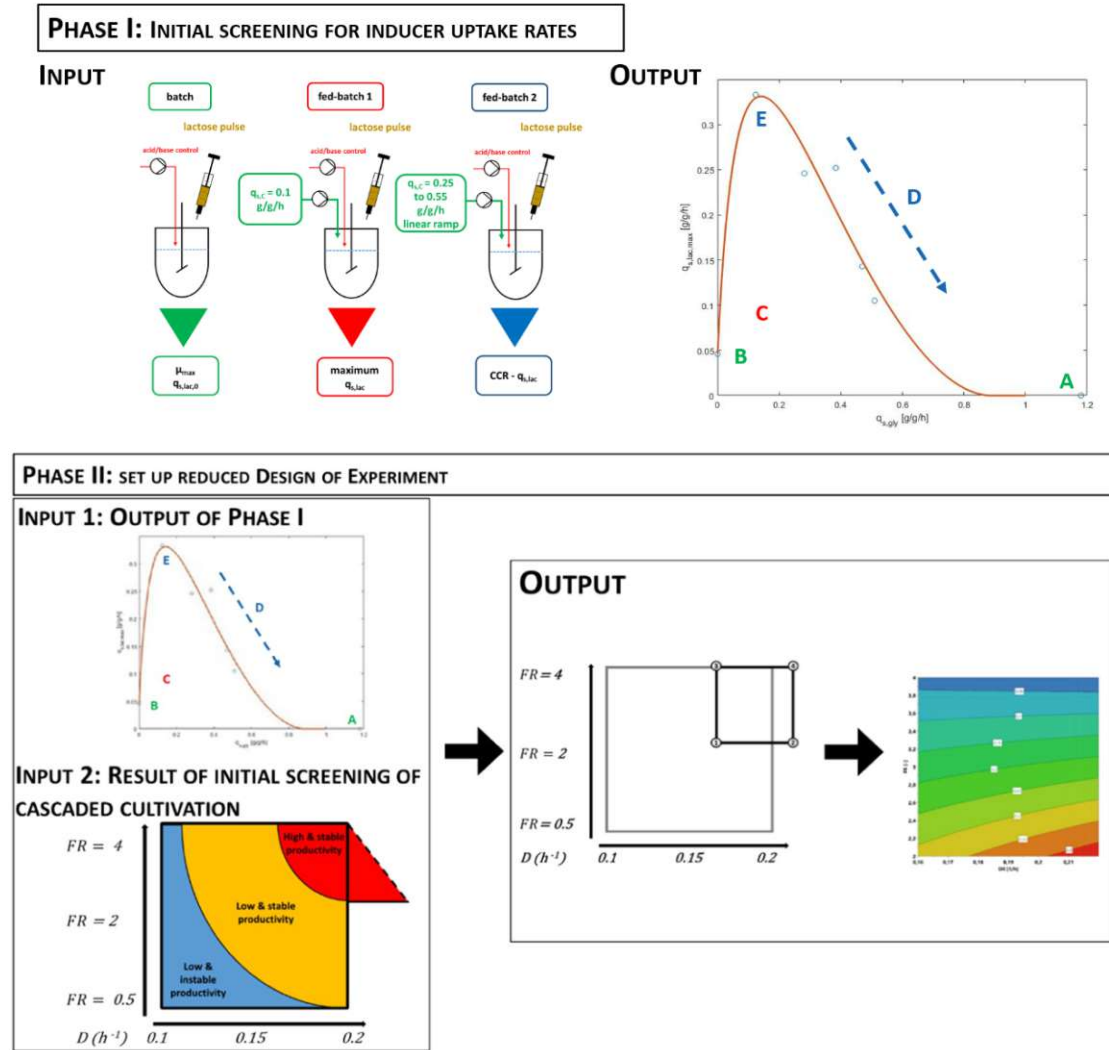


Figure 13: Proposed workflow to accelerate the establishment of a cascaded continuous cultivation. In phase I three experiments are required: (1) a batch cultivation for maximum growth rate (A) and inducer uptake without C-source (B), (2) a fed-batch cultivation for the maximum inducer uptake rate (C) and (3) a fed-batch cultivation for inducer uptake rates between a  $q_{s,glc}$  set point from 0.25 to 0.55 g/g/h using a linear ramp approach to screen for carbon catabolite repression (CCR). These results are used to determine applicable feed ratios (FR) of glycerol to lactose in the induction feed. In combination with the the constricted design space in phase II the process to find optimal process conditions is accelerated. FR feed ratio, D dilution rate.

To validate the workflow, we used an BL21(DE3) strain expressing mCherry. First, we conducted the proposed screening to determine specific inducer and substrate uptake rates (phase I). These results in combination with the reduced design space were then used to find suitable process conditions for a high STY and  $q_p$ . Finally, we were able to identify the best process performance (highest STY and  $q_p$ ) ( $D=0.22$  h<sup>-1</sup>,  $FR=2$ ) with the proposed workflow within one month. For both tested proteins (N-pro and mCherry) similar process parameters led to stable long-term productivities, even though one was expressed as IB (N-Pro) and one as soluble protein (mCherry). High dilution rates were beneficial to increase the product formation, which might be caused by a decreased risk of subpopulation formation due to shorter residence times ( $1/D$ ). Furthermore, higher dilution rates increase the bleed volume and thus leading to higher STYs.

In summary, the proposed workflow enabled to implement a cascaded continuous cultivation, which was superior to fed-batch cultivations regarding the STY. In addition, we showed that the spatial separation of biomass growth and protein expression allows stable continuous cultivations for up to 200 h of process time.

Authors: Stefan Kittler, Christoph Slouka, Andreas Pell, Roman Lamplot, Mihail Besleaga, Sarah Ablasser, Christoph Herwig, Oliver Spadiut and Julian Kopp

Published: *Scientific Reports* 11, 11477 (2021). <https://doi.org/10.1038/s41598-021-90899-9>  
IF: 4.996 (2022)

Contribution: I, Christoph Slouka and Julian Kopp planned the experimental design and carried out the data treatment. I, Andreas Pell, Roman Lamplot, Mihail Besleaga, and Sarah Ablasser performed the cultivations and analytics. Christoph Slouka., Christoph Herwig and Oliver Spadiut gave major scientific input. Julian Kopp founded the idea of this study. I, Oliver Spadiut and Julian Kopp wrote the manuscript. Oliver Spadiut critically reviewed the manuscript. All authors contributed to the article and approved the submitted version.

## 4. Conclusion and Outlook

**Fed-batch cultivations** are the gold standard in academia and industry to produce recombinant proteins, because high product titers are reached in short cultivation times and the process mode is operationally simple [7, 9]. One of the most established expression systems is the T7-based pET system, which leads to fast transcription rates [63, 64]. However, the application of an inducer is required, influencing process design and production costs which can be avoided by using an auto-inducible promoter, like the pAT system [78, 101]. In our study, process conditions leading to an enhanced soluble expression of a Fab in the periplasm were identified and PO<sub>4</sub> dependent product formation was extensively investigated. Based on these results, we propose an approach that intensifies the production process with this expression system by adjusting the PO<sub>4</sub> concentration in the feed medium. Moreover, a DoE approach was used to systematically optimize the recombinant protein expression in fed-batch cultivations, identifying  $q_s$  and temperature as critical process parameters. Using the best performing process parameters, we were able to achieve a fourfold improvement of the final product concentration.

**Repetitive fed-batches** have been applied to reduce the downtimes, leading to increased STYs. However, the specific productivity was declining and fed-batches are associated with high energy consumption, CO<sub>2</sub> emission and water usage [30, 31].

Therefore, **continuous cultivations** with *E. coli* were investigated, which would bring economic and environmental benefits. However, chemostats suffer from a declining productivity, thus, the effect of mixed feeds was studied. A resurgence of the productivity was observed for glycerol/lactose fed cultivations, but still the STYs were below fed-batches. Finally, a workflow for the implementation of **cascaded continuous cultivations** was developed and led to stable product expression levels over cultivation times of more than 220 h. This resulted in improved STYs compared to fed-batch cultivations, hence showing the potential for continuous biomanufacturing with *E. coli* BL21(DE3).

In summary, different process parameters in various bioprocess modes with the expression host *E. coli* were investigated to switch from established fed-batches towards continuous manufacturing. However, studies on the observed instabilities in recombinant protein expression need to be deepened, focusing on transcriptomic and metabolomic changes. These studies could give further insights into subpopulation formation to adapt strains, expression systems, process parameters and cultivation strategies with the aim to achieve stable long-term



cultivations. This will facilitate the development of more sustainable bioprocesses for the production of recombinant proteins.

## 5. References

1. Ferrer-Miralles, N., et al., *Microbial factories for recombinant pharmaceuticals*. Microbial Cell Factories, 2009. **8**(1): p. 17.
2. *Human insulin receives FDA approval*. (0361-4344 (Print)).
3. Mohammed, N.B., et al., *Production of Biopharmaceuticals in E. coli: Current Scenario and Future Perspectives*. Journal of Microbiology and Biotechnology, 2015. **25**(7): p. 953-962.
4. Hausjell, J., et al., *E. coli HMS174(DE3) is a sustainable alternative to BL21(DE3)*. Microb Cell Fact, 2018. **17**(1): p. 169.
5. Berkmen, M., *Production of disulfide-bonded proteins in Escherichia coli*. Protein Expression and Purification, 2012. **82**(1): p. 240-251.
6. Gaćiarz, A., et al., *Efficient soluble expression of disulfide bonded proteins in the cytoplasm of Escherichia coli in fed-batch fermentations on chemically defined minimal media*. Microbial Cell Factories, 2017. **16**(1): p. 108.
7. Lindskog, E.K., *Chapter 31 - The Upstream Process: Principal Modes of Operation*, in *Biopharmaceutical Processing*, G. Jagschies, et al., Editors. 2018, Elsevier. p. 625-635.
8. Cardoso, V.M., et al., *Cost analysis based on bioreactor cultivation conditions: Production of a soluble recombinant protein using Escherichia coli BL21(DE3)*. Biotechnology Reports, 2020. **26**: p. e00441.
9. Chen, C., H.E. Wong, and C.T. Goudar, *Upstream process intensification and continuous manufacturing*. Current Opinion in Chemical Engineering, 2018. **22**: p. 191-198.
10. Lee, J., et al., *Control of fed-batch fermentations*. Biotechnology advances, 1999. **17**(1): p. 29-48.
11. Mears, L., et al., *A review of control strategies for manipulating the feed rate in fed-batch fermentation processes*. Journal of Biotechnology, 2017. **245**: p. 34-46.
12. Kittler, S., *Inclusion body production in fed-batch and continuous cultivation*, in *Inclusion Bodies*. in press, Springer Nature: Methods in Molecular Biology.
13. Levisauskas, D., *Inferential control of the specific growth rate in fed-batch cultivation processes*. Biotechnology Letters, 2001. **23**(15): p. 1189-1195.
14. Jobé, A.M., et al., *Generally applicable fed-batch culture concept based on the detection of metabolic state by on-line balancing*. Biotechnol Bioeng, 2003. **82**(6): p. 627-39.
15. Shiloach, J. and R. Fass, *Growing E. coli to high cell density—a historical perspective on method development*. Biotechnology Advances, 2005. **23**(5): p. 345-357.
16. Huang, C.-J., H. Lin, and X. Yang, *Industrial production of recombinant therapeutics in Escherichia coli and its recent advancements*. Journal of Industrial Microbiology and Biotechnology, 2012. **39**(3): p. 383-399.
17. Wechselberger, P., et al., *Efficient feeding profile optimization for recombinant protein production using physiological information*. Bioprocess and Biosystems Engineering, 2012. **35**(9): p. 1637-1649.
18. Kopp, J., et al., *Boosting Recombinant Inclusion Body Production-From Classical Fed-Batch Approach to Continuous Cultivation*. Frontiers in bioengineering and biotechnology, 2019. **7**: p. 297-297.
19. Sandén, A.M., et al., *Limiting factors in Escherichia coli fed-batch production of recombinant proteins*. Biotechnology and Bioengineering, 2003. **81**(2): p. 158-166.
20. Hammerschmidt, N., et al., *Economics of recombinant antibody production processes at various scales: Industry-standard compared to continuous precipitation*. Biotechnol J, 2014. **9**(6): p. 766-75.

21. Yang, O., S. Prabhu, and M. Ierapetritou, *Comparison between Batch and Continuous Monoclonal Antibody Production and Economic Analysis*. Industrial & Engineering Chemistry Research, 2019. **58**(15): p. 5851-5863.
22. Liu, L., et al., *Repeated fed-batch strategy and metabolomic analysis to achieve high docosahexaenoic acid productivity in *Cryptocodinium cohnii**. Microbial Cell Factories, 2020. **19**(1): p. 91.
23. Kuo, H.P., et al., *Pilot scale repeated fed-batch fermentation processes of the wine yeast *Dekkera bruxellensis* for mass production of resveratrol from *Polygonum cuspidatum**. Bioresour Technol, 2017. **243**: p. 986-993.
24. Kopp, J., et al., *Repetitive Fed-Batch: A Promising Process Mode for Biomanufacturing With *E. coli**. Frontiers in Bioengineering and Biotechnology, 2020. **8**: p. 1312.
25. Qu, L., et al., *Batch, fed-batch and repeated fed-batch fermentation processes of the marine thraustochytrid *Schizochytrium sp.* for producing docosahexaenoic acid*. Bioprocess and Biosystems Engineering, 2013. **36**(12): p. 1905-1912.
26. Martens, S., et al., *Fully automated production of potential Malaria vaccines with *Pichia pastoris* in integrated processing*. Engineering in Life Sciences, 2011. **11**(4): p. 429-435.
27. Li, G., et al., *Enhancing the efficiency of L-tyrosine by repeated batch fermentation*. Bioengineered, 2020. **11**(1): p. 852-861.
28. Zelić, B., et al., *Process strategies to enhance pyruvate production with recombinant *Escherichia coli*: From repetitive fed-batch to in situ product recovery with fully integrated electrodialysis*. Biotechnology and Bioengineering, 2004. **85**(6): p. 638-646.
29. Zhang, Y., et al.,  *$\epsilon$ -Poly-L-lysine production by immobilized cells of *Kitasatospora sp. MY 5-36* in repeated fed-batch cultures*. Bioresource Technology, 2010. **101**(14): p. 5523-5527.
30. Hewitt, C.J. and A.W. Nienow, *The Scale-Up of Microbial Batch and Fed-Batch Fermentation Processes*, in *Advances in Applied Microbiology*. 2007, Academic Press. p. 105-135.
31. Crater, J.S. and J.C. Lievens, *Scale-up of industrial microbial processes*. FEMS Microbiology Letters, 2018. **365**(13): p. fny138.
32. Peebo, K. and P. Neubauer, *Application of Continuous Culture Methods to Recombinant Protein Production in Microorganisms*. Microorganisms, 2018. **6**(3).
33. Kopp, J., et al., *The Rocky Road From Fed-Batch to Continuous Processing With *E. coli**. Frontiers in bioengineering and biotechnology, 2019. **7**: p. 328-328.
34. Konstantinov, K.B. and C.L. Cooney, *White Paper on Continuous Bioprocessing. May 20–21, 2014 Continuous Manufacturing Symposium*. Journal of Pharmaceutical Sciences, 2015. **104**(3): p. 813-820.
35. Schmieder, A. and D. Weuster-Botz, *High-performance recombinant protein production with *Escherichia coli* in continuously operated cascades of stirred-tank reactors*. Journal of Industrial Microbiology and Biotechnology, 2017. **44**(7): p. 1021-1029.
36. Wong, H.E., et al., *From chemostats to high-density perfusion: the progression of continuous mammalian cell cultivation*. Journal of Chemical Technology & Biotechnology, 2022. **97**(9): p. 2297-2304.
37. Karst, D.J., et al., *Process performance and product quality in an integrated continuous antibody production process*. Biotechnology and Bioengineering, 2017. **114**(2): p. 298-307.
38. Steinebach, F., et al., *Design and operation of a continuous integrated monoclonal antibody production process*. Biotechnology Progress, 2017. **33**(5): p. 1303-1313.
39. Burgstaller, D., et al., *Continuous cell flocculation for recombinant antibody harvesting*. J Chem Technol Biotechnol, 2018. **93**(7): p. 1881-1890.

40. Monod, J.L. *LA TECHNIQUE DE CULTURE CONTINUE THÉORIE ET APPLICATIONS*. 1978.
41. NOVICK, A. and L. SZILARD, *Description of the chemostat*. Science, 1950. **112**(2920): p. 715-6.
42. NOVICK, A. and L. SZILARD, *Experiments with the Chemostat on spontaneous mutations of bacteria*. Proc Natl Acad Sci U S A, 1950. **36**(12): p. 708-19.
43. Croughan, M.S., K.B. Konstantinov, and C. Cooney, *The future of industrial bioprocessing: batch or continuous?* Biotechnol Bioeng, 2015. **112**(4): p. 648-51.
44. Zinn, M., et al., *Editorial: Recent Advances in Continuous Cultivation*. Front Bioeng Biotechnol, 2021. **9**: p. 641249.
45. Seifert, T., et al., *Small scale, modular and continuous: A new approach in plant design*. Chemical Engineering and Processing: Process Intensification, 2012. **52**: p. 140-150.
46. Striedner, G., et al., *Tuning the Transcription Rate of Recombinant Protein in Strong Escherichiacoli Expression Systems through Repressor Titration*. Biotechnology Progress, 2003. **19**(5): p. 1427-1432.
47. Heins, A.-L., et al., *Quantitative Flow Cytometry to Understand Population Heterogeneity in Response to Changes in Substrate Availability in Escherichia coli and Saccharomyces cerevisiae Chemostats*. Frontiers in Bioengineering and Biotechnology, 2019. **7**: p. 187.
48. Rugbjerg, P. and M.O.A. Sommer, *Overcoming genetic heterogeneity in industrial fermentations*. Nature Biotechnology, 2019. **37**(8): p. 869-876.
49. Rugbjerg, P. and L. Olsson, *The future of self-selecting and stable fermentations*. Journal of Industrial Microbiology & Biotechnology, 2020. **47**(11): p. 993-1004.
50. Rhee, J.I. and K. Schügerl, *Continuous cultivation of recombinant Escherichia coli JM109 in a two-stage cascade reactor and production of the fusion protein EcoRI::SPA*. Process Biochemistry, 1998. **33**(2): p. 213-224.
51. Blount, Z.D., *The unexhausted potential of E. coli*. eLife, 2015. **4**: p. e05826.
52. Daegelen, P., et al., *Tracing Ancestors and Relatives of Escherichia coli B, and the Derivation of B Strains REL606 and BL21(DE3)*. Journal of Molecular Biology, 2009. **394**(4): p. 634-643.
53. Rosano, G.L., E.S. Morales, and E.A. Ceccarelli, *New tools for recombinant protein production in Escherichia coli: A 5-year update*. Protein Sci, 2019. **28**(8): p. 1412-1422.
54. Yoon, S.H., et al., *Comparative multi-omics systems analysis of Escherichia coli strains B and K-12*. Genome Biology, 2012. **13**(5): p. R37.
55. Marisch, K., et al., *A Comparative Analysis of Industrial Escherichia coli K-12 and B Strains in High-Glucose Batch Cultivations on Process-, Transcriptome- and Proteome Level*. PLOS One, 2013. **8**(8): p. e70516.
56. Studier, F.W. and B.A. Moffatt, *Use of Bacteriophage-T7 Rna-Polymerase to Direct Selective High-Level Expression of Cloned Genes*. Journal of Molecular Biology, 1986. **189**(1): p. 113-130.
57. Steen, R., et al., *T7 RNA polymerase directed expression of the Escherichia coli rrnB operon*. EMBO J, 1986. **5**(5): p. 1099-103.
58. Tegel, H., J. Ottosson, and S. Hober, *Enhancing the protein production levels in Escherichia coli with a strong promoter*. The FEBS Journal, 2011. **278**(5): p. 729-739.
59. Kim, S., et al., *Genomic and transcriptomic landscape of Escherichia coli BL21(DE3)*. Nucleic acids research, 2017. **45**(9): p. 5285-5293.
60. Hayashi, K., et al., *Highly accurate genome sequences of Escherichia coli K-12 strains MG1655 and W3110*. Molecular Systems Biology, 2006. **2**(1): p. 2006.0007.
61. Khankal, R., et al., *Comparison between Escherichia coli K-12 strains W3110 and MG1655 and wild-type E. coli B as platforms for xylitol production*. Biotechnology Letters, 2008. **30**(9): p. 1645-1653.

62. Chen, C., et al., *High-level accumulation of a recombinant antibody fragment in the periplasm of Escherichia coli requires a triple-mutant (degP prc spr) host strain*. Biotechnol Bioeng, 2004. **85**(5): p. 463-74.
63. Shilling, P.J., et al., *Improved designs for pET expression plasmids increase protein production yield in Escherichia coli*. Communications Biology, 2020. **3**(1): p. 214.
64. Studier, F.W. and B.A. Moffatt, *Use of bacteriophage T7 RNA polymerase to direct selective high-level expression of cloned genes*. Journal of Molecular Biology, 1986. **189**(1): p. 113-130.
65. Sørensen, H.P. and K.K. Mortensen, *Advanced genetic strategies for recombinant protein expression in Escherichia coli*. Journal of Biotechnology, 2005. **115**(2): p. 113-128.
66. Marbach, A. and K. Bettenbrock, *lac operon induction in Escherichia coli: Systematic comparison of IPTG and TMG induction and influence of the transacetylase LacA*. Journal of Biotechnology, 2012. **157**(1): p. 82-88.
67. Neubauer, P. and K. Hofmann, *Efficient use of lactose for the lac promotercontrolled overexpression of the main antigenic protein of the foot and mouth disease virus in Escherichia coli under fed-batch fermentation conditions*. FEMS Microbiology Reviews, 1994. **14**(1): p. 99-102.
68. Wurm, D.J., et al., *The E. coli pET expression system revisited-mechanistic correlation between glucose and lactose uptake*. Applied microbiology and biotechnology, 2016. **100**(20): p. 8721-8729.
69. Wurm, D.J., et al., *Teaching an old pET new tricks: tuning of inclusion body formation and properties by a mixed feed system in E. coli*. Applied microbiology and biotechnology, 2018. **102**(2): p. 667-676.
70. Wurm, D.J., et al., *Mechanistic platform knowledge of concomitant sugar uptake in Escherichia coli BL21(DE3) strains*. Scientific reports, 2017. **7**: p. 45072-45072.
71. Dvorak, P., et al., *Exacerbation of substrate toxicity by IPTG in Escherichia coli BL21 (DE3) carrying a synthetic metabolic pathway*. Microbial cell factories, 2015. **14**(1): p. 201.
72. Kopp, J., et al., *Impact of Glycerol as Carbon Source onto Specific Sugar and Inducer Uptake Rates and Inclusion Body Productivity in E. coli BL21(DE3)*. Bioengineering, 2017. **5**(1).
73. Lübke, C., W. Boidol, and T. Petri, *Analysis and optimization of recombinant protein production in Escherichia coli using the inducible pho A promoter of the E. coli alkaline phosphatase*. Enzyme and Microbial Technology, 1995. **17**(10): p. 923-928.
74. Bhatwa, A., et al., *Challenges Associated With the Formation of Recombinant Protein Inclusion Bodies in Escherichia coli and Strategies to Address Them for Industrial Applications*. Front Bioeng Biotechnol, 2021. **9**: p. 630551.
75. Schlegel, S., et al., *Optimizing heterologous protein production in the periplasm of E. coli by regulating gene expression levels*. Microbial Cell Factories, 2013. **12**(1): p. 24.
76. Luo, M., et al., *A general platform for efficient extracellular expression and purification of Fab from Escherichia coli*. Applied Microbiology and Biotechnology, 2019. **103**(8): p. 3341-3353.
77. Gundinger, T., et al., *Recombinant Protein Production in E. coli Using the phoA Expression System*. Fermentation, 2022. **8**(4).
78. Wang, Y., et al., *Production of phoA promoter-controlled human epidermal growth factor in fed-batch cultures of Escherichia coli YK537 (pAET-8)*. Process Biochemistry, 2005. **40**(9): p. 3068-3074.
79. Hoffmann, D., et al., *Reassessment of inclusion body-based production as a versatile opportunity for difficult-to-express recombinant proteins*. Critical Reviews in Biotechnology, 2018. **38**(5): p. 729-744.

80. Thomas, J.G. and F. Baneyx, *Protein Misfolding and Inclusion Body Formation in Recombinant Escherichia coli Cells Overexpressing Heat-shock Proteins (\*)*. Journal of Biological Chemistry, 1996. **271**(19): p. 11141-11147.
81. Kamionka, M., *Engineering of therapeutic proteins production in Escherichia coli*. Curr Pharm Biotechnol, 2011. **12**(2): p. 268-74.
82. Sørensen, H.P. and K.K. Mortensen, *Soluble expression of recombinant proteins in the cytoplasm of Escherichia coli*. Microbial Cell Factories, 2005. **4**(1): p. 1.
83. Sahdev, S., S.K. Khattar, and K.S. Saini, *Production of active eukaryotic proteins through bacterial expression systems: a review of the existing biotechnology strategies*. Molecular and Cellular Biochemistry, 2008. **307**(1-2): p. 249-264.
84. Cornelis, P., *Expressing genes in different Escherichia coli compartments*. Curr Opin Biotechnol, 2000. **11**(5): p. 450-4.
85. Rinas, U., et al., *Bacterial Inclusion Bodies: Discovering Their Better Half*. Trends Biochem Sci, 2017. **42**(9): p. 726-737.
86. Choi, J.H. and S.Y. Lee, *Secretory and extracellular production of recombinant proteins using Escherichia coli*. Applied Microbiology and Biotechnology, 2004. **64**(5): p. 625-635.
87. Farkade, V.D., S. Harrison, and A.B. Pandit, *Heat induced translocation of proteins and enzymes within the cell: an effective way to optimize the microbial cell disruption process*. Biochemical Engineering Journal, 2005. **23**(3): p. 247-257.
88. Mirzadeh, K., et al., *Increased production of periplasmic proteins in Escherichia coli by directed evolution of the translation initiation region*. Microbial Cell Factories, 2020. **19**(1): p. 85.
89. Malik, A., *Protein fusion tags for efficient expression and purification of recombinant proteins in the periplasmic space of E. coli*. 3 Biotech, 2016. **6**(1): p. 44.
90. Thie, H., et al., *SRP and Sec pathway leader peptides for antibody phage display and antibody fragment production in E. coli*. New Biotechnology, 2008. **25**(1): p. 49-54.
91. Kastenhofer, J., et al., *Economic and ecological benefits of a leaky E. coli strain for downstream processing: a case study for staphylococcal protein A*. Journal of Chemical Technology & Biotechnology, 2021. **96**(6): p. 1667-1674.
92. Ni, Y. and R. Chen, *Extracellular recombinant protein production from Escherichia coli*. Biotechnology Letters, 2009. **31**(11): p. 1661.
93. Yang, J., et al., *One hundred seventy-fold increase in excretion of an FV fragment-tumor necrosis factor alpha fusion protein (sFV/TNF-alpha) from Escherichia coli caused by the synergistic effects of glycine and triton X-100*. Appl Environ Microbiol, 1998. **64**(8): p. 2869-74.
94. Wurm, D.J., et al., *How to trigger periplasmic release in recombinant Escherichia coli: A comparative analysis*. Engineering in life sciences, 2017. **17**(2): p. 215-222.
95. Bäcklund, E., et al., *Fedbatch design for periplasmic product retention in Escherichia coli*. Journal of Biotechnology, 2008. **135**(4): p. 358-365.
96. Shokri, A., A.M. Sandén, and G. Larsson, *Growth rate-dependent changes in Escherichia coli membrane structure and protein leakage*. Appl Microbiol Biotechnol, 2002. **58**(3): p. 386-92.
97. Kadokura, H., F. Katzen, and J. Beckwith, *Protein disulfide bond formation in prokaryotes*. Annu Rev Biochem, 2003. **72**: p. 111-35.
98. Shin, P.K. and J.H. Seo, *Analysis of E. coli phoA-lacZ fusion gene expression inserted into a multicopy plasmid and host cell's chromosome*. Biotechnol Bioeng, 1990. **36**(11): p. 1097-104.
99. Baneyx, F., *Recombinant protein expression in Escherichia coli*. Current Opinion in Biotechnology, 1999. **10**(5): p. 411-21.

100. Schottroff, F., et al., *Selective Release of Recombinant Periplasmic Protein From E. coli Using Continuous Pulsed Electric Field Treatment*. *Frontiers in Bioengineering and Biotechnology*, 2021. **8**.
101. Agbogbo, F.K., et al., *Upstream development of Escherichia coli fermentation process with PhoA promoter using design of experiments (DoE)*. *J Ind Microbiol Biotechnol*, 2020. **47**(9-10): p. 789-799.
102. Rao, N.N., S. Liu, and A. Kornberg, *Inorganic polyphosphate in Escherichia coli: the phosphate regulon and the stringent response*. *Journal of bacteriology*, 1998. **180**(8): p. 2186-2193.
103. Wanner, B.L., *Phosphorus assimilation and control of the phosphate regulon*. *Escherichia coli and Salmonella: cellular and molecular biology*, 1996. **1**: p. 1357-1381.
104. Formenti, L.R., et al., *Challenges in industrial fermentation technology research*. *Biotechnology Journal*, 2014. **9**(6): p. 727-738.
105. Kumar, V., A. Bhalla, and A.S. Rathore, *Design of experiments applications in bioprocessing: Concepts and approach*. *Biotechnology Progress*, 2014. **30**(1): p. 86-99.
106. Kopp, J., et al., *Fundamental insights in early-stage inclusion body formation*. *Microbial Biotechnology*, 2022. **n/a**(n/a).
107. Slouka, C., et al., *Custom made inclusion bodies: impact of classical process parameters and physiological parameters on inclusion body quality attributes*. *Microb Cell Fact*, 2018. **17**(1): p. 148.
108. Takagi, H., et al., *Control of Folding of Proteins Secreted by a High Expression Secretion Vector, pIN-III-ompA: 16-Fold Increase in Production of Active Subtilisin E in Escherichia Coli*. *Bio/Technology*, 1988. **6**: p. 948.
109. Harrison, J.S. and E. Keshavarz-Moore, *Production of antibody fragments in Escherichia coli*. *Ann N Y Acad Sci*, 1996. **782**: p. 143-58.
110. Lee, S.L., et al., *Modernizing Pharmaceutical Manufacturing: from Batch to Continuous Production*. *Journal of Pharmaceutical Innovation*, 2015. **10**(3): p. 191-199.
111. Bren, A., et al., *Glucose becomes one of the worst carbon sources for E.coli on poor nitrogen sources due to suboptimal levels of cAMP*. *Scientific Reports*, 2016. **6**(1): p. 24834.
112. Hogema, B.M., et al., *Inducer exclusion in Escherichia coli by non-PTS substrates: the role of the PEP to pyruvate ratio in determining the phosphorylation state of enzyme IIAGlc*. *Mol Microbiol*, 1998. **30**(3): p. 487-98.
113. Brückner, R. and F. Titgemeyer, *Carbon catabolite repression in bacteria: choice of the carbon source and autoregulatory limitation of sugar utilization*. *FEMS Microbiology Letters*, 2002. **209**(2): p. 141-148.
114. Deutscher, J., C. Francke, and P.W. Postma, *How phosphotransferase system-related protein phosphorylation regulates carbohydrate metabolism in bacteria*. *Microbiol Mol Biol Rev*, 2006. **70**(4): p. 939-1031.
115. Stulke, J. and W. Hillen, *Carbon catabolite repression in bacteria*. *Current Opinion in Microbiology*, 1999. **2**(2): p. 195-201.
116. Görke, B. and J. Stülke, *Carbon catabolite repression in bacteria: many ways to make the most out of nutrients*. *Nature Reviews Microbiology*, 2008. **6**(8): p. 613-624.
117. Kremling, A., et al., *Understanding carbon catabolite repression in Escherichia coli using quantitative models*. *Trends in Microbiology*, 2015. **23**(2): p. 99-109.
118. Aidelberg, G., et al., *Hierarchy of non-glucose sugars in Escherichia coli*. *BMC Syst Biol*, 2014. **8**: p. 133.
119. Inada, T., K. Kimata, and H. Aiba, *Mechanism responsible for glucose-lactose diauxie in Escherichia coli: challenge to the cAMP model*. *Genes Cells*, 1996. **1**(3): p. 293-301.

120. Kimata, K., et al., *cAMP receptor protein-cAMP plays a crucial role in glucose-lactose diauxie by activating the major glucose transporter gene in Escherichia coli*. Proc Natl Acad Sci U S A, 1997. **94**(24): p. 12914-9.
121. Martínez-Gómez, K., et al., *New insights into Escherichia coli metabolism: carbon scavenging, acetate metabolism and carbon recycling responses during growth on glycerol*. Microb Cell Fact, 2012. **11**: p. 46.
122. Murarka, A., et al., *Fermentative utilization of glycerol by Escherichia coli and its implications for the production of fuels and chemicals*. Appl Environ Microbiol, 2008. **74**(4): p. 1124-35.
123. Boecker, S., et al., *Enabling anaerobic growth of Escherichia coli on glycerol in defined minimal medium using acetate as redox sink*. Metabolic Engineering, 2022. **73**: p. 50-57.
124. Chiang, C.-J., et al., *Rewiring of glycerol metabolism in Escherichia coli for effective production of recombinant proteins*. Biotechnology for Biofuels, 2020. **13**(1): p. 205.
125. Blommel, P.G., et al., *Enhanced bacterial protein expression during auto-induction obtained by alteration of lac repressor dosage and medium composition*. Biotechnol Prog, 2007. **23**(3): p. 585-98.
126. Ukkonen, K., et al., *Use of slow glucose feeding as supporting carbon source in lactose autoinduction medium improves the robustness of protein expression at different aeration conditions*. Protein Expression and Purification, 2013. **91**(2): p. 147-54.
127. Walther, J., et al., *The business impact of an integrated continuous biomanufacturing platform for recombinant protein production*. Journal of Biotechnology, 2015. **213**: p. 3-12.
128. Binder, D., et al., *Homogenizing bacterial cell factories: Analysis and engineering of phenotypic heterogeneity*. Metab Eng, 2017. **42**: p. 145-156.
129. DeLisa, M.P., et al., *Monitoring GFP-operon fusion protein expression during high cell density cultivation of Escherichia coli using an on-line optical sensor*. Biotechnology and Bioengineering, 1999. **65**(1): p. 54-64.



## 6. Scientific Publications

### 6.1. Scientific Publication 1



fermentation



Article

## Recombinant Protein Production in *E. coli* Using the phoA Expression System

Thomas Gundinger <sup>†</sup>, Stefan Kittler <sup>†</sup>, Sabine Kubicek, Julian Kopp <sup>ORCID</sup> and Oliver Spadiut <sup>\*ORCID</sup>

Research Group Integrated Bioprocess Development, Institute of Chemical, Environmental and Bioscience Engineering, TU Wien, Gumpendorferstraße 1a, 1060 Vienna, Austria; thomas.gundinger@gmx.net (T.G.); stefan.kittler@tuwien.ac.at (S.K.); sabine.kubicek@tuwien.ac.at (S.K.); julian.kopp@tuwien.ac.at (J.K.)

\* Correspondence: oliver.spadiut@tuwien.ac.at; Tel.: +43-1-58801-166473; Fax: +43-1-58801-166980

<sup>†</sup> These authors contributed equally to this work.

**Abstract:** Auto-inducible promoter systems have been reported to increase soluble product formation in the periplasm of *E. coli* compared to inducer-dependent systems. In this study, we investigated the phosphate (PO<sub>4</sub>)-sensitive phoA expression system (pAT) for the production of a recombinant model antigen-binding fragment (Fab) in the periplasm of *E. coli* in detail. We explored the impact of non-limiting and limiting PO<sub>4</sub> conditions on strain physiology as well as Fab productivity. We compared different methods for extracellular PO<sub>4</sub> detection, identifying automated colorimetric measurement to be most suitable for at-line PO<sub>4</sub> monitoring. We showed that PO<sub>4</sub> limitation boosts phoA-based gene expression, however, the product was already formed at non-limiting PO<sub>4</sub> conditions, indicating leaky expression. Furthermore, cultivation under PO<sub>4</sub> limitation caused physiological changes ultimately resulting in a metabolic breakdown at PO<sub>4</sub> starvation. Finally, we give recommendations for process optimization with the phoA expression system. In summary, our study provides very detailed information on the *E. coli* phoA expression system, thus extending the existing knowledge of this system, and underlines its high potential for the successful production of periplasmic products in *E. coli*.

**Keywords:** *E. coli*; phoA promoter; T7lac promoter; pAT; pET; antibody fragment; periplasm; inclusion body



**Citation:** Gundinger, T.; Kittler, S.; Kubicek, S.; Kopp, J.; Spadiut, O. Recombinant Protein Production in *E. coli* Using the phoA Expression System. *Fermentation* **2022**, *8*, 181. <https://doi.org/10.3390/fermentation8040181>

Academic Editor: Francesca Berini

Received: 11 March 2022

Accepted: 6 April 2022

Published: 11 April 2022

**Publisher's Note:** MDPI stays neutral with regard to jurisdictional claims in published maps and institutional affiliations.



**Copyright:** © 2022 by the authors. Licensee MDPI, Basel, Switzerland. This article is an open access article distributed under the terms and conditions of the Creative Commons Attribution (CC BY) license (<https://creativecommons.org/licenses/by/4.0/>).

### 1. Introduction

Besides mammalian cells, the bacterium *Escherichia coli* represents the most commonly used production host for biopharmaceuticals, especially antigen binding fragments (Fabs, [1–3]). *E. coli* provides several benefits, as simple genetic manipulation, high cell densities and productivities, as well as cultivation on inexpensive media [4]. The production of functional Fabs in *E. coli*, however, requires secretion into the periplasmic space as only the oxidizing conditions present there enable the correct formation of disulfide bonds [5]. Periplasmic translocation is directed by addition of an N-terminal leader peptide, which typically originates from a natively translocated protein [6], such as phoA [7], ompA [7], pelB [8] or stII [3,9]. Successful production of functional Fabs by periplasmic expression in *E. coli* was first reported by Skerra et al. [7] and Better et al. in the 1990s [10]. Skerra produced a Fab under the control of the lac promoter, whereas Better expressed a Fab under the control of the araB promoter. In both cases, however, the obtained product yields did not exceed 2 mg/L. Other promoter systems used for Fab production were the phoA promoter [3,9] and the tac promoter [8,11,12]. Since then, several studies have dealt with the commonly observed low expression levels of Fabs [13], which are mainly attributed to toxicity effects, protein degradation, inclusion body (IB) formation and translocation inefficiencies [14,15]. In this regard, different cultivation conditions, vector elements [4,16,17],

medium compositions and aeration strategies [8,18] have been investigated to boost productivity. Furthermore, the impact of co-expressed chaperones and application of protease deficient strains [11] as well as the influence of gene order (heavy and light chain), temperature and DNA sequence [13,19,20] on soluble Fab expression have been investigated.

Based on these studies, the product yield could be pushed to nearly 5 g/L for certain Fabs [9,11,21,22]. However, in most cases obtained yields are still quite low (<200 mg/L) even in high cell density cultivations (OD > 100) [12,23]. Several working groups have attributed these low yields to an uncontrolled loss of product into the culture medium, due to leakiness of the *E. coli* outer cell membrane [8,10,13]. Furthermore, intracellular protein loss in the form of IBs is a common phenomenon for *E. coli*. This undesired IB formation can be attributed to several reasons: (1) overexpression imposes metabolic burden on the biosynthetic machinery of the cell [24]; (2) non-optimal cultivation conditions affect soluble protein production [25,26] and (3) the use of strong promoters and high inducer concentrations leads to increased expression rates overcoming the capacity of the native translocation system [27,28]. Based on that, the application of strong expression systems, such as the well-established and widely used T7lac system, might not be suitable for soluble Fab production in the *E. coli* periplasm. However, the T7 system is still used for the production of Fabs both in academia and industry (e.g., [29–31]).

In a recent study, Luo et al. used the alkaline phosphatase (*phoA*) promoter (pAT system) and the *stII* leader peptide to successfully produce five different Fabs extracellularly in *E. coli* BL21DE3 [3]. They also demonstrated the superiority of the *phoA*-based pAT system over the commonly used T7-based pET system. Based on these interesting findings, we (1) directly compared the production of a recombinant Fab under the control of the *E. coli phoA* expression system (hereafter called pAT) and the T7lac expression system (hereafter called pET) under different cultivation conditions and (2) investigated in more detail the impact of extracellular PO<sub>4</sub> concentration on strain physiology and product formation during cultivation starting at high PO<sub>4</sub> content (30 mM) until PO<sub>4</sub> starvation (<0.1 mM). Since appropriate PO<sub>4</sub> analysis is essential for bioprocess control, we also analyzed and compared different methods for determination of extracellular PO<sub>4</sub> in the culture broth. Finally, we give recommendations for process intensification using the *phoA* expression system. In summary, this study extends current knowledge on the *phoA* expression system.

## 2. Materials and Methods

### 2.1. Strains and Product

The gene encoding the model Fab (50 kD, pI 7.4, 5 S-S bonds) was codon-optimized for *E. coli* and obtained from GenScript. The antibody chains coding for light chain and heavy chain were placed under the control of the promoter (order: 1. Promoter—2. light chain—3. heavy chain). Furthermore, both antibody chains were preceded by the *E. coli* enterotoxin II (*stII*) signal sequence to allow translocation to the *E. coli* periplasm, as shown before for five different Fabs [3]. For pET cultivations, *E. coli* BL21(DE3) (NEB, Ipswich, MA, USA) transformed with a pET26(+) vector carrying the gene coding for the Fab—placed between the restriction sites *XhoI* and *XbaI*—under the transcriptional control of the T7lac promoter was used (T7lac strain). For pAT cultivations, *E. coli* W3110 (DSMZ, Braunschweig, Germany) transformed with a modified pAT153 vector (*Amp<sup>R</sup>* gene was removed) carrying the gene coding for the Fab—placed between the restriction sites *NotI* and *EcoRI*—under the transcriptional control of the *E. coli phoA* promoter was used (*phoA* strain).

### 2.2. Bioreactor Cultivations

#### 2.2.1. Strain Characterization

Cultivations for characterization of both the T7lac strain and the *phoA* strain were carried out in a DASGIP® Parallel Bioreactor System (Eppendorf, Hamburg, Germany) with a working volume of 2 L. The CO<sub>2</sub> and O<sub>2</sub> in the off-gas were analyzed by a DASGIP® GA gas analyzer (Eppendorf, Hamburg, Germany), pH by a pH-sensor EasyFerm Plus

(Hamilton, Reno, NV, USA) and dissolved oxygen ( $dO_2$ ) by a Visiferm DO 225 electrode (Hamilton, Reno, NV, USA). The  $dO_2$  was kept above 20% oxygen saturation throughout the whole cultivation by supplying 2 vvm of a mixture of pressurized air and pure oxygen. The pH was kept at 7.2 by supplying 12.5%  $NH_4OH$  and 10% HCl and stirring speed was set to maximum (2000 rpm) to reduce the required pure oxygen consumption. Fed-batch cultivations were performed using a soft-sensor controlled feeding strategy. The applied soft-sensor, using online measurement of  $CO_2$  in the off-gas for estimation of biomass concentration, was described in detail by Wechselberger et al. [32]. Calculated feed-flowrates were adjusted with the DASbox<sup>®</sup> MP8 Multi Pump Module. All process parameters were logged and controlled by the DASware<sup>®</sup> control.

#### T7lac-Based Expression (pET Cultivations)

In total, 500 mL sterile DeLisa pre-culture medium [33] supplemented with 0.05 g/L kanamycin and 8 g/L glucose was aseptically inoculated from frozen stocks (T7lac strain, 3 mL,  $-80^\circ C$ ). Pre-cultures were grown in two 500-mL high-yield shake flasks in an Infors HR Multitronshaker (Infors, Bottmingen, Switzerland) at  $37^\circ C$  and 230 rpm overnight (15 h). For batch cultivation, 900 mL DeLisa batch medium [33] supplemented with 20 g/L glucose was inoculated with 100 mL of pre-culture and temperature was set to  $35^\circ C$ . After sugar depletion (indicated by a drop of  $CO_2$  in the off-gas signal), a non-induced fed-batch phase using a feed with 400 g/L glucose was carried out. The temperature was kept at  $35^\circ C$  and the feed flow rate was adjusted to correspond to a specific growth rate ( $\mu$ ) of  $0.1\ h^{-1}$ . At a biomass concentration of around 30 g/L dry cell weight (DCW), induction was performed by addition of 0.1 mM Isopropyl- $\beta$ -D-thiogalactopyranoside (IPTG). Temperature and feed rate (corresponding to  $\mu$ ) for the different cultivations were set as following: pET 1:  $\mu = 0.1\ h^{-1}$ ,  $35^\circ C$ ; pET 2:  $\mu = 0.1\ h^{-1}$ ,  $30^\circ C$ ; pET 3:  $\mu = 0.05\ h^{-1}$ ,  $35^\circ C$ ; pET 4:  $\mu = 0.05\ h^{-1}$ ,  $30^\circ C$ . Each culture was induced for 8 h. Applied feed flow rates ranged from 8 mL/h (start fed-batch) to 80 mL/h (end fed-batch).

#### phoA-Based Expression (pAT Cultivations)

A total of 500 mL sterile DeLisa pre-culture medium [33] supplemented with 0.01 g/L tetracycline and 8 g/L glucose was aseptically inoculated from frozen stocks (phoA strain, 3 mL,  $-80^\circ C$ ). Pre-cultures were grown as described above. For batch cultivation, 900 mL DeLisa batch medium [33] containing only 1.09 g/L  $KH_2PO_4$  and 6.04 g/L  $(NH_4)_2HPO_4$  as P-source was used. These amounts account for approx. 50 g/L DCW based on the elemental biomass composition of *E. coli* W3110, and were supplemented with 20 g/L glucose. Batch was inoculated with 100 mL of pre-culture and temperature was set to  $35^\circ C$ . After sugar depletion, a fed-batch phase using a glucose feed with 400 g/L glucose was carried out. Temperature and feed rate (corresponding to  $\mu$ ) for the different cultivations were set as following: pAT 1:  $\mu = 0.1\ h^{-1}$ ,  $35^\circ C$ ; pAT 2:  $\mu = 0.1\ h^{-1}$ ,  $30^\circ C$ ; pAT 3:  $\mu = 0.05\ h^{-1}$ ,  $35^\circ C$ ; pAT 4:  $\mu = 0.05\ h^{-1}$ ,  $30^\circ C$ . The fed-batch was terminated at  $PO_4$  starvation, indicated by a stagnation of  $CO_2$  in the off-gas signal. Applied feed flow rates ranged from 8 mL/h (start fed-batch) to 80 mL/h (end fed-batch).

#### Sampling

For evaluation of pET cultivations, samples were taken at the beginning and end of batch and non-induced fed-batch, and after 4 h and 8 h of induction. For evaluation of pAT cultivations, samples were taken at the beginning and end of the batch phase, during the fed-batch phase at a  $PO_4$  concentration of  $>1\ mM$  (before  $PO_4$  limitation) and at  $PO_4$  starvation. Determination of biomass DCW was completed gravimetrically in triplicates [6]. Optical density at 600 nm ( $OD_{600}$ ) was determined photometrically in triplicates (Photometer Genesys 20; Thermo Fisher, Waltham, MA, USA). Glucose and acetate were measured in cell-free culture broth HPLC [34]. The inorganic  $PO_4$  concentration in the cell-free culture broth was determined colorimetrically using the Cedex Bio HT analyzer (Roche, Basel, Switzerland) applying the Phosphate Bio HT test kit (Ref 06990088001). Based on

the measured  $\text{PO}_4$  concentrations, the respective biomass concentrations and the time intervals between sampling points, the respective specific  $\text{PO}_4$  uptake rate ( $\text{mmol/g/h}$ ) was calculated.

### 2.2.2. Characterization of the pAT System

Cultivations were carried out in a Cplus Biostat Bioreactor System (Sartorius, Göttingen, Germany) with a total volume of 15 L and a working volume of 10 L.  $\text{CO}_2$  and  $\text{O}_2$  in the off-gas were analyzed by an off-gas analysis system (Dr. Marino Müller Systems, Esslingen, Switzerland), pH was monitored by a pH-sensor 405-DPAS-SC-K8S/120 (Mettler Toledo, Columbus, OH, USA), and dissolved oxygen ( $\text{dO}_2$ ) by an InPro 6860i nA electrode (Mettler Toledo, Columbus, OH, USA). The  $\text{dO}_2$  was kept above 20% oxygen saturation throughout the whole cultivation by supplying 2 vvm of a mixture of pressurized air and pure oxygen. The pH was kept at 7.2 by supplying 12.5%  $\text{NH}_4\text{OH}$  and 10% HCl and stirring speed was set to 1200 rpm (the commonly applied stirrer speed for *E. coli* cultivation in our lab). All process parameters were logged and controlled by the Process Information Management System Lucullus (Securecell, Urdorf, Switzerland).

Pre-culture was grown in 2500-mL high-yield shake flasks in an Infors HR Multi-tronshaker (Infors, Bottmingen, Switzerland) at 37 °C and 230 rpm overnight (15 h). A total of 550 mL of sterile DeLisa pre-culture medium [35] supplemented with 0.01 g/L tetracycline and 8 g/L glucose was aseptically inoculated from frozen stocks (phoA strain, 3 mL, −80 °C). For batch cultivation, 4500 mL of DeLisa batch medium [35] containing 1.09 g/L  $\text{KH}_2\text{PO}_4$  and 6.04 g/L  $(\text{NH}_4)_2\text{HPO}_4$  as P-source, accounting for approx. 50 g/L DCW, and supplemented with 20 g/L glucose was inoculated with 500 mL of pre-culture and temperature was set to 35 °C. After sugar depletion (indicated by a drop of the  $\text{CO}_2$  off-gas signal), a fed-batch phase using a glucose feed with 400 g/L glucose was carried out. Temperature and feed rate (corresponding to  $\mu$ ) were set to 30 °C and  $\mu = 0.05 \text{ h}^{-1}$ . Fed-batch cultivations were performed using a feed-forward strategy (exponential feed rate as well as initial feed rate were based on Equations (1) and (2)). The cultivations were performed in triplicates.

Equation (1). Formula for feed rate  $F_t$

$$F_t = F_0 \times e^{\mu t} \quad (1)$$

$F_t$  feed rate [g/h];

$F_0$  initial feed rate [g/h];

$\mu$  specific growth rate [1/h];

$t$  cultivation time [h].

Equation (2). Formula for initial feed rate  $F_0$

$$F_0 = \frac{\mu \times x_0 \times V_0}{c_{s, \text{Feed}} \times Y_{X/S}} \times \rho_{\text{Feed}} \quad (2)$$

$F_0$  initial feed rate at time point 0 [g/h];

$\mu$  specific growth rate [1/h];

$x_0$  biomass conc. at time point 0 [g/L];

$V_0$  culture volume at time point 0 [L];

$c_{s, \text{Feed}}$  glucose conc. in feed medium [g/L];

$Y_{X/S}$  biomass yield on glucose [g/g].

The feed-flowrate was adjusted with a Preciflow peristaltic pump (Lambda, Baar, Switzerland). Cultivations were performed until  $\text{PO}_4$  starvation (indicated by stagnation of the  $\text{CO}_2$  off-gas signal). Applied feed flow rate ranged from 18 mL/h (start fed-batch) to 125 mL/h (end fed-batch). For evaluation, samples were taken in a 2 h interval starting at a  $\text{PO}_4$  concentration of 35 mM until  $\text{PO}_4$  starvation. Determination of biomass DCW was completed gravimetrically [14]. Optical density at 600 nm (OD600) was determined photometrically (Photometer Genesys 20; Thermo Fisher, Waltham, MA, USA). Glucose

and acetate were measured in fermentation supernatant and quantified via HPLC [36]. The inorganic  $\text{PO}_4$  concentration in the cell-free culture broth was determined colorimetrically using the Cedex Bio HT analyzer (Roche, Basel, Switzerland) applying the Phosphate Bio HT test kit (Ref 06990088001).

### 2.3. Analytics

#### 2.3.1. Sample Preparation for Product Analysis

Cell pellets of 50 mL cultivation broth were resuspended (20 mM  $\text{NaH}_2\text{PO}_4$ , 100 mM NaCl, pH 7.0) to 100 g/L DCW and homogenized at 1000 bar for 10 passages (Panda 2000 Plus, GEA, Düsseldorf, Germany). After centrifugation (20 min, 14,000 rcf, 4 °C), the obtained supernatant was analyzed for soluble product, whereas the solid pellet (cell debris) was used for IB quantification.

#### 2.3.2. Soluble Product Quantification by Affinity HPLC

Crude cell lysates were pre-treated with a de-lipidation step prior to analysis [37] Fab quantification was carried out by HPLC analysis (UltiMate 3000; Thermo Fisher, Waltham, MA, USA) using a Protein L-based affinity chromatography column (POROS Capture Select LC Kappa, Applied Biosystems, Foster City, CA, USA) [37]. The product was quantified using purified Fab as standard. The standard deviation was quantified with 9.69% by performing triplicates of Fab standards (no technical triplicates of the single samples from the bioreactor cultivations were performed).

#### 2.3.3. Product IB Quantification by Size Exclusion HPLC

The cell debris was washed twice with deionized water and aliquoted (200 mg DCW/tube). Washed aliquots were solubilized in 2 mL of a solution containing 1 part Tris-buffer (50 mM Tris, pH 8.0) and 1 part solubilization buffer (50 mM Tris, 8 M guanidine hydrochloride (GnHCl), pH 8.0) and incubated on a shaker at room temperature for 2 h. Centrifugation (30 min, 14,000 rcf) was performed to remove particles prior to analysis. Product quantification was carried out by HPLC analysis (UltiMate 3000; Thermo Fisher, Waltham, MA, USA) using a size exclusion column (BioBasic SEC 300, Thermo Fisher, Waltham, MA, USA). A total of 50 mM BisTris, pH 6.8, supplemented with 4 M GnHCl and 150 mM NaCl, was used as mobile phase with a constant flow of 0.2 mL/min and the system was run isocratically at 25 °C. The product was quantified with an UV detector (Thermo Fisher, Waltham, MA, USA) at 280 nm using purified Fab as standard. The standard deviation was quantified with 1.04% by performing triplicates of all the samples.

#### 2.3.4. Investigation of $\text{PO}_4$ Quantification Methods

Phosphate/phosphorus was measured in cell-free culture broth (centrifugation at 14,000 rcf 4 °C and 2 min) by (1) Inductively Coupled Plasma—Optical Emission Spectroscopy (ICP-OES); (2) Ion exchange—Ion Chromatography (IC); (3) a Phosphate ( $\text{PO}_4$ ) Colorimetric Assay Kit and (4) a Cedex Bio HT analyzer. Depending on the analytical method, samples were diluted in deionized water to give results within the detection range.

##### ICP-OES

The phosphorus concentration was determined by ICP-OES using an iCAP 6000 ICP-OES instrument. Measurements and calibration, as well as standard and sample preparation, were conducted as described by Kamravamesh et al. [33].

##### IC

The inorganic  $\text{PO}_4$  concentration was determined by IC analysis (Dionex ICS 5000+ chromatography including a Dionex AERS 500 conductivity suppressor, Thermo Fisher, Waltham, MA, USA) using an anion exchange column (Dionex IonPac AS11, Thermo Fisher, Waltham, MA, USA). A guard column (Dionex IonPac AG11, Thermo Fisher, Waltham, MA, USA) was connected upstream for protection of the analytical column and the system was

saturated with N<sub>2</sub> to prevent dissolution of atmospheric CO<sub>2</sub> forming undesired carbonates. A total of 12 mM NaOH was used as mobile phase with a constant flow of 1.2 mL/min and the system was run isocratically at 25 °C. Remaining trace anion contaminants in the hydroxide eluent were removed using an anion trap column (Dionex ASTC 500, Thermo Fisher, Waltham, MA, USA). PO<sub>4</sub> was quantified with a conductivity detector (Thermo Fisher, Waltham, MA, USA) using dilutions of NaH<sub>2</sub>PO<sub>4</sub> as standards [34].

#### Colorimetric Assay Kit

The inorganic PO<sub>4</sub> concentration was determined colorimetrically using a colorimetric assay kit [37]. Measurements and the calibration curve were conducted according to the product manual [37]. Two hundred µL samples (or diluted samples) were mixed with 30 µL PO<sub>4</sub> reagent on a 96-well plate. After 30 min incubation at room temperature, absorbance at 650 nm was measured for PO<sub>4</sub> quantification.

#### Cedex Bio HT Analyzer

The inorganic PO<sub>4</sub> concentration was determined colorimetrically using the Cedex Bio HT analyzer (Roche, Basel, Switzerland) applying the Phosphate Bio HT test kit (Ref 06990088001).

### 3. Results

In this study we directly compared the production of a recombinant model Fab in *E. coli* using the T7lac (pET) and the phoA (pAT) expression system under equal cultivation conditions. We analyzed and compared cell physiology as well as soluble and IB product formation.

#### 3.1. Characterization of T7lac-Based Fab Production (pET)

In all pET cultivations we performed a non-induced fed-batch ( $\mu = 0.1 \text{ h}^{-1}$ , 35 °C) to a biomass concentration of 30 g/L DCW, followed by an IPTG induction phase at different  $\mu$  (0.1 h<sup>-1</sup> and 0.05 h<sup>-1</sup>) and cultivation temperatures (35 °C and 30 °C). Induction was completed by commonly performed one-point addition of IPTG to a final concentration of 0.1 mM [35,36]. Strain physiology and product-related data were evaluated after 4 h and 8 h of induction which was comparable to reported induction times in literature [12,38].

##### 3.1.1. Strain Physiology

The most important strain physiological parameters are summarized in Table 1 and extended data are given in Supplementary Table S1. Obtained  $Y_{X/S}$  (biomass/substrate yield) and  $Y_{\text{CO}_2/S}$  (CO<sub>2</sub>/substrate yield) of the strain cultivated under different conditions were comparable, however, at the higher  $\mu = 0.1 \text{ h}^{-1}$  glucose accumulated over time indicating cellular stress. This was also underlined by calculating the real  $\mu$  of the cultures, which were only half of the set values at the end of cultivation (Supplementary Table S1). Although the  $Y_{\text{CO}_2/S}$  changed over time, indicating a metabolic shift [39], even the soft-sensor was not able to react properly to these physiological changes, leading to overfeeding of the cells and consequent glucose accumulation. At  $\mu = 0.1 \text{ h}^{-1}$  and 35 °C we also observed cell lysis (indicated by foam formation and an increase in extracellular DNA content) (Supplementary Table S5). In contrast, in cultivations completed at a lower  $\mu = 0.05 \text{ h}^{-1}$  the calculated  $\mu$  corresponded well to the set values. Recoveries of total carbon in all cultivations were similar, resulting in C-balances of 0.78–0.85 (Table 1). We attribute minor cell lysis to be the reason for non-closing C-balances [40,41]. As also shown before [42], we demonstrated that even a relatively low  $\mu = 0.1 \text{ h}^{-1}$  during induction of a pET system negatively impacts cell physiology and leads to cell lysis.

Table 1. Strain physiological parameters for pET cultivations.

Cultivation	$\mu$	Temp.	Induction	DCW	Glucose	Acetate	$Y_{X/S}$	$Y_{CO_2/S}$	C-Balance
	(h <sup>-1</sup> )								
pET 1	0.1	35	4 h	40.1	1.52	0	0.33	0.47	0.80
			8 h	40.3 <sup>+</sup>	93.1	0.42	n.d.*	n.d.*	n.d.*
pET 2	0.1	30	4 h	41.3	0.93	0.87	0.36	0.47	0.85
			8 h	42.6	21.7	0	0.25	0.61	0.84
pET 3	0.05	35	4 h	33.9	0	0.33	0.33	0.52	0.85
			8 h	36.9	0	0	0.27	0.56	0.83
pET 4	0.05	30	4 h	36.4	0	0.52	0.37	0.48	0.85
			8 h	40.4	0	0.59	0.27	0.51	0.78

<sup>+</sup> biomass concentration was calculated from OD<sub>600</sub> due to unreliable values obtained from gravimetric determination resulting from cell lysis (OD<sub>600</sub>/DCW correlation: DCW = 0.3077 × OD<sub>600</sub>; R<sup>2</sup> = 1). \* not determined due to cell lysis. Abbr.:  $Y_{X/S}$ , biomass/substrate yield;  $Y_{CO_2/S}$ , CO<sub>2</sub>/substrate yield.

### 3.1.2. Fab Productivity

Most of the recombinant Fab was found as IBs in all pET cultivations independent from the cultivation conditions and induction time (Table 2)—in fact 5–10 times more IBs than soluble product was formed (Supplementary Table S2). We confirmed that a higher temperature during induction favored IB formation [43,44]. However, we could still find soluble Fab. At 30 °C we obtained specific titers of up to 2.89 mg/g DCW resulting in a volumetric titer of nearly 120 mg Fab/L cultivation broth. We confirmed that a lower temperature during induction of a pET system favored the formation of soluble product [26,45]. In contrast to the temperature,  $\mu$  had no considerable impact on specific Fab titers—neither soluble nor IBs. As expected, extended induction times led to a shift from the production of soluble Fab towards IB formation (Table 2) which can be addressed to an extended exposure to metabolic stress [24]. Possibilities to overcome this problem could be a reduction of applied inducer concentration or the continuous addition of IPTG in a specific ratio to the biomass during induction [35,46]. Summarizing, the highest specific soluble Fab titer was achieved at 30 °C after 4 h induction independent from  $\mu$ . This result is comparable to data published previously [12].

Table 2. Fab productivity for pET cultivations.

Cult.	$\mu$	Temp.	Ind.	Fab Insoluble (IBs)			Fab Soluble			Ratio
				Spec. Titer	Vol. Titer	STY	Spec. Titer	Vol. Titer	STY	
	(h <sup>-1</sup> )	(°C)	(h)	(mg/g)	(mg/L)	(mg/L/h)	(mg/g)	(mg/L)	(mg/L/h)	IB:SP *
pET 1	0.1	35	4 h	19.5	782.6	33.4	2.22	89.0	3.79	8.8
			8 h	22.2	896.6	32.2	1.89	76.5	2.75	11.8
pET 2	0.1	30	4 h	14.9	613.0	26.0	2.89	119.5	5.07	5.1
			8 h	22.1	942.4	33.9	2.42	102.9	3.71	9.1
pET 3	0.05	35	4 h	20.4	693.6	29.3	2.38	80.6	3.41	8.6
			8 h	24.6	907.7	33.5	2.20	82.0	2.99	11.2
pET 4	0.05	30	4 h	12.0	436.5	18.3	2.81	102.9	4.32	4.2
			8 h	20.9	841.0	30.4	2.50	101.5	3.67	8.3

\* ratio of insoluble (IB) Fab titer compared to soluble (SP) Fab titer. Abbr.: STY, space-time yield.

### 3.2. Characterization of phoA-Based Fab Production (pAT)

The main goal of the study was to investigate Fab production under the control of the *E. coli* phoA system in detail. In contrast to the T7lac promoter, the phoA promoter is recognized by the *E. coli* RNA polymerase and is regulated under PO<sub>4</sub>-limiting conditions [3,24,47]. Successful Fab production under control of the phoA promoter has been reported before (e.g., [3,9,48]). In this study we performed a batch cultivation at 35 °C followed by a single-phase fed-batch until PO<sub>4</sub> starvation (indicated by stagnation of the CO<sub>2</sub> off-gas signal) at different  $\mu$  and temperatures. Required PO<sub>4</sub> in the cultivation medium for generation of 50 g/L DCW was calculated based on the elemental biomass composition of *E. coli* W3110 and provided in the batch medium considering the PO<sub>4</sub> carry-over from the

pre-culture. Physiology and productivity were evaluated at PO<sub>4</sub> starvation, but also before PO<sub>4</sub> limitation was reached (>1 mM PO<sub>4</sub>) since the shake flask screening experiments indicated product formation already at non-limiting PO<sub>4</sub> conditions (data not shown).

### 3.2.1. Impact of Cultivation Conditions on the Overall Cultivation Time

In contrast to pET cultivations, which were all induced for 8 h, the end of pAT cultivations was determined by the time point of PO<sub>4</sub> starvation, indicated by the stagnation of CO<sub>2</sub> in the off-gas signal. Obviously, the overall cultivation time strongly depended on set cultivation conditions (Table 3).

**Table 3.** Impact of cultivation conditions on cultivation times for pAT cultivations.

Cultivation	$\mu$	Temp.	Sample	PO <sub>4</sub> Conc.	Cultivation Time
	(h <sup>-1</sup> )	(°C)	(-)	(mM)	(h)
pAT 1	0.1	35	>1 mM PO <sub>4</sub>	2.37	22.3
			PO <sub>4</sub> starvation	0.16	27.3
pAT 2	0.1	30	>1 mM PO <sub>4</sub>	2.82	22.4
			PO <sub>4</sub> starvation	<0.10	25.2
pAT 3	0.05	35	>1 mM PO <sub>4</sub>	4.57	43.2
			PO <sub>4</sub> starvation	0.39 *	54.8
pAT 4	0.05	30	>1 mM PO <sub>4</sub>	4.46	37.1
			PO <sub>4</sub> starvation	0.10	47.3

\* higher due to potential cell lysis.

Interestingly, at  $\mu = 0.05 \text{ h}^{-1}$  we observed an impact of the cultivation temperature on the time needed until PO<sub>4</sub> starvation: at 35 °C the cultivation took significantly longer than at 30 °C (Table 3). Since the specific PO<sub>4</sub> uptake rates ( $q_{\text{PO}_4}$ ) in cultivations pAT 3 and pAT 4 were similar (Table 4), we believe that the increased temperature in combination with the low  $\mu = 0.05 \text{ h}^{-1}$  caused partial cell lysis, thus the release of intracellular PO<sub>4</sub> into the broth. This hypothesis was underlined by the higher PO<sub>4</sub> concentration (Table 3; pAT 3) as well as significant lower  $Y_{X/S}$  and biomass concentration at the end of the cultivation (Table 4).

### 3.2.2. Strain Physiology

The most important strain physiological parameters are summarized in Table 4 and extended data are shown in Supplementary Table S3. Physiological yields obtained under non-limiting conditions (>1 mM PO<sub>4</sub>) were similarly independent from cultivation conditions, except for cultivation pAT 3. It seems that for the strain harboring the *phoA* system, a combination of low  $\mu$  and high temperature (pAT 3) implies increased metabolic burden leading to cell lysis (indicated by foam formation and an increased extracellular DNA content; Supplementary Table S5). Despite this, we observed a shift towards decreased  $Y_{X/S}$  and increased  $Y_{\text{CO}_2/S}$  during the phase of PO<sub>4</sub> starvation in all cultivations, indicating metabolic change [49]. At 35 °C, C-balances were between 0.8 and 0.9, whereas at 30 °C C-balances were close to 1. Determined  $q_{\text{PO}_4}$  correlated with the applied  $\mu$  at >1 mM PO<sub>4</sub>, giving a two-fold higher  $q_{\text{PO}_4}$  at  $\mu = 0.1 \text{ h}^{-1}$ . Although hardly any PO<sub>4</sub> uptake was determined during the PO<sub>4</sub> limitation phase (Table 4), surprisingly the biomass concentration still increased. We hypothesized a metabolic shift from uptake of extracellular towards utilization of intracellular, stored PO<sub>4</sub> to be the reason [50,51]. The calculated  $\mu$  correlated well with the set  $\mu$  (except for cultivation pAT 3) underlining the stability of these cultivations as well as the applicability of the soft-sensor-based feeding control. Overall, strain physiological parameters of pAT cultivations showed that 35 °C negatively affects physiology and viability, especially at a low  $\mu = 0.05 \text{ h}^{-1}$ .



**Table 4.** Strain physiological parameters for pAT cultivations.

Cult.	$\mu$ (h <sup>-1</sup> )	Temp. (°C)	Sample ( $\epsilon$ )	DCW (g/L)	qPO <sub>4</sub> (mmol/g/h)	Glucose (g/L)	Acetate (g/L)	Y <sub>xs</sub> (C-mol/C-mol)	Y <sub>CO<sub>2</sub>s</sub> (C-mol/C-mol)	C-Balance ( $\epsilon$ )
pAT 1	0.1	35	>1 mM PO <sub>4</sub> PO <sub>4</sub> starvation	42.8 53.2	0.112 0.008	0 1.70	0.28 0.99	0.45 0.30	0.42 0.49	0.87 0.80
pAT 2	0.1	30	>1 mM PO <sub>4</sub> PO <sub>4</sub> starvation	47.6 52.0	0.097 0.018	0 0	0.46 0.69	0.44 0.27	0.52 0.85	0.96 1.13
pAT 3	0.05	35	>1 mM PO <sub>4</sub> PO <sub>4</sub> starvation	31.8 47.1	0.052 0.008	0 0	- 0.34	0.20 0.32	0.65 0.57	0.85 0.89
pAT 4	0.05	30	>1 mM PO <sub>4</sub> PO <sub>4</sub> starvation	43.0 52.6	0.055 0.008	0 0	0.28 0.58	0.47 0.29	0.49 0.70	0.97 0.99

 Abbr.: qPO<sub>4</sub>, specific phosphate uptake rate; Y<sub>xs</sub>, biomass/substrate yield; Y<sub>CO<sub>2</sub>s</sub>, CO<sub>2</sub>/substrate yield.

### 3.2.3. Fab Productivity

Independent of cultivation conditions, we observed soluble Fab production already at non-limiting  $\text{PO}_4$  conditions ( $>1 \text{ mM PO}_4$ ), indicating incomplete promoter repression (Table 5 and Supplementary Table S4). Although the *phoA* promoter is usually tightly controlled, protein expression at increased  $\text{PO}_4$  concentrations has been reported before [24]. Since the *phoA* promoter also controls chromosomal alkaline phosphatase, it is hypothesized that competition between chromosomal and plasmid DNA for the repressors involved in regulation of *phoA*-based gene expression might be the reason for leaky expression [24,52].

In all pAT cultivations, soluble Fab was produced with specific titers ranging from 2.28–6.09 mg/g DCW. Interestingly, only during  $\text{PO}_4$  starvation of cultivations at  $\mu = 0.05 \text{ h}^{-1}$  IB formation was observed, indicating a high metabolic burden under these conditions—probably due to increased recombinant expression [53]. Cultivation of pAT 4 at  $\mu = 0.05 \text{ h}^{-1}$  and  $30 \text{ }^\circ\text{C}$  delivered the highest soluble Fab titer yielding 6.09 mg/g DCW and 321 mg/L cultivation broth. However, due to the long cultivation time the space-time yield (STY) was only 6.77 mg/L/h. Summarizing, *phoA*-based Fab production is favored at low temperatures as well as low  $\mu$ , which leads to long cultivation times, but results in high titers of soluble Fab.

### 3.3. Direct Comparison of T7lac- and *phoA*-Based Fab Production

Important criteria for industrial production processes are volumetric product titer as well as STY, whereas the latter is more important regarding economic feasibility by incorporation of process time [54]. In Figure 1 we compare the pET and the pAT system under the conditions giving the highest productivity of soluble Fab, namely cultivation pET 2 after 4 h induction time (called pET 2\_a4; Table 2) as well as cultivation pAT 4 at  $\text{PO}_4$  starvation (called pAT 4\_st; Table 5). Under these conditions, Fab expression under the control of the T7lac promoter led to five-fold higher formation of IBs compared to soluble Fab, whereas *phoA*-based expression gave comparable amounts of IBs and soluble Fab. Cultivation pAT 4\_st resulted in a three times higher volumetric soluble Fab titer compared to the pET cultivation and, despite the long cultivation time, the final STY was 1.3-fold higher. Thus, we underline the great potential of the easy-to-use pAT system as an interesting alternative to the well-known pET system for the production of periplasmic products, as also reported before [3].

**Table 5.** Fab productivity for pAT cultivations.

Cult.	$\mu$ $h^{-1}$	Temp. (°C)	Sample (-)	Fab Insoluble (IBs)			Fab Soluble			Ratio IB:SP *
				Spec. Titer (mg/g)	Vol. Titer (mg/L)	STY (mg/L/h)	Spec. Titer (mg/g)	Vol. Titer (mg/L)	STY (mg/L/h)	
pAT 1	0.1	35	>1 mM PO <sub>4</sub>	0	0	0	2.28	97.30	4.36	n.a.
			PO <sub>4</sub> starvation	0	0	0	3.21	170.9	6.24	n.a.
pAT 2	0.1	30	>1 mM PO <sub>4</sub>	0	0	0	2.95	140.4	6.27	n.a.
			PO <sub>4</sub> starvation	0	0	0	2.91	150.1	5.98	n.a.
pAT 3	0.05	35	>1 mM PO <sub>4</sub>	0	0	0	2.53	80.62	1.86	n.a.
			PO <sub>4</sub> starvation	8.16	385.0	7.02	2.54	119.5	2.18	3.2
pAT 4	0.05	30	>1 mM PO <sub>4</sub>	0	0	0	4.63	198.8	5.37	n.a.
			PO <sub>4</sub> starvation	7.88	414.2	8.76	6.09	321.1	6.77	1.3

\* ratio of insoluble (IB) Fab titer compared to soluble (SP) Fab titer: n.a., not applicable. Abbr.: STY, space-time yield.

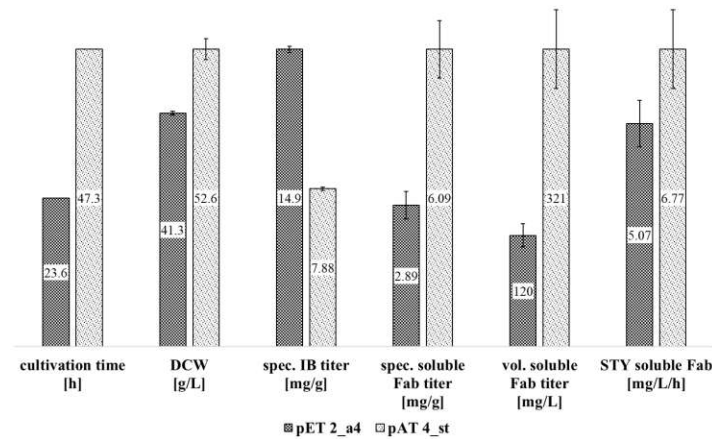


**Figure 1.** Comparison of cultivation times, biomass concentrations and Fab production of the T7lac (pET 2\_a4) and the phoA expression system (pAT 4\_st) under conditions resulting in the highest space-time yield (STY) of soluble Fab. Fab production using the pET system gave highest productivity in cultivation at  $\mu = 0.1 \text{ h}^{-1}$  and 30 °C after 4 h induction time (pET 2\_a4). The pAT system gave highest productivity in cultivation at  $\mu = 0.05 \text{ h}^{-1}$  and 30 °C until PO<sub>4</sub> starvation (pAT 4\_st). Presented standard deviations result from analytical measurements which were performed in triplicates.

3.4. Detailed Characterization of the pAT System

3.4.1. PO<sub>4</sub> Monitoring

In this study we explored the impact of extracellular PO<sub>4</sub> concentration on strain physiology and product formation of the pAT system in more detail, to extend knowledge about this valuable system. In this respect, we also investigated and compared different methods for determination of extracellular PO<sub>4</sub> in the culture broth for their suitability as an at-line PO<sub>4</sub> monitoring tool. An overview of the evaluated methods is given in Table 6.

**Table 6.** Overview of investigated analytical methods for PO<sub>4</sub> monitoring.

	ICP-OES	IC	Colorimetric Kit	Cedex Bio HT
Analyte	P	PO <sub>4</sub>	PO <sub>4</sub>	PO <sub>4</sub>
Limit of Quantification	65 µmol/L	4 µmol/L	5 µmol/L	100 µmol/L
Equipment costs	-	-	+	-
Sample preparation	-	-	-	+
Operator's impact	~	~	-	+
Time	>>30 min	>>30 min	>>30 min	15 min
Automation	-	-	-	+
At-line measurement	-	-	-	+

Features are evaluated to be (1) advantageous (+); (2) disadvantageous (-) or (3) intermediate (~). Abbr.: ICP-OES, inductively coupled plasma-optical emission spectroscopy; IC, ion chromatography; P, phosphorus; PO<sub>4</sub>, phosphate.

ICP-OES

In contrast to the other investigated methods, ICP-OES determines elemental phosphorus (P) instead of inorganic PO<sub>4</sub>. In case PO<sub>4</sub> describes the only P source of the sample, obtained P contents correlated well with PO<sub>4</sub> concentrations (data not shown). However, contamination of the sample with other P sources, e.g., organophosphates from complex media or polyphosphates, nucleic acids and membrane lipids from cells [25,27], complicate a valid correlation with PO<sub>4</sub>. In this regard, missing selectivity for PO<sub>4</sub> describes a major

drawback of this method. In addition, the limit of quantification (LOQ) of 65  $\mu\text{M}$  is also rather high compared to other methods (Table 6). ICP-OES also requires costly equipment as well as an argon supply for measurement. Furthermore, the method needs expertise and routine by the analyst, and is time consuming concerning sample preparation (HCl treatment) and manual dilution, which hampers the usage for at-line monitoring.

#### IC

IC allows direct quantification of inorganic  $\text{PO}_4$  with a very low LOQ of 4  $\mu\text{M}$ . However,  $\text{PO}_4$  detection is highly affected by contaminating anions in the eluent, which have to be either removed (anion trap column) or their formation prevented (saturation with  $\text{N}_2$ ). Furthermore, the impact of the sample matrix (*E. coli* culture broth) on the detection performance (peak fronting and peak maxima shifts) describes a major drawback of this method (data not shown). Acquisition costs for equipment (IC system and chromatography columns) are considerable as well as the requirement for continuous  $\text{N}_2$  supply. Performance of IC is usually quite simple; however, the required sample treatment and manual dilution describe potential error risks. Finally, the overall procedure, comprising sample preparation and IC sequence (30 min), may take up more than 60 min, which makes IC-based  $\text{PO}_4$  detection not suitable for at-line monitoring.

#### Phosphate Colorimetric Assay Kit

Performance of a  $\text{PO}_4$  colorimetric assay (PCA) allows quantification of inorganic  $\text{PO}_4$ . The method is based on the reaction of  $\text{PO}_4$  with a chromogenic complex that results in a colorimetric product. The PCA provides a low LOQ (5  $\mu\text{M}$ ; Table 6) and only requires a plate reader or simple photometer. The PCA is intended for measurement of low  $\text{PO}_4$  concentrations (blood or wastewater) [37], which explains the very low linear detection range (5–25  $\mu\text{M}$ ). However, high sample dilutions are necessary, which requires tedious pipetting work. Therefore, the overall procedure (sample preparation, incubation time and measurement) can take up 1–1.5 h.

#### Cedex Bio HT

The Cedex Bio HT analyzer is a completely automated instrument that allows simultaneous measurement of up to 90 samples. Furthermore, up to 32 test kits can be loaded at the same time [39]. Application of the Phosphate Bio HT kit [40] allows the quantitative determination of inorganic  $\text{PO}_4$ . The LOQ is rather high (100  $\mu\text{M}$ ; Table 6), which describes the major drawback of this method. Furthermore, acquisition costs for the analyzer and the test kits are significantly higher compared to PCA. However,  $\text{PO}_4$  measurement using the Cedex Bio HT provides several advantages as sample preparation is quite simple and samples are diluted automatically. Therefore, measurement results can be obtained within 15 min, which is essential for at-line based  $\text{PO}_4$  monitoring.

Summarizing, investigation of described  $\text{PO}_4/\text{P}$  detection methods revealed the Cedex Bio HT system to be most suitable for required at-line  $\text{PO}_4$  monitoring. Therefore, this method was chosen to be used for the detailed investigation of the pAT system.

#### 3.4.2. Impact of $\text{PO}_4$ Conditions on Strain Physiology

To analyze the pAT system in more detail, we performed batch cultivations at 35  $^\circ\text{C}$ , followed by a single-phase fed-batch until  $\text{PO}_4$  starvation at  $\mu = 0.05 \text{ h}^{-1}$  and 30  $^\circ\text{C}$ . The main strain physiological parameters are summarized in Table 7 and extended data are shown in Supplementary Table S6. The bioreactor cultivation was performed in triplicates. The standard deviations for all calculated rates and yields were below 10%. The required process time (45 h) and obtained biomass concentration at cultivation end (49 g/L DCW) were comparable to the respective small-scale experiment in the 2 L scale. The  $\text{CO}_2$  off-gas signal was monitored for process evaluation and determination of cultivation end (Figure 2).

**Table 7.** Strain physiological parameters of *E. coli* W3110 harboring the *phoA* expression system at different extracellular  $\text{PO}_4$  concentrations.

Process Time (h)	DCW (g/L)	$\mu$ ( $\text{h}^{-1}$ )	$c\text{PO}_4$ (mM)	$q\text{PO}_4$ (mmol/g/h)	$Y_{\text{CO}_2/\text{S}}$ (C-mol/C-mol)	$Y_{\text{X}/\text{S}}$ (C-mol/C-mol)	C-Balance (-)
27.4	29.0	n.a.	33.5	n.a.	0.54	0.55	1.09
29.3	30.7	0.040	27.5	0.090	0.58	0.38	0.98
31.3	32.0	0.036	24.3	0.059	0.59	0.32	0.89
33.3	34.3	0.049	20.2	0.053	0.58	0.42	0.99
35.3	37.0	0.054	14.6	0.070	0.57	0.45	1.01
37.3	39.0	0.045	8.7	0.071	0.56	0.36	0.91
39.3	41.4	0.049	3.6	0.061	0.56	0.38	0.93
41.3	45.5	0.070	1.9	0.018	0.54	0.54	1.07
43.3	48.7	0.057	0.13	0.018	0.56	0.43	0.99
45.0 *	48.9	0.021	<0.10	0.0003	0.82	0.19	0.99

n.a. not applicable, since this is the initial sample for characterization and calculation of specific rates. \* time point of harvest. Abbr.: DCW, dry cell weight;  $\mu$ , specific growth rate;  $c\text{PO}_4$ , extracellular phosphate concentration;  $q\text{PO}_4$ , specific  $\text{PO}_4$  uptake rate;  $Y_{\text{CO}_2/\text{S}}$ ,  $\text{CO}_2$ /substrate yield;  $Y_{\text{X}/\text{S}}$ , biomass/substrate yield.

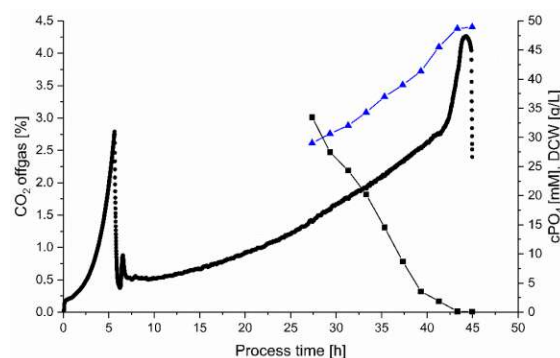


**Figure 2.** Time courses of  $\text{CO}_2$  off-gas signal (black dots); extracellular  $\text{PO}_4$  concentration ( $c\text{PO}_4$ ; black squares) and *E. coli* dry cell weight (DCW; blue triangles) during fed-batch cultivation until  $\text{PO}_4$  starvation (indicated by a stagnation of the  $\text{CO}_2$  off-gas signal at around 43 h). The sudden drop of the  $\text{CO}_2$  off-gas signal at the end of cultivation (45 h) resulted from stopping the feed pump (C-source limitation) prior to cultivation end.

Under non-limiting  $\text{PO}_4$  conditions ( $>1$  mM), the  $\text{CO}_2$  signal showed the expected trend for an exponential feeding regime. However, during  $\text{PO}_4$  limitation we observed a fast increase in the  $\text{CO}_2$  signal indicating a metabolic shift of the *E. coli* cells. This assumption was confirmed by evaluation of physiological yields, which were quite constant under non-limiting  $\text{PO}_4$  conditions, but shifted towards increased  $Y_{\text{CO}_2/\text{S}}$  and decreased  $Y_{\text{X}/\text{S}}$  during  $\text{PO}_4$  limitation (Supplementary Table S6). Our results confirm that  $\text{PO}_4$  limitation triggers metabolic burden and physiological changes [55]. However, no considerable cell lysis was observed, which was supported by obtained C-balances between 0.9 and 1.1, even under  $\text{PO}_4$  limitation (Table 7). Although hardly any  $\text{PO}_4$  was taken up during  $\text{PO}_4$  limitation, interestingly the biomass concentration still slightly increased (Supplementary Table S6). We assume a metabolic shift from uptake of extracellular towards consumption of intracellular, stored  $\text{PO}_4$  to be the reason [50,51]. Therefore, we investigated the intracellular phosphorus (P) content during cultivation under non-limiting and limiting  $\text{PO}_4$  conditions (Supplementary Figure S1). The intracellular P content (initial value of 2.3%; [56]) started to decrease already at a  $\text{PO}_4$  concentration of around 5 mM. At this  $\text{PO}_4$  concentration also  $q\text{PO}_4$  strongly decreased (Table 7). These results confirmed our hypothesis that *E. coli* accumulates polyphosphate as  $\text{PO}_4$  reservoir that is reused, when needed [57,58]. At  $\text{PO}_4$  starvation, cell metabolism started to break down, indicated by the stagnation of

the CO<sub>2</sub> off-gas signal and glucose accumulation in the culture broth (data not shown). In conclusion, limiting PO<sub>4</sub> conditions highly affect cell physiology and PO<sub>4</sub> starvation, ultimately results in collapsing cell metabolism (data not shown).

### 3.4.3. Impact of PO<sub>4</sub> Conditions on Fab Productivity

Recombinant Fab production was already observed at non-limiting PO<sub>4</sub> conditions indicating incomplete repression of the *phoA* promoter (Table 8). Although the *phoA* promoter system is usually tightly controlled, protein expression at increased PO<sub>4</sub> concentrations has been reported before [24,59]: competition of plasmid and chromosomal DNA for the repressors involved in regulation of *phoA*-controlled gene expression have been reported to be the reason for leaky expression [24,52,59]. However, we clearly see a boost in qFab at PO<sub>4</sub> concentrations of <1 mM (Table 8; Figure 3). Finally, a maximum specific and volumetric Fab titer of 7.2 mg/g DCW and 350 mg/L cultivation broth, respectively, was obtained at the end of cultivation.

**Table 8.** Fab productivity of *E. coli* W3110 harboring the pAT expression system at different PO<sub>4</sub> concentrations.

Process Time (h)	cPO <sub>4</sub> (mM)	qPO <sub>4</sub> (mmol/g/h)	Spec. Fab Titer (mg/g)	Vol. Fab Titer (mg/L)	qFab (mg/g/h)	Fab STY (mg/L/h)
27.4	33.5	n.a.	5.26	153	n.a.	n.a.
29.3	27.5	0.090	5.46	167	0.31	9.4
31.3	24.3	0.059	5.65	181	0.29	9.2
33.3	20.2	0.053	5.56	191	0.23	7.6
35.3	14.6	0.070	5.49	203	0.26	9.3
37.3	8.7	0.071	5.72	223	0.37	14.0
39.3	3.6	0.061	5.77	239	0.31	12.4
41.3	1.9	0.018	5.73	261	0.38	16.6
43.3	0.13	0.018	6.43	313	0.69	32.5
45.0 *	<0.10	0.0003	7.15	350	0.59	28.6

n.a. not applicable, since this is the initial sample for characterization and calculation of specific rates. \* time point of harvest. Abbr.: qFab, specific product formation rate; Fab STY, Fab space-time yield.

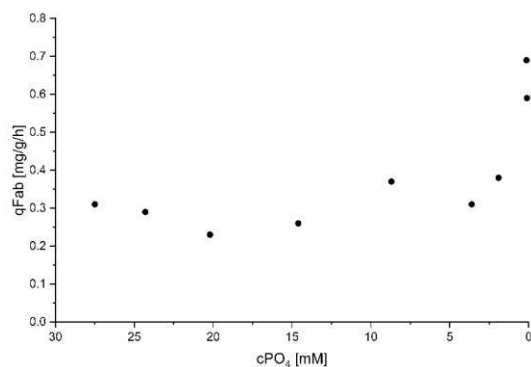


**Figure 3.** Specific product formation rate (qFab) as a function of the extracellular PO<sub>4</sub> concentration (cPO<sub>4</sub>) during fed-batch cultivation until PO<sub>4</sub> starvation. The average standard deviation was quantified with 9.69%.

## 4. Discussion

In a recent study, Luo et al. showed the high potential of the pAT system for the extracellular production of a series of Fabs [3]. The pAT system allows auto-induction regulated by limitation of phosphate (PO<sub>4</sub>) in the cultivation broth. In contrast to the

established pET system, it does not require the addition of expensive/toxic inducers and allows simple process regimes. However, detailed information regarding performance under different cultivation conditions, especially  $\text{PO}_4$  concentrations, is scarce.

In this study we directly compared the commonly used T7-based pET expression system and the pAT system for the recombinant production of a model Fab in *E. coli* under equal cultivation conditions and then investigated the pAT system in detail. For directly comparing the pET and the pAT system we chose cultivation conditions which (1) have been reported in literature for these systems before (e.g., [60–63]), and (2) can be also implemented on an industrial scale. Even though literature also discusses much lower cultivation temperatures below 30 °C especially for the T7 expression system (e.g., [64–68]), we chose 30 °C and 35 °C as these temperatures are feasible and can be controlled at large scales [69]. Even though we believe that lower temperatures during induction boost the formation of soluble product, we considered potential limitations in cooling capacities at large scales for our experimental design. Besides, we aimed for a direct comparison of the two-expression systems pET and pAT under equal cultivation conditions and thus chose conditions which have been reported for both systems before [3]. We also neglected the use of an autoinduction medium based on lactose for the T7 system (e.g., [68,70,71]) in the current study, as this type of medium is not widely accepted in the biopharmaceutical industry. For T7-based pET expression systems induction by IPTG is still the state-of-the-art. Since the DE3 system is not required for phoA-based recombinant protein production, we used an *E. coli* W3110 chassis strain for investigating the pAT system. This *E. coli* strain has been used for such purposes before [50,72]. The cultivations for strain characterization of the pET and the pAT system were performed only once—however, closing C-balances confirm the accuracy of the data.

In our study, we underline the recent findings of Luo et al. [3] of the superiority of the pAT system compared to the T7-based pET system. Under comparable cultivation conditions, the pET system resulted in a five-fold higher formation of Fab IBs compared to soluble Fab, whereas the pAT system gave comparable amounts of IBs and soluble Fab. To get better understanding and extend the current knowledge of the valuable pAT system we characterized this system in more detail. The phoA-based recombinant protein production in *E. coli* is typically executed until  $\text{PO}_4$  starvation (<0.1 mM; [3,9,24,73]). However, in this study we showed that cultivation until  $\text{PO}_4$  starvation induces drastic physiological changes (Table 7), ultimately resulting in collapsing cell metabolism and potential product loss. As extracellular  $\text{PO}_4$  already depletes several hours before  $\text{PO}_4$  starvation it is tricky to identify the optimal time point of harvest in a typical fed-batch cultivation. Based on our findings that qFab is already quite high at  $\text{PO}_4$  concentrations >0.1 mM (Table 8), we recommend to use the CEDEX Bio HT device to monitor the fed-batch until a  $\text{PO}_4$  concentration close to 0.1 mM is reached. Then we suggest to add  $\text{PO}_4$  to the feed medium to allow extended cultivation at this  $\text{PO}_4$  concentration in the bioreactor and thus obtain a boosted STY. Summarizing, our study extends the knowledge on the *E. coli* phoA expression system and demonstrates its high potential for the successful production of periplasmic products in *E. coli*.

**Supplementary Materials:** The following supporting information can be downloaded at: <https://www.mdpi.com/article/10.3390/fermentation8040181/s1>, Figure S1: Time courses of extracellular  $\text{PO}_4$  concentration in the culture broth (black circles) and intracellular P content of the *E. coli* W3110 biomass (blue squares) during fed-batch cultivation until  $\text{PO}_4$  starvation; Table S1: Extended strain physiological parameters for pET cultivations; Table S2: Extended Fab production data for pET cultivations; Table S3: Extended strain physiological parameters for pAT cultivations.; Table S4: Extended Fab production data for pAT cultivations.; Table S5: Extracellular DNA contents of pET and pAT cultivations; Table S6: Extended overview of strain physiological parameters of *E. coli* W3110 harboring the phoA expression system at different extracellular  $\text{PO}_4$  concentrations.

**Author Contributions:** All authors contributed substantially to this work, in the form of: Conceptualization, O.S.; Methodology, O.S., S.K. (Stefan Kittler), T.G.; Formal Analysis, S.K. (Stefan Kittler),



T.G., J.K.; Investigation, S.K. (Stefan Kittler), T.G., S.K. (Sabine Kubicek); Writing—Original Draft Preparation, S.K. (Stefan Kittler), T.G.; Writing—Review & Editing, J.K., O.S.; Visualization, S.K. (Stefan Kittler), T.G., S.K. (Sabine Kubicek); Supervision, J.K., O.S.; Project Administration, O.S. All authors have read and agreed to the published version of the manuscript.

**Funding:** This research was funded by the Austrian Research Promotion Agency (FFG), project number 874206. The authors acknowledge TU Wien Bibliothek for financial support through its Open Access Funding by TU Wien.

**Institutional Review Board Statement:** Not applicable.

**Informed Consent Statement:** Not applicable.

**Data Availability Statement:** Not applicable.

**Acknowledgments:** Andreas Limbeck (TU Wien) is gratefully acknowledged for ICP-OES analyses. Mag. Johannes Theiner from University of Vienna (Microanalytical Laboratory) is gratefully acknowledged for determination of elemental biomass composition (intracellular phosphorus content). Peter Flotz assisted in the lab work. Alfred Gruber GmbH is gratefully thanked for supporting the research and being a project partner.

**Conflicts of Interest:** The authors declare no conflict of interest.

## References

- Holt, L.J.; Herring, C.; Jespers, L.S.; Woolven, B.P.; Tomlinson, I.M. Domain antibodies: Proteins for therapy. *Trends Biotechnol.* **2003**, *21*, 484–490. [[CrossRef](#)] [[PubMed](#)]
- Rodrigo, G.; Gruvegard, M.; Van Alstine, J.M. Antibody Fragments and Their Purification by Protein L Affinity Chromatography. *Antibodies* **2015**, *4*, 259–277. [[CrossRef](#)]
- Luo, M.; Zhao, M.; Cagliero, C.; Jiang, H.; Xie, Y.; Zhu, J.; Yang, H.; Zhang, M.; Zheng, Y.; Yuan, Y.; et al. A general platform for efficient extracellular expression and purification of Fab from *Escherichia coli*. *Appl. Microbiol. Biotechnol.* **2019**, *103*, 3341–3353. [[CrossRef](#)] [[PubMed](#)]
- Rosano, G.L.; Ceccarelli, E.A. Recombinant protein expression in *Escherichia coli*: Advances and challenges. *Front. Microbiol.* **2014**, *5*, 172. [[CrossRef](#)] [[PubMed](#)]
- Kadokura, H.; Katzen, F.; Beckwith, J. Protein disulfide bond formation in prokaryotes. *Annu. Rev. Biochem.* **2003**, *72*, 111–135. [[CrossRef](#)] [[PubMed](#)]
- Gundinger, T.; Spadiut, O. A comparative approach to recombinantly produce the plant enzyme horseradish peroxidase in *Escherichia coli*. *J. Biotechnol.* **2017**, *248*, 15–24. [[CrossRef](#)]
- Skerra, A.; Pluckthun, A. Assembly of a functional immunoglobulin Fv fragment in *Escherichia coli*. *Science* **1988**, *240*, 1038–1041. [[CrossRef](#)]
- Ukkonen, K.; Veijola, J.; Vasala, A.; Neubauer, P. Effect of culture medium, host strain and oxygen transfer on recombinant Fab antibody fragment yield and leakage to medium in shaken *E. coli* cultures. *Microb. Cell Fact.* **2013**, *12*, 73. [[CrossRef](#)]
- Carter, P.; Kelley, R.F.; Rodrigues, M.L.; Snedecor, B.; Covarrubias, M.; Velligan, M.D.; Wong, W.L.; Rowland, A.M.; Kotts, C.E.; Carver, M.E.; et al. High level *Escherichia coli* expression and production of a bivalent humanized antibody fragment. *Biotechnology* **1992**, *10*, 163–167. [[CrossRef](#)]
- Better, M.; Chang, C.P.; Robinson, R.R.; Horwitz, A.H. *Escherichia coli* secretion of an active chimeric antibody fragment. *Science* **1988**, *240*, 1041–1043. [[CrossRef](#)]
- Ellis, M.; Patel, P.; Edon, M.; Ramage, W.; Dickinson, R.; Humphreys, D.P. Development of a high yielding *E. coli* periplasmic expression system for the production of humanized Fab' fragments. *Biotechnol. Prog.* **2017**, *33*, 212–220. [[CrossRef](#)]
- Shibui, T.; Munakata, K.; Matsumoto, R.; Ohta, K.; Matsushima, R.; Morimoto, Y.; Nagahari, K. High-level production and secretion of a mouse-human chimeric Fab fragment with specificity to human carcino embryonic antigen in *Escherichia coli*. *Appl. Microbiol. Biotechnol.* **1993**, *38*, 770–775. [[CrossRef](#)] [[PubMed](#)]
- Kulmala, A.; Huovinen, T.; Lamminmaki, U. Effect of DNA sequence of Fab fragment on yield characteristics and cell growth of *E. coli*. *Sci. Rep.* **2017**, *7*, 3796. [[CrossRef](#)] [[PubMed](#)]
- Levy, R.; Ahluwalia, K.; Bohmann, D.J.; Giang, H.M.; Schwimmer, L.J.; Issafras, H.; Reddy, N.B.; Chan, C.; Horwitz, A.H.; Takeuchi, T. Enhancement of antibody fragment secretion into the *Escherichia coli* periplasm by co-expression with the peptidyl prolyl isomerase, FkpA, in the cytoplasm. *J. Immunol. Methods* **2013**, *394*, 10–21. [[CrossRef](#)] [[PubMed](#)]
- Lin, B.; Renshaw, M.W.; Autote, K.; Smith, L.M.; Calveley, P.; Bowdish, K.S.; Frederickson, S. A step-wise approach significantly enhances protein yield of a rationally-designed agonist antibody fragment in *E. coli*. *Protein Expr. Purif.* **2008**, *59*, 55–63. [[CrossRef](#)]
- Frenzel, A.; Hust, M.; Schirrmann, T. Expression of recombinant antibodies. *Front. Immunol.* **2013**, *4*, 217. [[CrossRef](#)]
- Rosano, G.A.-O.; Morales, E.S.; Ceccarelli, E.A.-O. New tools for recombinant protein production in *Escherichia coli*: A 5-year update. *Protein Sci.* **2019**, *28*, 1412–1422. [[CrossRef](#)]

18. Ukkonen, K.; Vasala, A.; Ojamo, H.; Neubauer, P. High-yield production of biologically active recombinant protein in shake flask culture by combination of enzyme-based glucose delivery and increased oxygen transfer. *Microb. Cell Fact.* **2011**, *10*, 107. [[CrossRef](#)]
19. Nadkarni, A.; Kelley, L.L.; Momany, C. Optimization of a mouse recombinant antibody fragment for efficient production from *Escherichia coli*. *Protein Expr. Purif.* **2007**, *52*, 219–229. [[CrossRef](#)]
20. Friedrich, L.; Stangl, S.; Hahne, H.; Kuster, B.; Kohler, P.; Multhoff, G.; Skerra, A. Bacterial production and functional characterization of the Fab fragment of the murine IgG1/lambda monoclonal antibody cmHsp70.1, a reagent for tumour diagnostics. *Protein Eng. Des. Sel. PEDS* **2010**, *23*, 161–168. [[CrossRef](#)]
21. Gupta, S.K.; Shukla, P. Microbial platform technology for recombinant antibody fragment production: A review. *Crit. Rev. Microbiol.* **2017**, *43*, 31–42. [[CrossRef](#)]
22. De Palma, A. Advances in protein expression. *Genet. Eng. Biotechnol. News* **2014**, *34*, 24–25, 27. [[CrossRef](#)]
23. Pack, P.; Kujau, M.; Schroeckh, V.; Knupfer, U.; Wenderoth, R.; Riesenberger, D.; Pluckthun, A. Improved bivalent miniantibodies, with identical avidity as whole antibodies, produced by high cell density fermentation of *Escherichia coli*. *Biotechnology* **1993**, *11*, 1271–1277. [[CrossRef](#)]
24. Shin, P.K.; Seo, J.H. Analysis of *E. coli* phoA-lacZ fusion gene expression inserted into a multicopy plasmid and host cell's chromosome. *Biotechnol. Bioeng.* **1990**, *36*, 1097–1104. [[CrossRef](#)] [[PubMed](#)]
25. Takagi, H.; Morinaga, Y.; Tsuchiya, M.; Ikemura, H.; Inouye, M. Control of Folding of Proteins Secreted by a High Expression Secretion Vector, pIN-III-ompA: 16-Fold Increase in Production of Active Subtilisin E in *Escherichia coli*. *Biotechnology* **1988**, *6*, 948. [[CrossRef](#)]
26. Harrison, J.S.; Keshavarz-Moore, E. Production of antibody fragments in *Escherichia coli*. *Ann. N. Y. Acad. Sci.* **1996**, *782*, 143–158. [[CrossRef](#)] [[PubMed](#)]
27. Baneyx, F. Recombinant protein expression in *Escherichia coli*. *Curr. Opin. Biotechnol.* **1999**, *10*, 411–421. [[CrossRef](#)]
28. Mergulhao, F.J.; Monteiro, G.A. Secretion capacity limitations of the Sec pathway in *Escherichia coli*. *J. Microb. Biotechnol.* **2004**, *14*, 128–133.
29. Zhang, L.; Cao, Y.; Liu, M.; Chen, X.; Xiang, Q.; Tian, J. Functional recombinant single-chain variable fragment antibody against *Agkistrodon acutus* venom. *Exp. Med* **2019**, *17*, 3768–3774. [[CrossRef](#)]
30. Ge, S.; Xu, L.; Li, B.; Zhong, F.; Liu, X.; Zhang, X. Canine Parvovirus is diagnosed and neutralized by chicken IgY-scFv generated against the virus capsid protein. *Vet. Res.* **2020**, *51*, 110. [[CrossRef](#)]
31. Sharma, S.K.; Suresh, M.R.; Wuest, F.R. Improved soluble expression of a single-chain antibody fragment in *E. coli* for targeting CA125 in epithelial ovarian cancer. *Protein Expr. Purif.* **2014**, *102*, 27–37. [[CrossRef](#)] [[PubMed](#)]
32. Wechselberger, P.; Sagmeister, P.; Herwig, C. Real-time estimation of biomass and specific growth rate in physiologically variable recombinant fed-batch processes. *Bioprocess Biosyst. Eng.* **2013**, *36*, 1205–1218. [[CrossRef](#)] [[PubMed](#)]
33. DeLisa, M.P.; Li, J.; Rao, G.; Weigand, W.A.; Bentley, W.E. Monitoring GFP-operon fusion protein expression during high cell density cultivation of *Escherichia coli* using an on-line optical sensor. *Biotechnol. Bioeng.* **1999**, *65*, 54–64. [[CrossRef](#)]
34. Wurm, D.J.; Veiter, L.; Ulonska, S.; Eggenreich, B.; Herwig, C.; Spadiut, O. The *E. coli* pET expression system revisited—mechanistic correlation between glucose and lactose uptake. *Appl. Microbiol. Biotechnol.* **2016**, *100*, 8721–8729. [[CrossRef](#)]
35. Marschall, L.; Sagmeister, P.; Herwig, C. Tunable recombinant protein expression in *E. coli*: Enabler for continuous processing? *Appl. Microbiol. Biotechnol.* **2016**, *100*, 5719–5728. [[CrossRef](#)]
36. Larentis, A.L.; Nicolau, J.F.M.Q.; dos Santos Esteves, G.; Vareschini, D.T.; de Almeida, F.V.R.; dos Reis, M.G.; Galler, R.; Medeiros, M.A. Evaluation of pre-induction temperature, cell growth at induction and IPTG concentration on the expression of a leptospiral protein in *E. coli* using shaking flasks and microbioreactor. *BMC Res. Notes* **2014**, *7*, 671. [[CrossRef](#)]
37. Gundinger, T.; Pansy, A.; Spadiut, O. A sensitive and robust HPLC method to quantify recombinant antibody fragments in *E. coli* crude cell lysate. *J. Chromatogr. B Anal. Technol. Biomed. Life Sci.* **2018**, *1083*, 242–248. [[CrossRef](#)]
38. Wurm, D.J.; Quehenberger, J.; Mildner, J.; Eggenreich, B.; Slouka, C.; Schwaighofer, A.; Wieland, K.; Lendl, B.; Rajamanickam, V.; Herwig, C.; et al. Teaching an old pET new tricks: Tuning of inclusion body formation and properties by a mixed feed system in *E. coli*. *Appl. Microbiol. Biotechnol.* **2018**, *102*, 667–676. [[CrossRef](#)]
39. Marisch, K.; Bayer, K.; Cserjan-Puschmann, M.; Luchner, M.; Striedner, G. Evaluation of three industrial *Escherichia coli* strains in fed-batch cultivations during high-level SOD protein production. *Microb. Cell Fact.* **2013**, *12*, 58. [[CrossRef](#)]
40. Rajamanickam, V.; Wurm, D.; Slouka, C.; Herwig, C.; Spadiut, O. A novel toolbox for *E. coli* lysis monitoring. *Anal. Bioanal. Chem.* **2017**, *409*, 667–671. [[CrossRef](#)]
41. Wurm, D.J.; Marschall, L.; Sagmeister, P.; Herwig, C.; Spadiut, O. Simple monitoring of cell leakiness and viability in *Escherichia coli* bioprocesses—A case study. *Eng. Life Sci.* **2017**, *17*, 598–604. [[CrossRef](#)] [[PubMed](#)]
42. Kopp, J.; Slouka, C.; Ulonska, S.; Kager, J.; Fricke, J.; Spadiut, O.; Herwig, C. Impact of Glycerol as Carbon Source onto Specific Sugar and Inducer Uptake Rates and Inclusion Body Productivity in *E. coli* BL21(DE3). *Bioengineering* **2017**, *5*, 1. [[CrossRef](#)] [[PubMed](#)]
43. Klumpp, S.; Zhang, Z.; Hwa, T. Growth rate-dependent global effects on gene expression in bacteria. *Cell* **2009**, *139*, 1366–1375. [[CrossRef](#)] [[PubMed](#)]
44. Terpe, K. Overview of bacterial expression systems for heterologous protein production: From molecular and biochemical fundamentals to commercial systems. *Appl. Microbiol. Biotechnol.* **2006**, *72*, 211. [[CrossRef](#)] [[PubMed](#)]

45. Takkinen, K.; Laukkanen, M.L.; Sizmann, D.; Alftan, K.; Immonen, T.; Vanne, L.; Kaartinen, M.; Knowles, J.K.; Teeri, T.T. An active single-chain antibody containing a cellulase linker domain is secreted by *Escherichia coli*. *Protein Eng.* **1991**, *4*, 837–841. [\[CrossRef\]](#)
46. Striedner, G.; Cserjan-Puschmann, M.; Pötschacher, F.; Bayer, K. Tuning the Transcription Rate of Recombinant Protein in Strong *Escherichiacoli* Expression Systems through Repressor Titration. *Biotechnol. Prog.* **2003**, *19*, 1427–1432. [\[CrossRef\]](#)
47. Kikuchi, Y.; Yoda, K.; Yamasaki, M.; Tamura, G. The nucleotide sequence of the promoter and the amino-terminal region of alkaline phosphatase structural gene (*phoA*) of *Escherichia coli*. *Nucleic Acids Res.* **1981**, *9*, 5671–5678. [\[CrossRef\]](#)
48. Wang, Z.; Gao, Y.; Luo, M.; Cagliero, C.; Jiang, H.; Xie, Y.; Zhu, J.; Lu, H. A PhoA-STII Based Method for Efficient Extracellular Secretion and Purification of Fab from *Escherichia coli*. *Bio-Protocol* **2019**, *9*, e3370. [\[CrossRef\]](#)
49. Schuhmacher, T.; Löffler, M.; Hurler, T.; Takors, R. Phosphate limited fed-batch processes: Impact on carbon usage and energy metabolism in *Escherichia coli*. *J. Biotechnol.* **2014**, *190*, 96–104. [\[CrossRef\]](#)
50. Rao, N.N.; Liu, S.; Kornberg, A. Inorganic polyphosphate in *Escherichia coli*: The phosphate regulon and the stringent response. *J. Bacteriol.* **1998**, *180*, 2186–2193. [\[CrossRef\]](#)
51. Wanner, B.L. Phosphorus assimilation and control of the phosphate regulon. In *Escherichia coli and Salmonella: Cellular and Molecular Biology*, 2nd ed.; ASM Press: Washington, DC, USA, 1996; Volume 41, pp. 1357–1381.
52. Wanner, B. Phosphate regulation of gene expression in *E. coli*. In *Escherichia coli and Salmonella typhimurium: Cellular and Molecular Biology*; ASM Press: Washington, DC, USA, 1987; Volume 2, pp. 1326–1333.
53. Marzan, L.W.; Shimizu, K. Metabolic regulation of *Escherichia coli* and its *phoB* and *phoR* genes knockout mutants under phosphate and nitrogen limitations as well as at acidic condition. *Microb. Cell Fact.* **2011**, *10*, 39. [\[CrossRef\]](#) [\[PubMed\]](#)
54. Baca, M.; Wells, J.A. Anti-VEGF Antibodies. US Patent 6,884,879, 26 April 2005.
55. Romano, S.; Schulz-Vogt, H.N.; González, J.M.; Bondarev, V. Phosphate limitation induces drastic physiological changes, virulence-related gene expression, and secondary metabolite production in *Pseudovibrio* sp. strain FO-BEG1. *Appl. Environ. Microbiol.* **2015**, *81*, 3518–3528. [\[CrossRef\]](#) [\[PubMed\]](#)
56. Doran, P.M. *Bioprocess Engineering Principles*, 2nd ed.; Elsevier: Amsterdam, The Netherlands, 2012.
57. Santos-Beneit, F. The Pho regulon: A huge regulatory network in bacteria. *Front. Microbiol.* **2015**, *6*, 402. [\[CrossRef\]](#)
58. Ghorbel, S.; Smirnov, A.; Chouayekh, H.; Sperandio, B.; Esnault, C.; Kormanec, J.; Virole, M.J. Regulation of *ppk* expression and in vivo function of *Ppk* in *Streptomyces lividans* TK24. *J. Bacteriol.* **2006**, *188*, 6269–6276. [\[CrossRef\]](#) [\[PubMed\]](#)
59. Wanner, B.L. Signal transduction in the control of phosphate-regulated genes of *Escherichia coli*. *Kidney Int.* **1996**, *49*, 964–967. [\[CrossRef\]](#)
60. Muller, J.M.; Wetzel, D.; Flaschel, E.; Friehs, K.; Risse, J.M. Constitutive production and efficient secretion of soluble full-length streptavidin by an *Escherichia coli* “leaky mutant”. *J. Biotechnol.* **2016**, *221*, 91–100. [\[CrossRef\]](#)
61. Morowvat, M.H.; Babaeipour, V.; Rajabi-Memari, H.; Vahidi, H.; Maghsoudi, N. Overexpression of Recombinant Human Beta Interferon (rhINF-beta) in Periplasmic Space of *Escherichia coli*. *Iran. J. Pharm. Res.* **2014**, *13*, 151–160.
62. Song, H.; Jiang, J.; Wang, X.; Zhang, J. High purity recombinant human growth hormone (rhGH) expression in *Escherichia coli* under *phoA* promoter. *Bioengineered* **2017**, *8*, 147–153. [\[CrossRef\]](#)
63. Agbogbo, F.K.; Ramsey, P.; George, R.; Joy, J.; Srivastava, S.; Huang, M.; McCool, J. Upstream development of *Escherichia coli* fermentation process with *PhoA* promoter using design of experiments (DoE). *J. Ind. Microbiol. Biotechnol.* **2020**, *47*, 789–799. [\[CrossRef\]](#)
64. Sohoni, S.V.; Nelapati, D.; Sathé, S.; Javadekar-Subhedar, V.; Gaikawari, R.P.; Wangikar, P.P. Optimization of high cell density fermentation process for recombinant nitrilase production in *E. coli*. *Bioresour. Technol.* **2015**, *188*, 202–208. [\[CrossRef\]](#)
65. Maldonado, L.M.; Hernandez, V.E.; Rivero, E.M.; Barba de la Rosa, A.P.; Flores, J.L.; Acevedo, L.G.; De Leon Rodriguez, A. Optimization of culture conditions for a synthetic gene expression in *Escherichia coli* using response surface methodology: The case of human interferon beta. *Biomol. Eng.* **2007**, *24*, 217–222. [\[CrossRef\]](#) [\[PubMed\]](#)
66. Saida, F. Overview on the expression of toxic gene products in *Escherichia coli*. *Curr. Protoc. Protein Sci.* **2007**. [\[CrossRef\]](#)
67. Grunberg, S.; Wolf, E.J.; Jin, J.; Ganatra, M.B.; Becker, K.; Ruse, C.; Taron, C.H.; Correa, I.R., Jr.; Yigit, E. Enhanced expression and purification of nucleotide-specific ribonucleases MC1 and Cusativin. *Protein Expr. Purif.* **2022**, *190*, 105987. [\[CrossRef\]](#) [\[PubMed\]](#)
68. Fathi-Roudsari, M.; Maghsoudi, N.; Maghsoudi, A.; Niazi, S.; Soleiman, M. Auto-induction for high level production of biologically active replease in *Escherichia coli*. *Protein Expr. Purif.* **2018**, *151*, 18–22. [\[CrossRef\]](#) [\[PubMed\]](#)
69. Cardoso, V.M.; Campani, G.; Santos, M.P.; Silva, G.G.; Pires, M.C.; Goncalves, V.M.; de Giordano, C.R.; Sargo, C.R.; Horta, A.C.L.; Zangirolami, T.C. Cost analysis based on bioreactor cultivation conditions: Production of a soluble recombinant protein using *Escherichia coli* BL21(DE3). *Biotechnol. Rep.* **2020**, *26*, e00441. [\[CrossRef\]](#)
70. Tahara, N.; Tachibana, I.; Takeo, K.; Yamashita, S.; Shimada, A.; Hashimoto, M.; Ohno, S.; Yokogawa, T.; Nakagawa, T.; Suzuki, F.; et al. Boosting Auto-Induction of Recombinant Proteins in *Escherichia coli* with Glucose and Lactose Additives. *Protein Pept. Lett.* **2020**, *28*, 1180–1190. [\[CrossRef\]](#)
71. Studier, F.W. Use of T7 RNA polymerase to direct expression of cloned genes. *Methods Enzymol.* **1990**, *185*, 60–89.
72. Rao, N.N.; Wang, E.; Yashpbe, J.; Torriani, A. Nucleotide pool in *pho* regulon mutants and alkaline phosphatase synthesis in *Escherichia coli*. *J. Bacteriol.* **1986**, *166*, 205–211. [\[CrossRef\]](#)
73. Wang, Y.; Ding, H.; Du, P.; Gan, R.; Ye, Q. Production of *phoA* promoter-controlled human epidermal growth factor in fed-batch cultures of *Escherichia coli* YK537 (pAET-8). *Process Biochem.* **2005**, *40*, 3068–3074. [\[CrossRef\]](#)

## 6.2. Scientific Publication 2

Journal of Biotechnology 359 (2022) 108–115



Contents lists available at ScienceDirect

Journal of Biotechnology

journal homepage: [www.elsevier.com/locate/jbiotec](http://www.elsevier.com/locate/jbiotec)

## Recombinant Protein L: Production, Purification and Characterization of a Universal Binding Ligand

Stefan Kittler<sup>a,b,1</sup>, Julian Ebner<sup>a,b,1</sup>, Mihail Besleaga<sup>a</sup>, Johan Larsbrink<sup>c</sup>, Barbara Darnhofer<sup>d</sup>, Ruth Birner-Gruenberger<sup>d,e</sup>, Silvia Schobesberger<sup>f</sup>, Christopher K. Akhgar<sup>g</sup>, Andreas Schwaighofer<sup>g</sup>, Bernhard Lendl<sup>g</sup>, Oliver Spadiut<sup>a,\*</sup>

<sup>a</sup> Research Division Integrated Bioprocess Development, Institute of Chemical, Environmental and Bioscience Engineering, TU Wien, Gumpendorfer Strasse 1a, 1060 Vienna, Austria

<sup>b</sup> Alfred Gruber GmbH, Nordstrasse 6, 5301 Eugendorf, Austria

<sup>c</sup> Wallenberg Wood Science Center, Division of Industrial Biotechnology, Department of Biology and Biological Engineering, Chalmers University of Technology, Gothenburg, Sweden

<sup>d</sup> Research Division Functional Proteomics and Metabolic Pathways, Diagnostic and Research Institute of Pathology, Medical University of Graz, Stiftingtalstrasse 24, 8010 Graz, Austria

<sup>e</sup> Research Division Bioanalytics, Institute of Chemical Technology and Analytics, TU Wien, Getreidemarkt 9/164, 1060 Vienna, Austria

<sup>f</sup> Research Division Organic & Biological Chemistry, Institute of Applied Synthetic Chemistry, TU Wien, Getreidemarkt 9/163, 1060 Vienna, Austria

<sup>g</sup> Research Division Environmental Analytics, Process Analytics and Sensors, Institute of Chemical Technology and Analytics, TU Wien, Getreidemarkt 9/164, 1060 Vienna, Austria

## ARTICLE INFO

## Keywords:

Protein L  
E. coli  
Recombinant production  
Bioreactor  
Affinity ligand

## ABSTRACT

Protein L (PpL) is a universal binding ligand that can be used for the detection and purification of antibodies and antibody fragments. Due to the unique interaction with immunoglobulin light chains, it differs from other affinity ligands, like protein A or G. However, due to its current higher market price, PpL is still scarce in applications. In this study, we investigated the recombinant production and purification of PpL and characterized the product in detail. We present a comprehensive roadmap for the production of the versatile protein PpL in *E. coli*.

## 1. Introduction

The affinity protein protein L (PpL) originates from *Fingoldia magna* (formerly *Peptostreptococcus magnus*) and was identified by Myhre and Erntell as a membrane protein (Björck, 1988; Nilson et al., 1992; Rosenthal et al., 2012). PpL has up to 5B (binding) domains, which selectively bind to kappa light chains of immunoglobulins (Igs) and, unlike protein A and G, do not interfere with the Fc region during binding (Kittler et al., 2021; Rodrigo et al., 2015; Zheng et al., 2012). In biotechnology, PpL is of high interest due to its ability not only to bind whole Igs, but also antibody fragments containing light chains, such as single chain variable fragments (scFvs) and fragments antigen binding (Fabs) (Kittler et al., 2021; Nilson et al., 1993; Rodrigo et al., 2015;

Zheng et al., 2012). Different commercial versions (4 or 5B domains) are available, as the fifth binding domain has only minor effects on the binding affinity of the protein (Kittler et al., 2021). It was shown that PpL binds to kappa subtypes 1, 3 and 4, and is therefore applicable for more Ig classes compared to protein A and G (Nilson et al., 1992; Rodrigo et al., 2015). However, all three proteins are currently used in downstream processing (DSP) and bioanalytics due to their binding abilities. Ig binding proteins enable the purification of high value products (i.e. antibodies and antibody fragments) in the pharmaceutical industry, where most of the processes use protein A, G or L affinity columns as a first chromatography capture step. Other applications encompass site-specific immobilization of Igs to maintain high functionality, including enzyme-linked immunosorbent assay (ELISA) and

\* Corresponding author.

E-mail addresses: [stefan.kittler@tuwien.ac.at](mailto:stefan.kittler@tuwien.ac.at) (S. Kittler), [julian.ebner@tuwien.ac.at](mailto:julian.ebner@tuwien.ac.at) (J. Ebner), [mihail.besleaga@tuwien.ac.at](mailto:mihail.besleaga@tuwien.ac.at) (M. Besleaga), [johan.larsbrink@chalmers.se](mailto:johan.larsbrink@chalmers.se) (J. Larsbrink), [b.darnhofer@medunigraz.at](mailto:b.darnhofer@medunigraz.at) (B. Darnhofer), [ruth.birner-gruenberger@tuwien.ac.at](mailto:ruth.birner-gruenberger@tuwien.ac.at) (R. Birner-Gruenberger), [silvia.schobesberger@tuwien.ac.at](mailto:silvia.schobesberger@tuwien.ac.at) (S. Schobesberger), [christopher.akhgar@tuwien.ac.at](mailto:christopher.akhgar@tuwien.ac.at) (C.K. Akhgar), [andreas.schwaighofer@tuwien.ac.at](mailto:andreas.schwaighofer@tuwien.ac.at) (A. Schwaighofer), [bernhard.lendl@tuwien.ac.at](mailto:bernhard.lendl@tuwien.ac.at) (B. Lendl), [oliver.spadiut@tuwien.ac.at](mailto:oliver.spadiut@tuwien.ac.at) (O. Spadiut).

<sup>1</sup> These authors contributed equally to the work.

<https://doi.org/10.1016/j.jbiotec.2022.10.002>

Received 21 August 2022; Received in revised form 28 September 2022; Accepted 1 October 2022

Available online 4 October 2022

0168-1656/© 2022 The Author(s). Published by Elsevier B.V. This is an open access article under the CC BY license (<http://creativecommons.org/licenses/by/4.0/>).

immunoprecipitation (Bohinski, 2000; Shen et al., 2017). Furthermore, they are used as binding ligand for surface plasmon resonance (SPR) and biolayer interferometry (BLI) to determine binding kinetics of Igs and antibody fragments (Douzi, 2017; Kittler et al., 2021; Sultana and Lee, 2015).

However, the number of applications of PpL lag behind those of protein A and G, even though the use of PpL is the only viable alternative for binding antibody fragments missing the Fc region. To our knowledge, there is no literature describing the production of PpL available to date (process mode and conditions, purification, etc.), even though recombinant PpL versions can be purchased. Furthermore, the commercial price is approximately twice as high as for protein G and even three times higher than that of protein A (Kittler et al., 2021). We hypothesize that this is caused by the lower number of approved antibody fragments on the biopharmaceutical market compared to antibodies, reducing the need of PpL.

The goal of this study was to recombinantly produce 5B domain His<sub>6</sub>-tagged PpL in *Escherichia coli* and test its functionality in comparison with a commercially available PpL with 4B domains (purchased from Sigma-Aldrich). In the upstream process (USP), product localization (inclusion body (IB) vs. soluble) and protein quantity were investigated by altering specific substrate uptake rate ( $q_s$ ) and temperature. The downstream processing aimed to obtain a high purity (>80%) without using an expensive affinity column. In this respect, the attachment of a His<sub>6</sub>-tag presents several advantages: It enables simple DSP, composed of Immobilized Metal Affinity Chromatography (IMAC), resulting in an efficient capture step for proteins produced in soluble form (Bornhorst and Falke, 2000; Ley et al., 2011). Furthermore, the tag enables the immobilization in a specific orientation which benefits subsequent applications such as electrochemical assays, SPR and lateral flow assays (Andrescu et al., 2001; Kröger et al., 1999; Ley et al., 2011). In the last step the purified PpL was characterized to investigate any potential negative impact of the His<sub>6</sub>-tag on the binding characteristics of the protein.

## 2. Material and Methods

### 2.1. Strain

The cultivations were performed using an *E. coli* BL21(DE3) strain transformed with a pET-24a(+) plasmid carrying the codon-optimized gene for the 5B domain PpL (GenBank accession no. AAA67503) with a C-terminal His<sub>6</sub>-tag (restriction sites: *NheI/XhoI*). The encoded PpL has a theoretical size of 41.98 kDa and a theoretical pI of 4.82 (supplementary information: 1. Sequencing Result). The sequence for the 5B domains originates from *F. magna* and was adapted from ProSpec (PROTEIN-L, 2019).

### 2.2. Media

The bioreactor cultivations were carried out using a defined medium described by DeLisa et al. (DeLisa et al., 1999), supplemented with 0.02 g/L kanamycin to prevent plasmid loss (Table 1). Glycerol was used as sole carbon source since recent results showed that this can result in higher product titers due to a higher amount of accessible energy (Kopp et al., 2017).

### 2.3. Bioreactor Cultivations

For pre-culture, 500 mL of DeLisa medium (Table 1) in a 2500 mL high yield shake flask were inoculated with 1.5 mL frozen bacterial stock. The pre-culture was grown at 37 °C and 230 rpm in an Infors HR Multitron incubator (Infors, Bottmingen, Switzerland) for 16 h. The cultivations were carried out in a DASGIP parallel reactor system (Eppendorf, Hamburg, Germany) with four vessels having 2 L working volume each. The culture broth was aerated with 2 L/min and stirred at

**Table 1**

DeLisa medium used for all cultivation phases. 0.02 g/L kanamycin were added for all phases.

Component	Pre-culture	Batch	Feed	Sterilization
	Concentration [g/L]			
Citric acid	13.3	–	–	autoclave
(NH <sub>4</sub> ) <sub>2</sub> HPO <sub>4</sub>	4	–	–	–
Citric acid	1.7	–	–	–
MgSO <sub>4</sub> ·0.7 H <sub>2</sub> O (stock 500 x)	1.2	–	10.00	autoclave
Fe(III) citrate (stock 100 x)	0.1	–	0.02	autoclave
EDTA (stock 100 x)	0.0084	–	0.0065	autoclave
Zn(CH <sub>3</sub> COO) <sub>2</sub> ·H <sub>2</sub> O (stock 200 x)	0.013	–	0.008	filter sterile
TE <sup>a</sup> (stock 200 x)	5 mL/L	–	7.27 mL/L	filter sterile
Thiamine HCl (stock 1000 x)	0.0045	–	–	filter sterile
Glycerol	8	20	400	autoclave

<sup>a</sup> TE stock: CoCl<sub>2</sub>·0.6 H<sub>2</sub>O (2.5 mg/L); MnCl<sub>2</sub>·0.4 H<sub>2</sub>O (15 mg/L); CuCl<sub>2</sub>·0.2 H<sub>2</sub>O (1.2 mg/L); H<sub>3</sub>BO<sub>3</sub> (3 mg/L); Na<sub>2</sub>MoO<sub>4</sub>·0.2 H<sub>2</sub>O (2.5 mg/L)

1400 rpm. The pH was monitored with an Easyferm electrode (Hamilton, Reno, NV, USA) and kept constant at 6.7 via addition of NH<sub>4</sub>OH (12.5%). The dissolved oxygen was monitored using a Visiferm fluorescence dissolved oxygen electrode (Hamilton, Reno, NV, USA) and kept above 30% by supplying a mixture of pressurized air and pure oxygen if necessary. Off-gas was monitored using a DASGIP-GA gas analyzer (Eppendorf, Hamburg, Germany). The temperature was controlled with a heat jacket and cooling finger and kept at 37 °C for the batch and at 35 °C during the non-induced fed-batch phase. For process control and monitoring the DAS-GIP-control system (DASware-control) was used. The batch phase (volume = 1 L) was started by inoculating the reactor with 10% (v/v) of the pre-culture. Once all glycerol was depleted, as indicated by a drop of the CO<sub>2</sub> signal and vice versa a rise in the dO<sub>2</sub> signal, substrate was fed to reach a cell dry weight concentration of approx. 25 g/L. After the fed-batch, expression of PpL was induced by addition of Isopropyl β-D-1-thiogalactopyranoside (IPTG) to a final concentration of 0.5 mM (induced fed-batch). During the induction phase, the specific substrate uptake rate ( $q_s$ ) and temperature were altered using a design of experiment (DoE) approach. These process parameters have been shown to be crucial factors for protein quantity and localization (IB vs. soluble) (Kopp et al., 2017; Slouka et al., 2018). During the induced fed-batch, samples were drawn every two hours to monitor product formation. The factor  $q_s$  was adjusted at the start of induction and was altered in the range of 0.1 g/g/h to 0.5 g/g/h. The temperature was investigated in a range of 27–35 °C, while the center-point conditions (CP) ( $q_s = 0.3$  g/g/h; T = 31 °C) were performed three times to investigate reproducibility. We decided to perform a central composite circumscribed design to adequately describe potential quadratic interactions. In a first step the product localization and feasibility of a tunable production of IB or soluble PpL was investigated. For the design of DoE the volumetric product concentration in g/L was chosen as process response. The software MODDE 10 (Sartorius, Göttingen, Germany) was used for model design and to develop a multilinear regression model describing volumetric titer of PpL as a function of  $q_s$  and temperature over the induction time.

### 2.4. Bioreactor Cultivation Analytics

#### 2.4.1. Biomass

Biomass was quantified via optical density by measuring OD<sub>600</sub> using a UV/VIS photometer (Genisys 20, Thermo Scientific, Waltham, MA, USA) to monitor biomass growth during the process. Additionally, dry cell weight (DCW) was determined gravimetrically by centrifuging 1 mL of culture broth (9000 rcf, 10 min), subsequently washing the pellet with 0.9% (w/v) NaCl and centrifuging again. Afterwards the pellets were dried at 105 °C for 72 h.

#### 2.4.2. Metabolite Analysis

The concentration of glycerol in the supernatant was analyzed via high performance liquid chromatography (HPLC) (UltiMate 3000; Thermo Fisher, Waltham, MA) using a Supelcogel C-610 H column (Supelco, Bellefonte, PA, USA) (Kopp et al., 2017). For this method 0.1% H<sub>3</sub>PO<sub>4</sub> with a constant flow rate of 0.5 mL/min was used as eluent. The sugars were detected and quantified using respective standards, by a refractive index detector (Shodex RI-101, Ecom, Prague, Czech Republic) (Kopp et al., 2017). The  $q_s$  was calculated according to Eq. 1, taking accumulated glycerol into account.

$$q_s \left[ \frac{g}{g \cdot h} \right] = \frac{V_{in,feed,\Delta t} [L] * C_{feed} \left[ \frac{g}{L} \right] - V_{reactor,t_i} [L] * C_{acc,t_i} \left[ \frac{g}{L} \right]}{\Delta t [h] * X_{\Delta t} [g]} \quad (1)$$

- $q_s \left[ \frac{g}{g \cdot h} \right]$  ... specific substrate uptake rate.  
 $V_{in,feed,\Delta t} [L]$  ... feed volume in timespan  $\Delta t$ .  
 $C_{feed} \left[ \frac{g}{L} \right]$  ... glycerol concentration in the feed (400 g/L).  
 $V_{reactor,t_i} [L]$  ... reactor volume at time point  $i$ .  
 $C_{acc,t_i} \left[ \frac{g}{L} \right]$  ... concentration of glycerol in the supernatant at time point  $i$ .  
 $\Delta t [h]$  ... timespan ( $t_i - t_{i-1}$ ) for the calculation of  $q_s$ .  
 $X_{\Delta t} [g]$  ... average biomass in the reactor in the timespan  $\Delta t$ .

#### 2.4.3. Product Analysis

For determining the PpL concentration, 10 mL of the cultivation broth were centrifuged at 9000 rcf for 10 min at 4 °C. The supernatant was discarded and the product samples were stored at – 20 °C until further use. The cell pellet was suspended in 40 mL lysis buffer (100 mM Tris, 10 mM EDTA, pH = 7.4) and homogenized using a high-pressure homogenizer at 1200 bar for 7 passages (PandaPLUS, Gea AG, Germany). Subsequently, the cell suspension was centrifuged at 20,380 rcf for 20 min at 4 °C, and supernatant and IB pellet were further analyzed as described in the sections below. a) **SDS-PAGE** For SDS-PAGE, Mini-PROTEAN® TGX Stain-Free™ (BioRad, Hercules, CA, USA) gels were used. The IB pellet were dissolved in 1x Laemmli buffer containing 100  $\mu$ L  $\beta$ -mercaptoethanol (reducing conditions) (Laemmli, 1970). The soluble fraction was mixed in a 1–2 ratio with 2x Laemmli buffer. All samples were incubated at 95 °C for 10 min and subsequently spun down. Five  $\mu$ L of a protein molecular weight standard (precision plus protein standard dual color, BioRad) and 10  $\mu$ L of each sample were loaded in the respective wells. The gel was run at 180 V for 30 min. Staining was performed using Coomassie brilliant blue and gels were analyzed using a Gel Doc (Universal Hood II, BioRad, Hercules, CA, USA) and the ImageLab software (Version 6.0.1, BioRad, Hercules, CA, USA). b) **HPLC** Reversed Phase-HPLC: The product concentration was determined using a BioResolve reversed phase (RP) Polyphenyl column (dimensions 100  $\times$  3 mm, particle size 2.7  $\mu$ m) (Waters Corporation, MA, USA) equipped with a pre-column (3.9  $\times$  5 mm, 2.7  $\mu$ m) (Kopp et al., 2020). Eluent A was ultrapure water (MQ) and eluent B was acetonitrile, both supplemented with 0.1% (v/v) trifluoroacetic acid. A sample volume of 2  $\mu$ L was injected. The flow was kept constant at 0.4 mL/min and the measurement performed at 70 °C. A detailed description of the used method is given by Kopp et al. (Kopp et al., 2020). The soluble fractions were filtered with a 0.2  $\mu$ m syringe filter (CHROMAFIL® Xtra PVDF-20/25, Pall, New York, USA), while the IB pellets were first solubilized with 7.5 M guanidine hydrochloride, 62 mM Tris and 100 mM DTT at pH = 8 and filtered afterwards. To determine the protein concentration, BSA (bovine serum albumin) standards with concentrations between 0.1 and 2 g/L were measured. Size Exclusion Chromatography-HPLC: PpL concentration and purity during the DSP was measured using a size exclusion chromatography (SEC)-HPLC method. A BEH 200 A SEC 1.7  $\mu$ m 4.6  $\times$  300 mm, 3.5  $\mu$ m (Waters Corporation, MA, USA) column was run isocratically with SEC buffer (80 mM phosphate, 250 mM KCl, pH = 6.8) (Kittler et al., 2020). The method run time was 18 min with a flow rate of 0.5 mL/min and an

injection volume of 2  $\mu$ L was used. Column temperature was kept constant at 25 °C and absorbance was recorded at 280 nm and 214 nm. For quantification purposes, BSA protein standards were measured between 0.125 and 2 g/L and PpL concentrations calculated based on the calibration curve.

#### 2.5. Downstream Processing

The biomass of each cultivation was harvested 12 h after induction, centrifuged at 17,000 rcf, 4 °C, 30 min and the biomass pellet stored at – 20 °C until further use. For the described DSP protocol, biomass produced at  $q_s = 0.3$  g/g/h and  $T = 31$  °C was used. For preparative chromatography, an ÄKTA pure™ system (Cytiva Life Sciences, MA, USA) was used, monitoring conductivity and UV absorbance at three wavelengths (280 nm, 260 nm, 214 nm).

The DSP comprised the following steps:

- Cell lysis via high pressure homogenization
- Capture via IMAC chromatography
- Purification via anion exchange chromatography (AEC)

##### 2.5.1. High Pressure Homogenization

In order to release intracellularly produced soluble PpL, cell lysis was performed via high pressure homogenization using a PandaPLUS (Gea AG, Germany). Frozen biomass was resuspended in Buffer A (50 mM phosphate, pH = 7.4) containing protease inhibitor (cOmplete™ Mini, EDTA-free, Roche, Switzerland) to a final concentration of 13 g DCW/L buffer A. Homogenization was performed at 1200 bar for 7 passages and the homogenized sample was kept at 4 °C afterwards. In order to separate cell debris from the soluble fraction containing PpL, the sample was centrifuged at 20,380 rcf for 20 min at 4 °C. The supernatant was used in the following chromatography step and the pellet discarded.

##### 2.5.2. Capture Chromatography: IMAC

As a capture step for the His<sub>6</sub>-tagged PpL, a 5 mL HiTrap™ IMAC FF (Cytiva Life Sciences, MA, USA) with a flowrate of 0.2 column volumes (CV)/min was used. The column was equilibrated with buffer A (50 mM phosphate, pH = 7.4) until all signals were stable. The supernatant (35 mL) after homogenization was loaded onto the column, followed by a wash step with 4 CVs of buffer A. Elution was performed using a step gradient with 40% buffer B (50 mM phosphate, 500 mM imidazole, pH = 7.4). During elution, fractions of 1 mL were collected, pooled based on the UV 280 nm signal and analyzed for their respective concentration and purity using SEC-HPLC.

##### 2.5.3. Purification Chromatography: AEC

As purification step, a 1 mL HiTrap™ Capto Q (Cytiva Life Sciences, MA, USA) column with a flowrate of 1 CV/min was used. The column was equilibrated with buffer A (50 mM phosphate, pH = 7.4). The pooled fractions containing PpL obtained from the capture chromatography step (IMAC) were used as load (6 mL load volume) (Cytiva, 2021a, 2021b). After loading was completed, the column was washed with 5 CVs buffer A. PpL was eluted using a step gradient with 25% buffer C (50 mM phosphate, 1 M NaCl, pH = 7.4). As for IMAC, fractions of 1 mL were collected, pooled based on the UV 280 nm signal and analyzed for their respective concentration and purity using SEC-HPLC.

#### 2.6. Characterization and Protein Functionality

##### 2.6.1. Mass Spectrometry

The primary structure and mass of the purified His<sub>6</sub>-tagged PpL was confirmed using digestion followed by LC/MS (liquid chromatography/mass spectrometry). Additionally, the total mass of the produced PpL and the commercial PpL (for comparison) was measured using intact protein mass spectrometry. A detailed description of the performed

measurements can be found in the [supplementary information \(supplementary information: 6. Mass spectrometry\)](#).

### 2.6.2. Infrared Spectroscopy

Both PpL variants were measured using laser-based mid-infrared spectroscopy to obtain structural information. A detailed description of the applied external cavity-quantum cascade laser (EC-QCL) setup has previously been reported (Akhgar et al., 2020). Briefly, the laser (Hedgehog, Daylight Solutions Inc., San Diego USA) was operated in a tuning range between 1470  $\text{cm}^{-1}$  and 1730  $\text{cm}^{-1}$  with a scan speed of 3600  $\text{cm}^{-1}$  and pulse rate and width of 1 MHz and 200 ns, respectively. The IR light was attenuated by optical filters, divided into two beams and directed into a two-path transmission flow cell with a path length of 26  $\mu\text{m}$ . Approximately 500  $\mu\text{L}$  of sample solution were injected into the signal cell, while the reference cell was filled with the pure buffer solution. The intensity of both beams was detected by a thermoelectrically cooled mercury cadmium telluride balanced detector (Vigo System S.A., Poland) to compensate the noise introduced by the EC-QCL. A previously described pre-processing routine (Schwaighofer et al., 2018), including similarity index evaluation, scan averaging (300 single scans = 45 s acquisition time) and fast Fourier transform (FFT) filtering, was applied in order to obtain the final protein spectra with a spectral resolution of 2.6  $\text{cm}^{-1}$ .

### 2.6.3. Surface Plasmon Resonance

Surface plasmon resonance spectroscopy (SPR) was performed at the core facility at the University of Natural Resources and Life Sciences in Vienna. For the measurement, a Bioacore T200 (Cytiva Life Sciences, MA, USA) was used. For measuring the binding affinity of both PpL samples, a commercial protein A chip was used. In the first step, a 10  $\mu\text{g}/\text{mL}$  Herceptin solution was applied to bind the antibody to the protein A chip. Subsequently, to monitor the binding affinity, different PpL concentrations (0.617, 1.85, 5.55, 16.6, and 50 nM respectively) were loaded for 10 min. The flow rate for all loading steps was 10  $\mu\text{L}/\text{min}$ . The general running buffer was HBS-EP buffer (Cytiva Life Sciences, MA, USA). The obtained RPU (response) was plotted versus the time and fitted with a one site saturation model (Eq. 1) using Sigma plot (Systat Software GmbH) to determine the response at equilibrium. The RPU at equilibrium of all measurements was then plotted against the respective concentration and fitted with a one site saturation equation to determine the  $K_D$  value (Eq. 2) (Moscetti et al., 2017; Sparks et al., 2019).

$$y = \frac{B_{\max} * x}{K_D + x} \quad (2)$$

y ... y - value e.g. response of the SPR measurement  $B_{\max}$  ... maximal y-value x ... x - value e.g. concentration of the analyte  $K_D$  ... analyte concentration at  $B_{\max}/2$ .

### 2.6.4. Structure Analysis

Finally, the 3D structure of PpL was predicted using AlphaFold (Jumper et al., 2021; Varadi et al., 2022). For the analysis, the full amino acid sequence including the His6-tag was used and the prediction computed using the Alvis cluster within the Chalmers Centre for Computational Science and Engineering (C3SE), Sweden.

### 2.6.5. ELISA

To evaluate the functionality of the purified PpL, the purified protein was conjugated to recombinant horseradish peroxidase (HRP) and ELISA was performed. A detailed description of the protocol for conjugation, which was adapted from Nygren et al. and Molin et al. is given in the [supplementary information \(supplementary information: 2. ELISA Conjugation\)](#) (Molin So Fau - Nygren et al., 1978a, 1978b; Nygren et al., 1981).

For the ELISA, 100  $\mu\text{L}$  Herceptin (200  $\mu\text{g}/\text{mL}$ ) in phosphate buffered saline (PBS, pH = 7.4) was incubated at 4  $^{\circ}\text{C}$  in high binding ELISA

plates (Greiner Bio-One, Kremsmünster, Austria) for 16 h. Afterwards, the Herceptin solution was removed and the wells were washed four times with PBS containing 0.05% Tween20 (=wash buffer). Subsequently, to block open binding positions, the wells were incubated with 200  $\mu\text{L}$  1% BSA in PBS (=blocking solution) for 60 min at RT. Then the wells were washed again four times with wash buffer. Subsequently, the respective detection complex with a concentration of 0.2  $\mu\text{g}/\text{mL}$  was incubated at RT for 30 min (Table 2). The solution in the wells was discarded and wells were washed seven times with wash buffer to remove non-specifically bound HRP.

Bound HRP-PpL conjugates were quantified immediately after the last washing step using a S2,2'-azino-bis(3-ethylbenzothiazoline-6-sulfonic acid) (ABTS) assay. 180  $\mu\text{L}$  of 8 mM ABTS in 50 mM phosphate-citrate buffer, pH = 5, were pipetted in each well and the reaction was started by adding 20  $\mu\text{L}$  10 mM  $\text{H}_2\text{O}_2$ . The change of absorbance at 420 nm was monitored for 45 min using a Tecan plate reader (Spark®, Tecan, Männedorf, Switzerland) at 30  $^{\circ}\text{C}$ . For each well, the volumetric activity was calculated according to Eq. 3.

$$A \left[ \frac{\text{U}}{\text{mL}} \right] = \frac{V_{\text{total}} [\mu\text{L}] * \Delta A / \text{min} * \text{dilution}}{V_{\text{sample}} [\mu\text{L}] * d [\text{cm}] * \epsilon [\text{mM}^{-1} * \text{cm}^{-1}]} \quad (3)$$

$V_{\text{total}}$  [ $\mu\text{L}$ ] ... total volume in well.  
 $\Delta A / \text{min}$  ... change in absorption ( $\Delta\text{Abs}$  420 nm/min).  
 Dilution ... dilution of the sample.  
 $V_{\text{sample}}$  [ $\mu\text{L}$ ] ... volume of sample.  
 $d$  [ $\text{cm}$ ] ... length of the beam path through the cuvette ( $d = 0.58 \text{ cm}$ ).  
 $\epsilon$  [ $\text{mM}^{-1} * \text{cm}^{-1}$ ] ... extinction coefficient ( $\epsilon_{420} = 36 \text{ mM}^{-1} * \text{cm}^{-1}$ ).

## 3. Results and Discussion

### 3.1. Production and Purification of Recombinant Protein L

The goal of this study was to develop a production process for recombinant PpL that enables production of a high amount of biologically active protein with high purity (>80%). The investigated variables in the USP and DSP are listed in Table 3.

For the recombinant production of His<sub>6</sub>-tagged PpL, the specific substrate uptake rate and temperature ( $q_s$ , T) were investigated in a DoE approach. In previous studies it was shown that these process variables influence localization (IB or soluble) and quantity of produced recombinant protein (Kopp et al., 2017; Slouka et al., 2018). For all tested fermentation conditions, an excess of soluble PpL compared to IBs (9 g/L to <0.5 g/L) was observed (supplementary information: Fig. S1). Since PpL originates from a bacterial host, we believe that expression has a low burden on *E. coli* due to low protein complexity (no disulfide bridges or other post-translational modifications) and therefore only low amounts of IB were produced (Bhatwa et al., 2021). As depicted in Fig. 1a, high specific substrate uptake rates ( $\geq 0.5 \text{ g/g/h}$ ) led to an increase of the volumetric product titer in the beginning of the induction phase. However, after four to six hours, glycerol started to accumulate (data not shown) as the biomass growth stopped (DCW decreased) and the volumetric productivity declined. The observed drop in the specific growth rate correlated with the mentioned accumulation of glycerol, caused by a high metabolic stress using a  $q_s$  higher than 0.5 g/g/h. Lower temperatures (25.3  $^{\circ}\text{C}$  and 27  $^{\circ}\text{C}$ ) did not increase the amount of

**Table 2**  
 Tested combination of samples and conjugation-complex. HRP: horseradish peroxidase; PpL: protein L; BSA: bovine serum albumin.

Immobilized protein	Detection complex
Herceptin	HRP
Herceptin	PpL
Herceptin	PpL-HRP
BSA	PpL-HRP

S. Kitzler et al.

Journal of Biotechnology 359 (2022) 108–115

**Table 3**  
Overview of investigated factors in the production process of recombinant protein L. USP: upstream processing; DSP: downstream processing;  $q_s$ : specific substrate uptake rate; IMAC: immobilized metal affinity chromatography.

Unit operation	Factors	Range
USP	$q_s$	0.1 g/g/h – 0.5 g/g/h
	Temperature	27–35 °C
DSP - IMAC	NaCl	0 mM or 500 mM

PpL, independent of the adjusted  $q_s$ . The CP conditions ( $q_s = 0.3$  g/g/h, temperature 31 °C) resulted in an almost linear increase of the volumetric titer, while higher temperatures did not lead to an increase of

product formation.

The regression model for the volumetric titer showed that longer induction time had a positive influence on productivity (Fig. 1b). Furthermore, increasing temperature led to an increase of the volumetric titer, while the quadratic terms of all tested parameters had a negative impact on product formation (supplementary information: Fig. S2). The highest volumetric product titer (>9 g/L) was achieved at a  $q_s = 0.3$  g/g/h, a temperature of 31 °C and an induction time of 12 h, leading to a specific product titer of 0.17 g/g with a final biomass concentration of 55 g DCW/L (process data: supplementary information: Figs. S3 and S4).

After cell lysis, the His<sub>6</sub>-tagged PpL was purified to achieve purities

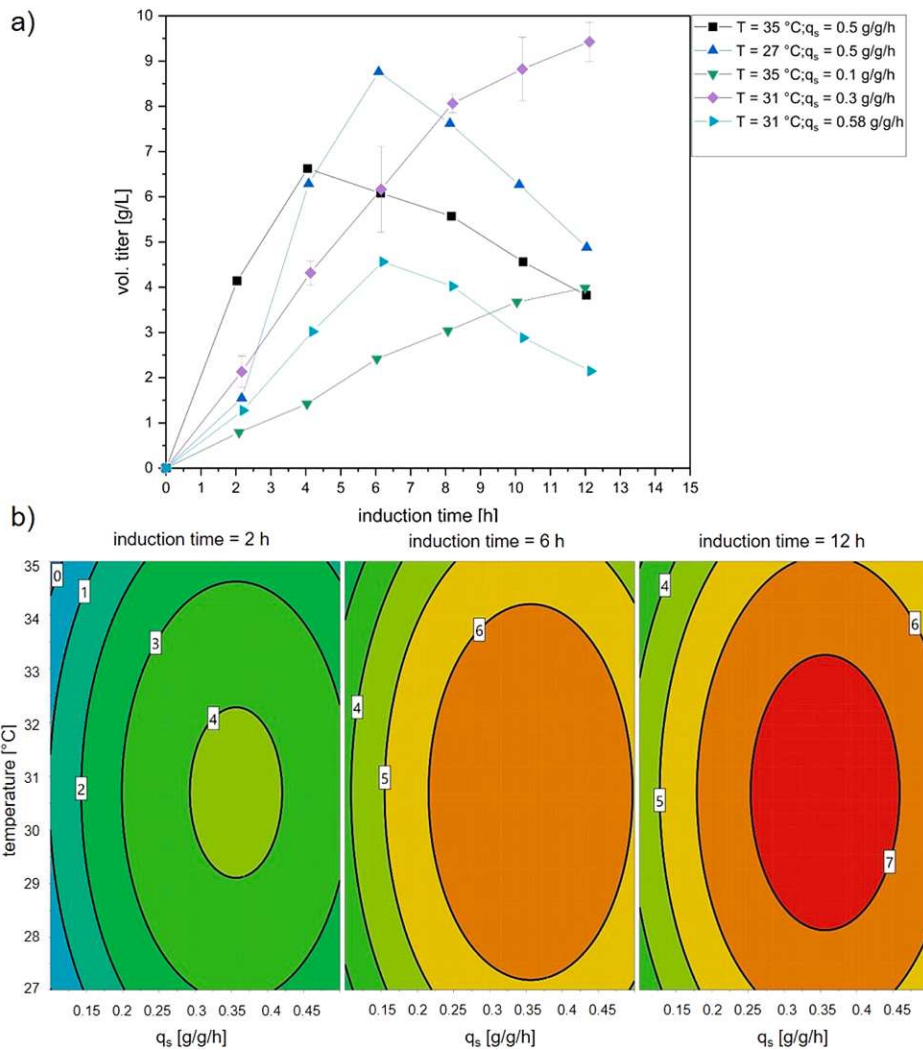


**Fig. 1.** a: Time resolved trend of volumetric titer [g/L] of performed cultivations according to the design of experiment (DoE). b: Contour plot of the volumetric titer [g/L]. The optimum in the tested design space is at a specific substrate uptake rate ( $q_s = 0.3$  g/g/h and temperature 31 °C after 12 h. These conditions led to a product concentration of about 9 g/L.



similar to the commercial PpL (i.e. 80%, determined by SEC). A standard protocol for IMAC, including 20 mM imidazole in the sample and the binding buffer, led to unexpectedly low recoveries (<30%, data not shown). In order to improve binding capacity and recovery, sample and binding buffers were prepared without imidazole. This adaptation resulted in improved recovery (59%) and purity (67%). Still, a second chromatography step was required to reach the targeted purity of > 80%. Due to the pI of 4.82, an anion exchange chromatography (AEC) step was chosen. However, the used salt (500 mM NaCl) in the IMAC buffers requires a buffer exchange to ensure sufficient binding in the subsequent AEC step. Therefore, we investigated whether NaCl can be omitted in the IMAC step without negative effects on recovery and purity. Summarized in Table 4, the final process using IMAC buffers without salt showed increased recovery and purity, resulting in a final PpL purity of 92% and a final yield of 5 g PpL / L fermentation broth (57%) after the second AEC step. As an additional advantage, the eluate of the capture step (IMAC) could directly be used to load the column in the second purification step, circumventing additional unit operations such as e.g. pH-adjustment or buffer exchange (Cytiva, 2021a, 2021b). The presented process might be a viable alternative to industrial production processes in which far more expensive Ig containing resins are used for the capture step (Cytiva). Furthermore, the purified 5B domain His<sub>6</sub>-tagged PpL had a higher purity (92%) compared to the commercial protein (80%). However, it is important to mention that DNA and endotoxin concentrations were not analyzed.

### 3.2. Protein Structure and Functionality Analysis

First, the primary structure of both PpL variants (TU Wien: 5B domain His<sub>6</sub>-tagged PpL and Sigma-Aldrich: 4B domain PpL) was confirmed using enzymatic digestion followed by LC/MS. However, due to the existence of repetitive B domains, the exact mass of the proteins could not be determined by analyzing the fragments. For this purpose, whole protein LC/MS was performed of each PpL variant. The 5B domain His<sub>6</sub>-tagged PpL, had a mass of 41816 Da (supplementary information: Fig. S5), while the commercial 4B domain PpL (one binding domain less) had a mass of 36038 Da (supplementary information: Fig. S6). Moreover, for both PpL variants, a distribution of different mass fragments was observed. This size heterogeneity has been reported for different Ig-binding proteins of Gram-positive bacteria (Kastern et al., 1992).

Laser-based mid-IR spectroscopy was applied to record absorbance spectra across the amide I (1600–1700 cm<sup>-1</sup>) and amide II (1500–1600 cm<sup>-1</sup>) bands, since these represent the most important wavenumber regions for protein secondary structure determination (Barth, 2007). Compared to conventional Fourier-transform infrared (FTIR) instrumentation, EC-QCLs operate at significantly higher spectral power densities, thus allowing the application of larger optical path lengths that lead to improved robustness and sensitivity (Schwaighofer and Lendl, 2020). Fig. 2a shows a comparison of PpL from Sigma-Aldrich (4B domains) and PpL produced here (TU Wien; 5B domains His<sub>6</sub>-tagged). Positions and shapes of the IR absorbance bands show excellent comparability between the spectra. The maxima at 1640 cm<sup>-1</sup> in the amide I region, as well as the broad amide II bands at approximately 1550 cm<sup>-1</sup> indicate a high share of  $\beta$ -sheet secondary structure (Barth, 2007).

**Table 4**

Recovery and purity of the His<sub>6</sub>-tagged PpL comparing the IMAC runs with and without 500 mM NaCl.

Step	Recovery [%]	Purity [%]
Capture (IMAC) with NaCl	66	45
Whole DSP	44	72
Capture (IMAC) without NaCl	49	67
Whole DSP	57	92

For testing functionality and binding affinity, SPR measurements were performed to determine the K<sub>D</sub> value of both PpL variants. However, PpL has a very high affinity to Igs and antibody fragments, indicated by a small K<sub>D</sub> and a slow dissociation reaction. Therefore, the dissociation could not be determined with the used experimental set up, since no steady state was achieved (data not shown). As an alternative approach, the maximum signals for steady state conditions were calculated based on a one site saturation model. In Fig. 2b the maximum fitted response (RPU) for each tested concentration is plotted against the respective concentration (Moschetti et al., 2017; Sparks et al., 2019). The obtained values were fitted again using a one site saturation model to determine the K<sub>D</sub> values (Fig. 2b).

The determined K<sub>D</sub> value for the recombinant 5B His<sub>6</sub>-tagged PpL variant (K<sub>D</sub> = 2.93 × 10<sup>-10</sup> M) was lower than for the commercial 4B domain PpL (K<sub>D</sub> = 1.55 × 10<sup>-9</sup> M). This can likely be attributed to the additional B domain in the construct, which slightly increases the affinity (Kastern et al., 1992; Kittler et al., 2021).

After similarity of the secondary structure was validated for both variants and the functionality was demonstrated, the tertiary structure of the 5B His<sub>6</sub>-tagged PpL variant was modeled using AlphaFold (Jumper et al., 2021; Varadi et al., 2022). Since no amino acid sequence was available for the commercial PpL variant, a comparison of the modeled structures was not possible. However, the single B domains could be predicted with high confidence and are in accordance with literature (Kittler et al., 2021; Wikstroem et al., 1994). The linkers between the binding domains were found to have lower prediction scores and are most likely flexible and without a defined structures (Fig. 3, supplementary information: Fig. S7). These linkers as well as the unstructured N- and C- terminal ends of the protein (the latter incorporating the His<sub>6</sub>-tag) could be susceptible to some proteases, possibly explaining the size heterogeneity observed in mass analysis and the low recovery during the capture step (IMAC) (Shen et al., 1991).

### 3.3. Application of Protein L in an ELISA

For the purpose of using PpL in an ELISA, both PpL variants were conjugated to recombinant HRP and used to detect Herceptin. First, solely the HRP activity without the binding to Herceptin was measured. The recombinant His<sub>6</sub>-tagged 5B domain PpL conjugate showed an activity of 6.82 ± 0.27 × 10<sup>3</sup> U/mol, which was similar to the 4B domain conjugate PpL that showed an activity of 7.49 ± 0.91 × 10<sup>3</sup> U/mol. However, it was expected that the 5B domain PpL would exhibit a higher amount of conjugated HRP due to the higher number of primary amines (e.g. lysine), which act as conjugation partners. However, we assume that these additional primary amines were not accessible due to their position within the binding domains, resulting in similar amounts of conjugated HRP. In the ELISA, the His<sub>6</sub>-tagged PpL with 5B domains achieved a volumetric activity of 3.99 ± 0.86 U/mL, while for the commercial PpL (Sigma-Aldrich) with 4B domains showed an activity of 4.96 ± 0.92 U/mL. Conjugation of PpL to HRP without loss of activity and detection of an antibody was thus possible for both variants, showing that the tested HRP-PpL complex can be successfully used for ELISAs applied as in-process control e.g. in the early DSP or for refolding processes.

## 4. Conclusion

In this study we were able to successfully produce and purify recombinant His<sub>6</sub>-tagged PpL with 5B domains in *E. coli* with a final product yield of 5 g product per L fermentation broth. The produced protein was characterized and compared to a commercially available PpL regarding secondary structure and activity (Table 5). The initial DSP resulted in unexpectedly low recoveries and purities, but these could be significantly improved by optimization of the IMAC capture step and performing a second AEC step. The results from the performed MS indicate a size heterogeneity of PpL, which could possibly explain the

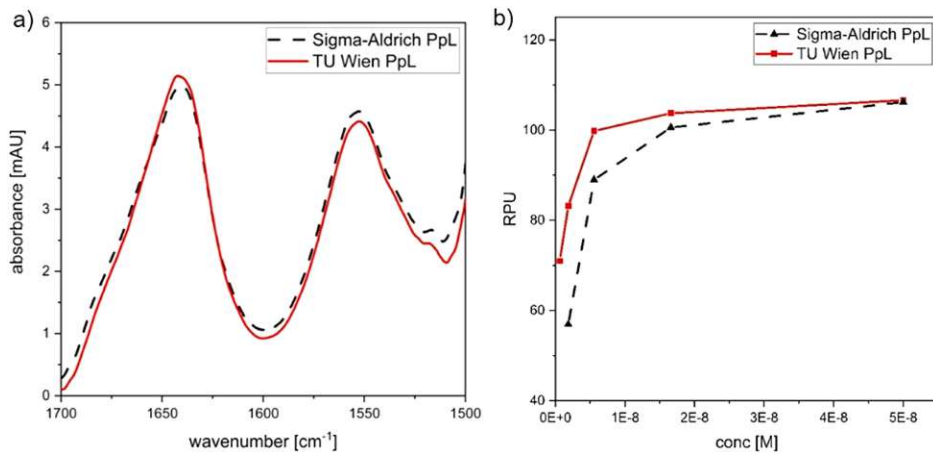


Fig. 2. a: IR spectrum of both protein L (PpL) variants. Both 4B domain and 5B domain His<sub>6</sub>-tagged PpL, from Sigma-Aldrich and TU Wien, respectively, show highly similar absorbance spectra indicating comparable secondary structure. b: Results of the SPR measurement of both protein L (PpL) variants. The calculated saturation values for each concentration is plotted against the respective concentration. The curve was fitted with a one-site saturation equation to determine the K<sub>D</sub> value. 4B domain PpL (Sigma-Aldrich PpL) K<sub>D</sub> = 1.5 × 10<sup>-9</sup> M; 5B domain His<sub>6</sub>-tagged PpL (TU Wien PpL): K<sub>D</sub> = 2.93 × 10<sup>-10</sup> M.

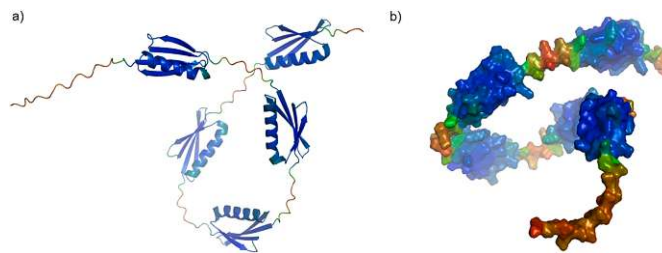


Fig. 3. a) Cartoon models colored by the prediction score, red-green-blue, from low to high, with the N-terminus on the left. b) Space-fill model of His<sub>6</sub>-tagged protein L, colored as in a), and with the N-terminus at the bottom. The structure of the B domains are confidently predicted, while the structure of the linkers and termini cannot be predicted reliably and are likely flexible in solution.

**Table 5**  
Summary of the results of the structural and functionality analysis of both protein L (PpL) variants. mAb: monoclonal antibody.

	TU Wien PpL	Sigma-Aldrich PpL
Mass [Da]	41816	36038
Structure of single B domain	4 beta sheets + 1 alpha helix	4 beta sheets + 1 alpha helix
B domains	5	4
K <sub>D</sub> [M]	2.93 × 10 <sup>-10</sup>	1.55 × 10 <sup>-9</sup>
Application in ELISA	Detection of mAb possible	Detection of mAb possible

still somewhat low overall recoveries. The structural analysis revealed unstructured protein parts that could be susceptible to cleavage, which would then result in different protein sizes and loss of the purification tag. We believe that further studies focusing on the structure of PpL will help to understand the observed results. Nevertheless, the secondary structure of the produced PpL was similar to the commercial variant with 4B domains. Furthermore, it was shown that the produced PpL is functional and active, without being negatively influenced by the HIS<sub>6</sub>-tag and the obtained K<sub>D</sub> value was lower compared to the 4B domain

PpL. Additionally, the application in an ELISA detecting Herceptin using a PpL-HRP conjugate was successful.

**Funding**

This research was funded by the Austrian Research Promotion Agency (FFG) (874206). The authors acknowledge the TU Wien Bibliothek for financial support through its Open Access Funding Program.

**CRediT authorship contribution statement**

SKI and JEB conducted most of the experiments and wrote the draft, MBE supported in the bioprocessing tasks, JLA did the protein model, BDA and RBG performed mass spectrometry, SSC assisted in the ELISA experiments, CAK, ASC and BLE did spectroscopic analyses, OSP initiated and supervised the study, secured funding and corrected the draft.

**Declaration of Competing Interest**

The authors declare that they have no known competing financial interests or personal relationships that could have appeared to influence the work reported in this paper.

S. Kittler et al.

Journal of Biotechnology 359 (2022) 108–115

**Data Availability**

Data will be made available on request.

**Acknowledgments**

Alfred Gruber GmbH is gratefully thanked for supporting the research and being project partner. This project was further supported by EQ-BOKU VIBT GmbH and the BOKU Core Facility Biomolecular & Cellular Analysis. Furthermore, we thank Karolina Golab for performing the conjugation and ELISA experiments.

**Appendix A. Supporting information**

Supplementary data associated with this article can be found in the online version at doi:10.1016/j.jbiotec.2022.10.002.

**References**

- Akhgar, C.K., Ramer, G., Zbik, M., Trajnerowicz, A., Pawluczyc, J., Schwaighofer, A., Lendl, B., 2020. The next generation of IR spectroscopy: EC-QCL-Based Mid-IR transmission spectroscopy of proteins with balanced detection. *Anal. Chem.* 92, 9901–9907.
- Andrescu, S., Magearu, V., Lougarre, A., Fournier, D., Marty, J.L., 2001. Immobilization of enzymes on screen-printed sensors via a histidine tail. Application to the detection of pesticides using modified cholinesterase. *Anal. Lett.* 34, 529–540.
- Barth, A., 2007. Infrared spectroscopy of proteins. *Biochim. Et Biophys. Acta (BBA) - Bioenergy* 1767, 1073–1101.
- Bhatwa, A., Wang, W., Hassan, Y.I., Abraham, N., Li, X.-Z., Zhou, T., 2021. Challenges associated with the formation of recombinant protein inclusion bodies in *Escherichia coli* and strategies to address them for industrial applications. *Front. Bioeng. Biotechnol.* 9, 65.
- Björck, L., 1988. Protein L. A novel bacterial cell wall protein with affinity for Ig L chains. *J. Immunol.* 140, 1194–1197.
- Bohinski, R.C., 2000. Immunoprecipitation of serum albumin with protein A-sepharose: a biochemistry laboratory experiment. *J. Chem. Educ.* 77, 1460.
- Bornhorst, J.A., Falke, J.J., 2000. Purification of proteins using polyhistidine affinity tags. *Methods Enzymol.* 326, 245–254.
- Cytiva, (https://www.cytivalifesciences.com/en/at) (accessed 10 August 2021a).
- Cytiva, (2021b) **Tips for successful ion exchange chromatography.**
- DeLisa, M.P., Li, J., Rao, G., Weigand, W.A., Bentley, W.E., 1999. Monitoring GFP-operon fusion protein expression during high cell density cultivation of *Escherichia coli* using an on-line optical sensor. *Biotechnol. Bioeng.* 65, 54–64.
- Douzi, B., 2017. Protein–protein interactions: surface plasmon resonance. In: *Journet, L., Cascales, E. (Eds.), Bacterial Protein Secretion Systems: Methods and Protocols.* Springer, New York, New York, NY, pp. 257–275.
- Jumper, J., Evans, R., Pritzel, A., Green, T., Figurnov, M., Ronneberger, O., Tunyasuvunakool, K., Bates, R., Zidek, A., Potapenko, A., Bridgland, A., Meyer, C., Kohli, S.A.A., Ballard, A.J., Cowie, A., Romera-Paredes, B., Nikolov, S., Jain, R., Adler, J., Back, T., Petersen, S., Reiman, D., Clancy, E., Zielinski, M., Steinegger, M., Pacholska, M., Berghammer, T., Bodenstein, S., Silver, D., Vinyals, O., Senior, A.W., Kavukcuoglu, K., Kohli, P., Hassabis, D., 2021. Highly accurate protein structure prediction with AlphaFold. *Nature* 596, 583–589.
- Kastern, W., Sjöbring, U., Björck, L., 1992. Structure of peptostreptococcal protein L and identification of a repeated immunoglobulin light chain-binding domain. *J. Biol. Chem.* 267, 12820–12825.
- Kittler, S., Kopp, J., Veelenfurt, P.G., Spadiut, O., Delvigne, F., Herwig, C., Slouka, C., 2020. The lazarus *Escherichia coli* effect: recovery of productivity on glycerol/lactose mixed feed in continuous biomanufacturing. *Front. Bioeng. Biotechnol.* 8, 993.
- Kittler, S., Besleaga, M., Ebner, J., Spadiut, O., 2021. Protein L—More Than Just an Affinity Ligand. *Processes* 9.
- Kopp, J., Slouka, C., Ulonska, S., Kager, J., Fricke, J., Spadiut, O., Herwig, C., 2017. Impact of Glycerol as Carbon Source onto Specific Sugar and Inducer Uptake Rates and Inclusion Body Productivity in *E. coli* BL21(DE3). *Bioeng. (Basel, Switz.)* 5, 1.
- Kopp, J., Zauner, F.B., Pell, A., Hausjell, J., Humer, D., Ebner, J., Herwig, C., Spadiut, O., Slouka, C., Pell, R., 2020. Development of a generic reversed-phase liquid chromatography method for protein quantification using analytical quality-by-design principles. *J. Pharm. Biomed. Anal.* 188, 113412.
- Kröger, D., Liley, M., Schiweck, W., Skerra, A., Vogel, H., 1999. Immobilization of histidine-tagged proteins on gold surfaces using chelator thioalkanes. *Biosens. Bioelectron.* 14, 155–161.
- Laemmli, U.K., 1970. Cleavage of structural proteins during the assembly of the head of bacteriophage T4. *Nature* 227, 680–685.
- Ley, C., Holtmann, D., Mangold, K.-M., Schrader, J., 2011. Immobilization of histidine-tagged proteins on electrodes. *Colloids Surf. B: Biointerfaces* 88, 539–551.
- Molin So Fau, -, Nygren, H., Nygren, H., Fau, -, Dolonius, L., Dolonius, L., 1978a. A new method for the study of glutaraldehyde-induced crosslinking properties in proteins with special reference to the reaction with amino groups. *J. Histochem. Cytochem.: Off. J. Histochem. Soc.* 26.
- Moscetti, L., Cannistraro, S., Bizzarri, A.R., 2017. Surface plasmon resonance sensing of biorecognition interactions within the tumor suppressor p53 network. *Sensors* 17, 2680.
- Nilson, B.H., Solomon, A., Björck, L., Akerström, B., 1992. Protein L from *Peptostreptococcus magnus* binds to the kappa light chain variable domain. *J. Biol. Chem.* 267, 2234–2239.
- Nilson, B.H., Löfdberg, L., Kastern, W., Björck, L., Akerström, B., 1993. Purification of antibodies using protein L-binding framework structures in the light chain variable domain. *J. Immunol. Methods* 164, 33–40.
- Nygren, H., Fau, -, Hansson, H.A., Hansson, H.A., 1981. Conjugation of horseradish peroxidase to staphylococcal protein A with benzoquinone, glutaraldehyde, or periodate as cross-linking reagents. The journal of histochemistry and cytochemistry: official journal of the Histochemistry. *J. Histochem. Cytochem.: Off. J. Histochem. Soc.* 29, 266–270.
- PROTEIN-L, HIS**, (https://www.prospebio.com/protein-l-his) (accessed 02.07.2019).
- Rodrigo, G., Cruvegård, M., Van Alstine, J.M., 2015. Antibody fragments and their purification by protein L affinity chromatography. *Antibodies* 4.
- Rosenthal, M.E., Rojzman Ad Fau, -, Frank, E., Frank, E., 2012. *Finogoldia magna* (formerly *Peptostreptococcus magnus*): an overlooked etiology for toxic shock syndrome? *Med. Hypotheses* 79, 138–140.
- Schwaighofer, A., Lendl, B., 2020. Chapter 3 - quantum cascade laser-based infrared transmission spectroscopy of proteins in solution. In: Ozaki, Y., Baranska, M., Lednev, I.K., Wood, B.R. (Eds.), *Vibrational Spectroscopy in Protein Research.* Academic Press, pp. 59–88.
- Schwaighofer, A., Montemurro, M., Freitag, S., Kristament, C., Culzoni, M.J., Lendl, B., 2018. Beyond fourier transform infrared spectroscopy: external cavity quantum cascade laser-based mid-infrared transmission spectroscopy of proteins in the amide I and amide II region. *Anal. Chem.* 90, 7072–7079.
- Shen, H., Schmuck, M., Pilz, L., Gilkes, N.R., Kilburn, D.G., Miller, R.C., Warren, R.A., 1991. Deletion of the linker connecting the catalytic and cellulose-binding domains of endoglucanase A (CenA) of *Cellulomonas fimi* alters its conformation and catalytic activity. *J. Biol. Chem.* 266, 11335–11340.
- Shen, M., Rusling, J., Dixit, C.K., 2017. Site-selective orientated immobilization of antibodies and conjugates for immunodiagnosis development. *Methods* 116, 95–111.
- Slouka, C., Kopp, J., Hutwimmer, S., Strahammer, M., Strohm, D., Eitenberger, E., Schwaighofer, A., Herwig, C., 2018. Custom made inclusion bodies: impact of classical process parameters and physiological parameters on inclusion body quality attributes. *Microb. Cell Factor.* 17, 148–148.
- So Fau, M., Nygren, H., Nygren, H., Fau, -, Dolonius, L., Dolonius, L., Fau, -, Hansson, H.A., Hansson, H.A., 1978b. A kinetic study of the reaction between glutaraldehyde and horseradish peroxidase. *J. Histochem. Cytochem.: Off. J. Histochem. Soc.* 26.
- Sparks, R.P., Jenkins, J.L., Fratti, R., 2019. Use of surface plasmon resonance (SPR) to determine binding affinities and kinetic parameters between components important in fusion machinery. *Methods Mol. Biol.* 1860, 199–210.
- Sultana, A., Lee, J.E., 2015. Measuring protein-protein and protein-nucleic acid interactions by bilayer interferometry. *Curr. Protoc. Protein Sci.* 79, 19.25.11–19.25.26.
- Varadi, M., Anyango, S., Deshpande, M., Nair, S., Natassia, C., Yordanova, G., Yuan, D., Stroe, O., Wood, G., Laydon, A., Zidek, A., Green, T., Tunyasuvunakool, K., Petersen, S., Jumper, J., Clancy, E., Green, R., Vora, A., Lutfi, M., Figurnov, M., Cowie, A., Hobbs, N., Kohli, P., Kleywegt, G., Birney, E., Hassabis, D., Velankar, S., 2022. AlphaFold Protein Structure Database: massively expanding the structural coverage of protein-sequence space with high-accuracy models. *Nucleic Acids Res.* 50, D439–D444.
- Wikstrom, M., Drakenberg, T., Forsen, S., Sjöbring, U., Bjoerck, L., 1994. Three-dimensional solution structure of an immunoglobulin light chain-binding domain of protein L. Comparison with the IgG-binding domains of protein G. *Biochemistry* 33, 14011–14017.
- Zheng, Z., Chinnasamy, N., Morgan, R.A., 2012. Protein L: a novel reagent for the detection of Chimeric Antigen Receptor (CAR) expression by flow cytometry. *J. Transl. Med.* 10, 29.

## 6.3. Scientific Publication 3



## Repetitive Fed-Batch: A Promising Process Mode for Biomanufacturing With *E. coli*

Julian Kopp<sup>†</sup>, Stefan Kittler<sup>†</sup>, Christoph Slouka, Christoph Herwig, Oliver Spadiut and David J. Wurm<sup>\*</sup>

Research Area Biochemical Engineering, Institute of Chemical Engineering, TU Wien, Vienna, Austria

Recombinant protein production with *Escherichia coli* is usually carried out in fed-batch mode in industry. As set-up and cleaning of equipment are time- and cost-intensive, it would be economically and environmentally favorable to reduce the number of these procedures. Switching from fed-batch to continuous biomanufacturing with microbials is not yet applied as these cultivations still suffer from time-dependent variations in productivity. Repetitive fed-batch process technology facilitates critical equipment usage, reduces the environmental fingerprint and potentially increases the overall space-time yield. Surprisingly, studies on repetitive fed-batch processes for recombinant protein production can be found for yeasts only. Knowledge on repetitive fed-batch cultivation technology for recombinant protein production in *E. coli* is not available until now. In this study, a mixed feed approach, enabling repetitive fed-batch technology for recombinant protein production in *E. coli*, was developed. Effects of the cultivation mode on the space-time yield for a single-cycle fed-batch, a two-cycle repetitive fed-batch, a three-cycle repetitive fed batch and a chemostat cultivation were investigated. For that purpose, we used two different *E. coli* strains, expressing a model protein in the cytoplasm or in the periplasm, respectively. Our results demonstrate that a repetitive fed-batch for *E. coli* leads to a higher space-time yield compared to a single-cycle fed-batch and can potentially outperform continuous biomanufacturing. For the first time, we were able to show that repetitive fed-batch technology is highly suitable for recombinant protein production in *E. coli* using our mixed feeding approach, as it potentially (i) improves product throughput by using critical equipment to its full capacity and (ii) allows implementation of a more economic process by reducing cleaning and set-up times.

**Keywords:** *E. coli*, repetitive fed-batch, process understanding, process intensification, recombinant protein production, continuous biomanufacturing

### OPEN ACCESS

#### Edited by:

Pau Ferrer,  
Autonomous University of Barcelona,  
Spain

#### Reviewed by:

Dongming Xie,  
University of Massachusetts Lowell,  
United States  
Stefan Junne,  
Technical University of Berlin,  
Germany

#### \*Correspondence:

David J. Wurm  
david.wurm@tuwien.ac.at

<sup>†</sup>These authors have contributed  
equally to this work

#### Specialty section:

This article was submitted to  
Bioprocess Engineering,  
a section of the journal  
Frontiers in Bioengineering and  
Biotechnology

**Received:** 17 June 2020

**Accepted:** 21 October 2020

**Published:** 10 November 2020

#### Citation:

Kopp J, Kittler S, Slouka C,  
Herwig C, Spadiut O and Wurm DJ  
(2020) Repetitive Fed-Batch:  
A Promising Process Mode  
for Biomanufacturing With *E. coli*.  
*Front. Bioeng. Biotechnol.* 8:573607.  
doi: 10.3389/fbioe.2020.573607

### INTRODUCTION

*Escherichia coli* serves as a beloved workhorse for the production of many recombinant proteins. Fast doubling times, little risk of contamination, cheap media and easy upscale are the most prominent benefits (Casali, 2003; Baeshen et al., 2015; Gupta and Shukla, 2017). The *E. coli* strain BL21(DE3) is the most commonly applied strain in industry with outstanding low acetate secretion and high product concentrations (Rosano and Ceccarelli, 2014; Wurm et al., 2017a; Rosano et al., 2019). The strain is regularly used for recombinant protein production with pET-plasmids, making use of the

integrated T7-promotor system (Wurm et al., 2016; Kopp et al., 2017; Rosano et al., 2019). For many applications IPTG (Isopropyl- $\beta$ -D-thiogalactopyranosid) is the inducer of choice, which leads to high levels of recombinant protein. Even though IPTG induction is described as tunable, toxic effects can be observed (Wurm et al., 2016; Hausjell et al., 2018). Several studies showed that the use of IPTG throughout long induction times leads to increased stress levels and thus to low viability (Dvorak et al., 2015; Slouka et al., 2018). Promotor systems, like araBAD and rhamBAD are not described to show any toxic effects (Marshall et al., 2016). The utilization of arabinose or rhamnose might enable long-term cultivation with *E. coli* (Marshall et al., 2016), however they are rarely used in industry due to the high price of these inducers (Kopp et al., 2019b). Thus, it is of great importance to find a suitable inducer that is affordable in large scale and shows no signs of toxicity onto host cells (Malakar and Venkatesh, 2012; Mühlmann et al., 2018). The disaccharide lactose is taken up via lactose permease. Upon uptake, lactose is either cleaved to glucose and galactose or converted to allolactose via  $\beta$ -galactosidase (Deutscher et al., 2006). Allolactose can then bind to the lac repressor and enable induction as described in various previous publications (Wurm et al., 2016; Kopp et al., 2017). Due to the non-toxicity and low cost of lactose compared to other inducers, this induction mechanism is tuneable and also economically feasible (9.39 €/g IPTG vs. 0.02 €/g lactose) (Yan et al., 2004; Briand et al., 2016). For mixed feed systems using lactose, an established mechanistic knowledge platform, which explains the correlation between sugar and inducer uptake by physiological parameters can be used (Wurm et al., 2017a). Furthermore, lactose has shown to boost productivity in soluble recombinant protein production when compared to IPTG (Wurm et al., 2016, 2017a). For periplasmic recombinant protein production soft induction by lactose is especially important as translocation to the periplasm is the rate limiting step (Gupta and Shukla, 2017; Karyolaimos et al., 2019; Hausjell et al., 2020).

Independent of product location, recombinant protein production in *E. coli* is commonly carried out in fed-batch cultivation mode (Slouka et al., 2018; Kopp et al., 2019b). However, in fed-batch cultivation sterilization, cleaning and biomass formation take up the majority of process time (Slouka et al., 2018). As industry is always aiming to increase the space-time yield, a continuous production system would be desirable to reduce down-times (Rathore, 2015; Tan et al., 2019; Zobel-Roos et al., 2019). Regulations of continuously produced products used to be an issue, however regulatory authorities have defined to separate production into diverse lot numbers according to ICH Q7: "The batch size can be defined either by a fixed quantity or by the amount produced in a fixed time interval" (EU GMP Guide, Part II). Compared to a batch system, continuous systems enable maximum utilization of equipment. By reducing down-times, production scale can be decreased or amounts of product can be gained within less time, or a combination of both factors (Glaser, 2015; Herwig et al., 2015; Rathore, 2015). Continuous production processes would allow increased product yields in smaller production facilities while obtaining the same amounts of

product (Allison et al., 2015; Konstantinov and Cooney, 2015; Nasr et al., 2017).

Aiming to establish time-independent microbial cultivation systems, evolutionary mechanisms, such as mutations (Rugbjerg and Sommer, 2019) and shifts in transcriptome and proteome (Peebo et al., 2015; Peebo and Neubauer, 2018) spoiled expectations of industry.

Repetitive fed-batch cultivation mode offers the chance of an immense down-time reduction, with multiple production cycles performed within one cultivation run (Bergmann and Trösch, 2016; Kuo et al., 2017; Zagrodnik and Łaniecki, 2017). While in fed-batch processes a complete harvest of the fermenter is performed at the end of cultivation, repetitive fed batch processing differs by performing only a partial harvest (Martens et al., 2011). Afterwards, the spared fermentation broth is diluted with fresh media and a new induction cycle can be started right away (Fricke et al., 2013). Repetitive fed-batch has proven to be a suitable cultivation mode to improve many processes in biotechnology and conducted studies and literature concerning repetitive fed-batch cultivations up to date are given in **Table 1**. However, studies on repetitive fed-batch using *E. coli* are scarce.

Repetitive fed-batch technology has shown promising effects in recombinant protein production mainly using *Pichia pastoris* (Ohya et al., 2005; Martens et al., 2011; Fricke et al., 2013). To our knowledge, a repetitive fed-batch cultivation mode using *E. coli* has only been implemented for pyruvate production (Zelić et al., 2004). However, the potential of using *E. coli* in repetitive fed-batch mode for recombinant protein production has not been investigated yet.

In this study we performed repetitive fed-batch cultivations for recombinant protein production using the production host *E. coli* in combination with lactose induction. In previous studies, the negative side effects of IPTG induction onto recombinant protein production in long-term fermentations were shown, whereas lactose was found to have a beneficial effect on productivity (Malakar and Venkatesh, 2012; Dvorak et al., 2015; Kopp et al., 2019a). We believe that no studies on repetitive fed-batch cultivation with *E. coli* for recombinant protein production have been published yet, either due to toxic effects of IPTG and the consequent decreasing productivity over time (Dvorak et al., 2015; Kopp et al., 2019b) or due to the absence of an induction strategy comparable to the established yeast system (Fricke et al., 2013). The goal of this study was to compare productivities and space-time yields of different production modes for *E. coli*. The assessment of changes in product quality and purity was not in the scope of this study. For the first time, we were able to show that a repetitive fed-batch cultivation mode using our developed lactose induction strategy is able to outperform conventional fed-batches and chemostat cultivations regarding the overall space-time yield.

## MATERIALS AND METHODS

### Strains

All cultivations were carried out with the strain *E. coli* BL21(DE3), transformed with a pET30a<sup>+</sup> plasmid carrying the gene for the cytoplasmic protein (CP) and periplasmic

**TABLE 1** | Summary of studies about repetitive fed-batch cultivations.

Microorganism	Product	Process description	Ref.
<i>Cryptocodinium cohnii</i>	docosahexaenoic acid	4 cycles, 80% medium replacement	Liu et al., 2020
<i>Aspergillus terreus</i>	Lovastatin	3 cycles, 37% yield in crease	Novak et al., 1997; Kumar et al., 2000
<i>Gluconobacter oxydans</i>	Dihydroxyacetone	4 cycles, repeated fed-batch process using two spatially separated vessels	Bauer et al., 2005
<i>Kluyveromyces marxianus</i>	Ethanol	5 cycles, product yield constant	Ozmihci and Kargi, 2007
<i>Kitasatospora</i>	$\epsilon$ -Poly-L-lysine	5 cycles	Zhang et al., 2010
<i>Yarrowia lipolytica</i>	Citric acid	10 cycles, productivity decrease over cultivation time	Moeller et al., 2011
<i>Pichia pastoris</i>	human serum albumin (rHSA)	4 cycles, 47% yield increase	Ohya et al., 2005
<i>Pichia pastoris</i>	Malaria vaccine candidates	stable productivity for 2-8 cycles, methanol induction	Martens et al., 2011; Fricke et al., 2013
<i>Escherichia coli</i>	Pyruvate	5 cycles, $q_p$ increased fivefold	Zelić et al., 2004

protein (PP), respectively. The cytoplasmic protein contained no disulfide bonds, had a isoelectric point (PI) of 5.62 and a protein size of 26.9 kDa. PI and protein size of the periplasmic protein were 5.42 and 32 kDa, respectively and it contained a single disulfide bond.

### Media

All cultivations were conducted using a defined minimal medium by DeLisa et al. (1999), supplemented with different amounts of glucose and lactose. 0.02 g/L kanamycin was added to prevent plasmid loss.

### Bioreactor Setup

All cultivations were performed in a Minifors 2 bioreactor system (max. working volume: 1 L; Infors HT, Bottmingen, Switzerland). The cultivation offgas was analyzed in online mode using gas sensors – IR for CO<sub>2</sub> and ZrO<sub>2</sub> based for Oxygen (Blue Sens Gas analytics, Herten, Germany).

Process control and exponential feeding was established using the process control system PIMS Lucullus (Securecell, Urdorf Switzerland). pH was monitored using an EasyFerm Plus pH-sensor (Hamilton, Reno, NV, United States) and was kept constant at 6.7 throughout all cultivations and controlled using a base only control (12.5% NH<sub>4</sub>OH), while acid (5% H<sub>3</sub>PO<sub>4</sub>) was added manually, if necessary. Stirrer speed was set to 1400 rpm. Dissolved oxygen (dO<sub>2</sub>) was kept above 30% oxygen saturation by supplying 2 vvm of a mixture of pressurized air and pure oxygen. The dO<sub>2</sub> was monitored using a Visiferm fluorescence dissolved oxygen electrode (Hamilton, Reno, NV, United States). Feed medium was added by using a PRECIFLOW pump (Lambda, Laboratory Instruments, Baar, Switzerland). Reactor weight and the depleted feed weight were monitored to determine exact feeding rates using a feed forward control as described here (Slouka et al., 2018). Harvest and fill-up step were conducted using a peristaltic pump (Watson-Marlow, Guntramsdorf, Austria).

### Cultivation Procedure

The pre-culture and batch phase was equivalent for all performed cultivations, followed by a single-cycle fed-batch, a two-cycle

fed-batch, a three-cycle fed-batch or a chemostat cultivation (**Supplementary Figure 1**).

### Pre-culture

Pre-culture was prepared using 2500 mL high yield flasks. 500 milliliter of DeLisa medium (DeLisa et al., 1999) supplemented with 8.8 g/L glucose were inoculated with 1.5 mL of bacteria solution stored in cryos at –80°C and subsequently cultivated for 16 h at 230 rpm in an Infors HR Multitron shaker (Infors, Bottmingen Switzerland) at 37°C.

### Batch Cultivation

Batch medium [DeLisa medium supplement with 20 g/L glucose (DeLisa et al., 1999)] was inoculated with 1/10th of the reactor volume using the previously described pre-culture. Batch process was carried out at 37°C and took approximately 6–7 h until sugar was depleted, monitored via a drop in the CO<sub>2</sub> signal or a pO<sub>2</sub> peak, respectively.

### Fed-Batch for Biomass Generation

After the batch phase, a non-induced fed-batch was carried out at 35°C over-night using carbon-limited feeding approaches. Non-induced fed-batch was carried out at a constant specific feeding rate (=q<sub>s</sub>) of 0.25 g/g/h to achieve a biomass concentration of approximately 35 g/L prior to induction (**Supplementary Figures 3a,b**). For exponential feeding, DeLisa medium (DeLisa et al., 1999) supplemented with 300 g/L glucose was used as feed medium. Equation 1 was used for the feed controller to calculate the feed-rate for maintaining a constant q<sub>s</sub> in feed forward mode (Kopp et al., 2017; Wurm et al., 2017a). Dry cell weight of biomass and feeding rates were determined as described here (Hausjell et al., 2018; Slouka et al., 2018). In short, triplicate at-line optical density (OD) measurements and a previously established OD to biomass correlation were used for calculation of the exponential feeding profile.

$$F(t) = \frac{q_s \times X(t) \times \rho_f}{c_f} \quad (1)$$

F, feed-rate (g/h); q<sub>s</sub>, specific glucose uptake rate (g/g/h); X(t), biomass (g);  $\rho_f$ , feed density (g/L); c<sub>f</sub>, feed concentration (g/L).

### Single-Cycle Fed-Batch

Prior to induction, temperature was decreased to 30°C, to reduce stress onto host cells and enhance soluble protein formation (Wurm et al., 2016). The induction phase was conducted for 12 h using a glucose–lactose mixed feed system according to a previous study (Slouka et al., 2018). For induction, DeLisa medium (DeLisa et al., 1999) supplemented with 250 g/L glucose and 141.2 g/L lactose, was fed at a constant specific feeding rate of 0.25 g/g/h, as these mixing ratios were found to show better results in previous cultivations (Wurm et al., 2017a). For single-cycle fed-batch cultivations, the cultivation was terminated after 12 h of induction and a full reactor harvest was conducted (Figure 1 and Supplementary Figure 1a), whereas for two-cycle and three-cycle fed-batches only a partial harvest was performed.

### Two-Cycle Repetitive Fed-Batch

Prior to the repetitive fed-batch the process cycles preculture, batch cultivation, fed-batch for biomass generation and the single-cycle fed-batch were performed. However, after the induction phase feeding was stopped and only a partial harvest was conducted leaving half of the initial volume for the ongoing process steps. In order to achieve the same biomass concentration as before induction, biomass was determined at-line and diluted to approximately 35 g/L using sterile DeLisa medium (DeLisa et al., 1999). Dilution media contained no carbon source but was double concentrated in salt and trace element concentration to avoid nutrient limitation throughout the following repeated cycles. Antibiotic was also added to the sterile medium to achieve the initial start concentration. After the refilling the feeding was started analogous to the single-cycle fed-batch for another 12 h. Complete harvest was conducted after the second cycle.

### Three-Cycle Repetitive Fed-Batch

Cultivation was carried out analog to the description in section “Two-Cycle Repetitive Fed-Batch.” However, after the second cycle was finished, again only a partial harvest was conducted. The refilling step was conducted analog to the procedure for the two-cycle repetitive fed-batch and the total fermentation broth was harvested after cycle 3 was finished.

### Chemostat Cultivation

After batch cultivation the continuous process mode was started. Dilution rate was set to  $D = 0.1 \text{ h}^{-1}$  and the volume in the reactor was kept constant at 750 mL using an immersion tube adjusted to the right height of the stirred liquid surface in the reactor which was connected to a bleed pump (Watson-Marlow, Guntramsdorf, Austria). Medium for chemostat cultivation was prepared as described by DeLisa (DeLisa et al., 1999) supplemented with 50 g/L glucose and 25 g/L lactose. To keep the growth rates of the performed repetitive fed-batch processes comparable to the performed chemostat processes, only dilution rates of  $0.1 \text{ h}^{-1}$  were investigated within this study. The overall induction time of the chemostat process was 90 h.

### Ideal Chemostat

In order to test advantages of a continuous cultivation system, an ideal chemostat was simulated. We calculated the ideal chemostat

with stable product formation at maximum specific productivity as shown in Figures 2B,3B.

### Sampling

Samples were taken at the end of the batch phase, after the fed-batch phase and regularly during the induced cycles of all cultivation modes. Biomass, optical density, viability and metabolite accumulation were determined for every sample taken. All samples taken during induction phase were additionally analyzed for product formation.

Samples during repetitive fed-batch cultivations were taken every three hours during the first and the third cycle, while the second cycle was conducted over night and therefore only the harvest sample was taken.

For the chemostat cultivation, samples were taken 3 h after start of the induced chemostat and from then on twice a day.

### Biomass, Viability, Substrate and Metabolite Analysis

Biomass was measured by optical density ( $OD_{600}$ ) and gravimetrically by dry cell weight (DCW), while flow cytometry analysis (FCM) was used for the determination of viability.

$OD_{600}$  was measured in triplicates using a Genesys 20 photometer (Thermo Scientific, Waltham, MA, United States). Since the linear range of the used photometer was between 0.2 and 0.8 (AU), samples were diluted with  $dH_2O$  to stay within the given range.

The DCW was determined by centrifugation (10,000 rpm for 10 min at 4°C) of 1 mL of homogenous sample solution in a prepared 2 mL Eppendorf-Safe-Lock Tube (Eppendorf, Hamburg, Germany). After centrifugation, the supernatant was withdrawn, frozen at  $-20^\circ\text{C}$  and used to determine sugar concentrations by HPLC measurements. The pellet was re-suspended with 1 mL of 0.9% NaCl solution and centrifuged again (10,000 rpm for 10 min at 4°C). Afterward, the pellet was dried for at least 48 h at  $105^\circ\text{C}$  and DCW was evaluated gravimetrically in triplicates.

For FCM, cultivation broth was diluted 1:100 with 0.9% NaCl solution, stored at 4°C and measured every day. The measurement was performed using a Cyflow® Cube 8 flow cytometer (Sysmex, Görlitz, Germany) according to Langemann et al. (2016) using DiBAC4(3) (bis-(1,3-dibutylbarbituric acid-trimethineoxonol) and Rh414 dye. Both dyes were purchased from AnaSpec (Fremont, CA, United States).

Sugar concentrations of feed and clarified fermentation broth were measured via anion exchange HPLC (Thermo Scientific, Waltham, MA, United States) using a Supelcogel-column (Sigma-Aldrich, St. Louis, MO, United States) and a refractive index detector (Agilent Technologies, Santa Clara, CA, United States). The mobile phase was 0.1%  $H_3PO_4$  with a constant flow rate of 0.5 mL/min, and the system was run isocratically at 30°C. Glucose, lactose, galactose, and acetate accumulation was monitored using calibration standards with a concentration of 1, 5, 10, 25, and 50 g/L of each analyte. Chromatograms were analyzed using Chromeleon Software (Thermo Scientific, Waltham, MA, United States).

Cultivation mode	$t_{\text{down}}$	$t_{\text{prod.}}$	Total product
Fed-batch	65.7%	34.3%	$P_{\text{conv.FB}} = V_{\text{Harvest}} * C_{\text{P Harvest}}$
Repetitive fed-batch (2 cycles)	48.9%	51.1%	$P_{\text{RFB 2 phase}} = ((V_{\text{H1}} - \frac{V_{\text{Batch}}}{2}) * C_{\text{PH1}}) + (V_{\text{H2}} * C_{\text{PH2}})$
Repetitive fed-batch (3 cycles)	39.0%	61.0%	$P_{\text{RFB 3 phase}} = ((V_{\text{H1}} - \frac{V_{\text{Batch}}}{2}) * C_{\text{PH1}}) + ((V_{\text{H2}} - \frac{V_{\text{Batch}}}{2}) * C_{\text{PH2}}) + (V_{\text{H3}} * C_{\text{PH3}})$
Chemostat	14.3%	85.7%	$P_{\text{Chemostat}} = \sum (V_{\text{Bleed}} * C_{\text{P Bleed}})$

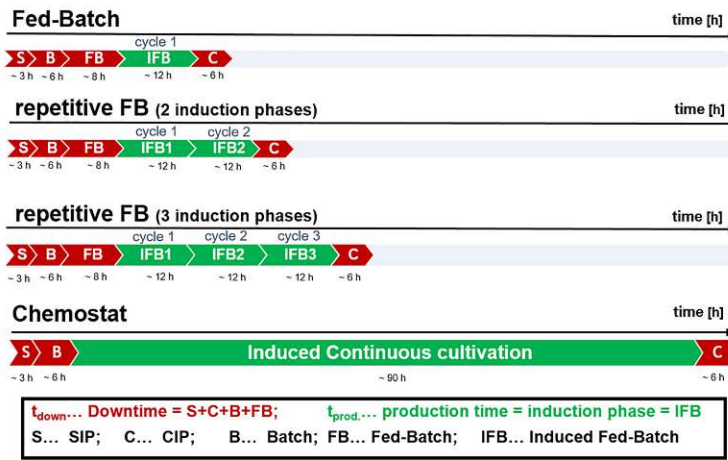


**FIGURE 1** | Comparison of cultivation durations of a fed-batch, a repetitive fed-batch consisting of two cycles, a repetitive fed-batch consisting of three cycles and a chemostat process; effective production time vs. downtime for a 10 m<sup>3</sup> fermenter scale is given for each process in percent relative to total process time; steam in place (SIP), cleaning in place (CIP).

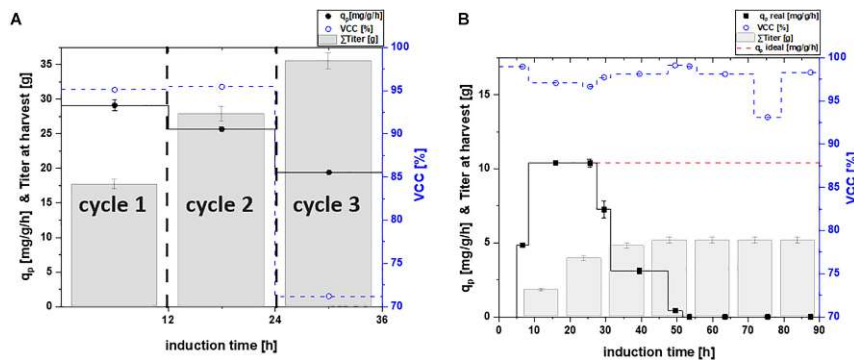


**FIGURE 2** | Specific productivity  $q_p$  (mg/g/h), viable cell concentration (=VCC) [%] and the harvested product titer for (A) a repetitive fed-batch cultivation and (B) a chemostat process; a theoretical ideal chemostat was simulated at  $q_{p,max}$ ; VCC was evaluated by flow cytometry analysis with an average standard deviation of 2%.

Die approbierte gedruckte Originalversion dieser Dissertation ist an der TU Wien Bibliothek verfügbar. The approved original version of this doctoral thesis is available in print at TU Wien Bibliothek.



### Product Quantification

Product samples were taken after the start of the induction phase. Five milliliter of cultivation broth were pipetted in a 50 mL falcon tube and centrifuged for 10 min at 5000 rpm at 4°C. The supernatant was discarded and the pellet was frozen at -20°C. Afterward, the samples were disrupted by homogenization as follows: The pellets were re-suspended in a buffer (0.1 M TRIS, 10 mM EDTA, pH 7.4) according to their dry cell weight to reach a biomass of 10 g/L prior to homogenization. After suspending the cells with a disperser (T10 basic ULTRA-TURRAX®, Staufen, Germany) they were treated with an EmusiflexC3 Homogenizer (Avestin, Ottawa, ON, United States) at 1400 bar for 4 passages, ensuring complete cell disruption. After homogenization the broth was centrifuged (14,000 rpm, 10 min, 4°C) and the supernatant was used immediately for HPLC quantification.

For soluble titer measurements of the cytoplasmic target protein, the supernatant derived after centrifugation of homogenized broth was filtered and then quantified via UHPLC (Thermo Scientific, Waltham, MA, USA). For quantification of cytoplasmic soluble protein, a size exclusion (=SEC) chromatography principle was applied, using a X-bridge column (Waters, Milford, DE, United States). The mobile phase was composed of 250 mM KCl and 50 mM of each KH<sub>2</sub>PO<sub>4</sub> and K<sub>2</sub>HPO<sub>4</sub> dissolved in Ultrapure water as describe elsewhere (Goyon et al., 2018). A constant flow rate of 0.5 mL/min was applied with an isocratic elution at 25°C for 18 min. BSA standards (50, 140, 225, 320, 500, 1000, and 2000 mg/mL; Sigma Aldrich, St. Louis, MO, United States) were used for quantification.

For soluble titer measurements of the periplasmic protein, clarified cultivation broth was analyzed by a BioResolve RP mAb Polyphenyl column (Waters, Milford, DE, United States), using a reversed-phase HPLC method published elsewhere (Kopp et al., 2020). Product was quantified with a UV detector (Thermo Fisher, Waltham, MA, United States) at 214 nm, using BSA as standard reference.

Specific productivity was calculated as a rate between two sampling points using Eq. 2:

$$q_p = \frac{\frac{c_i + c_{i-1}}{2}}{\frac{x_i + x_{i-1}}{2}} \times \frac{1}{t_i - t_{i-1}} \quad (2)$$

$q_p$  specific productivity (mg/g/h);  $c_i$ , product concentration of sample at timepoint  $i$  (mg/L);  $X_i$ , biomass concentration of sample at timepoint  $i$  (g/L);  $t_i$ , cultivation time at timepoint of sample  $i$  (h).

The experimentally evaluated  $q_p$  values were used for the calculation of the real chemostat. For the simulated ideal chemostat, stable product formation at maximum specific productivity was assumed, once the maximum productivity was reached, as shown in **Figures 2B,3B**.

### Reproducibility

To test the reproducibility of the equipment described in section "Bioreactor Setup," triplicates of a fed-batch cultivation were assessed by the same operator for one target protein. Found errors were not higher than  $\pm 0.35$  g/L for titer determination

[resulting in a maximum relative standard deviation (RSD) below 10%]. Specific feeding rates were found to be within a deviation of  $\pm 0.03$  g/g/h (max. RSD below 11%). Dry cell weights deviations between replicates were below 3.8 g/L (below a max. RSD of 9%). Set specific feeding rates require at-line OD<sub>600</sub> determination to estimate the biomass, before the exponential feeding ramp is calculated. Variances (i.e., due to dilution) in OD<sub>600</sub>-signals thus may cause differences in the resulting biomass and titer, as previously shown (Slouka et al., 2018).

## RESULTS AND DISCUSSION

### Experimental Design

The potential of achieving high recombinant protein titers in repetitive fed-batch cultivation mode was shown by Luttmann et al. for *P. pastoris* as production host (Martens et al., 2011). However, repetitive fed-batch technology for recombinant protein production using *E. coli* has not been investigated yet. As methanol was continuously fed throughout the repetitive fed-batch studies with *P. pastoris* (Martens et al., 2011; Fricke et al., 2013), we established a similar feeding strategy for the inducer lactose and *E. coli*. Hence a feed-forward feeding strategy according to Eq. 1 was applied throughout all cycles. Furthermore, we tested whether a single-cycle fed batch, a two-cycle repetitive fed-batch, a three-cycle repetitive fed-batch or a chemostat is the cultivation mode of choice regarding overall space-time yield. We tested the cultivation modes for two different recombinant products: one produced in the cytoplasm and one secreted to the periplasm. Establishing such a process is of high interest for industry, to reduce downtime. For the calculations within this study the duration of the cycles and downtimes of the cultivation were chosen as regularly applied in industry (Slouka et al., 2018). Downtime, production time as well as calculation of total product titer are depicted in **Figure 1**.

The fermenter scale for the calculations was assumed with 10 m<sup>3</sup>, which is a common scale for *E. coli* in industry. Thus, time for steam in place (SIP) and cleaning in place (CIP) takes 3 and 6 h, respectively (communication with industrial partner). Batch phase on glucose was 6 h (Slouka et al., 2018). Non-induced fed-batch time was 8 h, to achieve a biomass of 35–40 g/L before induction using a growth rate of  $\mu = 0.1$  h<sup>-1</sup> (equivalent to a  $q_s$  of 0.25 g/g/h using a biomass/substrate yield of 0.4 g/g for calculation, Kopp et al., 2017). Previous results indicate, that a  $q_s$  of 0.25 g/g/h, a cultivation temperature of 30°C and an induction time of 10–12 h is beneficial for the production of many recombinant proteins and was thus chosen for this study (Wurm et al., 2016; Wurm et al., 2017b; Slouka et al., 2018; Schein, 2019). As fed-batch cultivations were conducted at  $q_s = 0.25$  g/g/h (equivalent to  $\mu = 0.1$  h<sup>-1</sup>), dilution rates in chemostat cultivation were investigated for the same  $\mu = D = 0.1$  h<sup>-1</sup>.

The final product titer for the different cultivations modes was calculated according to **Figure 1**. Space-time yield was calculated according to Equation 3 to allow comparison of the different

process modes.

$$STY = \frac{\sum V_{Harvest} \times c_{Protein} \times 24}{V_{Reactor} \times t} \quad (3)$$

STY, space-time yield (g/L/day);  $\Sigma V_{Harvest}$ , sum of harvested volume (L);  $c_{Protein}$ , protein titer measured by HPLC analysis (g/L);  $V_{Reactor}$ , Reactor volume (L);  $t$ , process time (h).

### Cultivation Strategies and Their Results for Cytoplasmic Protein Formation

Mixed feed approaches, containing glucose and lactose, were found to enhance soluble protein formation (Wurm et al., 2016, 2017a,b). This is in accordance with our results obtained for the single-cycle fed-batch cultivation for the cytoplasmic protein, yielding a specific productivity of 29.12 mg/g/h. Other studies indicate stable viability throughout fed-batch cultivation using lactose induction at given feeding rates (Kopp et al., 2017), which we also confirmed in this study (95.1% viability at harvest).

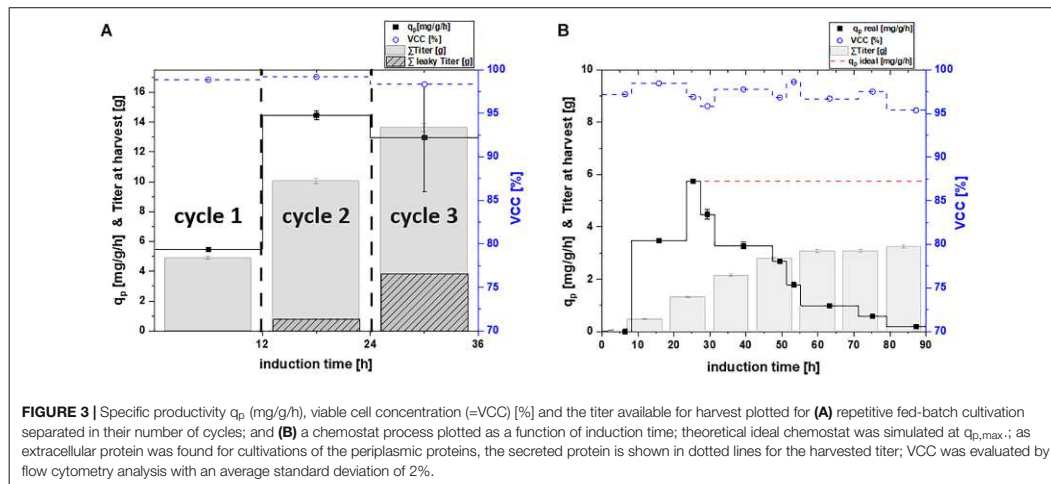
Throughout the two-cycle repetitive fed-batch cultivation a minor decrease in productivity from 29.12 to 25.67 mg/g/h could be observed. Even though productivity in cycle two decreased, the total titer obtained per liter reactor volume at harvest increased majorly (Table 2). As viability was also high with 95.4% throughout the second cycle, the reduction in cell specific productivity might be a result of metabolic burden. Kanamycin concentration was adapted to the starting concentration of 0.02 g/L before the start of each repeated cycle to avoid possible plasmid loss.

Throughout the third cycle, a rapid decrease of  $q_p$  to 19.51 mg/g/h was found. Viable cell concentration decreased by 30%, which is most likely the cause for the high decrease in productivity. Upon producing high amounts of recombinant protein the host cell needs to be divided into a physiological compartment and a recombinant compartment as described by Neubauer et al. (2003). High titers as needed to make recombinant protein formation industrially feasible can also be toxic for host cells. As accumulated recombinant protein can effect ATP and NADH balances negatively this might lead to a decrease in physiological functions of the cell and can potentially hinder cell doubling (Rugbjerg and Sommer, 2019). Even though the specific productivity declined over time, the harvested titers of cycle three (Figure 2A) still increased significantly, compared to the harvest of the previous cycles. As viability decreased majorly throughout the third cycle, no further cycle was conducted.

For the chemostat cultivation, product formation started after an adaption phase of 5 h post induction (Figure 2B). Specific productivity further increased until it peaked after 18 h of induction at a  $q_p$  of 10.4 mg/g/h. However, ongoing sampling points determined the product formation to decrease rapidly and to terminate after 50 h of induction. No decrease in viability was observed and kanamycin was continuously fed to the system to avoid plasmid loss. Still, reduced plasmid copy numbers might occur and thus could be an explanation for the decreasing productivity (Sieben et al., 2016). Recent results, however, show that the productivity can fluctuate in lactose induced chemostat with BL21(DE3) as a result of genotypic or phenotypic

TABLE 2 | Comparing specific productivity and the product titer at harvest for the production of a cytoplasmic protein; each cycle is investigated separately for fed-batch and repeated fed-batch cultivation; values for chemostat and theoretical "ideal" chemostat cultivations are given every 12 h (i.e., one cycle); calculation for  $q_p$  represents instantaneous values whereas titers are calculated as accumulated values.

induction time (h)	12	24	36	48	60	72	84
<b>Cytoplasmic protein</b>	$q_p$ (mg/g/h)	$q_p$ (mg/g/h)	$q_p$ (mg/g/h)	$q_p$ (mg/g/h)	$q_p$ (mg/g/h)	$q_p$ (mg/g/h)	$q_p$ (mg/g/h)
	Titer (g/L)	Titer (g/L)	Titer (g/L)	Titer (g/L)	Titer (g/L)	Titer (g/L)	Titer (g/L)
Fed-batch (1 cycle)	29.12 ± 0.82	17.64 ± 0.67					
Repeated fed-batch (2 cycles)		25.66 ± 0.32	27.85 ± 1.05				
Repeated fed-batch (3 cycles)			19.42 ± 0.14	35.51 ± 1.16			
Chemostat cultivation	8.00 ± 0.13	1.80 ± 0.07	9.18 ± 0.15	3.92 ± 0.15	4.75 ± 0.08	4.77 ± 0.19	5.14 ± 0.2
Theoretical "ideal" chemostat	8.00 ± 0.13	1.80 ± 0.07	9.18 ± 0.15	3.92 ± 0.15	10.4 ± 0.17	6.84 ± 0.27	11.52 ± 0.45
				10.4 ± 0.17	9.18 ± 0.36	10.4 ± 0.17	13.86 ± 0.54
					0.25 ± 0	5.14 ± 0.20	5.14 ± 0.2
					0.00	0.00	0.00
							16.2 ± 0.63



diversification (Kittler et al., 2020). Hence we believe effects causing the decrease in productivity derive from subpopulation diversification. Shifts in the transcriptome in combination with point mutations (Rugbjerg and Sommer, 2019), are known to cause the formation of non-producing subpopulations (Basan, 2018). Recent publications (Schreiber et al., 2016; Binder et al., 2017) showed that carbon limited feeding increases probability of phenotypic subpopulation diversification. These effects are described to increase with generation time (Rugbjerg et al., 2018). As cells in chemostat processes are cultivated for longer time-spans than fed-batch and repeated fed-batch processes, long-term cultures face a higher chance of being affected (Buerger et al., 2019). We believe that a fitter subpopulation, having altered levels of transcription, is avoiding the burden of production. As recombinant protein expression is referred to cause decreasing biomass yields, a non-productive subpopulation, showing no decrease in biomass yield thus could overgrow the initial population. Hence we believe that the productive subpopulation is washed-out over the time-course of the induction phase and a non-productive subpopulation takes over, explaining the decline in productivity (Peebo and Neubauer, 2018; Kopp et al., 2019b).

In order to test the applicability of continuous cultivations for industry, a theoretical “ideal” chemostat with constant productivity at maximum specific productivity was simulated. However, the maximum specific productivity during the chemostat cultivation is significantly lower compared to the repetitive fed-batch cultivation (2.9 times lower compared to productivity of cycle two, Figures 2A,B). Furthermore, higher biomass concentrations and thus higher volumetric titers can be achieved in fed-batch and repetitive fed-batch mode. As biomass yield is decreasing upon production of recombinant proteins, this can potentially lead to washout (Lis et al., 2019). Hence, trying to achieve “fed-batch like” biomass concentrations in chemostat cultivation is highly difficult. Our results are in favor of fed-batch and repetitive fed-batch cultivation for the cytoplasmic target

protein and will be compared in section “Targeting Maximum Space-Time Yield: The Cultivation Mode to Choose” regarding their space-time yield.

### Cultivation Strategies and Their Results for Periplasmic Protein Formation

In order to test and verify the effects monitored for the cytoplasmic protein, we investigated the same cultivation techniques for periplasmic protein production (Figure 3 and Table 3).

The measured cell specific productivity in the single-cycle fed-batch was  $q_p = 5.47$  mg/g/h, which was significantly lower compared to the cytoplasmic product. Production of the periplasmic protein started only 6 h post induction and low uptake rates of the inducer lactose potentially explain the low specific productivity during the single-cycle fed-batch. As production of periplasmic products depends on several factors (i.e., translocation to the periplasm), generally lower specific productivity can be expected, compared to protein expression in the cytoplasm (Kleiner-Grote et al., 2018; Karyolaimos et al., 2019). No decrease in viability could be observed throughout cycle one, as for the cytoplasmic product.

Cell specific productivity in the two-cycle repeated fed-batch cultivation was much higher compared to the first cycle ( $q_p = 14.44$  mg/g/h). Even though viability did not decrease in cycle two, leaky product (7.7% of total product) could be detected in the supernatant. This behavior has been observed for periplasmic proteins in literature before (Chen et al., 2014; Hausjell et al., 2020).

For repeated fed-batch technology carried out for three cycles, a minor decrease in productivity was found compared to cycle two, resulting in a  $q_p$  of 12.96 mg/g/h. The uptake rate of the inducer lactose increased during cycle two and three (Supplementary Figure 4b). Thus, we hypothesize that longer

**TABLE 3** | Comparing specific productivity and the product titer at harvest for the production of a periplasmic protein: each cycle is investigated separately for fed-batch and repeated fed-batch cultivation; values for chemostat and theoretical "ideal" chemostat cultivations are given every 12 h (i.e., one cycle); calculation for  $q_p$  represents instantaneous values whereas titers are calculated as accumulated values.

induction time (h)	12	24	36	48	60	72	84
periplasmic protein	$q_p$ (mg/g/h)	$q_p$ (mg/g/h)	$q_p$ (mg/g/h)	$q_p$ (mg/g/h)	$q_p$ (mg/g/h)	$q_p$ (mg/g/h)	$q_p$ (mg/g/h)
	$q_p$ (mg/g/h)	$q_p$ (mg/g/h)	$q_p$ (mg/g/h)	$q_p$ (mg/g/h)	$q_p$ (mg/g/h)	$q_p$ (mg/g/h)	$q_p$ (mg/g/h)
	Titer (g/L)	Titer (g/L)	Titer (g/L)	Titer (g/L)	Titer (g/L)	Titer (g/L)	Titer (g/L)
	Titer (g/L)	Titer (g/L)	Titer (g/L)	Titer (g/L)	Titer (g/L)	Titer (g/L)	Titer (g/L)
Fed-batch (1 cycle)	$5.47 \pm 0.06$	$4.87 \pm 0.09$					
Repeated fed-batch (2 cycles)		$14.44 \pm 0.30$	$10.03 \pm 0.19$				
Repeated fed-batch (3 cycles)				$12.96 \pm 3.65$	$13.61 \pm 0.26$		
Chemostat cultivation	$1.98 \pm 0.03$	$0.45 \pm 0.01$	$5.26 \pm 0.08$	$1.30 \pm 0.02$	$3.76 \pm 0.06$	$2.12 \pm 0.04$	$2.32 \pm 0.04$
Theoretical "ideal" chemostat	$1.98 \pm 0.03$	$0.45 \pm 0.01$	$5.26 \pm 0.08$	$1.30 \pm 0.02$	$3.16 \pm 0.05$	$5.75 \pm 0.04$	$5.02 \pm 0.07$

timespans of full lactose induction were the reason for the increase in specific productivity compared to cycle one. No cell death was monitored throughout cycle three, however higher amounts of leakiness were found (28.1% of total product). No fourth cycle was conducted, in order to make repetitive fed-batch cultivations for both target proteins comparable in their number of cycles. Moreover, levels of leakiness increased over the timespan of the cultivation, which was a further reason to terminate the process after cycle three.

For the chemostat cultivation no product formation was found for the first 8 h of induction. Product formation started after 8 h of induction and increased until reaching a peak of 5.75 mg/g/h after 20–25 h. The timespan until full induction was comparable for repetitive fed batch cultivations and chemostat cultivations (Figure 3). Therefore, it seems like the expression of the periplasmic protein required an adaption time after the start of induction, to establish protein translocation toward the periplasm (Kopp et al., 2017). Throughout chemostat cultivation maximum specific productivity was lower compared to repetitive fed-batch cultivation by a factor of 2.9 (which is in accordance with results obtained for the cytoplasmic product). However, we could not monitor any secretion of periplasmic protein during continuous cultivation. Chemostat cultivation was terminated after 90 h of induction as productivity was below the LOD for both products.

Again, a theoretical ideal chemostat was simulated, exhibiting time-independent productivity once cell specific productivity reached  $q_{p,max}$  (Figure 3B). Our results favor repetitive fed-batch cultivation mode for the periplasmic target protein over single cycle fed-batch and chemostat cultivations regarding the specific productivity. Achieved space-time yields of each cultivation mode will be compared in section "Targeting Maximum Space-Time Yield: The Cultivation Mode to Choose."

### Targeting Maximum Space-Time Yield: The Cultivation Mode to Choose

The goal of this study was to determine the cultivation strategy giving the highest space-time yield with recombinant *E. coli*. Thus, we calculated the overall space-time yield in  $g_{product}/L_{reactor}/day$ , including "downtimes" for each cultivation mode. Results are shown in Figure 4 and Supplementary Figure 2 for recombinant cytoplasmic and periplasmic protein production.

In fed-batch cultivations, cleaning and set-up take up a severe amount of time. Generally, this leads to a much shorter production time in comparison to the total process time. For repetitive fed-batch cultivations and continuous cultivations these downtimes can be reduced compared to single-cycle fed batches (Figure 1). Even though fed-batch cultivations usually give a high  $q_p$ , cultivation modes with a lower  $q_p$  in combination with a lower downtime might still result in an increase of the overall space-time yield.

For repetitive fed-batch cultivations and the cytoplasmic target protein, the highest space-time yield was found for a two-cycle process (Figure 4A). Even though  $q_p$  declined during cycles two and three (Figure 2A), the space-time yield for all repetitive fed batch cultivations was superior to a single-cycle fed batch.

**TABLE 4 |** Comparing substrate per product yield for the production of a cytoplasmic protein; each cycle is investigated separately for fed-batch and repeated fed-batch cultivation; chemostat cultivation is calculated as a rate every 12 h (i.e., one cycle).

induction time (h)	12	24	36	48	60	72	84
<b>cytoplasmic protein</b>	<b><math>Y_{P/S}</math> (mg/g)</b>						
Fed-batch (1 cycle)	86.8 ± 4.3						
Repeated fed-batch (2 cycles)		84.6 ± 4.2					
Repeated fed-batch (3 cycles)			77.9 ± 3.4				
Chemostat cultivation	241.7 ± 12.1	280.8 ± 14.0	176.3 ± 8.8	11.6 ± 0.6	0	0	0
Theoretical "ideal" chemostat	241.7 ± 12.1	280.8 ± 14.0	280.8 ± 14.0	280.8 ± 14.0	280.8 ± 14.0	280.8 ± 14.0	280.8 ± 14.0

**TABLE 5 |** Comparing substrate per product yield in mg/g for the production of a periplasmic protein; each cycle is investigated separately for fed-batch and repeated fed-batch cultivation; chemostat cultivation is calculated as a rate every 12 h (i.e., one cycle).

induction time (h)	12	24	36	48	60	72	84
<b>periplasmic protein</b>	<b><math>Y_{P/S}</math> (mg/g)</b>						
Fed-batch (1 cycle)	24.5 ± 0.9						
Repeated fed-batch (2 cycles)		135.4 ± 4.8					
Repeated fed-batch (3 cycles)			133.5 ± 4.7				
Chemostat cultivation	94.9 ± 3.3	133.6 ± 4.7	99.3 ± 3.5	58.4 ± 2.1	32.3 ± 1.1	7.8 ± 1.2	5.2 ± 0.8
Theoretical "ideal" chemostat	94.9 ± 3.3	133.6 ± 4.7	133.6 ± 4.7	133.6 ± 4.7	133.6 ± 4.7	133.6 ± 4.7	133.6 ± 4.7

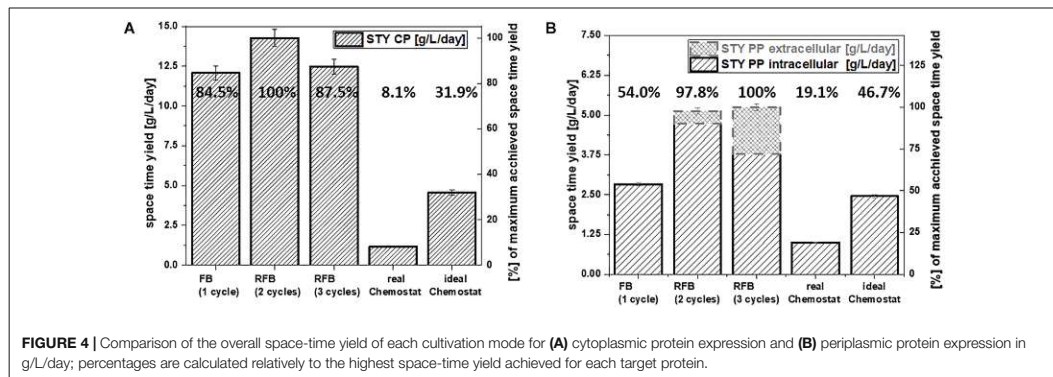


**FIGURE 4 |** Comparison of the overall space-time yield of each cultivation mode for (A) cytoplasmic protein expression and (B) periplasmic protein expression in g/L/day; percentages are calculated relatively to the highest space-time yield achieved for each target protein.

For processes conducted with the periplasmic target protein,  $q_p$  in cycle two and three was higher than productivity in cycle one (Figure 3A). Hence, it was obvious that repetitive fed-batch would be superior to a single-cycle cultivation regarding space-time yield. Even though the total space-time yield (Figure 4B) differed only by 2.2% when harvesting after cycle two or cycle three for the periplasmic protein, we want to highlight that by applying three induction cycles, total downtime can be reduced compared to the two-cycle repeated fed-batch.

A reduction of downtimes leads to reduced costs for chemicals and energy needed throughout SIP and CIP. Taking into account that CO<sub>2</sub>-taxes for industry will potentially be realized in near future, a reduction of energy consumption could also lead to higher profits (Kettner et al., 2018).

Continuous processes are generally described to lead to higher space-time yields (Lee et al., 2015). However, the monitored

space-time yield for the chemostat cultivations within this study was beneath 1/5th of the space-time yield received by the repetitive fed-batch cultivations, independent of the target product (Figures 4A,B). As (i) cell specific productivity and (ii) set biomass concentrations are lower in chemostat cultivation compared to repetitive fed-batch cultivation, this implies an overall reduction of space-time yield for chemostat processes. Product per Substrate Yield at the beginning of the continuous cultivation might compete with repetitive fed-batch cultivations (Tables 4, 5, and Supplementary Table 1). However, a severe decrease in productivity over time was monitored for chemostat cultivations, as microbial chemostat cultivations are known to result in fluctuating productivity (Peebo and Neubauer, 2018; Kopp et al., 2019a).

In order to simulate a steady state upon recombinant protein in chemostat cultivation, a stable productivity at  $q_{p,max}$  was

assumed for more than 6 residence times. The simulated space-time yield however was not superior compared to the repetitive fed batch cultivation. This is because  $q_p$  of chemostat cultivations was significantly lower compared to repeated fed-batch cultivations (Figures 2, 3). Hence, in this study chemostat cultivation led to a lower productivity and a lower space-time yield and would still need further investigation to achieve the high demands needed for recombinant protein formation.

## CONCLUSION

The goal of this study was to find out, whether a single-cycle fed-batch, a repetitive fed-batch consisting of two cycles or three cycles or a chemostat is the most suitable cultivation technique to achieve the highest space-time yield of soluble recombinant protein within *E. coli* BL21 (DE3). The impact of the cultivation technology on soluble protein formation was investigated for a cytoplasmic and a periplasmic model protein.

The results of this study show that a repetitive fed-batch approach leads to higher space-time yields compared to single-cycle fed-batches and chemostat cultures. For the cytoplasmic protein a two-cycle repetitive fed-batch was the most efficient cultivation mode, whereas for the periplasmic product a three-cycle repetitive fed-batch was found to be the most efficient cultivation method. Chemostat cultivations suffered from a low maximum specific productivity, which further decreased over time. Therefore, overall product throughput of the chemostat cultivations was much lower compared to other cultivation modes. Furthermore, a single-cycle fed batch was always outperformed by repeated fed-batch independent of the target product and number of applied cycles.

Production processes for recombinant proteins in large-scale are cost-intensive. Here, we were able to show that a repetitive

fed-batch cultivation leads to a higher space-time yield compared to a single-cycle fed-batch or a chemostat process. We can promote the developed mixed feeding approach in combination with the repetitive fed-batch cultivation mode, as it leads toward a more economic fingerprint and an increased space-time yield.

## DATA AVAILABILITY STATEMENT

The raw data supporting the conclusions of this article will be made available by the authors, without undue reservation.

## AUTHOR CONTRIBUTIONS

JK planned the experimental design and carried out the data treatment. SK performed the cultivations and analytics. CS, CH, and OS gave major scientific input. DW founded the idea of this study. JK and DW wrote the manuscript. OS critically reviewed the manuscript. All authors contributed to the article and approved the submitted version.

## ACKNOWLEDGMENTS

The authors acknowledge the TU Wien Bibliothek for financial support through its Open Access Funding Program.

## SUPPLEMENTARY MATERIAL

The Supplementary Material for this article can be found online at: <https://www.frontiersin.org/articles/10.3389/fbio.2020.573607/full#supplementary-material>

## REFERENCES

- Allison, G., Cain, Y. T., Cooney, C., Garcia, T., Bizjak, T. G., Holte, O., et al. (2015). Regulatory and Quality Considerations for Continuous Manufacturing. May 20–21, 2014 Continuous Manufacturing Symposium. *J. Pharm. Sci.* 104, 803–812. doi: 10.1002/jps.24324
- Baeshen, M. N., Al-Hejin, A. M., Bora, R. S., Ahmed, M. M., Ramadan, H. A., Saini, K. S., et al. (2015). Production of Biopharmaceuticals in *E. coli*: Current Scenario and Future Perspectives. *J. Microbiol. Biotechnol.* 25, 953–962. doi: 10.4014/jmb.1412.12079
- Basan, M. (2018). Resource allocation and metabolism: the search for governing principles. *Curr. Opin. Microbiol.* 45, 77–83. doi: 10.1016/j.mib.2018.02.008
- Bauer, R., Katsikis, N., Varga, S., and Hekmat, D. (2005). Study of the inhibitory effect of the product dihydroxyacetone on *Gluconobacter oxydans* in a semi-continuous two-stage repeated-fed-batch process. *Bioproc. Biosyst. Eng.* 28, 37–43. doi: 10.1007/s00449-005-0009-0
- Bergmann, P., and Trösch, W. (2016). Repeated fed-batch cultivation of *Thermosynechococcus elongatus* BP-1 in flat-panel airlift photobioreactors with static mixers for improved light utilization: Influence of nitrate, carbon supply and photobioreactor design. *Algal Res.* 17, 79–86. doi: 10.1016/j.algal.2016.03.040
- Binder, D., Drepper, T., Jaeger, K.-E., Delvigne, F., Wiechert, W., Kohlheyer, D., et al. (2017). Homogenizing bacterial cell factories: analysis and engineering of phenotypic heterogeneity. *Metab. Eng.* 42, 145–156. doi: 10.1016/j.ymben.2017.06.009
- Briand, L., Marcion, G., Kriznik, A., Heydel, J. M., Artur, Y., Garrido, C., et al. (2016). A self-inducible heterologous protein expression system in *Escherichia coli*. *Sci. Rep.* 6:33037. doi: 10.1038/srep33037
- Buerger, J., Gronenberg, L. S., Genee, H. J., and Sommer, M. O. A. (2019). Wiring cell growth to product formation. *Curr. Opin. Biotechnol.* 59, 85–92. doi: 10.1016/j.copbio.2019.02.014
- Casali, N. (2003). *Escherichia coli* host strains. *Methods Mol. Biol.* 235, 27–48. doi: 10.1385/1-59259-409-3:27
- Chen, Z.-Y., Cao, J., Xie, L., Li, X.-F., Yu, Z.-H., and Tong, W.-Y. (2014). Construction of leaky strains and extracellular production of exogenous proteins in recombinant *Escherichia coli*. *Microb. Biotechnol.* 7, 360–370. doi: 10.1111/1751-7915.12127
- DeLisa, M. P., Li, J., Rao, G., Weigand, W. A., and Bentley, W. E. (1999). Monitoring GFP-operon fusion protein expression during high cell density cultivation of *Escherichia coli* using an on-line optical sensor. *Biotechnol. Bioeng.* 65, 54–64.
- Deutscher, J., Francke, C., and Postma, P. W. (2006). How phosphotransferase system-related protein phosphorylation regulates carbohydrate metabolism in bacteria. *Microbiol. Mol. Biol. Rev.* 70, 939–1031. doi: 10.1128/MMBR.00024-06
- Dvorak, P., Chrast, L., Nikel, P. I., Fedr, R., Soucek, K., Sedlackova, M., et al. (2015). Exacerbation of substrate toxicity by IPTG in *Escherichia coli* BL21(DE3) carrying a synthetic metabolic pathway. *Microb. Cell. Fact.* 14:201. doi: 10.1186/s12934-015-0393-3
- Fricke, J., Pohlmann, K., Vefghi, E., Drews, M., Scheffler, U., and Luttmann, R. (2013). Advanced automation strategies for reliable, reproducible cultivation

- runs in a sequential/parallel operated multi-bioreactor plant. *IFAC Proc.* 46, 54–59 doi: 10.3182/20131216-3-IN-2044.00042
- Glaser, J. A. (2015). Continuous chemical production processes. *Clean Technol. Environ. Policy* 17, 309–316. doi: 10.1007/s10098-015-0903-3
- Goyon, A., Sciascera, L., Clarke, A., Guillaume, D., and Pell, R. (2018). Extending the limits of size exclusion chromatography: Simultaneous separation of free payloads and related species from antibody drug conjugates and their aggregates. *J. Chromatogr. A* 1539, 19–29. doi: 10.1016/j.chroma.2018.01.039
- Gupta, S. K., and Shukla, P. (2017). Microbial platform technology for recombinant antibody fragment production: A review. *Crit. Rev. Microbiol.* 43, 31–42. doi: 10.3109/1040841X.2016.1150959
- Hausjell, J., Kutscha, R., Gesson, D. J., Reinisch, D., and Spadiut, O. (2020). The Effects of Lactose Induction on a Plasmid-Free *E. coli* T7 Expression System. *Bioengineering* 7:8. doi: 10.3390/bioengineering7010008
- Hausjell, J., Weissensteiner, J., Molitor, C., Halbwirth, H., and Spadiut, O. (2018). *E. coli* HMS174(DE3) is a sustainable alternative to BL21(DE3). *Microb. Cell Fact.* 17:169. doi: 10.1186/s12934-018-1016-6
- Herwig, C., Garcia-Aponte, O. F., Golabgir, A., and Rathore, A. S. (2015). Knowledge management in the QbD paradigm: manufacturing of biotech therapeutics. *Trends Biotechnol.* 33, 381–387. doi: 10.1016/j.tibtech.2015.04.004
- Karyolimos, A., Ampah-Korsah, H., Hillenaar, T., Mestre Borrás, A., Dolata, K. M., Sievers, S., et al. (2019). Enhancing Recombinant Protein Yields in the *E. coli* Periplasm by Combining Signal Peptide and Production Rate Screening. *Front. Microbiol.* 10:1511. doi: 10.3389/fmicb.2019.01511
- Kettner, C., Kletzan-Slamani, D., Kirchner, M., Sommer, M., Kratena, K., Weishaar, S. E., et al. (2018). CATs–Carbon Taxes in Austria. *Implementation Issues and Impacts*. Vienna: WIFO.
- Kittler, S., Kopp, J., Veelenfurt, P. G., Spadiut, O., Delvigne, F., Herwig, C., et al. (2020). The Lazarus *Escherichia coli* Effect: Recovery of Productivity on Glycerol/Lactose Mixed Feed in Continuous Biomufacturing. *Front. Bioeng. Biotechnol.* 8:993. doi: 10.3389/fbioe.2020.00993
- Kleiner-Grote, G. R. M., Risse, J. M., and Friehs, K. (2018). Secretion of recombinant proteins from *E. coli*. *Eng. Life Sci.* 18, 532–550. doi: 10.1002/elsc.201700200
- Konstantinov, K. B., and Cooney, C. L. (2015). White Paper on Continuous Bioprocessing. May 20–21, 2014 Continuous Manufacturing Symposium. *J. Pharm. Sci.* 104, 813–820. doi: 10.1002/jps.24268
- Kopp, J., Kolkmann, A.-M., Veelenfurt, P. G., Spadiut, O., Herwig, C., and Slouka, C. (2019a). Boosting recombinant inclusion body production—from classical fed-batch approach to continuous cultivation. *Front. Bioeng. Biotechnol.* 7:297. doi: 10.3389/fbioe.2019.00297
- Kopp, J., Slouka, C., Spadiut, O., and Herwig, C. (2019b). The rocky road from fed-batch to continuous processing with *E. coli*. *Front. Bioeng. Biotechnol.* 7:328. doi: 10.3389/fbioe.2019.00328
- Kopp, J., Slouka, C., Ulonska, S., Kager, J., Fricke, J., Spadiut, O., et al. (2017). Impact of Glycerol as Carbon Source onto Specific Sugar and Inducer Uptake Rates and Inclusion Body Productivity in *E. coli* BL21(DE3). *Bioengineering* 5:1. doi: 10.3390/bioengineering5010001
- Kopp, J., Zauner, F. B., Pell, A., Hausjell, J., Humer, D., Ebner, J., et al. (2020). Development of a generic reversed-phase liquid chromatography method for protein quantification using analytical quality-by-design principles. *J. Pharm. Biomed. Anal.* 188:113412. doi: 10.1016/j.jpba.2020.113412
- Kumar, M. S., Jana, S. K., Senthil, V., Shashanka, V., Kumar, S. V., and Sadhukhan, A. K. (2000). Repeated fed-batch process for improving lovastatin production. *Process Biochem.* 36, 363–368. doi: 10.1016/S0032-9592(00)00222-3
- Kuo, H.-P., Wang, R., Lin, Y.-S., Lai, J.-T., Lo, Y.-C., and Huang, S.-T. (2017). Pilot scale repeated fed-batch fermentation processes of the wine yeast *Dekkera bruxellensis* for mass production of resveratrol from *Polygonum cuspidatum*. *Bioresour. Technol.* 243, 986–993. doi: 10.1016/j.biortech.2017.07.053
- Langemann, T., Mayr, U. B., Meitz, A., Lubitz, W., and Herwig, C. (2016). Multi-parameter flow cytometry as a process analytical technology (PAT) approach for the assessment of bacterial ghost production. *Appl. Microbiol. Biotechnol.* 100, 409–418. doi: 10.1007/s00253-015-7089-9
- Lee, S. L., O'Connor, T. F., Yang, X., Cruz, C. N., Chatterjee, S., Madurawe, R. D., et al. (2015). Modernizing Pharmaceutical Manufacturing: from Batch to Continuous Production. *J. Pharm. Innov.* 10, 191–199. doi: 10.1007/s12247-015-9215-8
- Lis, A. V., Schneider, K., Weber, J., Keasling, J. D., Jensen, M. K., and Klein, T. (2019). Exploring small-scale chemostats to scale up microbial processes: 3-hydroxypropionic acid production in *S. cerevisiae*. *Microb. Cell Fact.* 18, 50–50. doi: 10.1186/s12934-019-1101-5
- Liu, L., Wang, F., Pei, G., Cui, J., Diao, J., Lv, M., et al. (2020). Repeated fed-batch strategy and metabolomic analysis to achieve high docosahexaenoic acid productivity in *Cryptocodium cohnii*. *Microb. Cell Fact.* 19:91. doi: 10.1186/s12934-020-01349-6
- Malakar, P., and Venkatesh, K. V. (2012). Effect of substrate and IPTG concentrations on the burden to growth of *Escherichia coli* on glycerol due to the expression of Lac proteins. *Appl. Microbiol. Biotechnol.* 93, 2543–2549. doi: 10.1007/s00253-011-3642-3
- Marschall, L., Sagmeister, P., and Herwig, C. (2016). Tunable recombinant protein expression in *E. coli*: enabler for continuous processing? *Appl. Microbiol. Biotechnol.* 100, 5719–5728. doi: 10.1007/s00253-016-7550-4
- Martens, S., Borchert, S.-O., Faber, B. W., Cornelissen, G., and Luttmann, R. (2011). Fully automated production of potential Malaria vaccines with *Pichia pastoris* in integrated processing. *Eng. Life Sci.* 11, 429–435. doi: 10.1002/elsc.201000163
- Moeller, L., Grünberg, M., Zehndorf, A., Aurich, A., Bley, T., and Strehlitz, B. (2011). Repeated fed-batch fermentation using biosensor online control for citric acid production by *Yarrowia lipolytica*. *J. Biotechnol.* 153, 133–137. doi: 10.1016/j.jbiotec.2011.03.013
- Mühlmann, M. J., Forsten, E., Noack, S., and Büchs, J. (2018). Prediction of recombinant protein production by *Escherichia coli* derived online from indicators of metabolic burden. *Biotechnol. Prog.* 34, 1543–1552. doi: 10.1002/btpr.2704
- Nasr, M. M., Krumme, M., Matsuda, Y., Trout, B. L., Badman, C., Mascia, S., et al. (2017). Regulatory Perspectives on Continuous Pharmaceutical Manufacturing: Moving From Theory to Practice: September 26–27, 2016, International Symposium on the Continuous Manufacturing of Pharmaceuticals. *J. Pharm. Sci.* 106, 3199–3206. doi: 10.1016/j.xphs.2017.06.015
- Neubauer, P., Lin, H. Y., and Mathisizik, B. (2003). Metabolic load of recombinant protein production: inhibition of cellular capacities for glucose uptake and respiration after induction of a heterologous gene in *Escherichia coli*. *Biotechnol. Bioeng.* 83, 53–64. doi: 10.1002/bit.10645
- Novak, N., Gerdin, S., and Berovic, M. (1997). Increased lovastatin formation by *Aspergillus terreus* using repeated fed-batch process. *Biotechnol. Lett.* 19, 947–948. doi: 10.1023/A:1018322628333
- Ohya, T., Ohya, M., and Kobayashi, K. (2005). Optimization of human serum albumin production in methylotrophic yeast *Pichia pastoris* by repeated fed-batch fermentation. *Biotechnol. Bioeng.* 90, 876–887. doi: 10.1002/bit.20507
- Ozmilci, S., and Kargi, F. (2007). Ethanol fermentation of cheese whey powder solution by repeated fed-batch operation. *Enzyme Microb. Technol.* 41, 169–174. doi: 10.1016/j.enzmictec.2006.12.016
- Peebo, K., and Neubauer, P. (2018). Application of Continuous Culture Methods to Recombinant Protein Production in Microorganisms. *Microorganisms* 6:56. doi: 10.3390/microorganisms6030056
- Peebo, K., Valgepea, K., Maser, A., Nahku, R., Adamberg, K., and Vilu, R. (2015). Proteome reallocation in *Escherichia coli* with increasing specific growth rate. *Mol. Biosyst.* 11, 1184–1193.
- Rathore, A. S. (2015). Continuous Processing for Production of Biotech Therapeutics. *PDA J. Pharm. Sci. Technol.* 69:333. doi: 10.5731/pdajpst.2015.01072
- Rosano, G. L., and Ceccarelli, E. A. (2014). Recombinant protein expression in *Escherichia coli*: advances and challenges. *Front. Microbiol.* 5:172. doi: 10.3389/fmicb.2014.00172
- Rosano, G. L., Morales, E. S., and Ceccarelli, E. A. (2019). New tools for recombinant protein production in *Escherichia coli*: A 5-year update. *Protein Sci.* 28, 1412–1422. doi: 10.1002/pro.3668
- Rugbjerg, P., and Sommer, M. O. A. (2019). Overcoming genetic heterogeneity in industrial fermentations. *Nat. Biotechnol.* 37, 869–876. doi: 10.1038/s41587-019-0171-6
- Rugbjerg, P., Myling-Petersen, N., Porse, A., Sarup-Lytzen, K., and Sommer, M. O. A. (2018). Diverse genetic error modes constrain large-scale bio-based production. *Nat. Commun.* 9:787. doi: 10.1038/s41467-018-03232-w
- Schein, C. H. (2019). Production of Soluble Recombinant Proteins in Bacteria. *Biotechnology* 7:1141. doi: 10.1038/nbt1189-1141

- Schreiber, F., Littmann, S., Lavik, G., Escrig, S., Meibom, A., Kuypers, M. M. M., et al. (2016). Phenotypic heterogeneity driven by nutrient limitation promotes growth in fluctuating environments. *Nat. Microbiol.* 1:16055. doi: 10.1038/nmicrobiol.2016.55
- Sieben, M., Steinhorn, G., Müller, C., Fuchs, S., Chin, L. A., Regestein, L., et al. (2016). Testing plasmid stability of *Escherichia coli* using the continuously operated shaken BIOreactor system. *Biotechnol. Prog.* 32, 1418–1425. doi: 10.1002/btpr.2341
- Slouka, C., Kopp, J., Hutwimmer, S., Strahammer, M., Strohm, D., Eitenberger, E., et al. (2018). Custom Made Inclusion Bodies: Impact of classical process parameters and physiological parameters on Inclusion Body quality attributes. *Microb. Cell Fact.* 17:148. doi: 10.1186/s12934-018-0997-5
- Tan, Z. L., Zheng, X., Wu, Y., Jian, X., Xing, X., and Zhang, C. (2019). In vivo continuous evolution of metabolic pathways for chemical production. *Microb. Cell Fact.* 18:82. doi: 10.1186/s12934-019-1132-y
- Wurm, D. J., Hausjell, J., Ulonka, S., Herwig, C., and Spadiut, O. (2017a). Mechanistic platform knowledge of concomitant sugar uptake in *Escherichia coli* BL21 (DE3) strains. *Sci. Rep.* 7:45072.
- Wurm, D. J., Quehenberger, J., Mildner, J., Eggenreich, B., Slouka, C., Schwaighofer, A., et al. (2017b). Teaching an old pET new tricks: tuning of inclusion body formation and properties by a mixed feed system in *E. coli*. *Appl. Microbiol. Biotechnol.* 102, 667–676. doi: 10.1007/s00253-017-8641-6
- Wurm, D. J., Veiter, L., Ulonka, S., Eggenreich, B., Herwig, C., and Spadiut, O. (2016). The *E. coli* pET expression system revisited—mechanistic correlation between glucose and lactose uptake. *Appl. Microbiol. Biotechnol.* 100, 8721–8729. doi: 10.1007/s00253-016-7620-7
- Yan, J., Zhao, S. F., Mao, Y. F., and Luo, Y. H. (2004). Effects of lactose as an inducer on expression of *Helicobacter pylori* rUreB and rHpA, and *Escherichia coli* rLTkA63 and rLTB. *World J. Gastroenterol.* 10, 1755–1758. doi: 10.3748/wjg.v10.i12.1755
- Zagrodnik, R., and Łaniecki, M. (2017). Hydrogen production from starch by co-culture of *Clostridium acetobutylicum* and *Rhodobacter sphaeroides* in one step hybrid dark- and photofermentation in repeated fed-batch reactor. *Bioresour. Technol.* 224, 298–306. doi: 10.1016/j.biortech.2016.10.060
- Zelić, B., Gostović, S., Vuorilehto, K., Vasić-Rački, , and Takors, R. (2004). Process strategies to enhance pyruvate production with recombinant *Escherichia coli*: From repetitive fed-batch to in situ product recovery with fully integrated electro dialysis. *Biotechnol. Bioeng.* 85, 638–646. doi: 10.1002/bit.10820
- Zhang, Y., Feng, X., Xu, H., Yao, Z., and Ouyang, P. (2010). ε-Poly-L-lysine production by immobilized cells of *Kitasatospora* sp. MY 5-36 in repeated fed-batch cultures. *Bioresour. Technol.* 101, 5523–5527. doi: 10.1016/j.biortech.2010.02.021
- Zobel-Roos, S., Schmidt, A., Mestmäcker, F., Mouellef, M., Huter, M., Uhlenbrock, L., et al. (2019). Accelerating Biologics Manufacturing by Modeling or: Is Approval under the QbD and PAT Approaches Demanded by Authorities Acceptable without a Digital-Twin? *Processes* 7:94. doi: 10.3390/pr7020094

**Conflict of Interest:** The authors declare that the research was conducted in the absence of any commercial or financial relationships that could be construed as a potential conflict of interest.

Copyright © 2020 Kopp, Kittler, Slouka, Herwig, Spadiut and Wurm. This is an open-access article distributed under the terms of the Creative Commons Attribution License (CC BY). The use, distribution or reproduction in other forums is permitted, provided the original author(s) and the copyright owner(s) are credited and that the original publication in this journal is cited, in accordance with accepted academic practice. No use, distribution or reproduction is permitted which does not comply with these terms.



## 6.4. Scientific Publication 4



## The Lazarus *Escherichia coli* Effect: Recovery of Productivity on Glycerol/Lactose Mixed Feed in Continuous Biomanufacturing

Stefan Kittler<sup>1†</sup>, Julian Kopp<sup>2†</sup>, Patrick Gwen Veelenturf<sup>2</sup>, Oliver Spadiut<sup>1</sup>, Frank Delvigne<sup>3</sup>, Christoph Herwig<sup>1,2</sup> and Christoph Slouka<sup>1\*</sup>

### OPEN ACCESS

#### Edited by:

Miguel Cacho Teixeira,  
University of Lisbon, Portugal

#### Reviewed by:

Georg A. Sprenger,  
University of Stuttgart, Germany  
Cecilia Calado,  
Lisbon Higher Institute of Engineering  
(ISEL), Portugal

#### \*Correspondence:

Christoph Slouka  
christoph.slouka@tuwien.ac.at

<sup>†</sup> These authors have contributed  
equally to this work

#### Specialty section:

This article was submitted to  
Bioprocess Engineering,  
a section of the journal  
Frontiers in Bioengineering and  
Biotechnology

**Received:** 19 June 2020

**Accepted:** 29 July 2020

**Published:** 13 August 2020

#### Citation:

Kittler S, Kopp J, Veelenturf PG,  
Spadiut O, Delvigne F, Herwig C and  
Slouka C (2020) The Lazarus  
*Escherichia coli* Effect: Recovery  
of Productivity on Glycerol/Lactose  
Mixed Feed in Continuous  
Biomanufacturing.  
Front. Bioeng. Biotechnol. 8:993.  
doi: 10.3389/fbioe.2020.00993

<sup>1</sup> Research Division Biochemical Engineering, Research Group Integrated Bioprocess Development, Institute of Chemical, Environmental and Bioscience Engineering, Vienna University of Technology, Vienna, Austria, <sup>2</sup> Christian Doppler Laboratory for Mechanistic and Physiological Methods for Improved Bioprocesses, Institute of Chemical, Environmental and Bioscience Engineering, TU Vienna, Vienna, Austria, <sup>3</sup> TERRA Teaching and Research Centre, Microbial Processes and Interactions (MIP), Gembloux Agro-Bio Tech – Université de Liège, Gembloux, Belgium

Continuous cultivation with *Escherichia coli* has several benefits compared to classical fed-batch cultivation. The economic benefits would be a stable process, which leads to time independent quality of the product, and hence ease the downstream process. However, continuous biomanufacturing with *E. coli* is known to exhibit a drop of productivity after about 4–5 days of cultivation depending on dilution rate. These cultivations are generally performed on glucose, being the favorite carbon source for *E. coli* and used in combination with isopropyl  $\beta$ -D-1 thiogalactopyranoside (IPTG) for induction. In recent works, harsh induction with IPTG was changed to softer induction using lactose for T7-based plasmids, with the result of reducing the metabolic stress and tunability of productivity. These mixed feed systems based on glucose and lactose result in high amounts of correctly folded protein. In this study we used different mixed feed systems with glucose/lactose and glycerol/lactose to investigate productivity of *E. coli* based chemostats. We tested different strains producing three model proteins, with the final aim of a stable long-time protein expression. While glucose fed chemostats showed the well-known drop in productivity after a certain process time, glycerol fed cultivations recovered productivity after about 150 h of induction, which corresponds to around 30 generation times. We want to further highlight that the cellular response upon galactose utilization in *E. coli* BL21(DE3), might be causing fluctuating productivity, as galactose is referred to be a weak inducer. This “Lazarus” phenomenon has not been described in literature before and may enable a stabilization of continuous cultivation with *E. coli* using different carbon sources.

**Keywords:** *E. coli*, recombinant protein production, continuous biomanufacturing, mixed-feeding, productivity recovery

## INTRODUCTION

The gram-negative bacterium *Escherichia coli* is the expression host of choice to produce 30% to 40% of recombinant enzymes [recombinant protein production (RPP)] in industry (Walsh, 2010; Gupta and Shukla, 2016). This organism has fast replication rates and can be cultivated on comparatively cheap media (DeLisa et al., 1999) and has high intracellular product titers. These benefits often outweigh the numerous purification steps (Berlec and Strukelj, 2013; Gupta and Shukla, 2016) and the missing glycosylation pattern on the recombinant product (Spadiut et al., 2014; Baeshen et al., 2015). The strain BL21(DE3) generated by Studier and Moffatt (1986) is often used in industrial scale, because of showing low acetate formation, high replication rates as an effect of the integrated T7-polymerase (Steen et al., 1986; Studier and Moffatt, 1986; Studier et al., 1990; Dubendorff and Studier, 1991; Neubauer and Hofmann, 1994; Lyakhov et al., 1998), as well as the possibility of protein secretion into the fermentation broth due to a type 2 secretion pathway (Jeong et al., 2009, 2015; Tseng et al., 2009). The *lac* operon is still one of the most favored promoters in pET-expression-systems (Dubendorff and Studier, 1991; Marbach and Bettenbrock, 2012; Wurm et al., 2016), therefore it is generally used for insertion of the gene of interest. Induction can be performed by addition of lactose or a structural analog, e.g., the well-known inducer isopropyl  $\beta$ -D-1 thiogalactopyranoside (IPTG) (Burstein et al., 1965; Neubauer and Hofmann, 1994; Wurm et al., 2016). IPTG is known to bind directly to the *lacI* repressor protein after uptake, whereas lactose needs to be transformed to allolactose to cause the blockage of the repressor protein (Burstein et al., 1965). Still, these “low-cost” products in *E. coli* with the pET system, are expensive in their making (Jia and Jeon, 2016), as one gram of IPTG can exceed the price of one gram of 900 gold. For economic reasons and for reduction of metabolic/product burden (Malakar and Venkatesh, 2012), lactose, generally regarded as waste product, can be used for induction (Wurm et al., 2016, 2018; Wurm et al., 2017a). Apart from induction mechanism, a replacement of the primary carbon source is also frequently discussed. The most favored carbon source in *E. coli* cultivations has always been glucose (Postma et al., 1993; Ronimus and Morgan, 2003; Deutscher et al., 2006). However, compared to other carbon sources glucose is quite expensive and causes diauxic growth upon lactose induction (Monod, 1949; Loomis and Magasanik, 1967). Glycerol has shown quite promising results in terms of biomass/substrate yield in *E. coli* cultivations (Blommel et al., 2007). In addition, mixtures of glucose, glycerol and lactose have shown good results for diverse products gained via autoinduction systems (Monod, 1949; Viitanen et al., 2003; Blommel et al., 2007). Recently, we presented that glycerol used as primary carbon source for *E. coli* cultivations performed equally well during biomass production as glucose, but even increased the specific product titer in fed batches (Kopp et al., 2017).

Most processes today rely on fed batch mode, which are state-of-the-art in industry. They can be highly affected by different process parameters, like pH and T, physiological feeding (adaptation of the specific substrate uptake rate) and change

in induction agent. However, the time dependence of product quality is still a major drawback using this cultivation technique. This makes determination of the correct harvest time point often challenging, as the intracellular stress often leads to very quick lysis of the cells and product degradation. This results in variations in the downstream purification process. Continuous biomanufacturing is considered to increase product quality and therefore to a facilitation of the downstream process. However, up to now, only one stable microbial industrial chemostat process was established for *Saccharomyces cerevisiae* in the 90's for production of insulin (Diers et al., 1991). A drop of productivity after a certain process time and the lower time-space yield hinder continuous upstream using microbial hosts from being applied in industry (Peebo and Neubauer, 2018; Kopp et al., 2019b).

Several efforts have been made to enable continuous processes in *E. coli* (Kopp et al., 2019a), but we are still far away from application of such systems. Long-term cultivations with *E. coli* showed enhanced cell burden using IPTG induction and clearly favored feeding of the disaccharide lactose (Dvorak et al., 2015). From an engineering point of view, higher growth rates seem to be beneficial for RPP as shown in chemostat- and fed-batch experiments (Vaiphei et al., 2009; Slouka et al., 2019). Mutations and plasmid loss are expected during long time cultivation of *E. coli* (Weikert et al., 1997; Sieben et al., 2016; Peebo and Neubauer, 2018). However, constant supply of antibiotics is believed to prevent plasmid loss in continuous cultures (Sieben et al., 2016). Change in gene regulation of the transcription upon long time cultivation are often reported. The *lac* operon resulting in multistability of induction is well known and reported in literature (Ozbudak et al., 2004). Fluctuations in plasmid number, *lac*-repressor and cAMP levels may drastically influence RPP during long time cultivation. High concentrations of metabolites, like galactose upon feeding of lactose, are known to affect  $\beta$ -galactosidase concentrations (Llanes and McFall, 1969; Portaccio et al., 1998). Other approaches try to integrate the gene of interest into the genome to receive stable production in combination with strong inducible promoters (Striedner et al., 2010). Reactor design is a further screw to overcome stability issues in long-term RPP with *E. coli*, as recently published by Schmieder and Weuster-Botz (2017) who implemented a cascaded system, where two stirred tank reactors are operated in parallel at different conditions.

In this contribution, we present the results of chemostat cultures using mixed feed systems first applied by Wurm et al. (2016, 2018). The goal was to accomplish a continuous process with stable productivity outperforming the frequently used fed-batch. We tested mixed feeds with glucose/lactose and glycerol/lactose in chemostat for three model proteins and compared the performance to state-of-the-art fed batches induced with IPTG. In contrast to cultivations using BL21(DE3) with glucose/lactose, glycerol/lactose-based cultivations showed a recovery of productivity at elevated induction time. Alterations regarding the choice of carbon source thus might be a key driver to possibly enable stable productivity on a long-term basis. As an already lost productivity is recovered, we annotated this resurrection of productivity with the Christian term of “Lazarus” and the corresponding “Lazarus effect.”

## MATERIALS AND METHODS

### Strains

Cultivations were carried out with the strain *E. coli* BL21(DE3) using three different model proteins. All three protein sequences were cloned in a pET vectors, using pET21a<sup>+</sup> for green fluorescent protein (GFP), and pET28a for mCherry protein (mCherry) and Blitzenblue (BBlue). mCherry and BBlue were thankfully received from Prof. Maurer at FH Campus Wien. All cultures were kept at -80°C in 25% glycerol cryo stocks. The extracted pET21a<sup>+</sup> plasmid encoding for GFP was extracted and electroporated into an HMS174(DE3) strain (Novagen, Merck, Darmstadt, Germany).

### Cultivation and Process Modes

Cultivations were executed in a Minifors 2 bioreactor system (max. working volume: 1 L; Infors HT, Bottmingen, Switzerland). All cultivations were carried out using a defined minimal medium referred to DeLisa et al. (1999). Media had the same composition with different amounts of glycerol and glucose. Details on pre-culture, batch, fed batch and chemostat cultivation are given in Table 1. Induction was performed according to Table 1. The ratio of glycerol to lactose was calculated based on recent works in fed-batch regarding maximal lactose uptake versus applied  $q_{s,C}$  (Wurm et al., 2016). Fed batch was always cultivated to have a standard for protein production with similar specific growth rate as applied in the chemostat. The cultivation offgas flow was analyzed online using gas sensors – IR for CO<sub>2</sub> and ZrO<sub>2</sub> based for Oxygen (BlueSens Gas analytics, Herten, Germany). Process control and feeding was established using the process control system PIMS Lucullus (Securecell, Urdorf, Switzerland).

We used glucose or glycerol as carbon source and 0.5 mM IPTG for induction. During all induction phases pH is kept constant at 6.7 and temperature at 30°C. pH was controlled with base only (12.5% NH<sub>4</sub>OH), while acid (10% H<sub>3</sub>PO<sub>4</sub>) was added manually, if necessary. The pH was monitored using a pH-sensor EasyFerm Plus (Hamilton, Reno, NV, United States). Aeration

was carried out using a mixture of pressurized air and pure oxygen at about 2 vvm to keep dissolved oxygen (dO<sub>2</sub>) always higher than 30 %. The dissolved oxygen was monitored using a fluorescence dissolved oxygen electrode Visiferm DO (Hamilton, Reno, NV, United States).

For fed batches static feed forward  $q_{s,C}$ -controls were performed during induction phase. Exponential feed was established according to Eq. 1, to keep  $q_{s,C}$  constant (Slouka et al., 2016; Wurm et al., 2016):

$$F(t) = \frac{q_{s,C} * X(t) * \rho_f}{c_f} \quad (1)$$

With F being the feedrate [g/h],  $q_{s,C}$  the specific glycerol uptake rate [g/g/h], X(t) the absolute biomass [g],  $\rho_f$  the feed density [g/L], and  $c_f$  the feed concentration [g/L], respectively. For applied control strategies adaption of the  $q_{s,C}$  during the induction time was performed based on Eq. 1. Chemostat cultivations were set manually to a dilution rate of  $D = 0.1 \text{ h}^{-1}$  for all performed runs.

### Process Analytics

For fed batch, samples were always taken after inoculation, upon end of the batch-phase and after the non-induced-fed batch was finished. During the induction period, samples were taken in a maximum of 120 min intervals and analyzed subsequently. Details on the process analytics can be found elsewhere (Kopp et al., 2018; Slouka et al., 2018). For chemostat cultivations samples were collected after batch and afterward once or, if necessary, twice a day.

### Product Analytics

#### Preparation

A 5 mL fermentation broth samples were centrifuged at 4800 rpm at 4°C for 10 min. The supernatant was discarded, and the pellet was resuspended to a DCW of about 4 g/L in lysis buffer (100 mM Tris, 10 mM EDTA at pH = 7.4). Afterward the sample was homogenized using a Gea PandaPlus homogenizer (Gea, AG, Germany) at 1500 bar for 10 passages. After centrifugation at 10000 rpm and 4°C for 10 min 10 ml of the supernatant were kept for analysis of the soluble protein. Soluble protein was stored in 4°C. The resulting IB pellet was washed twice with ultrapure water. Aliquoted of pellets à 2 mL broth were centrifuged again (14000 rpm, 10 min 4°C) and finally stored at -20°C.

#### Inclusion Body Titer

Soluble protein samples were filtered (0.2 µm mesh) and directly used in the HPLC. Inclusion Body (IB) pellet samples were prepared according to Kopp et al. (2018), and subsequently solubilized using following buffer: 7.5 M guanidine hydrochloride, 62 mM Tris at pH = 8 and 125 mM DTT was added right before use. The filtered IB samples were quantified by HPLC analysis (UltiMate 3000; Thermo Fisher, Waltham, MA, United States). The used column was manufactured by Waters (BioResolve RPmab) and was designed for monoclonal antibody measurements (Waters Corporation, Milford, MA, United States). The product was quantified with an UV detector

TABLE 1 | C source and induction for the different cultivations.

	Glucose [g/L]		Glycerol [g/L]	
Pre-culture media	8		8	
Batch media	20		20	
Feed	Glucose [g/L]	Glycerol [g/L]	Inducer	Inducer concentration
GFP chemostat mode 1		50	Lactose	25 g/L
GFP chemostat mode 2	50		Lactose	25 g/L
GFP Fed-batch mode	300		IPTG	0.5 mM
mCherry chemostat mode		50	Lactose	25 g/L
mCherry Fed-batch mode	300		IPTG	0.5 mM
BBlue chemostat mode		50	Lactose	25 g/L
BBlue Fed-batch mode	400		IPTG	0.5 mM
HMS GFP chemostat 1		50	Lactose	25 g/L
HMS GFP chemostat 2	50		Lactose	25 g/L

(Thermo Fisher, Waltham, MA, United States) at 280 nm, respectively. Mobile phase was composed of water (ultrapure) (eluent A) and acetonitrile (eluent B) both supplemented with 0.1% (v/v) trifluoroacetic acid. Details on the method are given in Kopp et al. (2020). For quantification of soluble protein, a size exclusion (=SEC) chromatography principle was applied, using a X-bridge column (Waters Corporation, Milford, MA, United States). The mobile phase was composed of 250 mM KCl and 50 mM of each  $\text{KH}_2\text{PO}_4$  and  $\text{K}_2\text{HPO}_4$  dissolved in Ultrapure water as described elsewhere (Goyon et al., 2018). A constant flow rate of 0.5 mL/min was applied with an isocratic elution at 25°C for 18 min. BSA standards (50, 140, 225, 320, 500, 1000, and 2000 mg/mL; Sigma Aldrich, St. Louis, MO, United States) were used for quantification.

## RESULTS

Fed batch cultivations induced with IPTG are the golden standard for RPP with *E. coli*. To be able to compete with fed batches, the specific productivity in chemostat cultivations must be maximized and the duration of the productive phase prolonged, so that time space yields are significantly increased. We tested two mixed feed systems, glucose/lactose, and glycerol/lactose, to find conditions for stable protein expression in *E. coli* chemostats.

### Fed-Batch and Chemostats Using BI21(DE3) Expressing GFP as Model Protein

First, we compared three different cultivation modes using GFP as model protein. As IPTG is often referred to as toxic to the cells after a certain induction time, we used lactose as mild inducer in the first run (Dvorak et al., 2015). A mixed feed consisting of glucose and lactose (Table 1) was used for the first chemostat (Figure 1). To ease the comparability between fed batch and chemostat cultivation we aimed for similar specific substrate uptake rates  $-q_{s,C}$ , which resulted in a dilution rate for the chemostats of  $0.1 \text{ h}^{-1}$ . Respective process parameters are presented in Table 2.

While the fed batch gave the highest product titers after 10 h of induction, the glucose/lactose chemostat system had the maximum product titer at 20 h. In the glucose chemostat, productivity dropped below the limit of quantification (LoQ) of the HPLC method after around 3 days of cultivation, including batch of 6 h, and did not recover at later induction times. This phenomenon is well known for other strains cultivated with glucose as sole carbon source in chemostat mode (Peebo and Neubauer, 2018). Based on our recent results in fed batch using glycerol as carbon source (Kopp et al., 2017), we cultivated *E. coli* producing GFP with a mixed feed of glycerol/lactose. Highest specific titer (calculated by dividing titer through biomass), was found in the beginning of the glucose/lactose chemostat (Figure 1). There are high differences in terms of productivity between the three cultivations (Table 2).

In general, inclusion bodies and soluble protein were produced simultaneously during cultivations of *E. coli* expressing GFP (Wurm et al., 2018). For easy comparison, we calculated

the total productivity as a sum of IBs and soluble protein. Productivity and titer on glycerol were far lower in the beginning in comparison to the glucose/lactose fed chemostat (compare axes in Figure 1). In contrast to the glucose/lactose chemostat a recovery in productivity appeared at about 150 h of induction time. This renewed productivity dropped again at about 250 h of induction.

### Chemostat Cultivation Using *E. coli* HMS174 Expressing GFP

*Escherichia coli* BI21(DE3) lacks in a functioning Leloir pathway implementing lacking galactose uptake (Daegelen et al., 2009). To investigate effects of galactose metabolism, a recombinant *E. coli* HMS174(DE3) strain with a working galactose metabolism was examined. *E. coli* HMS174(DE3) was cultivated with glycerol and glucose as primary carbon source and lactose as inducer in chemostat cultures (Table 3). In Figure 2A, the chemostat cultivation with glucose/lactose is shown. HMS strain behaves like BI21 with initial high productivity of GFP expressed in similar specific titers. Biomass concentration was in overall higher using this strain, as galactose served as additional carbon source. The glycerol based chemostat, given in Figure 2B, showed also comparable productivity after induction to BI21, however, no recovery after 100 h of induction was observed using HMS174(DE3) strain.

### Chemostat Cultivation Using BI21(DE3) Expressing mCherry and Blitzenblue as Model Proteins

To check the effects of glycerol/lactose chemostats, we produced two further fluorescent model proteins with this respective system and compared them to glucose/IPTG fed batches using the strain BI21(DE3). In Table 4 results for cultivation using *E. coli* expressing mCherry are presented. Higher productivity and specific titer were found for the fed batch cultivations. However, induction with IPTG and product titers up to 18 g/L imposed stress to cells, obvious in the low substrate to biomass yield.

A similar result was obtained for cultivation for *E. coli* recombinantly expressing BBlue (Table 4). The magnitude of specific titer and  $q_{p,max}$  differed, but the trends were comparable. The substrate to biomass yield was even lower than for mCherry indicating that BBlue even imposed more stress to the host in the fed batch mode.

Chemostats for mCherry and BBlue resulted in less cellular stress compared to the fed batch cultivation. In Figure 3 DCW, specific titer and IB fraction over time are plotted for mCherry (Figure 3A) and BBlue (Figure 3B). mCherry produced a high amount of IBs in the beginning of the chemostat upon the first decrease in productivity during the cultivation. The recovery of productivity at about 200 h was exclusively soluble protein with no IB fraction anymore. BBlue showed no IB expression in fed batch nor in the chemostat and a high specific titer at the recovery at 200 h of induction time. This effect was highly different to the GFP glycerol run. While a high IB ratio was present in the GFP glycerol chemostat, the other *E. coli* expressing mCherry

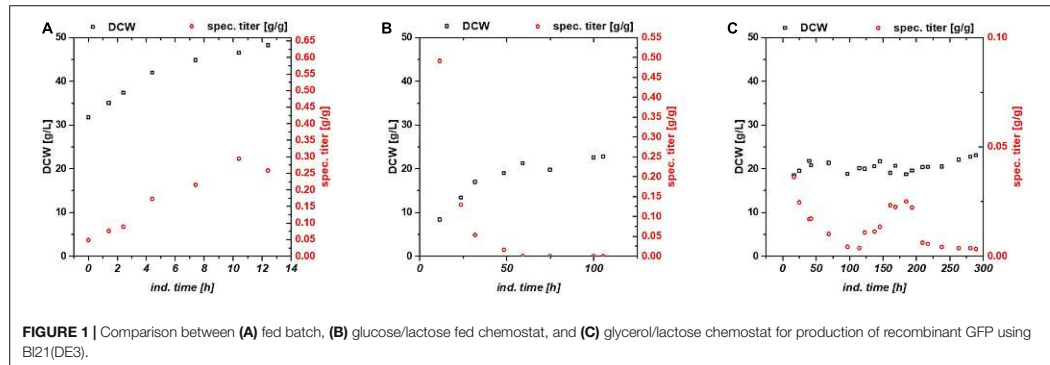


**FIGURE 1** | Comparison between (A) fed batch, (B) glucose/lactose fed chemostat, and (C) glycerol/lactose chemostat for production of recombinant GFP using BI21(DE3).

and BBlue produced mainly soluble protein in the recovery phase. During intermediate time between 100 and 200 h biomass concentration was generally higher (also indicated by higher yield coefficients), so metabolism was most likely regulated toward anabolism of host cell proteins. During the recovery, DCW started to drop again because of recombinant protein expression. In contrast to GFP and BBlue, mCherry had a high overall specific titer within the entire cultivation. Elucidating this metabolic shift in regulation may be a key parameter for maintaining constant productivity in chemostat cultures.

**DISCUSSION**

We tested the effects on productivity using mixed feed systems with glucose/lactose and glycerol/lactose in chemostats and compared them to classical fed batches with similar specific uptake rates. In the performed chemostat cultivation, we could

distinguish between three different metabolic states (Figure 4A). Phase I is the adaption phase after the batch. This phase resembled a fed batch like behavior for *E. coli* BI21(DE3) with GFP and mCherry including high RPP. This effect was most likely linked to high IB concentrations upon protein expression during this phase, which led to increased metabolic burden for the host (Figure 4B). Rise in IB concentrations was indicated by a change of the carbon dioxide to substrate yield ( $Y_{CO_2/S}$  not shown). Phase II was characterized by constant yields and carbon balance (C-balances). This phase overlapped with phase III, where recovery of productivity set in. Acetate formation measured by photometric assays (not shown) was always low for all cultivations. In contrast, BBlue chemostat did not show a phase I increase in yield coefficients of the C-balance. We believe that this was due to lack of IB expression in this strain. Surprisingly, a drop in C-balance was present upon recovery of productivity at 100–150 h (phase II and III). C-balance did not close to 1 during the entire cultivation, which indicated some other non-measured metabolites during this run. Reduction of biomass formation (decreased  $\mu$ ) is a common phenomenon upon RPP (Neubauer et al., 2003; Hoffmann and Rinas, 2004). Effects could be clearly seen for *E. coli* expressing GFP and mCherry in the beginning and for BBlue at the start of the recovery phase (Figures 1, 3). These effects were obviously strongly dependent on the expressed protein and could not be generalized. Comparing results of the mCherry chemostat cultivation to a chemostat cultivation for production of mCherry in literature (Schmideder and Weuster-Botz, 2017), maximum specific titer was found to be higher by a factor of 100, whereas average specific titer was higher by a factor of 10 (Table 4). As referred chemostat cultivation was induced with IPTG, we suppose that lactose induction facilitated the production of mCherry in chemostat cultivation.

Higher dilution rates are beneficial for productivity in chemostat, as described in literature before (Seo and Bailey, 1986; Reinikainen and Virkajärvi, 1989). However, no discussion on long term stability was given, as generally steady state was assumed after three residence times (Seo and Bailey, 1986), which corresponds to  $D = 0.1 \text{ h}^{-1}$  at 30 h. This would only result

**TABLE 2** | Process variables for three performed cultivations with BI21(DE3) expressing GFP.

Process parameters	Glucose-IPTG fed-batch	Glucose-lactose chemostat	Glycerol-lactose chemostat
spec. titer max. [g/g]	0.30	0.31	0.04
$q_{p,max}$ [g/g/h]	0.05	0.01	0.01
$q_{s,c}$ [g/g/h]	$0.23 \pm 0.02$	$0.24 \pm 0.04$	$0.27 \pm 0.04$
$Y_{X/S}$ [g/g]	$0.39 \pm 0.09$	$0.49 \pm 0.09$	$0.42 \pm 0.03$

**TABLE 3** | Process variables for performed chemostat cultivations with HMS174(DE3) expressing GFP.

Process parameters	Glucose-lactose chemostat	Glycerol-lactose chemostat
spec. titer max. [g/g]	0.27	0.35
$q_{p,max}$ [g/g/h]	0.02	0.039
$q_{s,c}$ [g/g/h]	$0.27 \pm 0.05$	$0.27 \pm 0.02$
$Y_{X/S}$ [g/g]	$0.37 \pm 0.04$	$0.43 \pm 0.03$

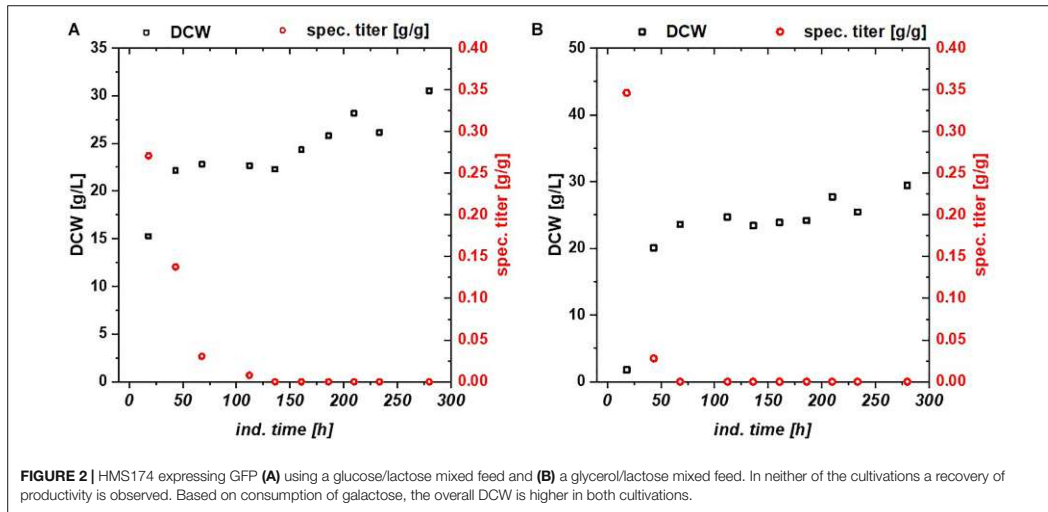


**FIGURE 2 |** HMS174 expressing GFP (A) using a glucose/lactose mixed feed and (B) a glycerol/lactose mixed feed. In neither of the cultivations a recovery of productivity is observed. Based on consumption of galactose, the overall DCW is higher in both cultivations.

in 17.3 generation times at the presented  $D = 0.4 \text{ h}^{-1}$ , where maximum productivity was found. The cultivations presented here, were cultivated for almost 40 generations. Stability of the long-time process is the main concern using *E. coli* as host (Peebo and Neubauer, 2018). Genetic instabilities, like plasmid loss and mutations, happen during this long term of cultivation. The recovery of the productivity in phase III was a strong indicator that only minor plasmid loss happened during cultivations and that no plasmid deficient hosts overgrew the culture.

All chemostat cultivations except for the glycerol-lactose chemostat cultivation on Bl21(DE3) follow the often describe bell-shaped decrease of productivity (Peebo and Neubauer, 2018). It is not clear yet, why glucose based chemostats showed a complete loss of productivity and glycerol-based cultivations recovered after a certain time span. Diauxic growth is known to downregulate  $\beta$ -galactosidase activity, leading to inducer exclusion often observed in batch cultivation (Monod, 1949;

Inada et al., 1996). As feeding of carbon source and inducer was conducted using previously established feeding protocols, growth rates never exceeded  $\mu_{\text{max}}$  (Wurm et al., 2017a). Both carbon sources were taken up at all time, except for a monitored adaption phase observed for HMS174 (Supplementary Figure 1). Therefore, diauxic growth can be excluded as a possible explanation. Even though IPTG transport was found to be highly dependent on lactose permease (Fernández-Castané et al., 2012), chemostat cultivations with Bl21(DE3) and IPTG induction also resulted in an irreversible drop of productivity (Kopp et al., 2019a). Only galactose accumulation was found to alter when comparing glucose and glycerol cultivations on Bl21(DE3), which will be discussed in more detail. Acetate formation was present in HMS174 strains for both carbon source, while acetate concentration was always below limit of detection of our respective HPLC method for Bl21(DE3) strains (Supplementary Figure 1).

Our recent work on fed batch cultivations using mixed feeds systems with glucose/lactose and glycerol/lactose showed a strong increase on productivity upon glycerol feeding (Kopp et al., 2017). Higher and better performance of cultivations using glycerol as carbon source was also found to produce different enzymes (Hansen and Eriksen, 2007; Liu et al., 2011). Difference in enzymatic regulations on glycerol consumption were reported by activation of gluconeogenesis also including “carbon stress responses” for batch culture approaches (Martínez-Gómez et al., 2012). However, in the performed chemostat cultures this glycerol carbon stress could be clearly seen for *E. coli* expressing GFP (Table 2) in yields and productivity compared to the glucose/lactose mixed feed system. Results indicate that glucose is the carbon source of choice in the beginning of a chemostat culture, as higher productivity upon glucose cultivation can be observed. As  $\mu_{\text{max}}$  is higher upon glucose cultivation compared to glycerol, energy (ATP) needed for recombinant protein

**TABLE 4 |** Cultivation variables for fed batch cultivation and continuous cultivation with the glycerol/lactose system for production of recombinant mCherry and recombinant Blitzenblue.

	Glucose-IPTG fed-batch	Glycerol-lactose chemostat
<b>Process variables mCherry</b>		
spec. titer max [g/g]	0.21	0.17
$q_{p,\text{max}}$ [g/g/h]	0.069	0.01
$q_{s,\text{c}}$ [g/g/h]	$0.28 \pm 0.02$	$0.22 \pm 0.2$
$Y_{x/s}$ [g/g]	$0.34 \pm 0.09$	$0.47 \pm 0.04$
<b>Process variables BBlue</b>		
spec. titer max [g/g]	0.13	0.035
$q_{p,\text{max}}$ [g/g/h]	0.033	0.002
$q_{s,\text{c}}$ [g/g/h]	$0.29 \pm 0.01$	$0.25 \pm 0.05$
$Y_{x/s}$ [g/g]	$0.18 \pm 0.05$	$0.30 \pm 0.03$

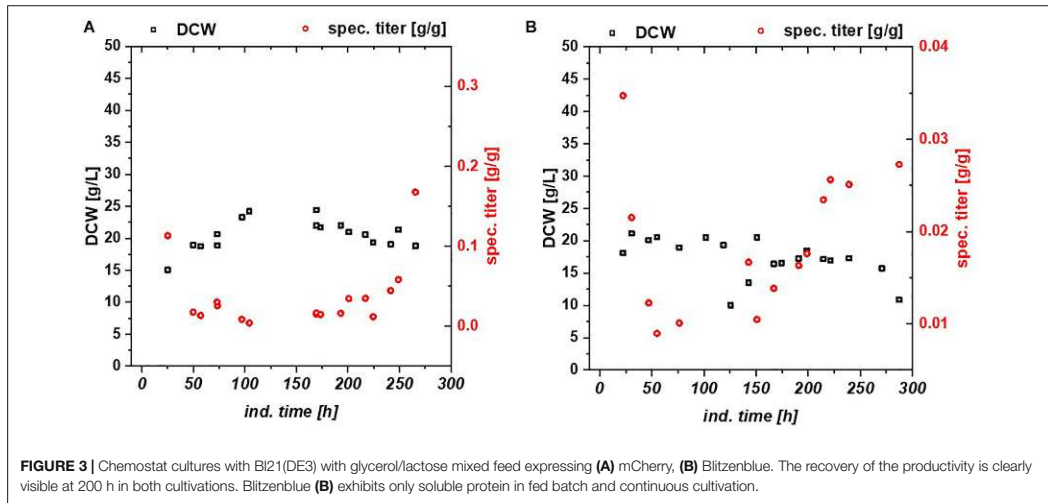


**FIGURE 3** | Chemostat cultures with BI21(DE3) with glycerol/lactose mixed feed expressing (A) mCherry, (B) Blitzenblue. The recovery of the productivity is clearly visible at 200 h in both cultivations. Blitzenblue (B) exhibits only soluble protein in fed batch and continuous cultivation.

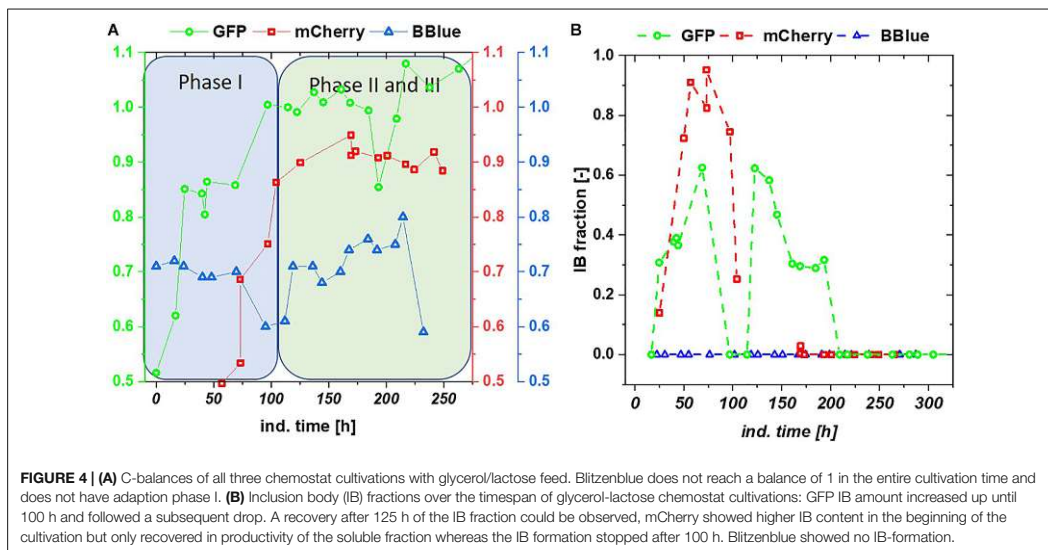


**FIGURE 4** | (A) C-balances of all three chemostat cultivations with glycerol/lactose feed. Blitzenblue does not reach a balance of 1 in the entire cultivation time and does not have adaption phase I. (B) Inclusion body (IB) fractions over the timespan of glycerol-lactose chemostat cultivations: GFP IB amount increased up until 100 h and followed a subsequent drop. A recovery after 125 h of the IB fraction could be observed, mCherry showed higher IB content in the beginning of the cultivation but only recovered in productivity of the soluble fraction whereas the IB formation stopped after 100 h. Blitzenblue showed no IB-formation.

formation might be faster accessible upon start of induction (Kopp et al., 2017; Wurm et al., 2017b).

The faster metabolism on glucose cultivation, compared to glycerol consumption (Wang and Yang, 2013) could possibly explain higher productivity for glucose fed chemostats in the beginning of the cultivation. NADPH formation on glycerol is also meager, when compared to glucose cultivation, emphasizing the previous statement (Yao et al., 2016). Still, in contrast to glucose, glycerol enabled a recovery of productivity at later stage. Reasons still need to be investigated but could

possibly result from different intracellular metabolism (i.e., pyruvate dehydrogenase and TCA activity) (Murarka et al., 2008; Yao et al., 2016).

Multistability of induction was described by Ozbudak et al. (2004) showing changes in expression. In this publication, it is shown that the lac system can remain in several states, depending on the amount of LacI and cAMP molecules. With constant process parameters, changes in plasmid number during the cultivation might be a reasonable explanation for the observed effects. Based on the strong metabolic

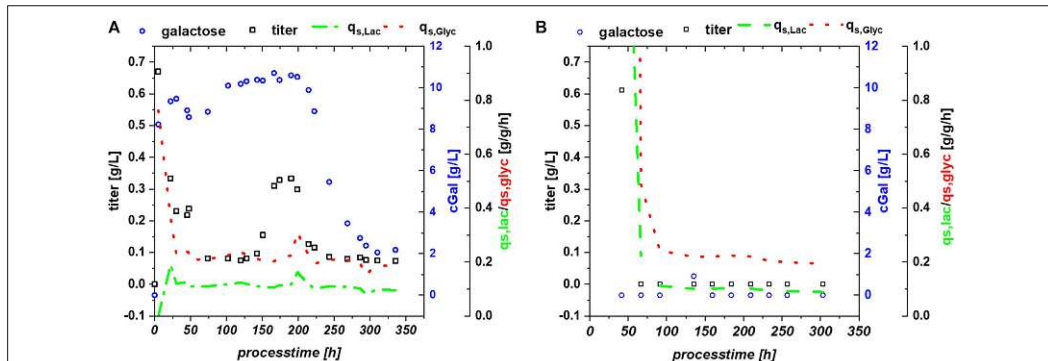


**FIGURE 5 | (A)** BL21(DE3) expressing GFP: glycerol/lactose cultivation: specific substrate uptake rates are constant throughout the whole induction time, while titer of the recombinant protein and extracellular galactose concentrations show high fluctuations; **(B)** HMS174 expressing GFP: glycerol/lactose cultivation with no accumulation of galactose and no respective recovery of productivity.

burden in the beginning, total number of plasmids might change and lead to a bi-stability of the cultivation system. Yet, pET plasmids generally carry a LacI gene, resulting in a direct relationship between lac repressor and plasmid number and may drastically reduce those observed effects during pET-based induction. Furthermore, the study by Ozbudak et al. (2004) was performed with a strong irreversible inducer [thiomethyl galactoside (TMG)], in comparison to lactose used for our experiments. Glycerol does not provoke a cAMP response directly, but cAMP response might be present based on the metabolized glucose (from lactose) as seen in fed batch cultivations (Kopp et al., 2017), which inherited a very different regulation compared to the glucose based cultivations. A further possible alternative for this fluctuation in productivity might be intracellular galactose accumulation (Supplementary Figure 1). Galactose is known to affect the cellular  $\beta$ -galactosidase concentrations (Llanes and McFall, 1969; Portaccio et al., 1998) and has been shown to function as a weak inducer (Ukkonen et al., 2013). High intracellular galactose concentration (drop in extracellular concentration), seen in Figure 5A, was accompanied by a drop of productivity. However, lactose consumption was not affected by the galactose fluctuations.

HMS174 can metabolize galactose upon induction with lactose (Hausjell et al., 2018), therefore this strain was investigated using a mixed feed with glycerol/lactose. However, previously mentioned advantages, such as overflow metabolism and overall titer formation favor B strains over K strains for the RPP (Shiloach and Fass, 2005; Rosano and Ceccarelli, 2014). HMS174(DE3) expressing GFP revealed no recovery on glycerol and no pronounced accumulation of neither glycerol, nor lactose or galactose, compare to Figure 5B. Still constant overflow metabolism was found for HMS174(DE3) chemostat cultivations whereas no acetate accumulation could be monitored for BL21(DE3) (Supplementary Figure 1). As galactose was

completely metabolized in HMS174(DE3) cultivations, biomass was found to be higher compared to BL21(DE3) cultivations. Specific uptake rates were also constant, expect for deviations upon start of the induction phase. Yet, we believe that galactose variations are the most reasonable explanation for the effects seen in BL21(DE3). It is not clear why galactose is stored inside the *E. coli* cells or expelled into the supernatant as seen in shifts of galactose concentration. Previous studies indicated galactose as main player for Lazarus effect. Based on these findings we expect a non-trivial interaction of multiple factors in BL21 resulting in the observed behavior.

Furthermore, the three analyzed fluorescence proteins exhibit several differences. GFP originates from jellyfish *Aequorea Victoria* while mCherry from *Discosoma* sp. (Shaner et al., 2004) and BBlue from *Actinia equina*. BBlue and mCherry show a homology of about 60% identical amino acids. GFP was found to be highly different, as overlap in gene sequence is below 30% of amino acids. All three analyzed proteins do not have any disulfide bonding, predicted via Disulfid server (Ceroni et al., 2006). However, a high difference is reported in maturation kinetics. While GFP only exhibits one maturation step (oxidation), for mCherry a two-step mechanism is described. Therefore, far longer maturation times for mCherry, than for GFP about a factor of 10 were reported (Hebisch et al., 2013). Both maturation kinetics exhibit a pronounced growth rate

**TABLE 5 |** Average time-space-yield (TSY) of fed batch and glycerol/lactose chemostat including running time of chemostat to reach the performance of the fed batch for BL21(DE3).

Protein	Glucose-IPTG fed-batch average TSY [g/l/h]	Glycerol-lactose chemostat TSY [g/l/h]	Cultivation time to reach fed-batch productivity at 10 h of induction [h]
GFP	1.28	0.022	581 h
mCherry	0.87	0.052	167 h
BBlue	0.56	0.017	215 h



dependency. Knowledge about the maturation may be a key parameter in further analysis of bacterial subpopulations during chemostat cultivations (Hebisch et al., 2013).

Finally, we compared time space yields for the three glycerol/lactose-based cultivations in BL21(DE3) to fed batches in Table 5. No continuous glycerol/lactose cultivations could compete with fed batch cultivation. mCherry showed the highest time space yield in tested cultivations. It needed at least 167 h of cultivation with an averaged time space yield to meet the performance of a classic fed-batch (which exhibits about 7.5 g/l titer after 10 h of induction).

Long-term *E. coli* cultivations are known to cause different mutants, showing different physiology (i.e.,  $\mu$ ,  $Y_{X/S}$ , etc.) compared to the original strain (Weikert et al., 1997; Binder et al., 2017; Delvigne et al., 2017; Heins et al., 2019). Long cultivation durations with wild-type strains revealed that changes in transcriptome and proteome can be already seen without recombinant protein formation (Wick et al., 2001; Peebo and Neubauer, 2018). As exact regulations in recombinant protein formation are still unknown, reasonable control strategies with further insight in the metabolic regulation are needed. We have ongoing projects identifying different productive subpopulations in *E. coli* being responsible for the change in productivity. However, new insights into the “black box” using transcriptomic analysis and measurement of plasmid and cAMP contents of the glycerol/lactose mixed feed system is mandatory and are ongoing in our group.

Summarizing, in this study we tested glycerol/lactose mixed feed systems in continuous culture using *E. coli* BL21(DE3) and HMS174 expressing different model proteins to find a system with long time stable productivity potentially outperforming fed-batches. Beside lower productivity of glycerol/lactose chemostats compared to glucose/lactose in the beginning, a recovery of productivity at times larger than 100 h (about 15 generation times) could be observed for all strains investigated. However,

further analysis like subpopulation monitoring is necessary to understand this “Lazarus” effect on a cellular level.

## DATA AVAILABILITY STATEMENT

The original contributions presented in the study are included in the article/Supplementary Material, further inquiries can be directed to the corresponding author.

## AUTHOR CONTRIBUTIONS

SK, JK, PV, and CS performed the bioreactor cultivations. SK, JK, and CS evaluated the data. CH, OS, and CS supervised the work. CH and FD gave valuable input for the manuscript. OS and CS drafted the manuscript. All authors contributed to the article and approved the submitted version.

## FUNDING

The authors thank the Christian Doppler Society for funding of this project.

## ACKNOWLEDGMENTS

The authors acknowledge TU Wien Bibliothek for financial support through its Open Access Funding Program.

## SUPPLEMENTARY MATERIAL

The Supplementary Material for this article can be found online at: <https://www.frontiersin.org/articles/10.3389/fbioe.2020.00993/full#supplementary-material>

## REFERENCES

- Baeshen, M. N., Al-Hejin, A. M., Bora, R. S., Ahmed, M. M., Ramadan, H. A., Saini, K. S., et al. (2015). Production of biopharmaceuticals in *E. coli*: current scenario and future perspectives. *J. Microbiol. Biotechnol.* 25, 953–962. doi: 10.4014/jmb.1412.12079
- Berlec, A., and Strukelj, B. (2013). Current state and recent advances in biopharmaceutical production in *Escherichia coli*, yeasts and mammalian cells. *J. Ind. Microbiol. Biotechnol.* 40, 257–274. doi: 10.1007/s10295-013-1235-1230
- Binder, D., Drepper, T., Jaeger, K.-E., Delvigne, F., Wiechert, W., Kohlheyer, D., et al. (2017). Homogenizing bacterial cell factories: analysis and engineering of phenotypic heterogeneity. *Metab. Eng.* 42, 145–156. doi: 10.1016/j.ymben.2017.06.009
- Blommel, P. G., Becker, K. J., Duvnjak, P., and Fox, B. G. (2007). Enhanced bacterial protein expression during auto-induction obtained by alteration of lac repressor dosage and medium composition. *Biotechnol. Prog.* 23, 585–598. doi: 10.1021/bp070011x
- Burstein, C., Cohn, M., Kepes, A., and Monod, J. (1965). Role du lactose et de ses produits métaboliques dans l'induction de l'opéron lactose chez *Escherichia coli*. *Biochimica et Biophysica Acta (BBA)-Nucleic Acids and Protein Synthesis* 95, 634–639. doi: 10.1016/0005-2787(65)90517-90514
- Ceroni, A., Passerini, A., Vullo, A., and Frasconi, P. (2006). DISULFIND: a disulfide bonding state and cysteine connectivity prediction server. *Nucleic Acids Res.* 34(Suppl\_2), W177–W181.
- Daegelen, P., Studier, F. W., Lenski, R. E., Cure, S., and Kim, J. F. (2009). Tracing ancestors and relatives of *Escherichia coli* B, and the derivation of B strains REL606 and BL21(DE3). *J. Mol. Biol.* 394, 634–643. doi: 10.1016/j.jmb.2009.09.022
- DeLisa, M. P., Li, J., Rao, G., Weigand, W. A., and Bentley, W. E. (1999). Monitoring GFP-operon fusion protein expression during high cell density cultivation of *Escherichia coli* using an on-line optical sensor. *Biotechnol. Bioeng.* 65, 54–64. doi: 10.1002/(SICI)1097-0290(19991005)65:1<54::AID-BIT7<3.0.CO;2-R
- Delvigne, F., Baert, J., Sassi, H., Fickers, P., Grünberger, A., and Dusny, C. (2017). Taking control over microbial populations: current approaches for exploiting biological noise in bioprocesses. *Biotechnol. J.* 12:1600549. doi: 10.1002/biot.201600549
- Deutscher, J., Francke, C., and Postma, P. W. (2006). How phosphotransferase system-related protein phosphorylation regulates carbohydrate metabolism in bacteria. *Microbiol. Mol. Biol. Rev.* 70, 939–1031. doi: 10.1128/MMBR.00024-26
- Diers, I., Rasmussen, E., Larsen, P., and Kjaersig, I. (1991). Yeast fermentation processes for insulin production. *Bioprocess. Technol.* 13:166.

- Dubendorff, J. W., and Studier, F. W. (1991). Controlling basal expression in an inducible T7 expression system by blocking the target T7 promoter with lac repressor. *J. Mol. Biol.* 219, 45–59. doi: 10.1016/0022-2836(91)90856-90852
- Dvorak, P., Chrast, L., Nikel, P. I., Fedr, R., Soucek, K., Sedlackova, M., et al. (2015). Exacerbation of substrate toxicity by IPTG in *Escherichia coli* BL21(DE3) carrying a synthetic metabolic pathway. *Microb Cell Fact* 14:201. doi: 10.1186/s12934-015-0393-393
- Fernández-Castané, A., Vine, C. E., Caminal, G., and López-Santín, J. (2012). Evidencing the role of lactose permease in IPTG uptake by *Escherichia coli* in fed-batch high cell density cultures. *J. Biotechnol.* 157, 391–398. doi: 10.1016/j.jbiotec.2011.12.007
- Goyon, A., Sciascera, L., Clarke, A., Guillaume, D., and Pell, R. (2018). Extending the limits of size exclusion chromatography: simultaneous separation of free payloads and related species from antibody drug conjugates and their aggregates. *J. Chromatogr. A* 1539, 19–29. doi: 10.1016/j.chroma.2018.01.039
- Gupta, S. K., and Shukla, P. (2016). Microbial platform technology for recombinant antibody fragment production: a review. *Crit. Rev. Microbiol.* 43, 31–42. doi: 10.3109/1040841X.2016.1150959
- Hansen, R., and Eriksen, N. T. (2007). Activity of recombinant GST in *Escherichia coli* grown on glucose and glycerol. *Process Biochem.* 42, 1259–1263. doi: 10.1016/j.procbio.2007.05.022
- Hausjell, J., Weissensteiner, J., Molitor, C., Halbwirth, H., and Spadiut, O. (2018). *E. coli* HMS174 (DE3) is a sustainable alternative to BL21 (DE3). *Microb Cell Fact* 17:169. doi: 10.1186/s12934-018-1016-1016
- Hebisch, E., Knebel, J., Landsberg, J., Frey, E., and Leisner, M. (2013). High variation of fluorescence protein maturation times in closely related *Escherichia coli* strains. *PLoS One* 8:e75991. doi: 10.1371/journal.pone.0075991
- Heins, A.-L., Johanson, T., Han, S., Lundin, L., Carlquist, M., Gernaey, K. V., et al. (2019). Quantitative flow cytometry to understand population heterogeneity in response to changes in substrate availability in *Escherichia coli* and *Saccharomyces cerevisiae* chemostats. *Front. Bioeng. Biotech.* 7:187. doi: 10.3389/fbioe.2019.00187
- Hoffmann, F., and Rinas, U. (2004). Stress induced by recombinant protein production in *Escherichia coli*. *Adv. Biochem. Eng. Biotechnol.* 89, 73–92. doi: 10.1007/b93994
- Inada, T., Kimata, K., and Aiba, H. (1996). Mechanism responsible for glucose–lactose diauxie in *Escherichia coli*: challenge to the cAMP model. *Genes Cells* 1, 293–301. doi: 10.1046/j.1365-2443.1996.24025.x
- Jeong, H., Barbe, V., Lee, C. H., Vallet, D., Yu, D. S., Choi, S. H., et al. (2009). Genome sequences of *Escherichia coli* B strains REL606 and BL21(DE3). *J. Mol. Biol.* 394, 644–652. doi: 10.1016/j.jmb.2009.09.052
- Jeong, H., Kim, H. J., and Lee, S. J. (2015). Complete genome sequence of *Escherichia coli* strain BL21. *Genome Announc.* 3:e00134-15. doi: 10.1128/genomeA.00134-15
- Jia, B., and Jeon, C. O. (2016). High-throughput recombinant protein expression in *Escherichia coli*: current status and future perspectives. *Open Biol.* 6:160196. doi: 10.1098/rsob.160196
- Kopp, J., Kolkman, A.-M., Veleenturf, P. G., Spadiut, O., Herwig, C., and Slouka, C. (2019a). Boosting recombinant inclusion body production—from classical fed-batch approach to continuous cultivation. *Front. Bioeng. Biotech.* 7:297. doi: 10.3389/fbioe.2019.00297
- Kopp, J., Slouka, C., Spadiut, O., and Herwig, C. (2019b). The rocky road from fed-batch to continuous processing with *E. coli*. *Front. Bioeng. Biotech.* 7:328. doi: 10.3389/fbioe.2019.00328
- Kopp, J., Slouka, C., Strohm, D., Kager, J., Spadiut, O., and Herwig, C. (2018). Inclusion Body Bead Size in *E. coli* controlled by physiological feeding. *Microorganisms* 6:116. doi: 10.3390/microorganisms6040116
- Kopp, J., Slouka, C., Ulonska, S., Kager, J., Fricke, J., Spadiut, O., et al. (2017). Impact of glycerol as carbon source onto specific sugar and inducer uptake rates and inclusion body productivity in *E. coli* BL21 (DE3). *Bioengineering* 5:1. doi: 10.3390/bioengineering5010001
- Kopp, J., Zauner, F. B., Pell, A., Hausjell, J., Humer, D., Ebner, J., et al. (2020). Development of a generic reversed-phase liquid chromatography method for protein quantification using analytical quality-by-design principles. *J. Pharmaceut. Biomed.* 188:113412. doi: 10.1016/j.jpba.2020.113412
- Liu, J.-F., Zhang, Z.-J., Li, A.-T., Pan, J., and Xu, J.-H. (2011). Significantly enhanced production of recombinant nitrilase by optimization of culture conditions and glycerol feeding. *Appl. Microbiol. Biot.* 89, 665–672. doi: 10.1007/s00253-010-2866-y
- Llanes, B., and McFall, E. (1969). Effect of galactose on  $\beta$ -Galactosidase synthesis in *Escherichia coli* K-12. *J. Bacteriol.* 97, 217–222. doi: jb.asm.org/content/97/1/217
- Loomis, W. F., and Magasanik, B. (1967). Glucose-lactose diauxie in *Escherichia coli*. *J. Bacteriol.* 93, 1397–1401. doi: jb.asm.org/content/93/4/1397
- Lyakhov, D. L., He, B., Zhang, X., Studier, F. W., Dunn, J. J., and McAllister, W. T. (1998). Pausing and termination by bacteriophage T7 RNA polymerase. *J. Mol. Biol.* 280, 201–213. doi: 10.1006/jmbi.1998.1854
- Malakar, P., and Venkatesh, K. (2012). Effect of substrate and IPTG concentrations on the burden to growth of *Escherichia coli* on glycerol due to the expression of Lac proteins. *Appl. Microbiol. Biot.* 93, 2543–2549. doi: 10.1007/s00253-011-3642-3643
- Marbach, A., and Bettenbrock, K. (2012). lac operon induction in *Escherichia coli*: systematic comparison of IPTG and TMG induction and influence of the transacetylase LacA. *J. Biotechnol.* 157, 82–88. doi: 10.1016/j.jbiotec.2011.10.009
- Martínez-Gómez, K., Flores, N., Castañeda, H. M., Martínez-Batallar, G., Hernández-Chávez, G., Ramírez, O. T., et al. (2012). New insights into *Escherichia coli* metabolism: carbon scavenging, acetate metabolism and carbon recycling responses during growth on glycerol. *Microb. Cell Fact* 11:46. doi: 10.1186/1475-2859-11-46
- Monod, J. (1949). The growth of bacterial cultures. *Annu. Rev. Microbiol.* 3, 371–394.
- Murarka, A., Dharmadi, Y., Yazdani, S. S., and Gonzalez, R. (2008). Fermentative utilization of glycerol by *Escherichia coli* and its implications for the production of fuels and chemicals. *Appl. Environ. Microbiol.* 74, 1124–1135. doi: 10.1128/AEM.02192-197
- Neubauer, P., and Hofmann, K. (1994). Efficient use of lactose for the lac promoter-controlled overexpression of the main antigenic protein of the foot and mouth disease virus in *Escherichia coli* under fed-batch fermentation conditions. *FEMS Microbiol. Rev.* 14, 99–102. doi: 10.1111/j.1574-6976.1994.tb00080.x
- Neubauer, P., Lin, H., and Mathisizik, B. (2003). Metabolic load of recombinant protein production: inhibition of cellular capacities for glucose uptake and respiration after induction of a heterologous gene in *Escherichia coli*. *Biotechnol. Bioeng.* 83, 53–64. doi: 10.1002/bit.10645
- Ozbudak, E. M., Thattai, M., Lim, H. N., Shraiman, B. I., and Van Oudenaarden, A. (2004). Multistability in the lactose utilization network of *Escherichia coli*. *Nature* 427:737. doi: 10.1038/nature02298
- Peebo, K., and Neubauer, P. (2018). Application of continuous culture methods to recombinant protein production in microorganisms. *Microorganisms* 6:56. doi: 10.3390/microorganisms6030056
- Portaccio, M., Stellato, S., Rossi, S., Bencivenga, U., Eldin, M. M., Gaeta, F., et al. (1998). Galactose competitive inhibition of  $\beta$ -galactosidase (*Aspergillus oryzae*) immobilized on chitosan and nylon supports. *Enzyme Microb. Tech.* 23, 101–106. doi: 10.1016/S0141-0229(98)00018-10
- Postma, P. W., Lengeler, J. W., and Jacobson, G. R. (1993). Phosphoenolpyruvate:carbohydrate phosphotransferase systems of bacteria. *Microbiol. Rev.* 57, 543–594.
- Reinikainen, P., and Virkajärvi, I. (1989). *Escherichia coli* growth and plasmid copy numbers in continuous cultivations. *Biotechnol. Lett.* 11, 225–230. doi: 10.1007/BF01031568
- Ronimus, R. S., and Morgan, H. W. (2003). Distribution and phylogenies of enzymes of the Embden-Meyerhof-Parnas pathway from archaea and hyperthermophilic bacteria support a gluconeogenic origin of metabolism. *Archaea* 1, 199–221. doi: 10.1155/2003/162593
- Rosano, G. L., and Ceccarelli, E. A. (2014). Recombinant protein expression in *Escherichia coli*: advances and challenges. *Front. Microbiol.* 5:172. doi: 10.3389/fmicb.2014.00172
- Schmideder, A., and Weuster-Botz, D. (2017). High-performance recombinant protein production with *Escherichia coli* in continuously operated cascades of stirred-tank reactors. *J. Ind. Microbiol. Biotechnol.* 44, 1021–1029. doi: 10.1007/s10295-017-1927-y
- Seo, J. H., and Bailey, J. E. (1986). Continuous cultivation of recombinant *Escherichia coli*: existence of an optimum dilution rate for maximum plasmid and gene product concentration. *Biotechnol. Bioeng.* 28, 1590–1594. doi: 10.1002/bit.260281018

- Shaner, N. C., Campbell, R. E., Steinbach, P. A., Giepmans, B. N., Palmer, A. E., and Tsien, R. Y. (2004). Improved monomeric red, orange and yellow fluorescent proteins derived from *Discosoma sp. red fluorescent protein*. *Nat. Biotechnol.* 22, 1567–1572. doi: 10.1038/nbt1037
- Shloach, J., and Fass, R. (2005). Growing *E. coli* to high cell density—a historical perspective on method development. *Biotechnol. Adv.* 23, 345–357. doi: 10.1016/j.biotechadv.2005.04.004
- Sieben, M., Steinhorn, G., Müller, C., Fuchs, S., Chin, L. A., Regestein, L., et al. (2016). Testing plasmid stability of *Escherichia coli* using the continuously operated shaken BIOreactor system. *Biotechnol. Prog.* 32, 1418–1425. doi: 10.1002/btpr.2341
- Slouka, C., Kopp, J., Hutwimmer, S., Strahammer, M., Strohm, D., Eitenberger, E., et al. (2018). Custom made inclusion bodies: impact of classical process parameters and physiological parameters on inclusion body quality attributes. *Microb Cell Fact* 17:148. doi: 10.1186/s12934-018-0997-995
- Slouka, C., Kopp, J., Strohm, D., Kager, J., Spadiut, O., and Herwig, C. (2019). Monitoring and control strategies for inclusion body production in *E. coli* based on glycerol consumption. *J. Biotechnol.* 296, 75–82. doi: 10.1016/j.jbiotec.2019.03.014
- Slouka, C., Wurm, D. J., Brunauer, G., Welzl-Wachter, A., Spadiut, O., Fleig, J., et al. (2016). A novel application for low frequency electrochemical impedance spectroscopy as an online process monitoring tool for viable cell concentrations. *Sensors (Basel)* 16:1900. doi: 10.3390/s16111900
- Spadiut, O., Capone, S., Krainer, F., Glieder, A., and Herwig, C. (2014). Microbials for the production of monoclonal antibodies and antibody fragments. *Trends Biotechnol.* 32, 54–60. doi: 10.1016/j.tibtech.2013.10.002
- Steen, R., Dahlberg, A. E., Lade, B. N., Studier, F. W., and Dunn, J. J. (1986). T7 RNA polymerase directed expression of the *Escherichia coli* rrnB operon. *EMBO J.* 5, 1099–1103. doi: 10.1002/j.1460-2075.1986.tb04328.x
- Striedner, G., Pfaffenweller, I., Markus, L., Nemecek, S., Grabherr, R., and Bayer, K. (2010). Plasmid-free T7-based *Escherichia coli* expression systems. *Biotechnol. Bioeng.* 105, 786–794. doi: 10.1002/bit.22598
- Studier, F. W., and Moffatt, B. A. (1986). Use of bacteriophage T7 RNA polymerase to direct selective high-level expression of cloned genes. *J. Mol. Biol.* 189, 113–130. doi: 10.1016/0022-2836(86)90385-2
- Studier, F. W., Rosenberg, A. H., Dunn, J. J., and Dubendorff, J. W. (1990). Use of T7 RNA polymerase to direct expression of cloned genes. *Methods Enzymol.* 185, 60–89. doi: 10.1016/0076-6879(90)85008-c
- Tseng, T. T., Tyler, B. M., and Setubal, J. C. (2009). Protein secretion systems in bacterial-host associations, and their description in the gene ontology. *BMC Microbiol.* 9(Suppl. 1):S2. doi: 10.1186/1471-2180-9-S1-S2
- Ukkonen, K., Mayer, S., Vasala, A., and Neubauer, P. (2013). Use of slow glucose feeding as supporting carbon source in lactose autoinduction medium improves the robustness of protein expression at different aeration conditions. *Protein Expr. Purif.* 91, 147–154. doi: 10.1016/j.pep.2013.07.016
- Vaiphei, S. T., Pandey, G., and Mukherjee, K. J. (2009). Kinetic studies of recombinant human interferon-gamma expression in continuous cultures of *E. coli*. *J. Ind. Microbiol. Biotechnol.* 36:1453. doi: 10.1007/s10295-009-0632-x
- Viitanen, M. I., Vasala, A., Neubauer, P., and Alatossava, T. (2003). Cheese whey-induced high-cell-density production of recombinant proteins in *Escherichia coli*. *Microb Cell Fact* 2:2. doi: 10.1186/1475-2859-2-2
- Walsh, G. (2010). Biopharmaceutical benchmarks 2010. *Nat. Biotechnol.* 28, 917–924. doi: 10.1038/nbt0910-917
- Wang, Z., and Yang, S.-T. (2013). Propionic acid production in glycerol/glucose co-fermentation by *Propionibacterium freudenreichii* subsp. *shermanii*. *Bioresour. Technol.* 137, 116–123. doi: 10.1016/j.biortech.2013.03.012
- Weikert, C., Sauer, U., and Bailey, J. E. (1997). Use of a glycerol-limited, long-term chemostat for isolation of *Escherichia coli* mutants with improved physiological properties. *Microbiology* 143, 1567–1574. doi: 10.1099/00221287-143-5-1567
- Wick, L. M., Quadroni, M., and Egli, T. (2001). Short-and long-term changes in proteome composition and kinetic properties in a culture of *Escherichia coli* during transition from glucose-excess to glucose-limited growth conditions in continuous culture and vice versa. *Environ. Microbiol.* 3, 588–599. doi: 10.1046/j.1462-2920.2001.00231.x
- Wurm, D. J., Hausjell, J., Ulonska, S., Herwig, C., and Spadiut, O. (2017a). Mechanistic platform knowledge of concomitant sugar uptake in *Escherichia coli* BL21 (DE3) strains. *Sci. Rep.* 7:45072. doi: 10.1038/srep45072
- Wurm, D. J., Herwig, C., and Spadiut, O. (2017b). How to determine interdependencies of glucose and lactose uptake rates for heterologous protein production with *E. coli*. *Methods Mol. Biol.* 1586, 397–408. doi: 10.1007/978-1-4939-6887-9\_26
- Wurm, D. J., Quehenberger, J., Mildner, J., Eggenreich, B., Slouka, C., Schwaighofer, A., et al. (2018). Teaching an old pET new tricks: tuning of inclusion body formation and properties by a mixed feed system in *E. coli*. *Appl. Microbiol. Biot.* 102, 667–676. doi: 10.1007/s00253-017-8641-8646
- Wurm, D. J., Veiter, L., Ulonska, S., Eggenreich, B., Herwig, C., and Spadiut, O. (2016). The *E. coli* pET expression system revisited—mechanistic correlation between glucose and lactose uptake. *Appl. Microbiol. Biotechnol.* 100, 8721–8729. doi: 10.1007/s00253-016-7620-7627
- Yao, R., Xiong, D., Hu, H., Wakayama, M., Yu, W., Zhang, X., et al. (2016). Elucidation of the co-metabolism of glycerol and glucose in *Escherichia coli* by genetic engineering, transcription profiling, and <sup>13</sup>C metabolic flux analysis. *Biotechnol. Biofuels* 9:175. doi: 10.1186/s13068-016-0591-591

**Conflict of Interest:** The authors declare that the research was conducted in the absence of any commercial or financial relationships that could be construed as a potential conflict of interest.

Copyright © 2020 Kittler, Kopp, Veelenurf, Spadiut, Delvigne, Herwig and Slouka. This is an open-access article distributed under the terms of the Creative Commons Attribution License (CC BY). The use, distribution or reproduction in other forums is permitted, provided the original author(s) and the copyright owner(s) are credited and that the original publication in this journal is cited, in accordance with accepted academic practice. No use, distribution or reproduction is permitted which does not comply with these terms.

## 6.5. Scientific Publication 5

www.nature.com/scientificreports

## scientific reports



## OPEN Cascaded processing enables continuous upstream processing with *E. coli* BL21(DE3)

Stefan Kittler<sup>1</sup>, Christoph Slouka<sup>1</sup>, Andreas Pell<sup>1</sup>, Roman Lamplot<sup>1</sup>, Mihail Besleaga<sup>1</sup>, Sarah Ablasser<sup>1</sup>, Christoph Herwig<sup>2</sup>, Oliver Spadiut<sup>1</sup> & Julian Kopp<sup>1✉</sup>

In many industrial sectors continuous processing is already the golden standard to maximize productivity. However, when working with living cells, subpopulation formation causes instabilities in long-term cultivations. In cascaded continuous cultivation, biomass formation and recombinant protein expression can be spatially separated. This cultivation mode was found to facilitate stable protein expression using microbial hosts, however mechanistic knowledge of this cultivation strategy is scarce. In this contribution we present a method workflow to reduce workload and accelerate the establishment of stable continuous processes with *E. coli* BL21(DE3) exclusively based on bioengineering methods.

*Escherichia coli* is frequently employed in research and industry for the production of recombinant proteins<sup>1–3</sup>. The advantages of a large toolbox for genetic modifications as well as fast doubling times outweigh the negative traits, such as the lack of posttranslational modifications<sup>3–6</sup>. Lactose and the synthetic structural analogue IPTG (Isopropyl- $\beta$ -D-thiogalactopyranosid) are common transcription inducers for T7-based *E. coli* expression hosts, like BL21(DE3)<sup>7–9</sup>. Whereas IPTG is known to cause cellular stress ensuing toxic effects at concentrations higher than 1 mM<sup>8,9</sup>, no such effects have been reported for lactose<sup>7,10–12</sup>. High concentrations of recombinant product additionally have been reported of causing host cell toxicity<sup>13</sup>, potentially favoring the use of lactose over IPTG due to slower heterologous protein expression. Furthermore, induction by lactose increases the production of soluble product<sup>6,14–16</sup>. Recently, we reported that co-utilization of glycerol and lactose promotes recombinant protein expression and increases viability compared to a mixed-feed with glucose<sup>17,18</sup>. Unlike glucose, glycerol is integrated into glycolysis and gluconeogenesis<sup>17,18</sup>. Results of other studies also indicate altered TCA-activity on glycerol compared to glucose metabolism potentially favoring recombinant protein production<sup>19–21</sup>.

For *E. coli* bioprocesses it is known that batch and fed-batch cultivations result in unwanted variable, time-dependent productivity<sup>22</sup>, however these processing modes are still state-of-the-art for industrial applications. Time-independent processing would reduce batch to batch variations and consequently allow stable productivity and robust downstream processing<sup>23,24</sup>. Furthermore, a change from fed-batch to continuous manufacturing would allow a reduction in scale and operating costs and thus should be pursued as the most efficient cultivation technique<sup>25–27</sup>. However, solutions for continuous cultivation with *E. coli* have not been realized yet, since subpopulations evolve over elongated cultivation times<sup>13,28–30</sup>, which are yet to be investigated<sup>13,31</sup>.

Previous studies highlighted a cascaded continuous operating system using two bioreactors, to reduce subpopulation formation compared to common continuous cultivations (i.e. chemostat, turbidostat, etc.)<sup>13,32–34</sup>. Even though a spatial separation of biomass formation and recombinant protein production seems promising, the effects of process parameters on productivity in such a cascaded continuous cultivation are barely known<sup>10,35</sup>. Further, long-term effects beyond 100 h of induction and thus the potential for continuous manufacturing with *E. coli* have not been investigated yet<sup>32,34,36</sup> because the development of continuous processes is highly time- and resource-dependent.

In this study, we investigated the cascaded continuous cultivation with a T7-based *E. coli* host over extended cultivation times of more than 220 h using cell specific productivity as a key performance indicator to determine cell equilibrium state. Glycerol-lactose systems were utilized solely for continuous process development, due to their beneficial results over glucose-fed and IPTG-induced systems in diverse pre-studies<sup>18,32,37</sup>. After intensive screening and variation of selected process parameters, a workflow on how to set-up continuous cultivations

<sup>1</sup>Research Division Integrated Bioprocess Development, Institute of Chemical, Environmental and Bioscience Engineering, TU Wien, Gumpendorfer Straße 1a, 1060 Vienna, Austria. <sup>2</sup>Institute of Chemical, Environmental and Bioscience Engineering, TU Wien, Getreidemarkt 9/166, 1060 Vienna, Austria. ✉email: julian.kopp@tuwien.ac.at

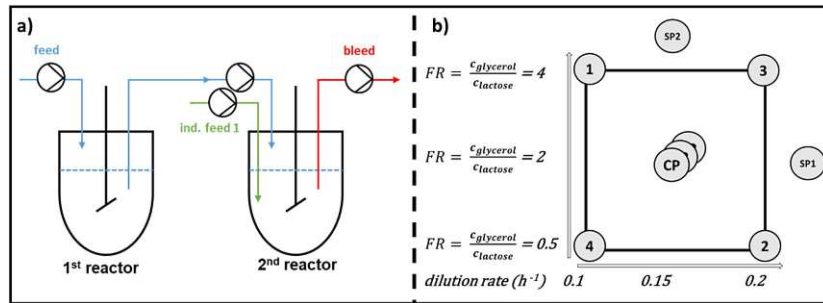


**Figure 1.** (a) Process overview of the cascaded continuous cultivation. Reactor 1 is used for biomass formation. Biomass stream is transferred to reactor 2, where recombinant protein production is induced; (b) showing the full factorial design of experiment (DoE) conducted for the factors dilution rate and feed ratio with the responses space-time yield and specific productivity, center point experiments were conducted in triplicates. (1–4 = run1 – run 4, SP starpoint, FR feed ratio).

Parameter	BL21(DE3) [N-Pro]	Refs.
Maximum specific growth rate— $\mu_{max}$ /h	0.38	18
Maximum specific lactose uptake rate— $q_{s,lac,max}$ [g/g/h]	0.23	18
Maximum specific productivity— $q_{p,max}$ [mg/g/h] in fed batch	70 at a $q_{s,gly}$ of 0.4–0.5 g/g/h	40,41
Induction temperature [°C]	31.5	22
Induction pH [–]	6.7	22

**Table 1.** Prior knowledge on the expression strain BL21(DE3) producing the N-Pro model protein.

with *E. coli* BL21(DE3) was developed, tested and verified. Consequently, we present a first workflow to set up and accelerate stable continuous process development with *E. coli* BL21(DE3).

### Results

Cascaded continuous biomanufacturing with *E. coli* BL21(DE3) was set up as shown in Fig. 1a. Process performance of the cascaded reactor system was evaluated via specific productivity ( $q_p$  [mg/g/h]) and space time yield (STY [mg/L/h]). The STY was chosen as indicator to determine the volumetric product throughput, which is frequently used to evaluate continuous processes. The process parameters dilution rate and glycerol-lactose mixed feed ratio were varied according to a multivariate design (Fig. 1b). The design space was based on recent findings on effects of the dilution rate<sup>32</sup> and the feeding rates using glycerol<sup>18</sup> in our group. Two model proteins with completely different expression behavior were chosen as model proteins in this study: The N-Pro fusion protein which is obligatory expressed as inclusion body in *E. coli* was used for initial screening<sup>38</sup>. The gained Know-how and the proposed workflow was then tested with the fluorescence protein mCherry, being predominantly expressed in soluble form<sup>39</sup>.

**Prior knowledge on the *E. coli* host producing N-Pro.** To screen the expression of recombinant proteins in a cascaded continuous operating system, we used a recombinant *E. coli* BL21(DE3) strain producing a N-Pro fusion protein. Essential physiological parameters, which are required for process development, have been determined in previous studies and are summarized in Table 1.

It is known that the dilution rate significantly affects the productivity in a cascaded cultivation system<sup>32,34</sup>. As a high number of variables in a multivariate design space would result in a remarkably high experimental load, we started with univariate experiments varying the specific glycerol uptake rate  $q_{s,gly}$  during induction, by keeping the total dilution rate constant (Reactor 2; Fig. 1a). Hence, the biomass flux and the induction feed flux into reactor 2 were varied in different percentages (10–30% induction feed of total volumetric stream in reactor 2; Eq. (1)) measuring STY and  $q_p$  as a response. We did not test percentages higher than 30% induction feed to prevent sugar accumulation in reactor 2. The concentration of carbon source to inducer was fixed at a 2:1 ratio. This ratio was based on fed-batch results for concomitant C-source and inducer uptake<sup>42</sup> to ensure complete uptake of the inducer lactose. Based on previous findings, where stable productivity was achieved for 36 generations<sup>32</sup>, we fixed the total dilution rate at 0.15/h.

$$D_{screening} = D_{reactor\ 1} + D_{mixed\ feed\ reactor\ 2} = 0.15/h. \quad (1)$$

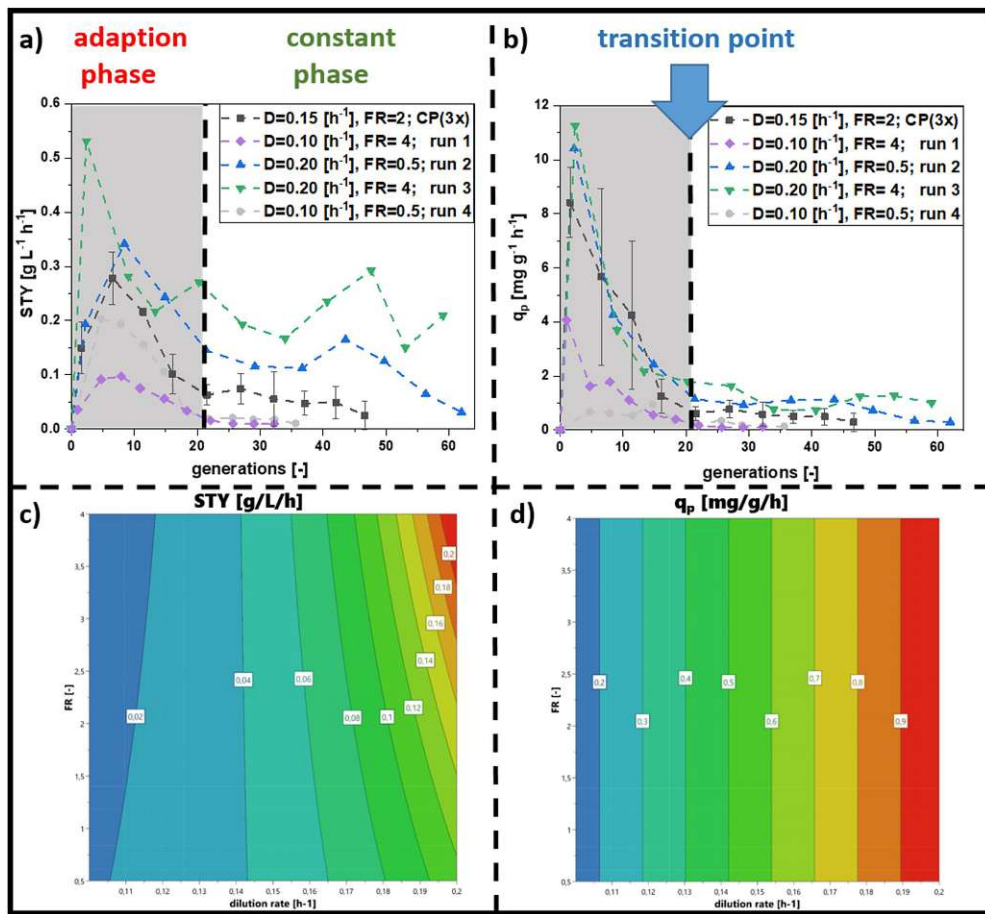


**Figure 2.** Results derived from the multivariate experiments carried out for cascaded continuous cultivation for the N-protein. Centerpoint runs (CP) were summed up in a trend line (triplicate). (a) Space-time-yield (STY), (b) specific productivity ( $q_p$ ), contour plot for (c) STY and (d) for  $q_p$ . High dilution rates, as well as a high uptake rates of glycerol and low rates of lactose seem to be preferable to achieve a high specific productivity and a high STY (FR feed ratio, D dilution rate).

First screening experiments showed best results when the total dilution rate in reactor 2 was composed of 30% mixed feed addition ( $=D_{\text{mixed feed reactor 2}}$  in Eq. (1)). The other 70% of the volumetric stream into reactor 2 were assembled via biomass and base addition. Details are given in Supplementary Data Sect. 1.1.

In the following multivariate design, we fixed the induction feed at 30% and changed the dilution rate and the induction feed ratio (Fig. 1b), which represents the influx of primary carbon source (glycerol) to inducer (lactose)<sup>18</sup>. All performed cultivations followed the same trend: STY and  $q_p$  reached a maximum after the start of induction and then decreased after 20 generations (Fig. 2a,b). Afterwards, productivity either stabilized at a certain level or further decreased to zero. The decrease of  $q_p$  in the adaption phase can be explained by the adaptation time of biomass to inducing conditions. Thus, we subdivided the process into an adaptation phase until 20 generations, before a “transition point” marked the switch towards a constant phase (Fig. 2).

Long-term recombinant protein production was possible in numerous cultivations in the design of experiment (DoE), however STY and  $q_p$  varied significantly. Runs at a dilution rate of 0.2/h and the feed ratio of 4 (Supplementary Data 2.1) led to the highest STY and  $q_p$ . However, these cultivations showed high fluctuations in STY and were not regarded as stable. The contour plots (Fig. 2c,d) visualize the results, tending towards higher dilution rates and higher feed ratio. Dilution rate showed the highest parameter impact, but also mixed feed composition influenced the model (Supplementary Data 2.2). As process conditions resulting in highest

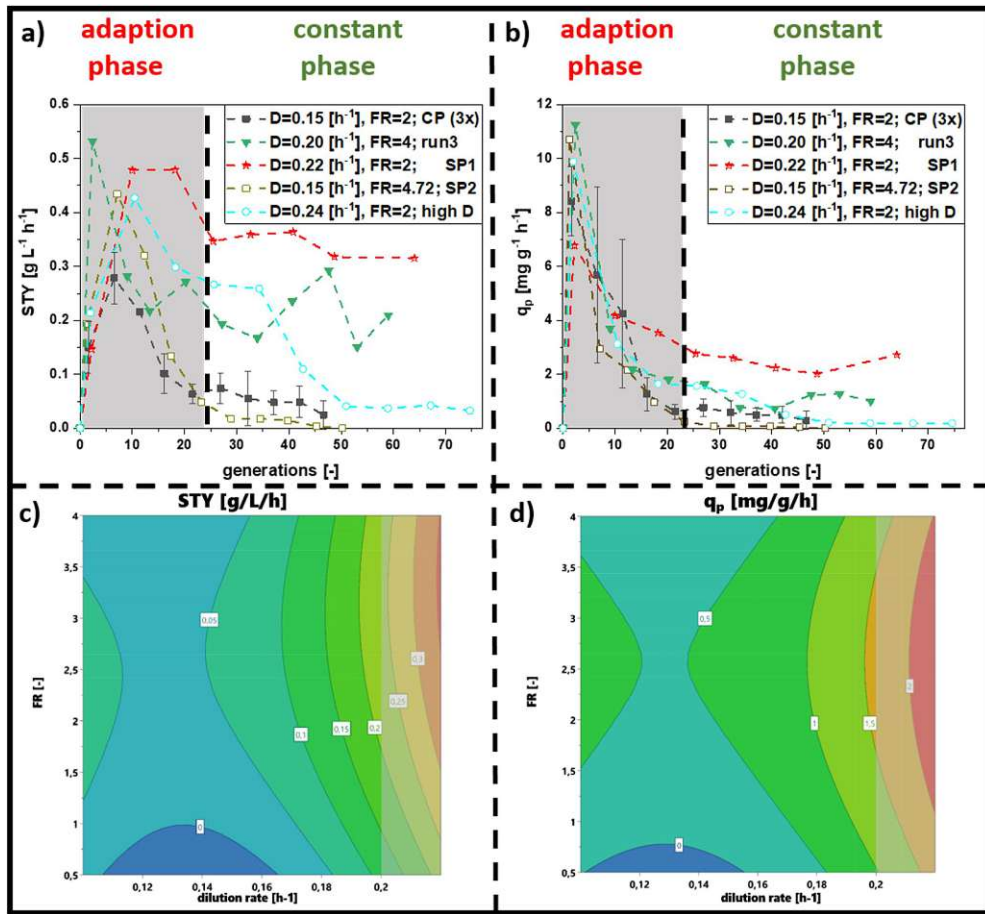


**Figure 3.** Comparing the optimum run of cascaded continuous cultivations derived from the DoE (design of experiment) (run 3) and the centerpoints, with star-point experiment 1 ( $D=0.22/h$  with  $F_{in, gly} = 6.6$  g/h and  $F_{in, lac} = 3.3$  g/h), star-point experiment 2 ( $D=0.15/h$  with  $F_{in, gly} = 14.25$  g/h and  $F_{in, lac} = 3.3$  g/h) and a further increase in dilution rate ( $D=0.24/h$  with  $F_{in, gly} = 6.6$  g/h and  $F_{in, lac} = 3.3$  g/h) (a) STY (space-time-yield) (b)  $q_p$  (specific productivity): Contour plots for (c) STY and (d)  $q_p$  (FR feed ratio, D dilution rate, SP star point).

productivity were at the edge of the design space (Fig. 2c,d), we added star-point experiments with a distance of  $\sqrt{2}$  according to a central composite circumscribed (CCC) model, namely (1)  $D=0.22/h$  with a feeding ratio = 2, and (2)  $D=0.15/h$  with feeding ratio = 4.72 (Fig. 3).

The process operated at a  $D=0.22/h$  with a feeding ratio = 2 gave a high productivity of 0.35 g/L/h even in the constant phase for a prolonged cultivation time of 250 h. At these conditions we further determined stable STY and  $q_p$ . We included the star point experiments in the multivariate design and modeled the response in terms of STY and  $q_p$  (Fig. 3c,d). All model parameters are given in the Supplementary Data 2.2.

As  $\mu_{max}$  for this strain was determined at 0.38/h, the known limit of a stable process was found at a dilution rate of 0.3/h considering biomass yield decrease upon recombinant protein production (Supplementary Data 1.2). To avoid wash-out of host cells, we tested yet another process condition between the new targeted optimum and 0.3/h, namely at  $D=0.24/h$  (with an identical feed ratio of 2). Specific productivity was found stable from 60 to 80 generations throughout the process operated at  $D=0.24/h$ . However, the process operated at star-point 1 with  $D=0.22/h$  achieved higher stable STY and  $q_p$  and was thus found to be optimal. Summing up, we could identify a narrow operating space for cascaded continuous processing using the N-Pro model protein in *E. coli* BL21 (DE3), which led to stable long-term protein expression. In a next step, we summarized our findings in a workflow protocol which comprises two phases.

Die approbierte gedruckte Originalversion dieser Dissertation ist an der TU Wien Bibliothek verfügbar. The approved original version of this doctoral thesis is available in print at TU Wien Bibliothek.

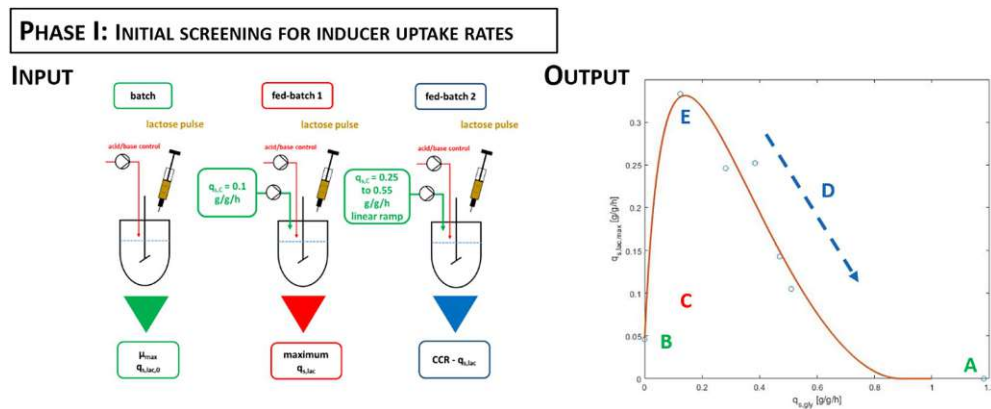


**Figure 4.** Phase I: Generic workflow for determination of maximum inducer uptake rates ( $q_s$ ) versus primary substrate uptake rates for *E. coli*. Therefore three experiments are necessary: (1st step) a batch cultivation for maximum growth rate (A) and inducer uptake without C-source (B); (2nd step) fed-batch cultivation for the maximum inducer uptake rate (C) (3rd step) fed-batch cultivation for inducer uptake rates between a  $q_{s,gly}$  set point from 0.25 to 0.55 g/g/h using a linear ramp approach to screen the regime of carbon catabolite repression (CCR) (E,D).

**2-phase workflow for setup of a cascaded continuous process for *E. coli* BL21(DE3).** *Phase I.* For the strain producing the N-pro fusion protein essential physiological data was already known from previous studies (Table 1). To determine this essential pre-knowledge, solely three bioreactor runs in a batch-/fed-batch mode without the need of sophisticated analytics (i.e. OMICs-studies) are necessary. Phase I is thus subdivided into three steps to obtain the required knowledge:

In step (I) the maximum growth rate and specific inducer uptake rates ( $q_{s,lac}$ ) are determined. Maximum growth rate is easily available upon a batch fermentation with excess carbon source. After the batch, lactose is pulsed in the reactor and uptake of lactose is monitored in a timely resolved way, e.g. by sampling every 30 min (Fig. 4, first reactor). The outcome of the first cultivation provides the maximum growth rate  $\mu_{max}$  and the inducer uptake rate at  $q_{s,gly} = 0$ , namely  $q_{s,lac,0}$ .

Furthermore, the mechanistic relation between  $q_{s,gly}$  and inducer uptake rate ( $q_{s,lac}$ ) must be determined. This can be done in a series of static experiments: A fixed  $q_{s,gly}$  is applied, inducer is pulsed in excess and lactose decrease in the broth is measured<sup>42</sup>. However, using this approach a high number of cultivations is necessary. We recently showed that this relation can be obtained more elegantly in only three experiments using dynamic feeding during induction<sup>42</sup>. Therefore, in step (II) a fed-batch is performed at  $q_{s,gly}$  of 0.1 g/g/h to determine the maximum  $q_{s,lac}$  (Fed-batch 1 in Fig. 4). In step (III)  $q_{s,lac}$  as function of  $q_{s,gly}$  can be identified using a linear  $q_{s,gly}$  ramp. Inducer is pulsed,  $q_{s,gly}$  is increased steadily from 0.25 to 0.55 g/g/h and regular samples are taken to determine  $q_{s,lac}$  in the regime of carbon catabolite repression (CCR) (Fed-batch 2, Fig. 4).

*Phase II.* As intensive screening of cascaded continuous cultivation has been conducted for the N-pro protein, we hypothesize that determined dilution rate optima for the N-pro protein can be transferred to the expression of other proteins using glycerol as C-source, reducing the experimental workload. Based on the previous findings, we recommend to alter the dilution rates in a narrow range of 0.16 to 0.22/h. In addition moderate to high uptake rates ( $q_{s,gly} = 0.25\text{--}0.55$  g/g/h) were found to result in high recombinant protein production in fed-batches<sup>22,32,40–43</sup>. Hence, we recommend to vary the feed ratio for screening near to the maximum inducer uptake rate, to prevent inducer deficiencies and also investigate moderate to high sugar uptake rates ( $q_{s,gly}$ ).

Consequently, our strategy to establish cascaded continuous cultivations for *E. coli* BL21(DE3) using glycerol as carbon source and lactose as inducer, can be summarized as: In phase I physiological parameters are determined (Fig. 4) to estimate a design space for proper feed ratios for cascaded continuous cultivation. In phase II, the output of phase I is combined with the results obtained from initial screening to set up a reduced design of experiment (DoE) in a constricted design space (Figs. 2, 3, 5).

**Testing the proposed workflow to establish cascaded cultivation using *E. coli* BL21(DE3).** To test whether the proposed workflow shows platform character, we conducted the procedure proposed in Figs. 4 and 5 for BL21(DE3) expressing the fluorescence protein mCherry. In phase I, inducer uptake rates at varying feeding rates were determined. This allowed to compose feed ratios for the mCherry protein in cascaded continuous cultivation (Outcome of phase I; Fig. 4).

The effect of the dilution rate was already screened intensively in previous cultivations conducted with the N-Pro protein. Hence, dilution rates were altered in a narrow range of 0.16 to 0.22/h.



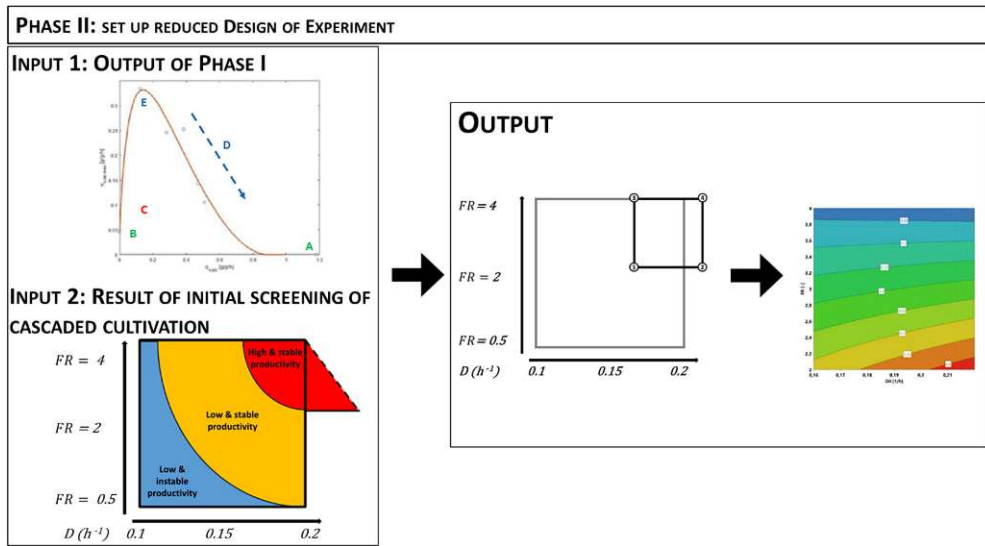


**Figure 5.** The previous findings of cascaded continuous cultivation are used and combined with the output of Phase I to choose a reduced design space. The obtained constricted design space in phase II accelerates the process to find optimal process conditions (*FR* feed ratio, *D* dilution rate).

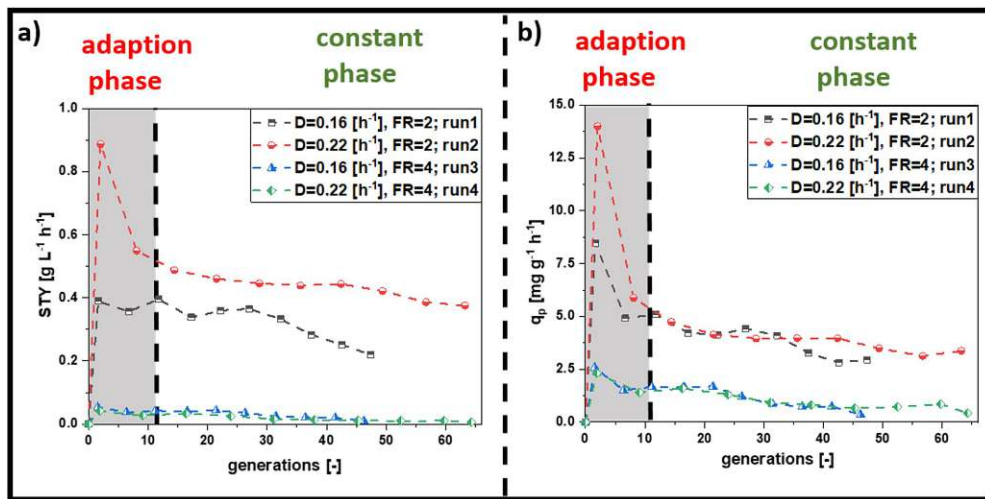


**Figure 6.** Results derived for cascaded continuous cultivation with mCherry, (a) showing the results for STY (space-time-yield) derived on a generation dependent manner, (b) showing  $q_p$  (specific productivity) on generation based behavior; high dilution rates and moderate feeding rates seem to be beneficial for production of mCherry (*FR* feed ratio, *D* dilution rate).

Assembling the gathered information allowed to set up a new screening strategy for mCherry, bearing a much lower experimental load, compared to the initial screening of Npro. The resulting constricted design space (Outcome of phase II, Fig. 5) was used to find suitable operation conditions for high STY and  $q_p$  in *E. coli* expressing mCherry (Fig. 6).

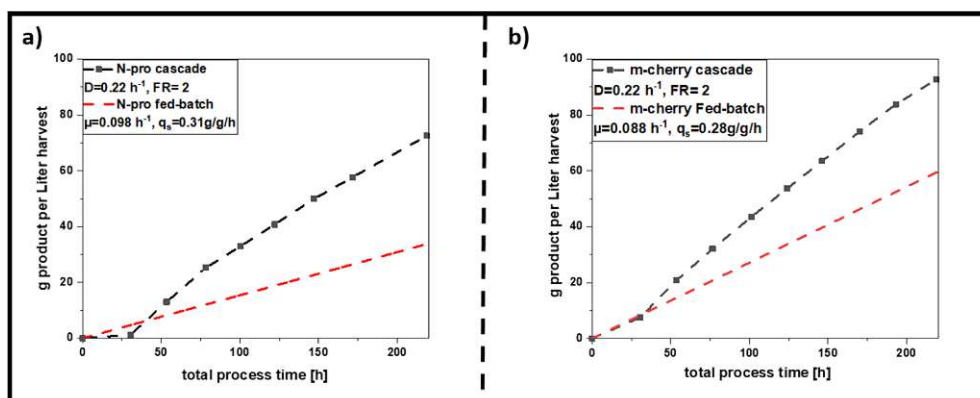


**Figure 7.** Space-time-yield calculated over the total process time for a fed batch and the cascaded continuous cultivation; For fed batches the maximum achieved titers were 5.09 g/L for the N-pro protein and 8.96 g/L for mCherry after each induction phase, CIP + SIP were assumed with 6 and 3 h respectively, batch phase with 6 h and non-induced fed-batch/continuous adaption phase with 12 h. Induction time for fed-batches was calculated with 10 h resulting in the dotted red lines, whereas cascaded continuous cultivation was calculated using cleaning and set-up times stated before, with the time-dependent results measured throughout induction phase given in the black curves for (a) N-pro and for (b) mCherry (*FR* feed ratio, *D* dilution rate, *CIP* clean-in-place, *SIP* sterilize-in-place).

Although the adaptation phase for the mCherry strain was found shorter compared to the N-Pro strain (10 generations vs 20 generations, respectively), chosen process parameters had a comparable impact on specific productivity (Fig. 6b). Model terms for the reduced DoE can be found in Supplementary Data 3.2. Again, the process operated at  $D = 0.22/h$  with a feeding ratio = 2 resulted in a stable, long-time productivity for 180 h. The best process performance was found at dilution rate 0.22/h and a feed ratio of 2 (run 2, Fig. 6a), identical to N-Pro).

The proposed workflow (Figs. 4, 5) thus was appropriate to find well suited operating conditions for an uncharacterized recombinant BL21(DE3) strain and enabled stable long-time productivity with a highly reduced experimental load. Results indicate that the proposed workflow shows platform character, which can be used to ease the set-up of cascaded continuous cultivation for other uncharacterized strains.

**Comparison of cascaded continuous cultivations to fed-batch cultivations.** We want to stress that the described process development for cascaded bio-manufacturing could be solely done with process engineering methods. This technique is thus ideal for being transferred to process development laboratories in industry. To strengthen this hypothesis STY from both processes were compared to state-of-the-art fed-batch cultivations which is the industrial golden standard. Total amount of produced protein was calculated for cascaded continuous process and fed-batch (Fig. 7a for N-pro and 7b for mCherry). As downtimes, such as CIP (clean-in-place), SIP (sterilize-in-place) and biomass cultivation times, can be reduced in cascaded processing, the total space time yield could be increased by a factor of 2.2 for N-pro protein cultivations () and 1.6-fold for mCherry STY.

## Discussion

Continuous cultivation with *E. coli* suffers from time-dependent productivity caused by the arising of non-producing subpopulations, which overgrow the producing population<sup>13,31,44</sup>. Hence, common continuous cultivations with microbials bear mutation rates, plasmid loss and further genetic errors<sup>13,31,44</sup>. The investigation of subpopulation evolution (i.e. via Flow cytometry analysis) was not within the scope of this study. In fact, for one of the chosen products such analytics would not have been technically feasible. In this study, we propose a workflow on how to set up continuous cultivations, keeping cells in an equilibrium state for induction times longer than 220 h using glycerol and lactose. Choosing recombinant protein titer (shown as  $q_p$  and STY) to determine cell equilibrium state in continuous cultivation, negligible long-time effects were observed at optimized process conditions. Results indicate low dilution rates ( $D = 0.1/h$ ) to be unsuitable for achieving long-term stable productivity, independent from the applied uptake rates<sup>32,34</sup>. We believe that high residence times (resulting from low dilution rates) enhance subpopulation diversification, as cells have more time to adapt to environmental conditions and to evolve a non-producing sub-population<sup>35,45,46</sup>. High dilution rates (implementing low residence times) were found to result in stable productivity. The principle facilitates continuous bio-manufacturing, as higher volumetric rates would lead to higher amount of bleed and consequently higher STY. Even though cultivations at higher dilution rates, such as  $D = 0.24/h$  and  $D = 0.3/h$  were found to result in stable productivity (Fig. 3a,b, Supplementary Data 1.2), the feed ratio had a severe impact on the level of cell specific productivity.

Careful optimizations in the feeding procedure (percentage of induction feed to feed) is thus necessary to achieve high and stable specific productivity.

As the ideal operating space for recombinant protein expression in cascaded continuous processing was intensively screened, obtained results were taken to propose a generic workflow for the establishment of cascaded continuous cultivation for *E. coli* BL21(DE3). We suggest to screen initial physiological parameters in a batch and two fed-batch runs (phase I) at first. Based on the initial screening experiments and the determination of physiological parameters (output of phase I) a reduced experimental design can be used to optimize process conditions in cascaded continuous cultivation (phase II). Testing the anticipated workflow showed that identical process parameters led to best results, independent from the recombinant protein. Stable specific productivity at highest space–time yield for the expression of both target proteins was found at a dilution rate of 0.22/h conducted at a feed ratio of 2 ( $q_p$  N-pro:  $2.47 \pm 13.3\%$ ;  $q_p$  mCherry =  $3.97 \pm 14.4\%$ ). Even though ideal cultivations were well comparable for both proteins exploitation of different carbon sources and inducers could lead to different effects (i.e. altered inducer uptake rates<sup>18,42</sup>).

Still, for new BL21(DE3) strains and products, we propose an experimental workflow with two phases using solely bioengineering methods. As parallelization of continuous processes can be used to speed up process development<sup>10</sup>, we were able to establish stable continuous cultivations for a new target product within less than a month. Results presented in this study also show that cascaded continuous cultivation is superior to fed-batch cultivation for *E. coli* BL21(DE3) and hence is a suitable tool for bio-manufacturing. Consequently, the demonstrated experimental workflow could be used to set up and accelerate the implementation of a stable continuous upstream process for *E. coli*.

## Material and methods

**Strains and media.** All performed cultivations were carried out using the *E. coli* strain BL21(DE3). The protein used for initial studies is an industrial protein (28.8 kDa), being linked to an N-pro fusion tag and integrated into a pET-30a plasmid system<sup>38</sup>. The protein used for verification and transfer studies was mCherry, being integrated also in a pET30a plasmid system. Expression for mCherry was dominantly soluble in the cytoplasm, with small fractions being expressed as an inclusion body.

For all cultivations, a defined minimal medium referred to DeLisa et al. was used (Supplementary Data, Chapter 4.5). To cope for the antibiotic selection of pET30a systems, Kanamycin was supplemented to the medium resulting in a final concentration of 0.02 g/L<sup>47</sup>.

Preculture was assembled of 8.2 g/L glycerol while batch medium contained 20.4 g/L glycerol. The feed for biomass formation (reactor 1) contained 25 g/L of glycerol, while the mixed feed was altered according to the DoE approach (Fig. 1). Each step was conducted using the referred media, with altered sugar and trace-element concentrations adapted for the corresponding growth phases.

The preculture was carried out in Ultra yield flasks using 500 mL sterile DeLisa medium. Preculture was inoculated with 1.5 mL frozen bacterial stocks, stored at  $-80^\circ\text{C}$  using 25% glycerol as antifreeze solution. They were cultivated over night at  $37^\circ\text{C}$ , 230 rpm and a pH of 6.7 in an Infors HR Multitron shaker (Infors, Bottmingen Switzerland). The batch medium was inoculated the next day with the preculture using 20% of the reactor volume.

**Cascaded continuous cultivation.** The used set up for the cascaded continuous cultivation is sketched in Fig. 1a. Biomass formation and protein expression were spatially separated, having sequentially operating chemostats implemented with separated feeds<sup>34</sup>. In each run, one reactor was used for biomass formation and the derived biomass stream was transferred to the second reactor, controlled via pumps monitored by the process system PIMS Lucullus (SecureCell, Urdorf, Swiss). Biomass formation (reactor 1) was performed in a Labfors 3 bioreactor (max. wV: 2 L; Infors HT, Bottmingen, Switzerland). The reactor was coupled to a continuously operated stirred-tank reactor—(Minifors 2, max. wV: 1 L; Infors HT, Bottmingen, Switzerland), used for recombinant protein expression. Reactor 1 was aerated with a mixture of pressurized air and pure oxygen at 3 vvm and constantly stirred at 1000 rpm. Minifors reactors were aerated with 2 vvm and stirred at 1400 rpm. The off-gas concentrations of  $\text{CO}_2$  and  $\text{O}_2$  were monitored via BlueSens Gas sensors (BlueSens Gas analytics, Herten, Germany). Throughout all cultivations the dissolved oxygen ( $\text{dO}_2$ ) was kept above 40% by adjusting the ratio of pure oxygen and pressurized air. The dissolved oxygen was monitored with a fluorescence dissolved oxygen electrode Visiform DO425 (Hamilton, Reno, NV, USA). As throughout the continuous phase the volume in the reactors was controlled with a dip pipe adjusted to the liquid surface, no stirrer cascade was implemented. pH was maintained at a constant value of 6.7 through all process phases and controlled by addition of  $\text{NH}_4\text{OH}$  (12.5%). The pH was monitored with an EasyFerm electrode (Hamilton, Reno, NV, USA). In all three reactors, a batch was conducted with carbon concentrations of 20.4 g/L, yielding in 9–10 g dry cell weight of biomass per litre of cultivation broth. The end of the batch phase was determined by a drop in the  $\text{CO}_2$  signal.

Afterwards, the non-induced chemostat system was started by supplying the biomass reactor with a dilution rate of 0.14/h feed 1 (Table 1) and starting the transfer of biomass. For the cascaded continuous cultivation, the temperature in reactor 1 was set to  $35^\circ\text{C}$ . To achieve an optimal protein expression the temperature in the second reactor was lowered to  $31.5^\circ\text{C}$  for the N-pro protein<sup>42</sup>, whereas  $30^\circ\text{C}$  where applied throughout induction phase for mCherry, due to previous results obtained for soluble protein expression<sup>43</sup>.

The so-called continuous adjustment phase and lasted over-night to achieve a steady state in all reactors, monitored by an equilibrium state of reactor 1 of derived  $\text{pO}_2$  and off gas signals. To initiate protein expression reactor 2 was supplied with the mixed feed containing glycerol and the inducer lactose, adjusted to the DoE approach. The volume throughput (Minifors 2, max. wV. 1 L) was adjusted to the desired dilution rate according to the design of experiment.

Experiments to determine uptake rates in mCherry, were performed in a Sartorius Biostat Cplus bioreactor (Sartorius, Göttingen, Germany) with 10 L working volume. Monitoring and control were performed via Lucillus (SecureCell, Urdorf, Swiss). The maximum glycerol uptake rate was determined in regularly sampling during the batch. Afterwards a lactose was added via pulse and uptake of solely lactose was evaluated. At a  $q_{s, gly}$  of about 0.15 g/g/h a static experiment was performed using a classic fed-forward approach and lactose pulses. Higher  $q_{s, gly}$  were screened using a linear ramp from about  $q_{s, gly}$  0.25 to 0.55 g/g/h of the glycerol feed in combination with lactose pulses. While for BL21, uptake rates are similar<sup>42</sup>, results might be different for other *E. coli* strains using lactose as inducing agent.

**Fed-batch cultivations.** Pre-culture and process analytics were performed equivalent to the cascaded continuous cultivations. Fed-batches were conducted with an exponential feeding approach at a constant  $q_{s, C}$ . Feed addition was started after the end of the batch, indicated by a drop of the CO<sub>2</sub> signal. Feeding was conducted at  $q_s = 0.2$  g/g/h and lasted over-night to generate 25–30 g/L biomass. Prior to induction temperature was adjusted to 31.5 °C for Npro and to 30 °C for mCherry. The exponential feeding was set to a  $q_s = 0.3$  g/g/h for both proteins. Induction was performed via a 0.5 mM IPTG pulse to the fermentation broth and induction lasted for 10 h.

**Multivariate data assessment and process analytics.** Multivariate data assessment of the performed experimental design was performed. Results were investigated for the statistical relevance of the model using the measure of fit ( $R^2$ ), the model predictability ( $Q^2$ ), the model validity and the model reproducibility, adjusted for degrees of freedom. Analysis of the process dataset was done by a multivariate data assessment (MODDE 12, Umetrics, Sweden). Time independent rates (space–time yield STY (mg/L/h) and specific productivity  $q_p$  (mg/g/h)) were chosen as responses to be evaluated for this study.

Process analytics were performed as described in previous studies<sup>18,22,32,40</sup> and further information can be found in Supplementary Sect. 4. Titer was determined using the described HPLC method<sup>48</sup>. For quantification of the N-pro fusion protein, our industrial partner provided a purified standard reference. mCherry was quantified via a commercial available protein standard. Protein size of the expressed target proteins was determined via SDS-PAGE (results not shown). Time independent rates (specific productivity  $q_p$  (mg/g/h) and space–time yield STY (g/L/h) were chosen as model responses to be evaluated for this study. Rates were calculated as stated beneath:

$$q_p = \frac{c_i + c_{i-1}}{2} \times \frac{X_i + X_{i-1}}{2} \times (t_i - t_{i-1})$$

$q_p$ : specific productivity [mg/g/h],  $c_i$ : product concentration of sample  $i$  [mg/L],  $X_i$ : biomass concentration of sample  $i$  [g/L],  $t_i$ : cultivation time at timepoint of sample  $i$  [mg/L].

Space–time–yield used for comparison, was calculated by the following Eqs. (2) and (3):

$$STY = \frac{c_i + c_{i-1}}{2} \times \frac{\Delta \dot{F}_i}{V_R} \quad (2)$$

$$\text{with } \Delta \dot{F}_i = \dot{F}_i - \dot{F}_{i-1} = \Delta \frac{\dot{X}_i}{2} + \Delta \dot{F}_{ind, Feed} + \Delta \dot{F}_{Base} \quad (3)$$

STY: space–time–yield [g/L/h],  $c_i$ : product concentration of sample  $i$  [g/L],  $F_i$ : volumetric flow through recombinant protein producing reactor at timepoint of sample  $i$  [L/h],  $\dot{X}_i$ : biomass flux derived from reactor 1 at timepoint of sample  $i$  [L/h],  $\dot{F}_{ind, Feed}$ : volumetric rate of inducer feed in reactor 2 [L/h] (comp. to Fig. 1a),  $\dot{F}_{Base}$ : volumetric rate of base in reactor 2 [L/h] (comp. to Fig. 1a).

Received: 18 December 2020; Accepted: 4 May 2021

Published online: 01 June 2021

## References

- Huang, C.-J., Lin, H. & Yang, X. Industrial production of recombinant therapeutics in *Escherichia coli* and its recent advancements. *J. Ind. Microbiol. Biotechnol.* **39**, 383–399 (2012).
- Baeshen, M. N. *et al.* Production of biopharmaceuticals in *E. coli*: Current scenario and future perspectives. *J. Microbiol. Biotechnol.* **25**, 953–962 (2015).
- Jia, B. & Jeon, C. O. High-throughput recombinant protein expression in *Escherichia coli*: Current status and future perspectives. *Open Biol.* **6**, 160196 (2016).
- Rosano, G. L. & Ceccarelli, E. A. Recombinant protein expression in *Escherichia coli*: Advances and challenges. *Front. Microbiol.* **5**, 172 (2014).
- Tegel, H., Ottosson, J. & Hober, S. Enhancing the protein production levels in *Escherichia coli* with a strong promoter. *FEBS J.* **278**, 729–739 (2011).
- Wurm, D. J. *et al.* The *E. coli* pET expression system revisited—mechanistic correlation between glucose and lactose uptake. *Appl. Microbiol. Biotechnol.* **100**, 8721–8729 (2016).
- Keiler, K. C. Biology of trans-translation. *Annu. Rev. Microbiol.* **62**, 133–151 (2008).
- Marbach, A. & Bettenbrock, K. lac operon induction in *Escherichia coli*: Systematic comparison of IPTG and TMG induction and influence of the transacetylase LacA. *J. Biotechnol.* **157**, 82–88 (2012).
- Neubauer, P. & Hofmann, K. Efficient use of lactose for the lac promoter-controlled overexpression of the main antigenic protein of the foot and mouth disease virus in *Escherichia coli* under fed-batch fermentation conditions. *FEMS Microbiol. Rev.* **14**, 99–102 (1994).

10. Peebo, K. & Neubauer, P. Application of continuous culture methods to recombinant protein production in microorganisms. *Microorganisms* **6**, 56 (2018).
11. Mainil, J. *Escherichia coli* virulence factors. *Vet. Immunol. Immunopathol.* **152**, 2–12 (2013).
12. Striedner, G., Cserjan-Puschmann, M., Pötschacher, F. & Bayer, K. Tuning the transcription rate of recombinant protein in strong *Escherichia coli* expression systems through repressor titration. *Biotechnol. Prog.* **19**, 1427–1432 (2003).
13. Rugbjerg, P. & Sommer, M. O. A. Overcoming genetic heterogeneity in industrial fermentations. *Nat. Biotechnol.* **37**, 869–876 (2019).
14. Blommel, P. G., Becker, K. J., Duvnjak, P. & Fox, B. G. Enhanced bacterial protein expression during auto-induction obtained by alteration of lac repressor dosage and medium composition. *Biotechnol. Prog.* **23**, 585–598 (2007).
15. Neubauer, P., Hofmann, K., Holst, O., Mattiasson, B. & Kruschke, P. Maximizing the expression of a recombinant gene in *Escherichia coli* by manipulation of induction time using lactose as inducer. *Appl. Microbiol. Biotechnol.* **36**, 739–744 (1992).
16. Bashir, H. *et al.* Simple procedure applying lactose induction and one-step purification for high-yield production of rhClIFN. *Biotechnol. Appl. Biochem.* **63**, 708–714 (2016).
17. Lin, E. C. Glycerol dissimilation and its regulation in bacteria. *Annu. Rev. Microbiol.* **30**, 535–578 (1976).
18. Kopp, J. *et al.* Impact of glycerol as carbon source onto specific sugar and inducer uptake rates and inclusion body productivity in *E. coli* BL21 (DE3). *Bioengineering* **5**, 1 (2017).
19. Heyland, J., Blank, L. M. & Schmid, A. Quantification of metabolic limitations during recombinant protein production in *Escherichia coli*. *J. Biotechnol.* **155**, 178–184 (2011).
20. Martínez-Gómez, K. *et al.* New insights into *Escherichia coli* metabolism: Carbon scavenging, acetate metabolism and carbon recycling responses during growth on glycerol. *Microb. Cell Fact.* **11**, 46 (2012).
21. Yao, R. *et al.* Elucidation of the co-metabolism of glycerol and glucose in *Escherichia coli* by genetic engineering, transcription profiling, and <sup>13</sup>C metabolic flux analysis. *Biotechnol. Biofuels* **9**, 175 (2016).
22. Slouka, C. *et al.* Custom made inclusion bodies: Impact of classical process parameters and physiological parameters on inclusion body quality attributes. *Microb. Cell Fact.* **17**, 148 (2018).
23. Sandén, A. M. *et al.* Limiting factors in *Escherichia coli* fed-batch production of recombinant proteins. *Biotechnol. Bioeng.* **81**, 158–166 (2003).
24. Konstantinov, K. B. & Cooney, C. L. White paper on continuous bioprocessing May 20–21 2014 continuous manufacturing symposium. *J. Pharm. Sci.* **104**, 813–820 (2015).
25. Glaser, J. A. *Continuous Chemical Production Processes* (Springer, 2015).
26. Lee, S. L. *et al.* Modernizing pharmaceutical manufacturing: From batch to continuous production. *J. Pharm. Innov.* **10**, 191–199 (2015).
27. Karst, D. J., Steinebach, F., Soos, M. & Morbidelli, M. Process performance and product quality in an integrated continuous antibody production process. *Biotechnol. Bioeng.* **114**, 298–307 (2017).
28. Heins, A.-L. *et al.* Quantitative flow cytometry to understand population heterogeneity in response to changes in substrate availability in *Escherichia coli* and *Saccharomyces cerevisiae* chemostats. *Front. Bioeng. Biotechnol.* <https://doi.org/10.3389/fbioe.2019.00187> (2019).
29. Binder, D. *et al.* Homogenizing bacterial cell factories: Analysis and engineering of phenotypic heterogeneity. *Metab. Eng.* **42**, 145–156 (2017).
30. Veening, J.-W., Smits, W. K. & Kuipers, O. P. Bistability, epigenetics, and bet-hedging in bacteria. *Annu. Rev. Microbiol.* **62**, 193–210 (2008).
31. Buerger, J., Gronenberg, L. S., Genee, H. J. & Sommer, M. O. Wiring cell growth to product formation. *Curr. Opin. Biotechnol.* **59**, 85–92 (2019).
32. Kopp, J. *et al.* Boosting recombinant inclusion body production—from classical fed-batch approach to continuous cultivation. *Front. Bioeng. Biotechnol.* **7**, 297 (2019).
33. Kopp, J., Slouka, C., Spadiut, O. & Herwig, C. The rocky road from fed-batch to continuous processing with *E. coli*. *Front. Bioeng. Biotechnol.* **7**, 328 (2019).
34. Schmideder, A. & Weuster-Botz, D. High-performance recombinant protein production with *Escherichia coli* in continuously operated cascades of stirred-tank reactors. *J. Ind. Microbiol. Biotechnol.* **44**, 1021–1029 (2017).
35. Delvigne, F. *et al.* Taking control over microbial populations: Current approaches for exploiting biological noise in bioprocesses. *Biotechnol. J.* **12**, 1600549 (2017).
36. Schmideder, A., Severin, T. S., Cremer, J. H. & Weuster-Botz, D. A novel milliliter-scale chemostat system for parallel cultivation of microorganisms in stirred-tank bioreactors. *J. Biotechnol.* **210**, 19–24 (2015).
37. Kittler, S. *et al.* The Lazarus *Escherichia coli* effect: Recovery of productivity on glycerol/lactose mixed feed in continuous biomanufacturing. *Front. Bioeng. Biotechnol.* **8**, 993 (2020).
38. Achmüller, C. *et al.* N(pro) fusion technology to produce proteins with authentic N termini in *E. coli*. *Nat. Methods* **4**, 1037–1043 (2007).
39. Kittler, S. *et al.* The Lazarus *E. coli* effect: Recovery of productivity on glycerol/lactose mixed feed in continuous biomanufacturing. *Front. Bioeng. Biotechnol.* **8**, 993 (2020).
40. Slouka, C. *et al.* Monitoring and control strategies for inclusion body production in *E. coli* based on glycerol consumption. *J. Biotechnol.* **296**, 75 (2019).
41. Kopp, J. *et al.* Inclusion body bead size in *E. coli* controlled by physiological feeding. *Microorganisms* **6**, 116 (2018).
42. Wurm, D. J., Hausjell, J., Ulonska, S., Herwig, C. & Spadiut, O. Mechanistic platform knowledge of concomitant sugar uptake in *Escherichia coli* BL21 (DE3) strains. *Sci. Rep.* **7**, 45072 (2017).
43. Wurm, D. J. *et al.* Teaching an old pET new tricks: Tuning of inclusion body formation and properties by a mixed feed system in *E. coli*. *Appl. Microbiol. Biotechnol.* **102**, 667–676 (2018).
44. Rugbjerg, P., Myling-Petersen, N., Porse, A., Sarup-Lytzen, K. & Sommer, M. O. Diverse genetic error modes constrain large-scale bio-based production. *Nat. Commun.* **9**, 1–14 (2018).
45. Fragosó-Jiménez, J. C. *et al.* Growth-dependent recombinant product formation kinetics can be reproduced through engineering of glucose transport and is prone to phenotypic heterogeneity. *Micro Cell Fact.* **18**, 26 (2019).
46. Sassi, H. *et al.* Segregostat: A novel concept to control phenotypic diversification dynamics on the example of Gram-negative bacteria. *Microb. Biotechnol.* **42**, 145 (2019).
47. DeLisa, M. P., Li, J., Rao, G., Weigand, W. A. & Bentley, W. E. Monitoring GFP-operon fusion protein expression during high cell density cultivation of *Escherichia coli* using an on-line optical sensor. *Biotechnol. Bioeng.* **65**, 54–64 (1999).
48. Kopp, J. *et al.* Development of a generic reversed-phase liquid chromatography method for protein quantification using analytical quality-by-design principles. *J. Pharmaceut. Biomed.* **188**, 113412 (2020).

### Acknowledgements

The authors acknowledge the TU Wien Bibliothek for financial support through its Open Access Funding Program. Furthermore the authors want to thank the Austrian Research Promotion Agency (FFG) for their funding facilitating this study (874206).

www.nature.com/scientificreports/

### Author contributions

S.K., C.S. and J.K. planned the experimental design and carried out the data treatment. S.K., A.P., R.L., M.B. and S.A. performed the cultivations and analytics. C.S., C.H. and O.S. gave major scientific input. J.K. founded the idea of this study. S.K., O.S. and J.K. wrote the manuscript. O.S. critically reviewed the manuscript. All authors contributed to the article and approved the submitted version.

### Competing interests

The authors declare no competing interests.

### Additional information

**Supplementary Information** The online version contains supplementary material available at <https://doi.org/10.1038/s41598-021-90899-9>.

**Correspondence** and requests for materials should be addressed to J.K.

**Reprints and permissions information** is available at [www.nature.com/reprints](http://www.nature.com/reprints).

**Publisher's note** Springer Nature remains neutral with regard to jurisdictional claims in published maps and institutional affiliations.



**Open Access** This article is licensed under a Creative Commons Attribution 4.0 International License, which permits use, sharing, adaptation, distribution and reproduction in any medium or format, as long as you give appropriate credit to the original author(s) and the source, provide a link to the Creative Commons licence, and indicate if changes were made. The images or other third party material in this article are included in the article's Creative Commons licence, unless indicated otherwise in a credit line to the material. If material is not included in the article's Creative Commons licence and your intended use is not permitted by statutory regulation or exceeds the permitted use, you will need to obtain permission directly from the copyright holder. To view a copy of this licence, visit <http://creativecommons.org/licenses/by/4.0/>.

© The Author(s) 2021

## 7. Appendix

### 7.1. Protein L – More Than Just an Affinity Ligand



Review

#### Protein L—More Than Just an Affinity Ligand

Stefan Kittler <sup>1,2</sup>, Mihail Besleaga <sup>1</sup>, Julian Ebner <sup>1,2</sup> and Oliver Spadiut <sup>1,\*</sup>

<sup>1</sup> Research Division Integrated Bioprocess Development, Institute of Chemical, Environmental and Bioscience Engineering, TU Wien, Gumpendorfer Strasse 1a, 1060 Vienna, Austria; stefan.kittler@tuwien.ac.at (S.K.); mihail.besleaga@tuwien.ac.at (M.B.); julian.ebner@tuwien.ac.at (J.E.)

<sup>2</sup> Alfred Gruber GmbH, Nordstrasse 6, 5301 Eugendorf, Austria

\* Correspondence: oliver.spadiut@tuwien.ac.at; Tel.: +43-1-58801-166473

**Abstract:** In the past 30 years, highly specific drugs, known as antibodies, have conquered the biopharmaceutical market. In addition to monoclonal antibodies (mAbs), antibody fragments are successfully applied. However, recombinant production faces challenges. Process analytical tools for monitoring and controlling production processes are scarce and time-intensive. In the downstream process (DSP), affinity ligands are established as the primary and most important step, while the application of other methods is challenging. The use of these affinity ligands as monitoring tools would enable a platform technology to monitor process steps in the USP and DSP. In this review, we highlight the current applications of affinity ligands (proteins A, G, and L) and discuss further applications as process analytical tools.

**Keywords:** monoclonal antibodies; antibody fragments; affinity ligands; process analytical technology; protein A; protein G; protein L



**Citation:** Kittler, S.; Besleaga, M.; Ebner, J.; Spadiut, O. Protein L—More Than Just an Affinity Ligand. *Processes* **2021**, *9*, 874. <https://doi.org/10.3390/pr9050874>

**Academic Editors:**  
Francesca Raganati and  
Alessandra Procentese

Received: 26 April 2021  
Accepted: 14 May 2021  
Published: 17 May 2021

**Publisher's Note:** MDPI stays neutral with regard to jurisdictional claims in published maps and institutional affiliations.



**Copyright:** © 2021 by the authors. Licensee MDPI, Basel, Switzerland. This article is an open access article distributed under the terms and conditions of the Creative Commons Attribution (CC BY) license (<https://creativecommons.org/licenses/by/4.0/>).

#### 1. Introduction

In 1986, a new type of drug was approved and introduced to the biopharmaceutical market—the first monoclonal antibody (mAb) with the trade name Orthoclone (OKT3), preventing rejection after kidney transplantation [1]. Ever since, the number of mAbs on the biopharmaceutical market has increased rapidly. Antibodies (Abs) are part of the adaptive immune response and formed by B cells as a response to a specific antigen [2]. They can be divided into five classes (IgG, IgA, IgM, IgD, and IgE), differing in their type and number of heavy chains [3–5], specifying their properties and functions. The majority of antibodies consist of at least two identical light and heavy chains, with each chain being subdivided into a constant and variable region (Figure 1) [5,6]. Antibodies bind via non-covalent interaction to antigens and provide a targeted and specific interaction [7,8]. The hypervariable region at the top of the Y structure, called the complementarity-determining region (CDR), is responsible for antigen-specific binding and consists of a light and a heavy chain [4–6]. Details about the function of each antibody class and reaction have been extensively discussed previously [2–6,9–17].

A wide range of applications for mAbs in therapeutics, biology, biochemistry, and bioanalytics, ranging from drugs against cancer and autoimmune diseases to labeling and detection of virulence factors, has been reported [18–20]. They are the largest product class on the biopharmaceutical market today, with a continuous increase in the number of approved products and over 75 currently available mAbs [17,21]. They have an annual market value of around 150 billion dollars, which is approximately 10% of the entire pharmaceutical turnover [21]. Monoclonal antibody production was initially developed by Kohler and Milstein by fusing an antibody-producing B cell and a myeloma cell, leading to the expression of large amounts of identical molecules, so-called monoclonal antibodies [22]. In recent years, mammalian cells lines have emerged as the standard expression host due to their ability to perform posttranslational modifications (PTMs) and extracellular

protein production [23,24]. In contrast, microorganisms, such as bacteria and yeast, are not capable of performing human-like glycosylation. However, recent approaches in strain engineering enable human-like glycosylation in microbial hosts [23,25,26]. In contrast to mAbs, microbes are perfectly suited to produce antibody fragments, which do not require glycosylation. Smaller antibody fragments can bind target molecules within the CDR region, which is located in the Fab (fragment antigen binding) region [6,13,17]. However, due to the missing Fc part, these fragments have different pharmacokinetic properties [17,27]. Fragments are no bigger than one-third of a full-length IgG (Fab ~55 kDa), and, as a result, tissues and tumors are penetrated faster, opening a broader field of applications regarding imaging and labeling [28–31]. On the downside, they show decreased half-life times in the human body [28]. However, this faster clearance can be used as an advantage for the transportation of toxic radioisotopes [28]. Fragments can be subdivided on the basis of the light and heavy chain, namely, Fab (Figure 2a), scFv (Figure 2b), sdAb (Figure 2c), and diabody (Figure 2d), to list the most important ones [32].

The economic success on the biopharmaceutical market is driven by the advances in the production processes. Mammalian cells are used for the production of mAbs, reaching titers above 5 g/L. Non-glycosylated or non-human-like glycosylated mAbs and antibody fragments are produced mainly in *Saccharomyces cerevisiae*, *Pichia pastoris*, and *Escherichia coli* [23,24]. All production processes require reliable and sensitive process analytical technological tools. The use of real-time monitoring would be beneficial to increase process efficiency and fulfill high-quality requirements [33,34]. Furthermore, recent advances in the productivity have shifted the focus in process development from upstream (USP) toward downstream processing (DSP) [24]. Efficient purification methods are necessary to reach high purity levels, ensuring drug safety. For both applications, affinity ligands can be used. Protein A is currently the state of the art for the purification of mAbs [35]. However, protein A is not applicable for the purification of fragments lacking the Fc region [35]. In contrast, protein L from *Peptostreptococcus magnus* binds kappa light chains and is, therefore, a promising tool for binding a multitude of mAbs, as well as antibody fragments. In this review, we focus on three different affinity ligands (proteins A, G, and L) and highlight their application ranges. We believe that these proteins can not only be used for common downstream applications, but also be employed as highly sensitive and accurate process analytical tools.

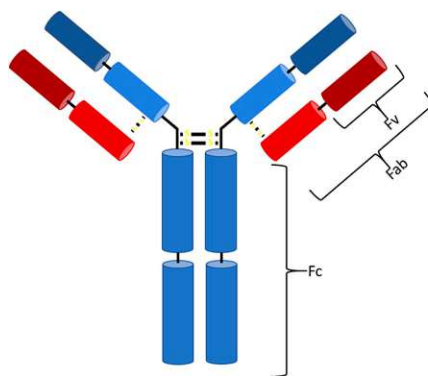


**Figure 1.** Structure of an IgG antibody. The Fc binding region consists of four heavy chains ( $2 \times C_{H3}$ ,  $2 \times C_{H2}$ ), and the Fab region consists of one constant heavy and one constant light chain, while, at the top, two variable chains of each type are located (Fv region).



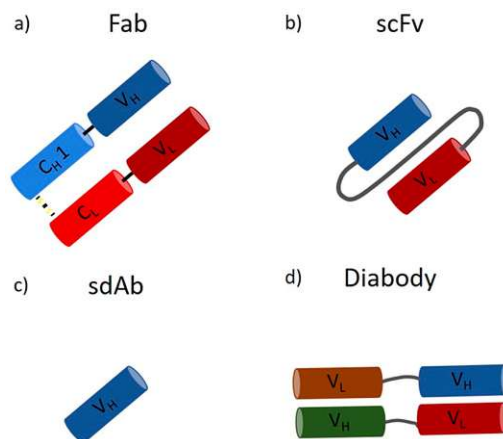


**Figure 2.** Antibody fragments: (a) the antigen-binding fragment (Fab) contains a variable and a constant domain of a light and heavy chain (size ~55 kDa); (b) the single-chain variable fragment (scFv) consists only of the variable domains, which form the antigen-binding part, linked together by a polypeptidlinker (size ~28 kDa); (c) the single-domain antibody (sdAb) consists of only one variable heavy chain (size ~15 kDa); (d) the diabody consists of two heavy and two light chains forming a bispecific fragment capable of binding two different antigens (size ~50 kDa).

## 2. Downstream Processing of mAbs and Fabs

Due to the high market competition and the need to decrease the time to market, it is crucial to determine optimal process conditions leading to high product yields while maintaining the highest quality [13,36]. In Figure 3, an overview of a typical recombinant bioprocess to produce antibody fragments in *E. coli* is given [24]. In addition to high product yields, strict critical quality attributes (CQAs) have to be reached, which are defined as “a physical, chemical, biological, or microbiological property or characteristic of the product that should be within an appropriate limit, range, or distribution to ensure the desired product quality” [37].

As shown in Figure 3, the intracellular protein production in microbial hosts requires several unit operations during the early DSP (harvest to filtration) [23,38]. In the subsequent capture step, large volumes with a low product concentration have to be processed. Furthermore, due to the presence of proteases, short process times are a necessity for this step. Even though a high purity after the capture step is not required, it can be provided using affinity chromatography during the capture step for mAbs and antibody fragments. Therefore, this technique is currently established as the gold standard, achieving not only high recoveries but also high purities. Nevertheless, several chromatography steps are required after the capture step in order to remove host cell proteins (HCPs), DNA, and product-related impurities to reach desired CQAs [39]. A further important reason for subsequent chromatographic steps is the leaching of affinity ligands due to harsh elution conditions [40,41]. The different chromatographic methods for capture and purification/polishing are listed in Table 1, with a focus on the methods used for mAbs and antibody fragments.

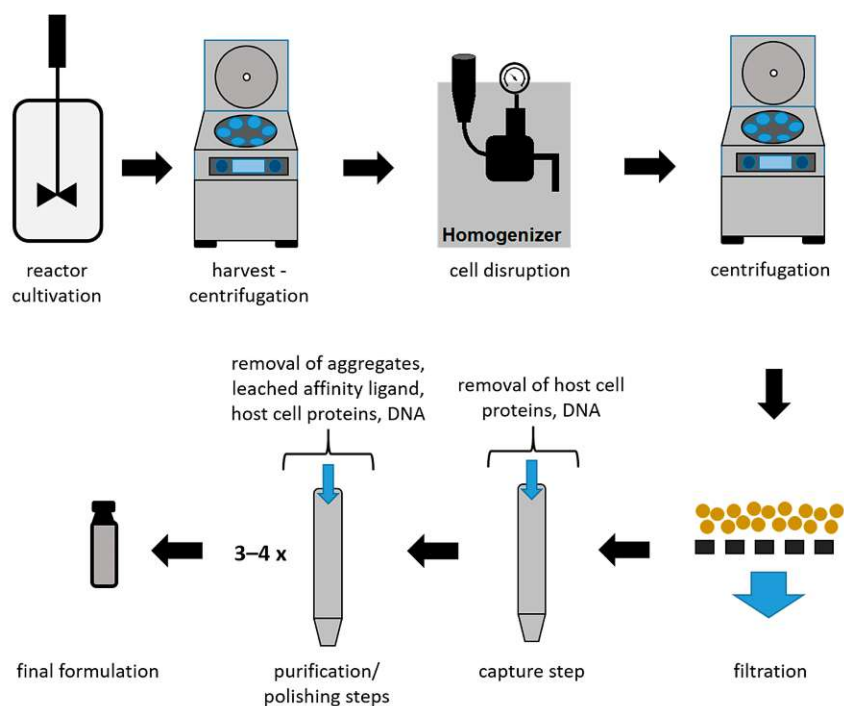


Figure 3. Schematic overview of a bioprocess using *E. coli* to produce antibody fragments.

Table 1. Comparison of chromatographic methods used for the purification of monoclonal antibodies (mAbs) and antibody fragments. AC (affinity chromatography); AEX (anion exchange chromatography); CEX (cation exchange chromatography); HIC (hydrophobic interaction chromatography); SEC (size-exclusion chromatography); DSP (downstream processing).

Method	Advantages	Disadvantages	DSP Step	References
AC	<ul style="list-style-type: none"> <li>- most applied method for purification of mAbs and antibody fragments</li> <li>- high yields and purity are reached in one step (&gt;90%)</li> </ul>	<ul style="list-style-type: none"> <li>- expensive</li> <li>- leaching of the ligand</li> <li>- requires low pH elution buffers which can denature mAbs</li> <li>- no alkaline stability</li> </ul>	capture	[42–45]
CEX	<ul style="list-style-type: none"> <li>- primary capture step for mAb fragments which lack Fc parts</li> <li>- separation of charge</li> <li>- removal of leached protein A</li> <li>- removal of aggregates, host DNA, and cell proteins</li> </ul>	<ul style="list-style-type: none"> <li>- many parameters to consider: mobile phase (pH, salt, composition); stationary phase (matrix type); operating variables (flow, elution gradient, etc.)</li> <li>- optimization is labor- and time-intensive</li> </ul>	capture (Fc lacking mAbs) purification polishing	[17,27,44,46,47]

Table 1. Cont.

Method	Advantages	Disadvantages	DSP Step	References
AEX	<ul style="list-style-type: none"> <li>- separation of biomolecules which have minor differences in their net charge</li> <li>- higher binding capacity than affinity columns</li> <li>- cheaper than affinity columns</li> <li>- removal of host cell DNA and proteins</li> </ul>	<ul style="list-style-type: none"> <li>- many parameters to consider: mobile phase (pH, salt, composition); stationary phase (matrix type); operating variables (flow, elution gradient, etc.)</li> <li>- optimization is labor- and time-intensive</li> </ul>	purification polishing	[13,44,46–48]
HIC	<ul style="list-style-type: none"> <li>- aggregate removal, good removal of process-related impurities</li> </ul>	<ul style="list-style-type: none"> <li>- binding capacity is limited (compared to IEX)</li> <li>- use of high salt concentrations, which affects mAbs</li> </ul>	polishing	[49,50]
SEC	<ul style="list-style-type: none"> <li>- good for isolation of immunoglobulins based on their classes</li> <li>- useful for small scale in case of product and process development</li> <li>- requires minimal process development</li> <li>- separation of aggregates</li> </ul>	<ul style="list-style-type: none"> <li>- low productivity since it is not adsorption-based and only a small amount of sample can be loaded</li> <li>- low selectivity</li> </ul>	polishing	[51]

To ensure an efficient capturing in the DSP, affinity resins have been established and are mainly used [13,52]. The capability to selectively capture target peptides, while host cell proteins and other molecules bind very weakly or not at all, outperforms other methods [53,54]. Although affinity chromatography is widely used as an initial step, it is expensive and requires harsh elution conditions (pH~3), leading to decreased column stability, ligand leaching, and possible activity loss of the target product [52,55,56]. However, the acidic conditions are an advantage for the required viral inactivation in mammalian production processes [41]. Other chromatographic methods, such as ion exchange (IEX), are mainly used as additional purification steps to remove leached affinity ligands, HCPs, and DNA [41]. These purification and polishing steps can include up to three or four different chromatographic steps to achieve the required product quality (Figure 3) [24].

Nevertheless, affinity resins have emerged as the gold standard for the first step of purification (capture step) of mAbs and antibody fragments; therefore, we explain the most important ligands below.

### 2.1. Protein A

Protein A originates from the human pathogen *Staphylococcus aureus* and has a molecular weight of 42 kDa [57–60]. The protein is anchored to the cell wall and protects the organism by binding IgGs produced by the immune system [59,61]. It contains five homologous binding domains A–E (Figure 4) [40,59,62], and each has the ability to bind IgG subclasses. The S region serves as a signal sequence, and the XM region is used as a cell anchor [56]. The binding domains are composed of three antiparallel alpha helices, and the interaction with the mAbs is primarily based on hydrophobic interaction [55]. In addition to the possibility of binding the Fc region, protein A has shown the ability to bind specific Fab domains [55,59].

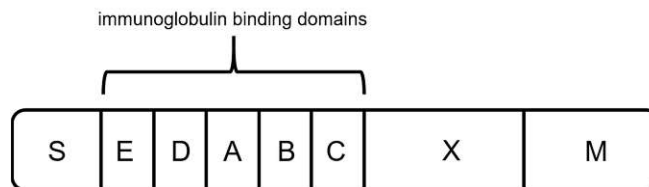


**Figure 4.** Schematic sketch of protein A, composed of a signal sequence (S) domain, five homologous immunoglobulin binding domains (E, D, A, B, and C), and a cell-wall anchoring domain (X, M) [56].

Each of the immunoglobulin-binding domains can bind to one Fc domain of an antibody or to the Fab region of  $V_{H3}$  human antibodies [55,57,62,63]. Staphylococcal protein A (SPA) binds strongly to Fc domains of IgG1, IgG2, and IgG4 and has a weaker ability to bind IgG3 [55,56,60]. Protein A is used for labeling and purification of mAbs [62], as well as indirect coating for enzyme-linked immunosorbent assays (ELISA) and other immunobinding assays. In nature, protein A makes only 1.7% of the total protein content of *Staphylococcus aureus* [64]. Since the approval of the first immunosorbent adsorption column by the FDA in 1998 for the therapy of autoimmune diseases, recombinant expression hosts, such as *E. coli* or *Pichia pastoris*, have been used for production [64]. Protein A affinity resins have emerged as the primary purification step (capturing) in mAb production processes [40,55]. The DSP of, e.g., Herceptin<sup>TM</sup>, Rituxan<sup>TM</sup>, MabCampath<sup>TM</sup>, Remicade<sup>TM</sup>, and Simulect<sup>TM</sup> includes a capture step using protein A affinity chromatography, already resulting in a purity of around 90% after this first chromatographic capture step [13].

## 2.2. Protein G

Protein G originates from the group *G streptococci* and has a molecular mass of around 65 kDa [65]. It is the second most used capture ligand in the DSP of mAbs and antibody fragments [55]. Protein G consists of a signal peptide, a cell-wall anchoring domain, and two different binding regions: one located at the N terminus, binding serum albumin, and the second one at the C terminus, interacting with immunoglobulins (Figure 5) [55,65]. For the purification of mAbs, recombinant Protein G is expressed lacking the serum albumin-binding region since albumin would be a contaminant in the formulation of mAbs as biopharmaceuticals [55,66].

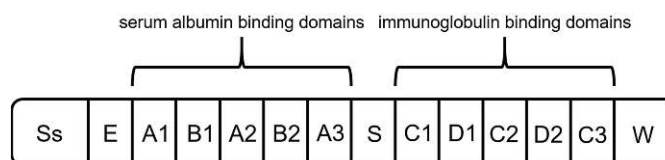


**Figure 5.** Schematic structure of protein G. It is composed of a signal peptide (Ss), an alanine-rich region (E), an albumin-binding site, an immunoglobulin-binding site, and a cell-wall anchoring region (W) [65].

Protein G interacts with the Fc region of immunoglobulins and binds via hydrogen bonds and salt bridges [55,66,67]. Additionally, protein G shows the capability of binding Fabs through the  $C_{H1}$  domain of  $Ig_{G1,3,4}$ . Nevertheless, due to the low affinity, purification of fragments is not applicable [55,60,68,69]. Therefore, protein G is mainly used for processes where protein A proves to be unsuitable, e.g., the purification of  $IgG_3$ . Due to a decreased stability and harsher elution conditions compared to protein A, the number of processes using protein G is considerably lower [55,56,70].

### 2.3. Protein L

As another alternative to previously mentioned capture ligands, protein L can be used for the binding of mAbs and fragments. Protein L was first isolated in 1985 by Myhre and Ertell as a surface protein of *Peptostreptococcus magnus*, showing binding activity against IgGs [71–73]. The native protein has a size between 76 to 106 kDa, depending on the number of B domains [27,74]. It consists of a signal sequence domain (SS), up to five binding domains (B1–B5), a short spacer region (S), two C repeats with an unknown function, and the wall anchor domain (W) with the transmembrane region (M) (Figure 6) [71]. It was shown that the fifth B domain slightly increases the affinity constant for interaction with kappa light chains ( $1.5 \times 10^9 \text{ M}^{-1}$  to  $2\text{--}3 \times 10^9 \text{ M}^{-1}$ ) [71,75]. Therefore, different versions of recombinant produced protein L consisting of either four or five binding domains are available.

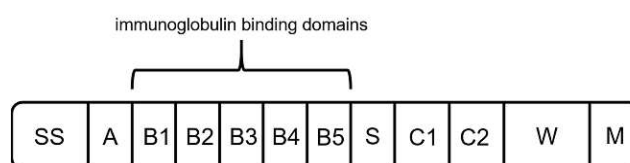


**Figure 6.** Schematic structure of protein L. It is composed of a hydrophobic signal sequence (SS), the  $\text{NH}_2$  terminal domain (A), repeated immunoglobulin-binding domains (B1–B5), a spacer region (S), C1 and C2 with unknown function, and the cell-wall anchoring domain [71].

All five binding domains (B1–B5) have a similar structure of an alpha helix and a beta sheet formed by four beta strands [55,76]. Unlike proteins A and G, protein L interacts with the  $V_L$  domain of kappa light chains [55,71]. It binds to kappa subtypes 1, 3, and 4, enabling the interaction with various types of antibody fragments [77,78]. Furthermore, compared to previously mentioned affinity ligands A and G, protein L binds to a wider range of Ig classes [27,73].

### 2.4. Comparison of Proteins A, G, and L

Protein A is the most common affinity ligand in the DSP of mAbs and has been investigated in numerous studies in the past years [27]. Protein G is only used in cases where protein A cannot be used, while protein L has only been established for the purification of fragments so far. A low price compared to the other affinity ligands and the suitability for common antibody types make protein A applicable for most capture steps in production processes of mAbs. As depicted in Figure 7, there is a huge price difference between proteins A, G, and L. This is caused by a decreased number of current applications for proteins G and L. Protein L is by far the most expensive ligand. To our knowledge there has been no publication about the large-scale production of protein L to date. Tocaj et al. produced recombinant protein L with four B domains using *E. coli* on a small scale, obtaining a concentration of 360 mg/L [79]. Nevertheless, recombinant versions produced in *E. coli* can be purchased from different vendors (Figure 7). The commercial proteins differ in the number of B domains, either four or five, and combinations with affinity tags are available.

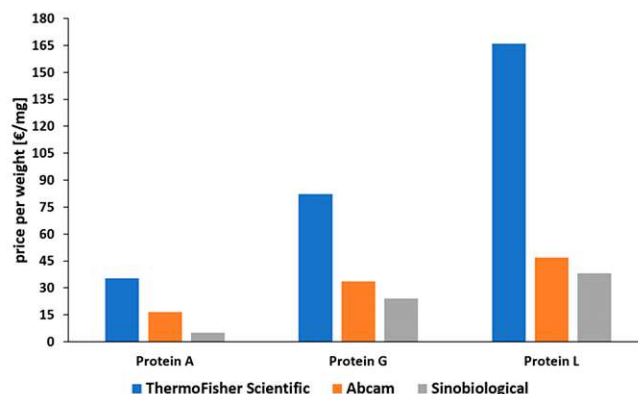


**Figure 7.** Comparison of prices for recombinantly produced proteins A, G, and L, normalized to EUR per mg [80–82]. Status: May 2021.

However, antibody fragments do not have an Fc domain, reducing the applicability of protein A [83,84]. Due to the rising applications and research regarding therapeutic antibody fragments, a modular capture step applicable for both mAbs and fragments is desirable—something that can be provided by protein L [27]. There is no doubt that protein L, due to its unique interaction with kappa light chains, has a huge market potential in the future. Additionally, it shows a high binding capability for human-derived antibodies and fragments [85]. Further interest in antibody fragments is also caused by the possibility to express these target molecules in microbials, such as *E. coli* [23]. Production costs are significantly lower, higher cell densities can be reached, and virus inactivation is not necessary [86]. However, applications of protein L are still scarce, and its development and improvement are behind that of other affinity ligands. Furthermore, regulatory challenges addressed for protein A are also applicable for protein L. Ligand leaching and limited lifetime would, thus, also be factors to consider.

However, we believe that, in addition to applications as an affinity ligand for product purification, protein L will also have an important role in analytical applications.

### 3. Is Protein L the Future?

Recombinant proteins in *E. coli* are usually located intracellularly [39,87]. However, during cultivation, *E. coli* cells often get leaky, causing an uncontrolled release and, thus, loss of highly valuable product—such as antibody fragments—into the fermentation broth [39]. Today, there is no online detection method for cell leakiness available. Results are obtained too late, and the product is lost in the fermentation broth. Another important analytical aspect in the recombinant production of antibody fragments in *E. coli* concerns the DSP. Harvested *E. coli* cells are disrupted, and the product is released together with proteases and other host-specific proteins, which are then removed by several chromatographic steps [39,87]. Furthermore, during the DSP process train, antibody fragments are usually analyzed offline, leading to great time delay. However, online monitoring and control using process analytical technology (PAT) are requested by Quality-by-design (QbD) principles [34,88]. This is particularly challenging for the production of antibody fragments in *E. coli*, which need to be analyzed in a complex sample background, limiting the applicability of robust and sensitive analytical methods [89]. Currently, recombinant fragments are quantified and analyzed by time-consuming and expensive offline methods, such as immunoassays (ELISA), high-performance liquid chromatography (HPLC), mass spectrometry (MS), or Western blot [89]. Even though LC–MS-based techniques are constantly being improved, automatization of these techniques is difficult, and they lack high

reproducibility [33,89]. More detailed information on currently available PAT tools can be found in a recent review by Wasalathanthri et al. [33].

The implementation of lateral flow, surface plasmon resonance (SPR), impedance, or electrochemical-based techniques as at-line or online tools in the USP and DSP of mAbs or antibody fragments would be highly beneficial. These methods are already used for the detection of virus particles and antibodies [90–92]. The use of affinity ligands, such as protein L, as biorecognition elements would provide a platform technology in this respect (Figure 8). The analyte (e.g., mAb, Fab) binds to the immobilized affinity ligand, causing a change in the readout signal (visual, refractive index, impedance, or resistance). Commercial sensors with immobilized protein L are already available to determine binding kinetics of mAbs/antibody fragments. These chips are used for a label-free analysis using SPR or biolayer interferometry (BLI) to determine kinetics and to quantify mAbs or antibody fragments containing kappa light chains [93,94].

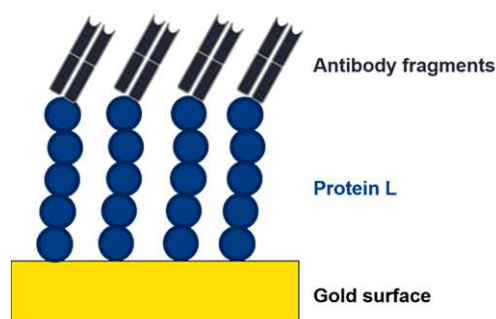


**Figure 8.** Depiction of an electrochemical impedance spectroscopy (EIS) sensor. An affinity ligand (e.g., protein L) is immobilized to a gold surface. Due to the interaction with an analyte, the charge transfer resistance changes, and the analyte can be detected and quantified.

Protein L is a highly important affinity ligand in these applications due to its interaction with kappa light chains. Antibody fragments and mAbs can be detected with high specificity, which enables universal application in different production processes. Furthermore, protein L shows the highest affinity constants to IgGs derived from human, which is the most important class of mAbs and antibody fragments.

#### 4. Further Applications of Protein L in Biomanufacturing

In addition to the possible application of protein L as a biorecognition element, it can further improve the DSP of *E. coli*. As extensive clarification of the lysate is required, membranes with immobilized protein L are an alternative to the traditional resin-based chromatography approach. Functionalized membrane adsorbers can be used, providing high flow rates and the great combination of filtration and chromatography [95,96]. With significantly higher flow rates, which are impracticable for packed bed columns due to high backpressure and the need for longer residence times, the space–time yield can be significantly increased [96]. The disadvantages of lower dynamic binding capacities caused by a decreased surface-to-volume ratio is of less concern during the capture step, where high volumes with relatively low product concentrations have to be processed. Here, membrane adsorbers with protein L would show highly interesting properties, especially for *E. coli* as an expression host [96].

A further application of protein L in the DSP is the separation of homodimers from heterodimeric bispecific antibodies (bsAbs). Due to a high similarity of the physiological properties, the separation is quite difficult. However, Chen et al. successfully used protein L-based affinity columns to differentiate between homodimers and target bsAbs [97].

## 5. Final Remarks

So far, protein A has mainly been used for the purification and as recognition element for antibodies. However, with a shift of the market situation toward antibody fragments and the use of microbials to produce them, protein A will definitely lose its blockbuster status. Antibody fragments have huge potential in the future of drug development, enabling fast tissue penetration due to a smaller size. The number of approved antibody fragments has increased from three to eight approved drugs in the past 7 years. In cancer treatment, the mentioned properties of antibody fragments are considered to be advantageous; however, so far, the number of approved drugs still lags behind mAbs [6,21].

Protein L would be a universal biorecognition element and ligand for both product purification and process analytical technology. Thus, we believe that this molecule will have a bright future in both research and industry.

**Author Contributions:** S.K., M.B., J.E., and O.S. drafted the manuscript; S.K., M.B., and J.E. performed the literature research; O.S. gave scientific input and finalized the manuscript. All authors have read and agreed to the published version of the manuscript.

**Funding:** This research was funded by the Austrian Research Promotion Agency (FFG), project number 874206. The authors acknowledge TU Wien Bibliothek for financial support through its Open Access Funding by TU Wien.

**Institutional Review Board Statement:** Not applicable.

**Informed Consent Statement:** Not applicable.

**Data Availability Statement:** Not applicable.

**Acknowledgments:** Alfred Gruber GmbH is gratefully thanked for supporting the research and being a project partner.

**Conflicts of Interest:** The authors declare no conflict of interest.

## References

1. Ecker, D.M.; Jones, S.D.; Levine, H.L. The therapeutic monoclonal antibody market. *mAbs* **2015**, *7*, 9–14. [[CrossRef](#)] [[PubMed](#)]
2. Grattendick, K.; Pross, S. Immunoglobulins. In *xPharm: The Comprehensive Pharmacology Reference*; Elsevier: Amsterdam, The Netherlands, 2007; pp. 1–6. [[CrossRef](#)]
3. Conroy, P.J.; Hearty, S.; Leonard, P.; O’Kennedy, R.J. Antibody production, design and use for biosensor-based applications. *Semin. Cell Dev. Biol.* **2009**, *20*, 10–26. [[CrossRef](#)] [[PubMed](#)]
4. Burrell, C.J.; Howard, C.R.; Murphy, F.A. Adaptive Immune Responses to Infection. In *Fenner and White’s Medical Virology*; Elsevier: Amsterdam, The Netherlands, 2017; pp. 65–76. [[CrossRef](#)]
5. Hnasko, R.M. The Biochemical Properties of Antibodies and Their Fragments. In *Methods in Molecular Biology*; Metzler, J.B., Ed.; Humana Press: New York, NY, USA, 2015; Volume 1318, pp. 1–14. [[CrossRef](#)]
6. Nelson, A.L. Antibody fragments. In *mAbs*; Taylor & Francis: Oxfordshire, UK, 2010; Volume 2, pp. 77–83. [[CrossRef](#)]
7. Esela-Culang, I.; Ekunik, V.; Eofran, Y. The Structural Basis of Antibody-Antigen Recognition. *Front. Immunol.* **2013**, *4*, 302. [[CrossRef](#)]
8. Wang, H.; Shen, G.; Yu, R. Aspects of recent development of immunosensors. *Electrochem. Biosens.* **2008**, 237–260. [[CrossRef](#)]
9. Schroeder, H.W.; Cavacini, L. Structure and function of immunoglobulins. *J. Allergy Clin. Immunol.* **2010**, *125*, S41–S52. [[CrossRef](#)]
10. Gould, H.J.; Beavil, R.L. IgE. In *Encyclopedia of Immunology*; Elsevier: Amsterdam, The Netherlands, 1998; pp. 1202–1208. [[CrossRef](#)]
11. Edholm, E.-S.; Bengten, E.; Wilson, M. Insights into the function of IgD. *Dev. Comp. Immunol.* **2011**, *35*, 1309–1316. [[CrossRef](#)]
12. Woof, J.M.; Kerr, M.A. The function of immunoglobulin A in immunity. *J. Pathol.* **2005**, *208*, 270–282. [[CrossRef](#)]
13. Sommerfeld, S.; Strube, J. Challenges in biotechnology production—generic processes and process optimization for monoclonal antibodies. *Chem. Eng. Process. Intensif.* **2005**, *44*, 1123–1137. [[CrossRef](#)]
14. Vidarsson, G.; Dekkers, G.; Rispens, T. IgG Subclasses and Allotypes: From Structure to Effector Functions. *Front. Immunol.* **2014**, *5*, 520. [[CrossRef](#)]
15. Painter, R.H. IgG. In *Encyclopedia of Immunology*; Elsevier: Amsterdam, The Netherlands, 1998; pp. 1208–1211. [[CrossRef](#)]
16. Rispens, T.; Vidarsson, G. Human IgG Subclasses. In *Antibody Fc*; Elsevier: Amsterdam, The Netherlands, 2014; pp. 159–177. [[CrossRef](#)]
17. Bates, A.; Power, C.A. David vs. Goliath: The Structure, Function, and Clinical Prospects of Antibody Fragments. *Antibodies* **2019**, *8*, 28. [[CrossRef](#)]



18. Grodzki, A.C.; Berenstein, E. Introduction to the Purification of Antibodies. In *Immunocytochemical Methods and Protocols; Methods in Molecular Biology (Methods and Protocols)*; Humana Press: Totowa, NJ, USA, 2010; Volume 588, pp. 11–13. [CrossRef]
19. Andrew, S.M.; Titus, J.A. Purification of Immunoglobulin G. In *Current Protocols in Immunology*; Wiley: Hoboken, NJ, USA, 2001.
20. Miller, L.G.; Goldstein, G.; Murphy, M.; Ginns, L.C. Reversible Alterations in Immunoregulatory T Cells in Smoking. *Chest* **1982**, *82*, 526–529. [CrossRef]
21. Lu, R.-M.; Hwang, Y.-C.; Liu, I.-J.; Lee, C.-C.; Tsai, H.-Z.; Li, H.-J.; Wu, H.-C. Development of therapeutic antibodies for the treatment of diseases. *J. Biomed. Sci.* **2020**, *27*, 1–30. [CrossRef]
22. Tomita, M.; Tsumoto, K. Hybridoma technologies for antibody production. *Immunotherapy* **2011**, *3*, 371–380. [CrossRef]
23. Spadiut, O.; Capone, S.; Krainer, F.; Glieder, A.; Herwig, C. Microbials for the production of monoclonal antibodies and antibody fragments. *Trends Biotechnol.* **2014**, *32*, 54–60. [CrossRef]
24. Shukla, A.A.; Thömmes, J. Recent advances in large-scale production of monoclonal antibodies and related proteins. *Trends Biotechnol.* **2010**, *28*, 253–261. [CrossRef]
25. Gerngross, T.U. Advances in the production of human therapeutic proteins in yeasts and filamentous fungi. *Nat. Biotechnol.* **2004**, *22*, 1409–1414. [CrossRef]
26. Gerngross, T. Production of Complex Human Glycoproteins in Yeast. *Adv. Exp. Med. Biol.* **2005**, *564*, 139. [CrossRef]
27. Rodrigo, G.; Gruvegård, M.; Van Alstine, J.M. Antibody Fragments and Their Purification by Protein L Affinity Chromatography. *Antibodies* **2015**, *4*, 259–277. [CrossRef]
28. Nelson, A.L.; Reichert, J.M. Development trends for therapeutic antibody fragments. *Nat. Biotechnol.* **2009**, *27*, 331–337. [CrossRef]
29. Xenaki, K.T.; Oliveira, S.; Henegouwen, P.M.P.V.B.E. Antibody or Antibody Fragments: Implications for Molecular Imaging and Targeted Therapy of Solid Tumors. *Front. Immunol.* **2017**, *8*, 1287. [CrossRef]
30. Ahamadi-Fesharaki, R.; Fateh, A.; Vaziri, F.; Solgi, G.; Siadat, S.D.; Mahboudi, F.; Rahimi-Jamrani, F. Single-Chain Variable Fragment-Based Bispecific Antibodies: Hitting Two Targets with One Sophisticated Arrow. *Mol. Ther. Oncolytics* **2019**, *14*, 38–56. [CrossRef]
31. Rader, C. Overview on Concepts and Applications of Fab Antibody Fragments. *Curr. Protoc. Protein Sci.* **2009**, *55*, 6.9.1–6.9.14. [CrossRef]
32. Holliger, P.; Hudson, P.J. Engineered antibody fragments and the rise of single domains. *Nat. Biotechnol.* **2005**, *23*, 1126–1136. [CrossRef]
33. Wasalathanthri, D.P.; Rehmann, M.S.; Song, Y.; Gu, Y.; Mi, L.; Shao, C.; Chemmalil, L.; Lee, J.; Ghose, S.; Borys, M.C.; et al. Technology outlook for real-time quality attribute and process parameter monitoring in biopharmaceutical development—A review. *Biotechnol. Bioeng.* **2020**, *117*, 3182–3198. [CrossRef]
34. Guerra, A.; Von Stosch, M.; Glassey, J. Toward biotherapeutic product real-time quality monitoring. *Crit. Rev. Biotechnol.* **2019**, *39*, 289–305. [CrossRef]
35. Arakawa, T.; Tsumoto, K.; Ejima, D. Alternative downstream processes for production of antibodies and antibody fragments. *Biochim. Biophys. Acta Proteins Proteom.* **2014**, *1844*, 2032–2040. [CrossRef]
36. Prasnkar, J.; Škerlj, T. New product development process and time-to-market in the generic pharmaceutical industry. *Ind. Mark. Manag.* **2006**, *35*, 690–702. [CrossRef]
37. ICH Guideline Q8 (R2) on Pharmaceutical Development. Available online: [https://www.ema.europa.eu/en/documents/scientific-guideline/international-conference-harmonisation-technical-requirements-registration-pharmaceuticals-human-use\\_en-11.pdf](https://www.ema.europa.eu/en/documents/scientific-guideline/international-conference-harmonisation-technical-requirements-registration-pharmaceuticals-human-use_en-11.pdf) (accessed on 13 June 2020).
38. Katsuda, T.; Sonoda, H.; Kumada, Y.; Yamaji, H. Production of Antibody Fragments in Escherichia coli. In *Antibody Engineering. Methods in Molecular Biology (Methods and Protocols)*; Humana Press: Totowa, NJ, USA, 2012; Volume 907, pp. 305–324. [CrossRef]
39. Wurm, D.J.; Slouka, C.; Bosilj, T.; Herwig, C.; Spadiut, O. How to trigger periplasmic release in recombinant Escherichia coli: A comparative analysis. *Eng. Life Sci.* **2016**, *17*, 215–222. [CrossRef]
40. Ramos-De-La-Peña, A.M.; González-Valdez, J.; Aguilar, O. Protein A chromatography: Challenges and progress in the purification of monoclonal antibodies. *J. Sep. Sci.* **2019**, *42*, 1816–1827. [CrossRef]
41. Shukla, A.A.; Hubbard, B.; Tressel, T.; Guhan, S.; Low, D. Downstream processing of monoclonal antibodies—Application of platform approaches. *J. Chromatogr. B* **2007**, *848*, 28–39. [CrossRef]
42. Mustafaoglu, N.; Kiziltepe, T.; Bilgicer, B. Antibody purification via affinity membrane chromatography method utilizing nucleotide binding site targeting with a small molecule. *Analyst* **2016**, *141*, 6571–6582. [CrossRef] [PubMed]
43. Ayyar, B.V.; Arora, S.; Murphy, C.; O’Kennedy, R. Affinity chromatography as a tool for antibody purification. *Methods* **2012**, *56*, 116–129. [CrossRef] [PubMed]
44. Chahar, D.S.; Ravindran, S.; Pisal, S. Monoclonal antibody purification and its progression to commercial scale. *Biologicals* **2020**, *63*, 1–13. [CrossRef] [PubMed]
45. Ghose, S.; Hubbard, B.; Cramer, S.M. Evaluation and comparison of alternatives to Protein A chromatography: Mimetic and hydrophobic charge induction chromatographic stationary phases. *J. Chromatogr. A* **2006**, *1122*, 144–152. [CrossRef]
46. Fahrner, R.L.; Knudsen, H.L.; Basey, C.D.; Galan, W.; Feuerhelm, D.; Vanderlaan, M.; Blank, G.S. Industrial Purification of Pharmaceutical Antibodies: Development, Operation, and Validation of Chromatography Processes. *Biotechnol. Genet. Eng. Rev.* **2001**, *18*, 301–327. [CrossRef]

47. Ishihara, T.; Yamamoto, S. Optimization of monoclonal antibody purification by ion-exchange chromatography: Application of simple methods with linear gradient elution experimental data. *J. Chromatogr. A* **2005**, *1069*, 99–106. [\[CrossRef\]](#)
48. Grodzki, A.C.; Berenstein, E. Antibody Purification: Ion-Exchange Chromatography. In *Immunocytochemical Methods and Protocols; Methods in Molecular Biology (Methods and Protocols)*; Humana Press: Totowa, NJ, USA, 2009; Volume 588, pp. 27–32. [\[CrossRef\]](#)
49. Ghose, S.; Tao, Y.; Conley, L.; Cecchini, D. Purification of monoclonal antibodies by hydrophobic interaction chromatography under no-salt conditions. *mAbs* **2013**, *5*, 795–800. [\[CrossRef\]](#)
50. Gagnon, P. Technology trends in antibody purification. *J. Chromatogr. A* **2012**, *1221*, 57–70. [\[CrossRef\]](#)
51. Ulmer, N.; Vogt, S.; Müller-Späh, T.; Morbidelli, M. Purification of Human Monoclonal Antibodies and Their Fragments. In *Human Monoclonal Antibodies: Methods and Protocols*; Steinitz, M., Ed.; Springer: New York, NY, USA, 2019; pp. 163–188. [\[CrossRef\]](#)
52. Strube, J.; Grote, F.; Ditz, R. Bioprocess Design and Production Technology for the Future. In *Biopharmaceutical Production Technology*; Wiley: Hoboken, NJ, USA, 2012; pp. 657–705.
53. Hage, D.S. Affinity Chromatography: A Review of Clinical Applications. *Clin. Chem.* **1999**, *45*, 593–615. [\[CrossRef\]](#)
54. Ståhl, S.; Kronqvist, N.; Jonsson, A.; Löfblom, J. Affinity proteins and their generation. *J. Chem. Technol. Biotechnol.* **2012**, *88*, 25–38. [\[CrossRef\]](#)
55. Kruljec, N.; Bratkovič, T. Alternative Affinity Ligands for Immunoglobulins. *Bioconjugate Chem.* **2017**, *28*, 2009–2030. [\[CrossRef\]](#)
56. Hober, S.; Nord, K.; Linhult, M. Protein A chromatography for antibody purification. *J. Chromatogr. B* **2007**, *848*, 40–47. [\[CrossRef\]](#)
57. Falugi, F.; Kim, H.K.; Missiakas, D.M.; Schneewind, O. Role of Protein A in the Evasion of Host Adaptive Immune Responses by *Staphylococcus aureus*. *mBio* **2013**, *4*, e00575-13. [\[CrossRef\]](#)
58. Kobayashi, S.D.; DeLeo, F.R. *Staphylococcus aureus* Protein A Promotes Immune Suppression. *mBio* **2013**, *4*, e00764-13. [\[CrossRef\]](#)
59. Palmqvist, N.; Foster, T.; Tarkowski, A.; Josefsson, E. Protein A is a virulence factor in *Staphylococcus aureus* arthritis and septic death. *Microb. Pathog.* **2002**, *33*, 239–249. [\[CrossRef\]](#)
60. Choe, W.; Durgannavar, T.A.; Chung, S.J. Fc-Binding Ligands of Immunoglobulin G: An Overview of High Affinity Proteins and Peptides. *Materials* **2016**, *9*, 994. [\[CrossRef\]](#)
61. Abouelkhair, M.A.; Bemis, D.A.; Kania, S.A. Characterization of recombinant wild-type and nontoxic protein A from *Staphylococcus pseudintermedius*. *Virulence* **2018**, *9*, 1050–1061. [\[CrossRef\]](#)
62. Graille, M.; Stura, E.A.; Corper, A.L.; Sutton, B.J.; Taussig, M.J.; Charbonnier, J.-B.; Silverman, G.J. Crystal structure of a *Staphylococcus aureus* protein A domain complexed with the Fab fragment of a human IgM antibody: Structural basis for recognition of B-cell receptors and superantigen activity. *Proc. Natl. Acad. Sci. USA* **2000**, *97*, 5399–5404. [\[CrossRef\]](#)
63. Romagnani, S.; Giudizi, M.G.; Del Prete, G.; Maggi, E.; Biagiotti, R.; Almerigogna, F.; Ricci, M. Demonstration on protein A of two distinct immunoglobulin-binding sites and their role in the mitogenic activity of *Staphylococcus aureus* Cowan I on human B cells. *J. Immunol.* **1982**, *129*, 596–602.
64. Hao, J.; Xu, L.; He, H.; Du, X.; Jia, L. High-level expression of *Staphylococcal* Protein A in *Pichia pastoris* and purification and characterization of the recombinant protein. *Protein Expr. Purif.* **2013**, *90*, 178–185. [\[CrossRef\]](#)
65. Sjöbring, U.; Björck, L.; Kastern, W. Streptococcal protein G. Gene structure and protein binding properties. *J. Biol. Chem.* **1991**, *266*, 399–405. [\[CrossRef\]](#)
66. Zhang, H.-C.; Yang, J.; Yang, G.-W.; Wang, X.-J.; Fan, H.-T. Production of recombinant protein G through high-density fermentation of engineered bacteria as well as purification. *Mol. Med. Rep.* **2015**, *12*, 3132–3138. [\[CrossRef\]](#)
67. Jha, R.K.; Gaiotto, T.; Bradbury, A.R.; Strauss, C.E. An improved Protein G with higher affinity for human/rabbit IgG Fc domains exploiting a computationally designed polar network. *Protein Eng. Des. Sel.* **2014**, *27*, 127–134. [\[CrossRef\]](#)
68. Derrick, J.P.; Wigley, D.B. Crystal structure of a streptococcal protein G domain bound to an Fab fragment. *Nat. Cell Biol.* **1992**, *359*, 752–754. [\[CrossRef\]](#) [\[PubMed\]](#)
69. Nilson, B.H.; Lögdberg, L.; Kastern, W.; Björck, L.; Åkerström, B. Purification of antibodies using protein L-binding framework structures in the light chain variable domain. *J. Immunol. Methods* **1993**, *164*, 33–40. [\[CrossRef\]](#)
70. Page, M.; Thorpe, R. Purification of IgG Using Protein A or Protein G. In *The Protein Protocols Handbook*; Humana Press: Totowa, NJ, USA, 2009; pp. 1761–1763. [\[CrossRef\]](#)
71. Kastern, W.; Sjöbring, U.; Björck, L. Structure of peptostreptococcal protein L and identification of a repeated immunoglobulin light chain-binding domain. *J. Biol. Chem.* **1992**, *267*, 12820–12825. [\[CrossRef\]](#)
72. Myhre, E.B.; Erntell, M. A non-immune interaction between the light chain of human immunoglobulin and a surface component of a *Peptococcus magnus* strain. *Mol. Immunol.* **1985**, *22*, 879–885. [\[CrossRef\]](#)
73. Darcy, E.; Leonard, P.; Fitzgerald, J.; Danaher, M.; O’Kennedy, R. Purification of Antibodies Using Affinity Chromatography. In *Protein Chromatography; Methods in Molecular Biology (Methods and Protocols)*; Humana Press: New York, NY, USA, 2011; pp. 369–382. [\[CrossRef\]](#)
74. Graille, M.; Stura, E.A.; Housden, N.G.; Beckingham, J.A.; Bottomley, S.P.; Beale, D.; Taussig, M.J.; Sutton, B.J.; Gore, M.G.; Charbonnier, J.-B. Complex between *Peptostreptococcus magnus* Protein L and a Human Antibody Reveals Structural Convergence in the Interaction Modes of Fab Binding Proteins. *Structure* **2001**, *9*, 679–687. [\[CrossRef\]](#)
75. Åkerström, B.; Björck, L. Protein L: An immunoglobulin light chain-binding bacterial protein. Characterization of binding and physicochemical properties. *J. Biol. Chem.* **1989**, *264*, 19740–19746. [\[CrossRef\]](#)

76. Wikstroem, M.; Drakenberg, T.; Forsen, S.; Sjoebing, U.; Bjoerck, L. Three-dimensional solution structure of an immunoglobulin light chain-binding domain of protein L. Comparison with the IgG-binding domains of protein G. *Biochemistry* **1994**, *33*, 14011–14017. [\[CrossRef\]](#)
77. Nilson, B.H.; Solomon, A.; Björck, L.; Akerström, B. Protein L from *Peptostreptococcus magnus* binds to the kappa light chain variable domain. *J. Biol. Chem.* **1992**, *267*, 2234–2239. [\[CrossRef\]](#)
78. Griep, R.; McDougall, J. Analysis and Purification of Antibody Fragments Using Protein A, Protein G, and Protein L. *Adv. Struct. Saf. Stud.* **2010**, 301–315. [\[CrossRef\]](#)
79. Toca, A.; Sjöbring, U.; Björck, L.; Holst, O. High level expression of protein L, an immunoglobulin-binding protein, in *Escherichia coli*. *J. Ferment. Bioeng.* **1995**, *80*, 1–5. [\[CrossRef\]](#)
80. ThermoScientific Fisher. Available online: <https://www.thermofisher.com/order/catalog/product/21189> (accessed on 10 December 2020).
81. Abcam. Available online: <https://www.abcam.com/recombinant-protein-l-ab155706.html> (accessed on 10 December 2020).
82. Sinobiological. Available online: <https://www.sinobiological.com/recombinant-proteins/protein-l-11044-h07e> (accessed on 10 December 2020).
83. Chateau, M.; Nilson, B.H.K.; Erntell, M.; Myhre, E.; Magnusson, C.G.M.; Åkerström, B.; Björck, L. On the Interaction between Protein L and Immunoglobulins of Various Mammalian Species. *Scand. J. Immunol.* **1993**, *37*, 399–405. [\[CrossRef\]](#) [\[PubMed\]](#)
84. Paloni, M.; Cavallotti, C. Molecular Modeling of the Interaction of Protein L with Antibodies. *ACS Omega* **2017**, *2*, 6464–6472. [\[CrossRef\]](#) [\[PubMed\]](#)
85. Sheng, S.; Kong, F. Separation of antigens and antibodies by immunoaffinity chromatography. *Pharm. Biol.* **2012**, *50*, 1038–1044. [\[CrossRef\]](#) [\[PubMed\]](#)
86. Rosano, G.L.; Ceccarelli, E.A. Recombinant protein expression in *Escherichia coli*: Advances and challenges. *Front. Microbiol.* **2014**, *5*, 172. [\[CrossRef\]](#)
87. Persson, T.; Eckersten, H.; Elen, O.; Hjelkrem, A.-G.R.; Markgren, J.; Söderström, M.; Börjesson, T. Predicting deoxynivalenol in oats under conditions representing Scandinavian production regions. *Food Addit. Contam. Part A* **2017**, *34*, 1026–1038. [\[CrossRef\]](#)
88. Su, Q.; Ganesh, S.; Moreno, M.; Bommireddy, Y.; Gonzalez, M.; Reklaitis, G.V.; Nagy, Z.K. A perspective on Quality-by-Control (QbC) in pharmaceutical continuous manufacturing. *Comput. Chem. Eng.* **2019**, *125*, 216–231. [\[CrossRef\]](#)
89. Gundinger, T.; Pansy, A.; Spadiut, O. A sensitive and robust HPLC method to quantify recombinant antibody fragments in *E. coli* crude cell lysate. *J. Chromatogr. B* **2018**, *1083*, 242–248. [\[CrossRef\]](#)
90. Nguyen, B.T.; Koh, G.; Lim, H.S.; Chua, A.J.S.; Ng, M.M.L.; Toh, C.-S. Membrane-Based Electrochemical Nanobiosensor for the Detection of Virus. *Anal. Chem.* **2009**, *81*, 7226–7234. [\[CrossRef\]](#)
91. Yu, H.; Kim, K.; Ma, K.; Lee, W.; Choi, J.-W.; Yun, C.-O.; Kim, D. Enhanced detection of virus particles by nanoisland-based localized surface plasmon resonance. *Biosens. Bioelectron.* **2013**, *41*, 249–255. [\[CrossRef\]](#)
92. Laghrib, F.; Saqrane, S.; El Bouabi, Y.; Farahi, A.; Bakasse, M.; Lahrich, S.; El Mhammedi, M. Current progress on COVID-19 related to biosensing technologies: New opportunity for detection and monitoring of viruses. *Microchem. J.* **2021**, *160*, 105606. [\[CrossRef\]](#)
93. Douzi, B. Protein–Protein Interactions: Surface Plasmon Resonance. In *Bacterial Protein Secretion Systems: Methods and Protocols*; Jourmet, L., Cascales, E., Eds.; Humana Press: New York, NY, USA, 2017; pp. 257–275. [\[CrossRef\]](#)
94. Sultana, A.; Lee, J.E. Measuring Protein-Protein and Protein-Nucleic Acid Interactions by Biolayer Interferometry. *Curr. Protoc. Protein Sci.* **2015**, *79*, 19.25.1–19.25.26. [\[CrossRef\]](#)
95. Anspach, F.B.; Petsch, D. Membrane adsorbers for selective endotoxin removal from protein solutions. *Process. Biochem.* **2000**, *35*, 1005–1012. [\[CrossRef\]](#)
96. Boi, C.; Malavasi, A.; Carbonell, R.G.; Gilleskie, G. A direct comparison between membrane adsorber and packed column chromatography performance. *J. Chromatogr. A* **2020**, *1612*, 460629. [\[CrossRef\]](#)
97. Chen, X.; Wang, Y.; Li, Y. Protein L chromatography: A useful tool for monitoring/separating homodimers during the purification of IgG-like asymmetric bispecific antibodies. *Protein Expr. Purif.* **2020**, *175*, 105711. [\[CrossRef\]](#)

## 7.2. Inclusion body production in fed-batch and continuous cultivation

### Inclusion body production in fed-batch and continuous cultivation

Running title: IB production in fed-batch and continuous cultivation

Stefan Kittler\*

Institute of Chemical, Environmental and Bioscience Engineering, Research Group Integrated Bioprocess Development, TU Wien, Gumpendorferstraße 1a, 1060 Vienna, Austria

\* Correspondence: stefan.kittler@tuwien.ac.at; Tel: +43 1 58801 166465

#### Abstract

Various fermentation strategies in industrial biotechnology are applied to produce recombinant target proteins using *Escherichia coli*. These proteins are often expressed as inclusion bodies (IBs), resulting in a high purity, high stability and high product titers. In state-of-the-art fed-batch processes, product formation takes place in a short period of time. Sterilization, cleaning and biomass growth are time consuming steps and reduce the space-time yield. Thus, the interest in establishing continuous cultivations, facilitating higher space-time yields, increased in recent years. In this protocol, we provide information and a guide to set up the production of recombinant proteins in fed-batch, as well as in chemostat continuous cultivations using *E. coli*.

**Keywords:** *E. coli*; inclusion body; fed-batch; chemostat; recombinant protein production

## 1. Introduction

Recombinant proteins originating from higher organisms (yeast, human etc.) can require post translational modifications (PTMs) to be functional [1, 2]. Hence, production of these proteins in *Escherichia coli* faces diverse challenges: *E. coli* has limitations to form disulphide bonds, when expressing recombinant proteins in the cytoplasm [1]. This can be bypassed by translocation into the periplasm, where disulfide bonds can be formed in the present oxidizing conditions [2-4]. Nevertheless, *E. coli* is one of the most used organisms in biotechnology since media components are cheap and the growth rate is high compared to various other hosts [1, 5-8]. Another industrially feasible option to express foreign proteins, is the formation of inclusion bodies (IBs). These are insoluble aggregates accumulating in the cytoplasm [9, 10]. Subsequent denaturing and refolding in the downstream process leads to the native structure and full functionality [2, 9, 10]. The production of IBs can be desirable since high product concentration and high purity can be achieved [10-12].

Fed-batch cultivations are currently state-of-the-art to produce recombinant proteins in industry using microbials. Using this cultivation mode, indeed a high biomass concentration can be achieved, however a time-dependent productivity can be observed. Additionally the recombinant protein formation phase itself is only a minor part of the total process time, thus causing low space-time yields [13]. To achieve time-independent processes, a change towards different cultivation modes is necessary. Higher space-time yields, lower set up costs and smaller cultivation vessels are benefits linked to continuous manufacturing. Furthermore, scalability of bioprocesses is simpler, as cultivation setups for production scale are more comparable [14, 15]. In chemostat cultivations, fermentation broth is steadily harvested, maintaining a constant reactor volume [14, 16]. In theory, cells reach a steady-state and constant product concentration and quality can be achieved. Even though equipment usage regarding recombinant protein production in *E. coli* can be increased applying continuous cultivation modes, implementations in industry are scarce [8, 16, 17]. This due to the fact, that microbial continuous cultivations suffer from an instable productivity, referred to the occurrence of subpopulations at elongated cultivation times (>100 h) [13, 15]. The simplicity of the fed-batch cultivation strategy yielding in high biomass concentrations and therefore high product titers in short time favor fed-batch cultivations over continuous cultivations still [16]. However, ongoing research and optimization of critical process parameters in continuous

manufacturing led to an increase of space-time yields compared to fed-batch cultivations and might change the paradigm of cultivation modes [15, 16, 18].

In this book chapter we will highlight recombinant protein production with the host *E. coli* BL21(DE3), enabling the use of a T7 based expression system [5, 7]. This system is well-known for high expression rates due to the strength of the T7 promotor. The induction can be performed either with isopropyl- $\beta$ -D-1-thiogalactopyranoside (IPTG) or the natural analogue allolactose, formed from added lactose. IPTG cannot be metabolized by cells, while fed lactose is partially metabolized by the strain BL21(DE3) and needs to be constantly supplied. Even though IPTG is favored over lactose in fed-batch cultivations, it was shown to be toxic at concentrations exceeding 1 mM [8, 19]. Furthermore, it is stated that mixed feeds of either glucose or glycerol combined with the inducer lactose can increase the productivity of recombinant proteins in fed-batch as well as in chemostat continuous cultivations [13, 19, 20]. As a result of partial degradation of the lactose, stress onto the host organism is minimized compared to an induction with IPTG. Thus, lactose is preferred in chemostat continuous cultivations, facilitating an increase of the recombinant protein expression. Non metabolized lactose is converted by  $\beta$ -galactosidase to allolactose, stopping repression of the lac operon. As primary C-source, glucose is conventionally favored for *E. coli* processes. Glucose is known to provide a high amount of energy due to affinity towards the phosphotransferase system and being used as glucose 6-phosphate in the glycolysis [6, 21, 22]. However, carbon catabolite repression is observed while feeding lactose and glucose in a mixed feed, minimizing lactose uptake from the broth and causing low induction levels [19]. As an alternative, glycerol showed less repression onto lactose uptake, resulting in higher and more stable expression rates of recombinant proteins [6]. Moreover, glycerol is introduced into glycolysis and gluconeogenesis, providing, like glucose, a high amount of energy for cell growth and recombinant protein expression [6, 23-25]. To summarize, the co-feeding of glycerol and lactose outperforms the feeding of a glucose-lactose mixture in chemostat continuous cultivations and can increase space-time yields therefore.

Various factors need to be considered to choose proper cultivation mode, carbon source and induction system (Note 1). In the following protocol we describe two cultivation modes (fed-batch and chemostat) and depict necessary analytics for characterization and optimization of the process.

3

## 2. Materials

### 2.1. Host Organism

For cultivations *E. coli* BL21(DE3) (Life technologies, Carlsbad, CA, USA) was used as a host strain (Note 2). The target plasmid (pET system) was transformed according to standard protocols described in detail elsewhere [26, 27]. Antibiotic must be adapted for cultivation, depending on the resistance gene of the used plasmid.

### 2.2. Cultivation Media

All cultivation steps were carried out using a defined medium described by DeLisa et al. [28], supplemented with 0.02 g/L of the respective antibiotic to prevent plasmid loss. The used concentrations of substrate and the contained supplements are depicted in Table 1 (Note 3).

*Table 1: DeLisa medium used for all cultivation phases. 0.02 g/L of the respective antibiotic were added for all phases [28]. As substrate either glycerol or glucose can be used.*

component	pre-culture	batch	feed	sterilization
	concentration [g/L]			
KH <sub>2</sub> PO <sub>4</sub>	13.3		-	autoclave
(NH <sub>4</sub> ) <sub>2</sub> HPO <sub>4</sub>	4		-	
Citric acid	1.7		-	
MgSO <sub>4</sub> *7H <sub>2</sub> O (stock 500 x)	1.2		10.00	autoclave
Fe(III) citrate (stock 100 x)	0.1		0.02	autoclave
EDTA (stock 100 x)	0.0084		0.0065	autoclave
Zn(CH <sub>3</sub> COO) <sub>2</sub> *H <sub>2</sub> O (stock 200 x)	0.013		0.008	filter sterilization
TE <sup>1</sup> (stock 200 x)	5 mL/L		7.27 mL/L	filter sterilization
Thiamine HCl (stock 1,000 x)	0.0045		-	filter sterilization
Substrate	8	20	400	autoclave

<sup>1</sup> TE stock: CoCl<sub>2</sub>\*6H<sub>2</sub>O (2.5 mg/L); MnCl<sub>2</sub>\*4H<sub>2</sub>O (15 mg/L); CuCl<sub>2</sub>\*2H<sub>2</sub>O (1.2 mg/L); H<sub>3</sub>BO<sub>3</sub> (3 mg/L); Na<sub>2</sub>MoO<sub>4</sub>\*2H<sub>2</sub>O (2.5 mg/L)

### 2.3. Devices and Equipment for Cultivation

#### I. Pre-culture:

Pre-culture requires growth for 16 h to reach an optical density ( $OD_{600}$ ) of  $> 5$  measured at a wavelength of 600 nm. An incubation shaker (250 rpm) equipped with a temperature control in the range of 30 - 40°C is required. The shake flask is inoculated with 0.3% (v/v) of the bacterial stock.

#### II. Bioreactor cultivation:

For all further cultivation steps at least one stirred-tank bioreactor is required, equipped with:

- Process control system:
  - o Controlling of pumps (e.g. exponential feeding)
  - o Data-recording scales for base and feed
  - o Monitoring of offgas signals
- PI- or PID-controller regulating the ratio of applied pressurized air and pure oxygen to keep  $dO_2 > 30\%$
- PI- or PID-controller connected to a pump to control the pH
- Gas flow controller for supplying pressurized air and oxygen if necessary
- Stirrer
- two pumps: feeding pump, base pump
- pH probe: The probe need to be calibrated within a pH-range of 4 - 7 prior usage. pH is controlled with 12.5%  $NH_4OH$  solution.
- Dissolved oxygen ( $=dO_2$ ): The probe needs to be calibrated before inoculation, however all medium supplements and process parameters should be adjusted.
- Offgas sensor for measuring residual offgas from reactors ( $CO_2$ ,  $O_2$ ).

For chemostat cultivation the bioreactor needs to be additionally equipped with:

- Pump for harvesting cultivation broth
- Dip-pipe adjusted to the desired volume



## 2.4. Process analysis

### 2.4.1. Biomass determination

#### OD<sub>600</sub>

- Photometer or plate reader
- Cuvettes or well plates

#### Dry Cell Weight (DCW)

- Oven (min. 105 °C)
- Centrifuge
- 2 mL Eppendorf Safe-Lock Tubes or glass Epprouvettes
- 0.9% NaCl solution

### 2.4.2. Metabolite determination

#### Option 1 - chromatography

- Liquid chromatography device. Equipped with:
  - o Refractory index (=RI) – detector
  - o Pump module
  - o Auto-sampler module
  - o Oven module
- Software for data analysis
- Anion exchange column
- HPLC-grade eluents
- HPLC (high performance liquid chromatography) vials
- Syringes and 0.2 µm syringe filters
- Calibration standards of respective metabolites which need to be quantified

#### Option 2 - automated analyser

- Respective test kits and calibration standards
- 1.5 mL Eppendorf Safe-Lock Tubes

#### 2.4.3. Inclusion body concentration determination

The analysis of inclusion bodies is highly product dependent. An example for product analysis applying liquid chromatography is given which is applicable for various recombinant proteins [29] (Note 4).

- High-pressure homogenizer
- Centrifuge
- 50 mL conic Greiner centrifuge tubes
- 2 mL Eppendorf Safe-Lock Tubes
- Vortex mixer
- Liquid chromatography device, equipped with:
  - o Pump module
  - o Auto-sampler module
  - o Oven module
  - o UV detector module
- Software for data analysis
- Reversed phase column
- HPLC-grade eluents
- HPLC (high performance liquid chromatography) vials
- Syringes and 0.2  $\mu\text{m}$  syringe filters

### 3. Methods

#### 3.1. Reactor set up and cultivation scheme

Figure 1 shows the cultivation set-up for both, fed-batch mode and chemostat mode.

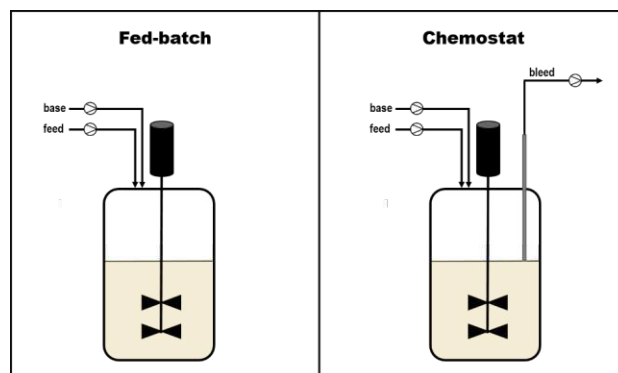


Figure 1: Process overview of a fed-batch cultivation, requiring at least two pumps (feed, base). The protein expression is triggered by supplementing an inducer (e.g.: IPTG (Isopropyl  $\beta$ -d-1-thiogalactopyranoside)). For chemostat continuous cultivation a dip-pipe is adjusted to a set height. By applying, a constant feed flow the dilution rate ( $D$ ) is specified. During the whole process, biomass is removed.

For both cultivation modes the reactors require the in section 2.3. described equipment. However, for chemostat cultivation additionally a dip-pipe and an additional pump for harvesting the bleed are required. In both cultivation modes first a batch is performed to reach a biomass concentration of approximately 8 g/L. Afterwards, for fed-batch cultivations, an exponential feeding is applied to reach a targeted biomass of e.g. 25 g/L. Subsequently, inducer can be applied either by one-point addition (IPTG (Isopropyl  $\beta$ -d-1-thiogalactopyranoside) or continuously in a mixed feed, containing e.g. lactose as inducer and glucose as the primary C-source (Note 5). For continuous cultivations a constant feeding is applied and biomass harvested, furthermore a perpetual supply of inducer is necessary. The cultivation scheme for both cultivation modes is depicted in Figure 2.

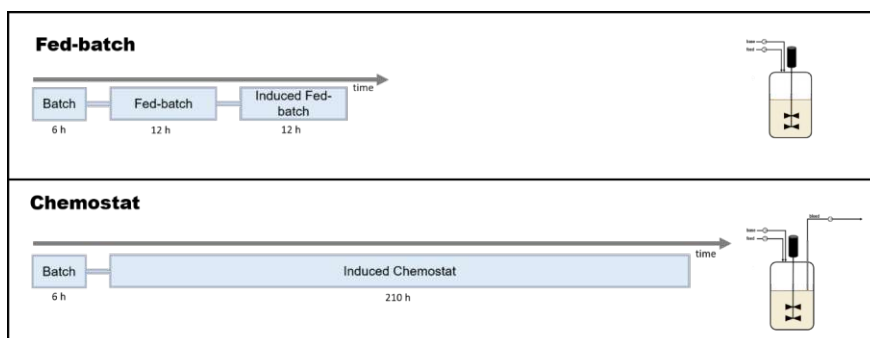


Figure 2: Exemplary process overview for estimated cultivation times. The classical fed-batch consists of a batch phase to grow cells reaching biomass concentration of approx. 8 g/L. Subsequently a feed is applied exponentially to increase biomass. This phase is then followed by an induction phase, where inducer is supplied and feeding continued. A chemostat consists of a batch phase and a subsequent continuous feed supply.

As mentioned above after the batch phase, further steps separate both cultivation modes.

#### 3.1.1.1. Pre-culture and Batch

1. Prior to sterilization, the pH of the pre-culture media needs to be adjusted to 7.2 using sodium hydroxide. Afterwards the required media components have to be sterilized according to Table 1.
2. Pre-culture is conducted at 37 °C and 230 rpm for 16 to 20 h (overnight) until an  $OD_{600}$  of >5 is reached.
3. Reactors need to be prepared before inoculation: 37 °C, 1,400 rpm, 2 vvm aeration and a pH of 6.7. The pH is set after sterilization using 12.5%  $NH_4OH$ . The  $dO_2$  probe is calibrated using a one-point calibration to 100% dissolved oxygen shortly before inoculation.
4. Inoculation: The batch medium is inoculated with 10% of the pre-culture (e.g.: 100 mL for 1 L batch). During the whole process dissolved oxygen is kept above 40% using pure oxygen if necessary.
5. The end of the batch phase is indicated by a drop of the  $CO_2$  signal or a rise of the  $dO_2$  signal.

## 3.1.2. Fed-batch vs Chemostat after batch phase

Fed-batch	Chemostat
<p>The goal for the non-induced fed-batch is to increase the biomass concentration. Therefore, an exponential feeding profile is used, to grow cells at a defined growth rate = <math>\mu</math> [<math>\text{h}^{-1}</math>]. After the targeted biomass concentration is reached, induction is performed either using IPTG or lactose. Feeding in the induced fed-batch phase can be varied and is described in more detail below.</p>	<p>In chemostat continuous cultivations feed is supplied and biomass harvested to achieve a cell equilibrium indicated by stable offgas signals. In this steady-state the biomass concentration is constant and therefore the dilution rate (<math>=D</math>) equals the growth factor (<math>=\mu</math>).</p>

The expression rates of recombinant proteins depend highly on expression host and target product. To boost the product titer an optimization of the induction phase is recommended (Note 1).

### Induced Fed-batch

Feeding can be performed using a) an exponential b) a linear or c) a constant profile. The different feeding strategies are illustrated in Figure 3.

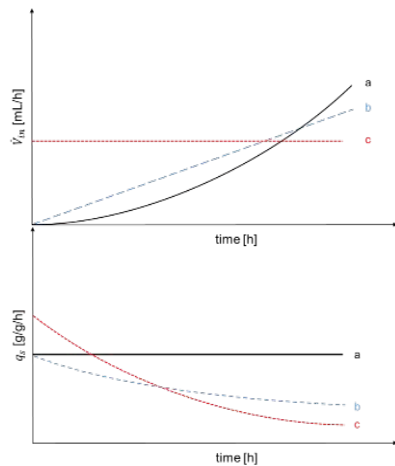


Figure 3: Overview of possible feeding strategies and the corresponding specific substrate uptake rate ( $q_s$  [g/g/h]) in a fed-batch. a: exponential feeding, b: linear feeding, c: constant feeding

$$\dot{V}_{in} \left[ \frac{mL}{h} \right] = \frac{q_s \left[ \frac{g}{g/h} \right] * X(t) [g]}{C_{feed} \left[ \frac{g}{L} \right]}$$

Equation 1

- Biomass ( $X(t)$ ) is determined by  $OD_{600}$  measurements and biomass is calculated using a previously determined  $OD$  to biomass correlation.
- For exponential feeding (a) an exponential ramp is used for calculating the biomass, which is used to adapt the  $\dot{V}_{in}$  automatically.

### Chemostat

- The dilution rate ( $D$ ) (or residence time) is calculated according the following equation 3:

$$D [h^{-1}] = \frac{\dot{V}_{in} \left[ \frac{mL}{h} \right]}{V [mL]}$$

Equation 3

- The trend of the feeding rate and the specific substrate uptake rate ( $q_s$ ) is depicted in Figure 4.

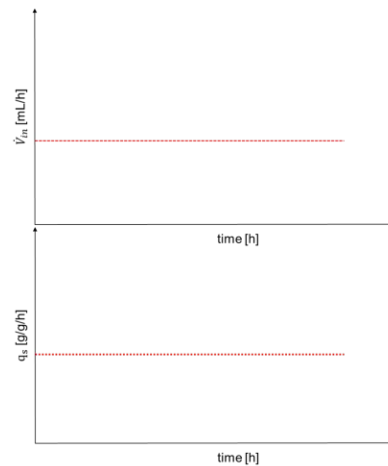


Figure 4: Overview of feeding profile and the corresponding specific substrate uptake rate ( $q_s$  [g/g/h]) in a chemostat continuous cultivation.

- $D$  can be adjusted with the volumetric flow ( $\dot{V}_{in}$ ) at a defined reactor volume ( $V$ ).
- Maintenance of constant volume can be ensured by a peristaltic pump, connected to the dip-pipe, with a flow rate ( $\dot{V}_{out}$ ) larger than  $\dot{V}_{in}$ .

11

### Induced Fed-batch

- For linear feeding (b) equation 1 is used to calculate the start value ( $\dot{V}_{in}$ ). The feed rate ( $\dot{V}_{in,t}$ ) is then increased linearly until a targeted final feed rate is reached. This can be done by a formula with a slope which represents the change of the feed rate per hour (Equation 2).

$$\dot{V}_{in,t} \left[ \frac{mL}{h} \right] = \dot{V}_{change} \left[ \frac{mL}{h^2} \right] * t[h] + \dot{V}_{in} \left[ \frac{mL}{h} \right]$$

Equation 2

$\dot{V}_{in,t} \left[ \frac{mL}{h} \right]$  ... feed rate into the reactor at time point t

$\dot{V}_{change} \left[ \frac{mL}{h^2} \right]$  ... slope for the change of the feed rate

t [h] ... feed rate at elapsed time in h

$\dot{V}_{in} \left[ \frac{mL}{h} \right]$  ... start feed rate into the reactor

- For constant feeding (c)  $\dot{V}_{in}$  is calculated at the beginning and kept constant during the whole induction phase.

### Chemostat

- Dip-pipe is adjusted to the required volume height: To adjust the dip-pipe at the required height, set up the reactor (probes, pipes etc.), fill the reactor with required volume prior to sterilization and adjust height at applied process parameters (e.g. 1400 rpm, 2 vvm).
- Continuous supply of inducer (e.g. IPTG, lactose) and antibiotic (selection pressure) etc. is necessary.

### 3.2. Sampling and Analysis

After batch, a first sample is taken. For fed-batch cultivation, this sample is used to determine the biomass concentration required for starting the exponential feed. At the end of the fed-batch again a sample is taken to determine biomass concentration for subsequent feeding during induction (Notes 6-8).

#### 3.2.1. Biomass determination

Biomass concentration is determined via OD<sub>600</sub> and gravimetrically by DCW.

##### OD<sub>600</sub>

- Procedure:
  1. Vortex sample for 5 – 10 sec
  2. Dilute sample to linear range of the photometer (e.g.: 0.2 – 0.8 AU)
  3. Blank the device with water
  4. Measure absorbance of the homogeneous sample at 600 nm

##### Dry Cell Weight (DCW)

- Preheat 2 mL Eppendorf Safe-Lock Tubes or glass Epprouvettes at >105 °C until weight stability is reached (3 – 4 days)
- Pre-weigh labelled tubes at room temperature (cooling for 1h recommended)
- Procedure:
  1. Vortex sample for 5 – 10 sec
  2. Pipette 1 mL of homogenous sample into the pre-weighted reaction tube
  3. Centrifuge at 4 °C and 10,000 rpm for 10 min
  4. Decant supernatant in other reaction tubes and store it at -20 °C for metabolite analysis
  5. Resuspend biomass pellet in 0.9% NaCl solution
  6. Centrifuge at 4 °C and 10,000 rpm for 10 min
  7. Discard supernatant
  8. Dry biomass pellet at 105 °C for 2 to 3 days
  9. Determine  $\Delta$ weight to pre-weighted reaction tube at room temperature



## 3.2.2. Metabolite determination

Samples of the supernatant from fermentation samples and feed can be measured using liquid chromatography or an automated analyzer

- Thaw supernatant from 3.2.1. DCW
- Filter supernatant using 0.2  $\mu\text{m}$  syringe filters prior analysis

Liquid chromatography:

1. Prepare eluent
2. Prepare HPLC using anion exchange chromatography
3. Prepare standards of the respective metabolites and substrate
4. Analyze of chromatogram with suitable software

Automated analyser:

1. Transfer filtered supernatant into 1.5 mL Eppendorf Safe-Lock Tubes
2. Select test kit and start measurement

## 3.2.3. Product determination

For the determination of product concentration a HPLC can be used. As mentioned above, analysis of inclusion bodies is highly product dependent, however an example for determining product concentration is given in Note 8.

## 3.3. Calculation of process parameters

## 3.3.1. Calculation of feed rate for Fed-batch cultivations

The feed flow into the reactor can be monitored gravimetrically. A desired rate can be calculated according to Equation 4.

$$\dot{V}_{in} \left[ \frac{\text{mL}}{\text{h}} \right] = \frac{q_s \left[ \frac{\text{g}}{\text{h}} \right] * X(t) [\text{g}]}{c_{feed} \left[ \frac{\text{g}}{\text{L}} \right]} * 1000$$

Equation 4

$\dot{V}_{in} \left[ \frac{\text{mL}}{\text{h}} \right]$  ... feed rate into the reactor

$q_s \left[ \frac{\text{g}}{\text{h}} \right]$  ... specific substrate uptake rate

$X(t) [\text{g}]$  ... biomass in the reactor at specific time point

$c_{feed} \left[ \frac{g}{L} \right]$  ... concentration of substrate in the feed

### 3.3.2. Calculation of dilution rate for Chemostat cultivations

The dilution rate can be calculated via the monitored feed volumes over time, while the reactor volume must be kept constant (Equation 5). Dilution rates exceeding  $D_{crit}$  must be avoided, to prevent a wash out of the cells.

$$D [h^{-1}] = \frac{\dot{V}_{in} \left[ \frac{mL}{h} \right]}{V [mL]}$$

Equation 5

$\dot{V}_{in} \left[ \frac{mL}{h} \right]$  ... feed rate into the reactor

$V[mL]$  ... reactor volume

### 3.3.3. Calculation of substrate uptake-rates

The real specific substrate uptake rate can be calculated according to Equation 6.

$$q_s \left[ \frac{g}{h} \right] = \frac{V_{in,feed,\Delta t} [L] * c_{feed} \left[ \frac{g}{L} \right] - V_{reactor,t_{i+1}} [L] * c_{acc,\Delta t} \left[ \frac{g}{L} \right]}{\Delta t [h] * X_{\Delta t} [g]}$$

Equation 6

$q_s \left[ \frac{g}{h} \right]$  ... specific substrate uptake rate

$V_{in,feed,\Delta t} [L]$  ... volume of applied feed in timespan  $\Delta t$

$c_{feed} \left[ \frac{g}{L} \right]$  ... concentration of substrate in the feed

$V_{reactor,t_{i+1}} [L]$  ... volume in the reactor at time point  $i+1$

$c_{acc,\Delta t} \left[ \frac{g}{L} \right]$  ... concentration of substrate accumulated in the reactor in time span  $\Delta t$

$\Delta t [h]$  ... timespan ( $t_{i+1} - t_i$ ) for calculated uptake rate

$X_{\Delta t} [g]$  ... average biomass in the reactor during timespan  $\Delta t$

#### 4. Notes

- 1.) For optimization of the protein expression rates, critical process parameters need to be determined. These parameters (Table 2) can be altered in a Design of Experiment (DoE) approach. First, the maximum specific growth rate ( $\mu_{max}$ ) needs to be determined either in shake flask experiments or using a plate reader, monitoring biomass growth over time,  $\mu_{max}$  is calculated according Equation 7.

$$\mu_{max} \left[ \frac{1}{h} \right] = \ln \left( \frac{X_{t_{i+1}} [g]}{X_{t_i} [g]} \right) * \frac{1}{\Delta t}$$

Equation 7

The determined  $\mu_{max}$  can be correlated to the specific substrate uptake rate which can be used for fed-batch cultivations. In chemostat continuous cultivations  $\mu$  equals  $D$ , in case the operation range is below the critical dilution rate.

Table 2: Parameters that can be considered to optimize recombinant protein expression rates.

Fed-batch	Chemostat
- Induction temperature	- Induction temperature
- Induction time	- Dilution rate
- Specific substrate uptake rate	- Ratio of primary carbon source to inducer in mixed feed approaches
- Type of inducer	- Specific substrate uptake rate
- Ratio of primary carbon source to inducer in mixed feed approaches	

As chemostat cultivations run for longer process times, screening the optimized induction temperature is recommended in fed-batch cultivations. The knowledge from these experiments can be used for chemostat cultivations to optimize the dilution rate.

- 2.) The described methods and process times are exemplarily given for *E. coli* BL21(DE3), however they depend highly on the used host organism and strain.
  - 3.) Glucose needs to be sterilized separately in a split volume in order to avoid Maillard reaction. Glycerol can be autoclaved with  $\text{KH}_2\text{PO}_4$ ,  $(\text{NH}_4)_2\text{HPO}_4$  and citric acid.
  - 4.) The given HPLC method is an example, applicable for some recombinant proteins. As a commonly used alternative, sodiumdodecyl sulfate polyacrylamide gel electrophoresis (SDS-PAGE) can be performed. To perform a SDS-PAGE, samples are mixed with a Laemmli buffer stock to achieve a 1× concentration of Laemmli buffer in the final dilution. Then samples need to be heated to 95 °C for 10 min and are subsequently spun down for 2 min. Five  $\mu\text{L}$  of each sample are loaded onto a pre-cast SDS gel and the gel is run for 30 min at 180 V. Subsequently the gel is stained with Coomassie Blue.
  - 5.) For mixed feeds (glucose/glycerol + lactose) the carbon source to inducer ratio must be calculated prior to utilization. Screening approaches therefore can be found in given citations [5, 6].
  - 6.) All samples can be stored at -20 °C until analysis, DCW and  $\text{OD}_{600}$  have to be determined immediately after sampling.
  - 7.) Sampling during induction depends on various factors:
    - growth rate of the host organism
    - expectations in productivity
    - cultivation mode:
      - a. induced fed-batch: sampling e.g. 2 h is recommended
      - b. chemostat: sampling once a day is recommended
  - 8.) Product determination
- Sampling:
1. Pipette approx. 10 mL of homogeneous fermentation broth into 50 mL conic Greiner centrifuge tubes to reach a wet cell weight of approx. 1 – 2 g

17

2. Centrifuge at 4 °C and 10,000 rpm for 10 min
3. Discard supernatant und store biomass pellet at -20 °C until further use

Homogenization:

1. Suspend biomass pellet in Lysis buffer (100 mM Tris, 10 mM EDTA, pH = 7.4)
2. Disrupt cells using a high-pressure homogenizer
3. Centrifuge at 4 °C and 10,000 rpm for 10 min
4. Discard supernatant
5. Suspend pellet in 30 mL MQ
6. Centrifuge at 4 °C and 10,000 rpm for 10 min
7. Discard supernatant
8. Suspend pellet in 10 mL MQ, aliquot 1 mL each into a 2 mL Eppendorf tube and centrifuge at 4 °C and 10,000 rpm for 10 min
9. Discard supernatant and freeze IB pellets at -20 °C until further use

IB concentration analysis:

1. Suspend IB pellet in IB buffer (7.5 M Gu-HCl, 62 mM Tris, 125 mM DTT, pH = 8)
2. Filter sample prior HPLC measurement using 0.2 µm syringe filter
3. Prepare eluents (A: MQ + 0.1% TFA, B: ACN + 0.1% TFA) [29]
4. Prepare HPLC using reversed phase column
5. Prepare standards of the respective protein standard
6. Analysis of chromatograms with a suitable software

**Figure caption:**

**Figure 1:** Process overview of a fed-batch cultivation, requiring at least two pumps (feed, base). The protein expression is triggered by supplementing an inducer (e.g.: IPTG (Isopropyl  $\beta$ -d-1-thiogalactopyranoside)). For chemostat continuous cultivation a dip-pipe is adjusted to a set height. By applying, a constant feed flow the dilution rate ( $D$ ) is specified. During the whole process, fermentation broth is removed.

**Figure 2:** Exemplary process overview for estimated cultivation times. The classical fed-batch consists of a batch phase to grow cells reaching biomass concentration of approx. 8 g/L. Subsequently a feed is applied exponentially to increase biomass. This phase is then followed by an induction phase, where inducer is supplied and feeding continued. A chemostat consists of a batch phase and a subsequent continuous feed supply.

**Figure 3:** Overview of possible feeding strategies and the corresponding specific substrate uptake rate ( $q_s$  [g/g/h]) in a fed-batch. a: exponential feeding, b: linear feeding, c: constant feeding

**Figure 4:** Overview of feeding profile and the corresponding specific substrate uptake rate ( $q_s$  [g/g/h]) in a chemostat continuous cultivation.

**Table caption:**

**Table 3:** DeLisa medium used for all cultivation phases. 0.02 g/L of the respective antibiotic were added for all phases [28]. As substrate either glycerol or glucose can be used.

**Table 4:** Parameters that can be considered to optimize recombinant protein expression rates.

## References

1. Demain, A.L. and P. Vaishnav, *Production of recombinant proteins by microbes and higher organisms*. Biotechnology Advances, 2009. **27**(3): p. 297-306.
2. Walsh, G., *Post-translational modifications of protein biopharmaceuticals*. Drug Discovery Today, 2010. **15**(17): p. 773-780.
3. Manta, B., et al., *Disulfide Bond Formation in the Periplasm of Escherichia coli*. EcoSal Plus, 2019. **8**(2).
4. Missiakas, D. and S. Raina, *Protein folding in the bacterial periplasm*. Journal of bacteriology, 1997. **179**(8): p. 2465-2471.
5. Wurm, D.J., et al., *Mechanistic platform knowledge of concomitant sugar uptake in Escherichia coli BL21(DE3) strains*. Scientific reports, 2017. **7**: p. 45072-45072.
6. Kopp, J., et al., *Impact of Glycerol as Carbon Source onto Specific Sugar and Inducer Uptake Rates and Inclusion Body Productivity in E. coli BL21(DE3)*. Bioengineering (Basel, Switzerland), 2017. **5**(1): p. 1.
7. Rosano, G.A.-O., E.S. Morales, and E.A.-O. Ceccarelli, *New tools for recombinant protein production in Escherichia coli: A 5-year update*. (1469-896X (Electronic)).
8. Kopp, J., et al., *Repetitive Fed-Batch: A Promising Process Mode for Biomanufacturing With E. coli*. Frontiers in Bioengineering and Biotechnology, 2020. **8**: p. 1312.
9. Singh, A., et al., *Protein recovery from inclusion bodies of Escherichia coli using mild solubilization process*. Microbial Cell Factories, 2015. **14**(1): p. 41.
10. Carrió, M.M. and A. Villaverde, *Localization of Chaperones DnaK and GroEL in Bacterial Inclusion Bodies*. Journal of Bacteriology, 2005. **187**(10): p. 3599-3601.
11. García-Fruitós, E., *Inclusion bodies: a new concept*. Microbial Cell Factories, 2010. **9**(1): p. 80.
12. Slouka, C.A.-O.X., et al., *Perspectives of inclusion bodies for bio-based products: curse or blessing?* (1432-0614 (Electronic)).
13. Kittler, S., et al., *Cascaded processing enables continuous upstream processing with E. coli BL21(DE3)*. Scientific Reports, 2021. **11**(1): p. 11477.
14. Adamberg, K., K. Valgepea, and R. Vilu, *Advanced continuous cultivation methods for systems microbiology*. Microbiology, 2015. **161**(9): p. 1707-1719.
15. Peebo, K. and P. Neubauer, *Application of Continuous Culture Methods to Recombinant Protein Production in Microorganisms*. Microorganisms, 2018. **6**(3): p. 56.
16. Kopp, J., et al., *The Rocky Road From Fed-Batch to Continuous Processing With E. coli*. (2296-4185 (Print)).
17. Lee, S., et al., *Modernizing Pharmaceutical Manufacturing: from Batch to Continuous Production*. Journal of Pharmaceutical Innovation, 2015. **10**: p. 191-199.
18. Curvers, S., et al., *Human chymotrypsinogen B production with Pichia pastoris by integrated development of fermentation and downstream processing. Part 1. Fermentation*. (8756-7938 (Print)).
19. Wurm, D.J., et al., *The E. coli pET expression system revisited-mechanistic correlation between glucose and lactose uptake*. Applied microbiology and biotechnology, 2016. **100**(20): p. 8721-8729.
20. Neubauer, P., et al., *Maximizing the expression of a recombinant gene in Escherichia coli by manipulation of induction time using lactose as inducer*. Applied Microbiology and Biotechnology, 1992. **36**(6): p. 739-744.



21. Deutscher, J., C. Francke, and P.W. Postma, *How phosphotransferase system-related protein phosphorylation regulates carbohydrate metabolism in bacteria*. Microbiology and molecular biology Reviews, 2006. **70**(4): p. 939-1031.
22. Postma, P.W., J.W. Lengeler, and G.R. Jacobson, *Phosphoenolpyruvate: carbohydrate phosphotransferase systems of bacteria*. Microbiological reviews, 1993. **57**(3): p. 543-594.
23. Lin, E., *Glycerol dissimilation and its regulation in bacteria*. Annual review of microbiology, 1976. **30**(1): p. 535-578.
24. Zwaig, N., W. Kistler, and E. Lin, *Glycerol kinase, the pacemaker for the dissimilation of glycerol in Escherichia coli*. Journal of bacteriology, 1970. **102**(3): p. 753-759.
25. Voegelé, R.T., G.D. Sweet, and W. Boos, *Glycerol kinase of Escherichia coli is activated by interaction with the glycerol facilitator*. Journal of bacteriology, 1993. **175**(4): p. 1087-1094.
26. Swords, W.E., *Chemical transformation of E. coli*. (1064-3745 (Print)).
27. Tomley, F.M., *Transformation of E. coli*. (1064-3745 (Print)).
28. DeLisa, M.P., et al., *Monitoring GFP-operon fusion protein expression during high cell density cultivation of Escherichia coli using an on-line optical sensor*. Biotechnology and Bioengineering, 1999. **65**(1): p. 54-64.
29. Kopp, J., et al., *Development of a generic reversed-phase liquid chromatography method for protein quantification using analytical quality-by-design principles*. Journal of Pharmaceutical and Biomedical Analysis, 2020. **188**: p. 113412.

## 7.3. Curriculum vitae

### Curriculum vitae

Dipl.-Ing. Stefan Kittler

**Date of Birth:** 18.08.1996

**E-Mail:** s.kittler@icloud.com



#### EDUCATION

- Since 12/2019** Doctoral program at the Institute of Chemical, Environmental and Biological Engineering at Technical University of Vienna
- 11/2017 – 11/2019** Master program: Technical Chemistry with focus on Biotechnology and Bioanalytics at Technical University of Vienna  
*Master thesis: "Optimization of a cascaded continuous cultivation mode using a Design of Experiment approach"*
- WS/2018** Semester abroad at Chalmers University of Technology
- 10/2014 -10/2017** Bachelor program: Technical Chemistry at Technical University of Vienna  
*Bachelor thesis: "Capture of a Fab from E. coli: HIC vs. AFFINITY CHROMATOGRAPHY"*

#### PROFESSIONAL EXPERIENCE AND SUMMER INTERNSHIPS

- 08/2017 – 10/2018** Project Assistant at Technical University of Vienna in the group *Integrated Bioprocess Development*
- 07/2016** Summer Internship at ESW Consulting Wruss
- 07/2013 & 07/2014** Summer Internship at Natural History Museum

SKILLS

<b>Languages</b>	German (mother tongue) English (fluent)	
<b>Computer literacy</b>	Microsoft Office MODDE Origin Matlab (basic knowledge)	Lucullus (PIMS) R Studio

PUBLICATIONS

**Kittler, S.**, Ebner, J., Besleaga, M., Larsbrink, J., et al., Recombinant Protein L: Production, Purification and Characterization of a Universal Binding Ligand. *Journal of Biotechnology* 2022, 359, 108-115.

Gundinger, T.; **Kittler, S.**; Kubicek, S.; Kopp, J.; Spadiut, O. Recombinant Protein Production in *E. coli* Using the phoA Expression System. *Fermentation* 2022, 8.

**Kittler, S.**; Slouka, C.; Pell, A.; Lamplot, R.; Besleaga, M.; Ablasser, S.; Herwig, C.; Spadiut, O.; Kopp, J. Cascaded processing enables continuous upstream processing with *E. coli* BL21(DE3). *Scientific Reports* 2021, 11, 11477.

**Kittler, S.**; Besleaga, M.; Ebner, J.; Spadiut, O. Protein L—More Than Just an Affinity Ligand. *Processes* 2021, 9, 874.

Kopp, J.; **Kittler, S.**; Slouka, C.; Herwig, C.; Spadiut, O.; Wurm, D.J. Repetitive Fed-Batch: A Promising Process Mode for Biomanufacturing With *E. coli*. *Frontiers in Bioengineering and Biotechnology* 2020, 8, 1312.

**Kittler, S.**; Kopp, J.; Veelenturf, P.G.; Spadiut, O.; Delvigne, F.; Herwig, C.; Slouka, C. The Lazarus *Escherichia coli* Effect: Recovery of Productivity on Glycerol/Lactose Mixed Feed in Continuous Biomanufacturing. *Frontiers in Bioengineering and Biotechnology* 2020, 8, 993.

CONFERENCES

**Poster Presentation** “Small scale mechanical cell disruption: A workflow to screen for ideal disruption conditions for recombinantly produced proteins in *E. coli*”; **Stefan Kittler**, Julian Ebner, Julian Kopp, Oliver Spadiut; 7<sup>th</sup> BioProscale 2022 in Berlin, 28-21 March 2022 (2<sup>nd</sup> place in the Best Poster Award)